

Escherichia coli response to nitrosative stress.

by

Claire Elizabeth Vine



A thesis submitted to the University of Birmingham
for the degree of DOCTOR OF PHILOSOPHY

School of Biosciences
College of Life and Environmental Sciences
University of Birmingham
November 2011

UNIVERSITY OF
BIRMINGHAM

University of Birmingham Research Archive

e-theses repository

This unpublished thesis/dissertation is copyright of the author and/or third parties. The intellectual property rights of the author or third parties in respect of this work are as defined by The Copyright Designs and Patents Act 1988 or as modified by any successor legislation.

Any use made of information contained in this thesis/dissertation must be in accordance with that legislation and must be properly acknowledged. Further distribution or reproduction in any format is prohibited without the permission of the copyright holder.

Abstract

Previous transcriptomic experiments have revealed that various *Escherichia coli* K-12 genes encoding proteins of unknown function are highly expressed during anaerobic growth in the presence of nitrate, or especially nitrite. Products of some of these genes, especially YeaR-YoaG, YgbA, YibIH and the hybrid cluster protein, Hcp, have been implicated in the response to nitrosative stress. The aims of this study were to investigate sources of nitrosative stress, and the possible roles of some of these proteins in protection against nitric oxide. The YtfE protein has been implicated in the repair of iron centres, especially in iron-sulphur proteins. The previously unexplained anaerobic growth defect of the *ytfE* strain LMS 4209 was shown to be due to a secondary 126-gene deletion rather than to the deletion of *ytfE*.

At the start of the project, the transcription factor, NsrR, was known to respond to low concentrations of intracellular NO, and to repress expression of *ytfE*, *hcp-hcr* encoding the hybrid cluster protein and its reductase, and *hmp* that encodes the flavohaemoglobin, Hmp. In this work, a biochemical assay of *hcp* promoter activity was developed as a reporter of intracellular NO generation. This assay was used in combination with a range of mutants to show that the major source of intracellular NO is the reduction of nitrite by the cytoplasmic nitrate reductase, NarG. Although the periplasmic cytochrome *c* nitrite reductase, NrfAB, and the cytoplasmic nitrite reductase, NirBD, decrease nitrosative stress by reducing nitrite to ammonia, at least one additional source of NO production from nitrite remains unidentified.

An assay for NO reduction using a Clark-Type electrode was validated. Rates of NO reduction were induced 2-fold in the presence of nitrate. Lowest rates of NO reduction were found in a mutant defective in *nsrR*. A quadruple mutant defective in Hmp, the flavorubredoxin, NorV, NrfAB and NirBD still reduced NO at more than half the rate of the parent. This residual activity was not due to YibIH, YeaR-YoaG or YgbA. Various *hcp-hcr* derivatives of strains defective in NO reductases revealed a severe growth defect under conditions of nitrosative stress, but Hcp was eliminated as a possible additional NO reductase. This growth defect was substantially suppressed by a further mutation in *ytfE*. Growth experiments with isogenic sets of mutant defective in all combinations of *hcp* and *ytfE* in addition to deletions in *hmp*, *norVW* and *nrfAB* implicated both YtfE and Hcp in repair of nitrosative damage. However, weaker phenotypes of these strains in absence of nitrate or nitrite are consistent with more general roles for these proteins in the repair of damage to protein iron centres.

Dedication

To my family and Sam.

Acknowledgements

Firstly I must thank my supervisor, Professor Jeff Cole, for his guidance, support, faith in my ability and pressure to do well, all as needed, throughout my PhD project! I must also thank Dr Derrick Squire for his involvement at the start of my project and also Lesley Griffiths for their guidance in finding my feet in the lab. I thank Dr Marta Justino and Dr Ligia Saraiva for allowing me to work in their laboratory, and FEMS for providing a Research Fellowship to fund my stay in Oeiras. I thank Professor Steve Busby for his input at our weekly lab meetings and other members of the Busby lab, past and present: Dr Doug Browning; Dr David Lee; Dr Kerry Hollands; Dr Maria Antonia Sanchez Romero; Dr David Chismon; Dr Mohammed Shahidul Islam; Jack Bryant; Laura Rowley and Patcharawarin Ruanto for their helpful comments. I acknowledge Cole lab members, past and present: Dr Sudesh Mohan, Dr Tim Overton; Dr Yanina Sevastyanovich; Dr Wenjing Jia; Dr Angeliki Marietou; Dr Ying Li; Dr Sara Alfasi; Amanda Hopper; Ian Cadby; Lenny Zaffaroni; Dr Masha Tutukina; Sukhjit Purewal and Charlene Bradley for their invaluable help and friendship.

I thank my Aunty, Dr Catherine Rees, for allowing me to work in her laboratory aged fifteen, for helping me to get the 'Science Bug' in the first place, and for her enthusiasm and support throughout my education! I also thank my wonderful friends for their help and support outside of the lab: Nyree; Barbara; Cass; Amy; Paddy; Fi; Hema; Rob; Will; Tom; Tim; Jeni; Sophie; Claire and Ellie, I couldn't have completed this without you. I must give a special mention to my gorgeous friend Louise, who has always provided me with fun times to forget about troubles at work, and has listened to my thoughts and presentations about Microbiology, despite being a Theologist! In particular I thank my parents, grandparents and my sister Laura for their love and support; I would not have believed in my ability to complete the undergraduate work, let alone a PhD, without you all. Finally to those that have been closest to me during the past four years, my wonderful husband Sam, Amanda, Jack and Ian – the countless cups of tea and coffee (and occasionally something stronger) in a time of need, listening to my worries and convincing me to carry on, I will never forget your help.

Contents list
Table of contents

Abstract.....	i
Dedication.....	ii
Acknowledgements.....	iii
List of figures.....	ix
List of tables.....	xiii
List of abbreviations.....	xiv
CHAPTER 1 – INTRODUCTION.....	1
Adaptation of <i>Escherichia coli</i> to anaerobic growth.....	1
Electron transfer components during anaerobic growth.....	2
Quinones used for electron transfer.....	2
Generation of a proton motive force.....	5
Regulation of the adaptation to anaerobic growth.....	5
The factor for inversion stimulation, Fis.....	11
Nitrate reductases in <i>E. coli</i>	12
Nitrite reductases in <i>E. coli</i>	15
TMAO and DMSO reductases.....	18
The twin-arginine transport system.....	19
<i>E. coli</i> encounters oxidative and nitrosative stress.....	21
Protein damage caused by nitrosative stress.....	22
DNA damage caused by nitrosative stress.....	24
Detoxification of NO in <i>E. coli</i>	25
Sensors of NO.....	28
The role of the di-iron protein, YtfE, in resisting nitrosative stress.....	29
Identification of <i>E. coli</i> genes of unknown function implicated in the response to nitrosative stress.....	31
The hybrid cluster protein, Hcp.....	32
YgbA.....	38
YeaR and YoaG.....	38
YibI and YibH.....	39
Ogt.....	39
Possible roles for the genes of unknown function.....	41
Aims of this work.....	41
CHAPTER 2 - MATERIALS AND METHODS.....	44
MATERIALS.....	44
Media.....	44

Antibiotics	44
Buffers	44
BACTERIAL METHODS	44
Bacterial strains	44
Preparing bacteria for long term storage	44
Plasmids	50
Preparation of competent <i>E. coli</i> cells	50
Transformation of <i>E. coli</i> with plasmid DNA	50
P1 transduction	54
Generation of <i>hmp</i> and <i>narL</i> deletion mutants	55
Removal of the antibiotic resistance cassette using FRT sites	57
Construction of an isogenic set of <i>nirBDC</i> and <i>nrfAB</i> mutants	58
Construction of an <i>nsrR</i> mutant	59
Construction of mutants defective in a combination of proteins implicated in nitrosative stress	59
Growth assays for comparison with experiments reported in Justino <i>et al.</i> , 2006	59
Growth assays	64
β -galactosidase assays	64
Preparation of nitric oxide saturated water (NOSW)	65
Growth and β -galactosidase assays in response to the addition of nitrate, nitrite or NO	66
.....	66
Growth and preparation of bacteria for use in the nitric oxide electrode	68
NO electrode assays	68
Qualitative determination of nitrite presence	71
Determination of nitrite concentration	71
Quantitative nitrite reduction assay	71
DNA AND RNA TECHNIQUES	72
The polymerase chain reaction (PCR)	72
pGEM®-T Easy cloning	73
Agarose gel electrophoresis	78
Restriction digests	78
Treatment of restriction digests with calf intestinal alkaline phosphatase (CIAP)	78
Ligations	78
Preparation of genomic DNA	78
Comparative genomic hybridisation microarray experiments	79
DNA Sequencing	80
Construction of plasmid pCV01	80

Construction of plasmid pSP01	81
PROTEIN TECHNIQUES	81
SDS polyacrylamide gel electrophoresis (SDS-PAGE) of proteins	81
Coomassie staining of SDS-PAGE gels	82
STATISTICAL ANALYSIS OF THE DATA	82
Calculation of p values	82
CHAPTER 3 – RESULTS	83
The generation of NO by <i>Escherichia coli</i>	83
Introduction	83
Detection of NO accumulation in the <i>E. coli</i> cytoplasm	85
Activity of the <i>hcp</i> promoter as a reporter of NO generation	86
The effect of an <i>nsrR</i> mutation on <i>hcp</i> transcription	86
Optimal conditions for transcription activation	89
The effect of NO concentration on the activity of NsrR regulated promoters	89
Enzymes implicated in NO production in the <i>E. coli</i> cytoplasm	93
The effect of nitrite and nitrate reductases on NO accumulation in the <i>E. coli</i> cytoplasm	95
Confirmation of the NsrR-based reporter system: can <i>ytfE::lacZ</i> also report NO accumulation?	95
Can a combination of deletions deplete NO generation in <i>E. coli</i> cultures supplemented with nitrite?	97
The effect of the periplasmic nitrate reductase, NapAB, on NO accumulation in <i>E. coli</i>	100
Does the accumulation of NO damage the transcription factor, Fnr?	103
Is NO generation reliant upon Fnr?	105
Conclusions	105
Discussion	108
CHAPTER 4. RESULTS	110
NO reduction by various strains of <i>E. coli</i>	110
The mechanisms of NO detoxification in <i>E. coli</i>	110
Validation of the assay: use of an NO electrode to quantify the rate of NO reduction by <i>E. coli</i> suspensions	111
The effect of substrate concentration on the rate of NO reduction	113
Response of bacteria in the electrode chamber to multiple pulses of NO	113
The effect of nitrate or nitrite during growth on potential rates of NO reduction	116
The effect of a single NarL or NsrR mutation on the rate of NO reduction	116
Rate of NO reduction by single mutants defective in known NO reductases	120

NO reduction rate of single mutants defective in proteins of unknown function.....	122
The contribution of a repair protein, YtfE, and the hybrid cluster protein, Hcp, to the rate of NO reduction.....	122
Rate of NO reduction of mutants defective in several known NO reductases.....	124
Growth of the strain defective in all known NO reductases.....	130
The effect of the nitrate reductase, NarG, on the rate of NO reduction.....	132
The effect of regulatory proteins on the rate of NO reduction by the quadruple mutant strain defective in all characterised NO reductases.....	134
Response of the <i>nirBDC nrfAB norV hmp fnr</i> strain to low nitrite concentrations...	137
Discussion.....	137
CHAPTER 5. RESULTS.....	143
Repair of nitrosative damage: regulation of <i>PytfE</i> transcription and phenotypes of <i>ytfE</i> mutants.....	143
Introduction.....	143
The role of the di-iron protein, YtfE, in resisting nitrosative stress.....	143
Construction of a new <i>ytfE</i> mutation in strain RK4353.....	144
Anaerobic growth of RK4353 mutants in medium supplemented with nitrate.....	145
Reconstruction and growth of <i>Escherichia coli</i> K-12 ATCC 26176 <i>ytfE</i>	147
Reconstruction of the <i>ytfE</i> mutation in <i>E. coli</i> K-12 ATCC 23716.....	147
Growth of K-12 ATCC 23716 <i>ytfE</i> mutants in the presence of DMSO, fumarate or nitrite.....	147
Comparative genomic hybridisation to locate any secondary mutations.....	150
Regulation of the <i>ytfE</i> promoter.....	159
The effect of growth conditions on the regulation of the <i>ytfE</i> promoter.....	160
The effect of Fnr on the <i>ytfE</i> promoter.....	160
The effect of NarL and NarP on the <i>ytfE</i> promoter.....	162
The effect of Fis on the <i>ytfE</i> promoter.....	164
The effect of NsrR on the <i>ytfE</i> promoter.....	164
The effect of exogenous NO on anaerobic growth of <i>E. coli</i> and on the <i>ytfE</i> promoter.....	167
Effect of exogenous NO on bacteria defective in <i>nrfA</i> in the periplasm.....	170
The role of the flavohaemoglobin, Hmp, in preventing exogenous NO from activating <i>ytfE</i> expression.....	170
Discussion.....	171
CHAPTER 6. RESULTS.....	176
Repair of nitrosative damage: the role of the hybrid cluster protein, flavohaemoglobin and YtfE.....	176

Introduction.....	176
The effect of the hybrid cluster protein, Hcp, and the flavohaemoglobin, Hmp, on growth of the triple mutant.....	176
The effect of an <i>hcp</i> mutation on growth of the quadruple mutant defective in previously characterised NO reductases.....	180
Complementation of the <i>hcp</i> mutation using a plasmid.....	181
The accumulation of nitrite in growth medium supplemented with nitrate.....	184
Nitrite removal in the absence of both nitrite reductases.....	184
A possible role for Hcp in repair of nitrosative damage.....	188
The role of Hcp and YtfE in strains defective in all characterised NO reductases....	190
The rate of NO reduction of a <i>ytfE</i> derivative of the quadruple mutant.....	196
The effect of nitrate and nitrite concentration on growth of the <i>hcp ytfE</i> derivative of the quadruple mutant.....	196
The effect of NarG on growth of the <i>nirBDC nrfAB norV hmp hcp</i> strain.....	199
Discussion.....	203
CHAPTER 7. DISCUSSION.....	208
The role of Fnr as a physiological sensor of NO.....	208
Another NO reductase must remain to be characterised.....	211
Exogenous NO does not derepress transcription of <i>pytFE</i> : is there a barrier to NO equilibration?.....	214
The role of Hcp as a hydroxylamine reductase.....	215
Regulation of <i>pytFE</i> transcription and function of the YtfE protein in different bacterial species.....	216
The role of Hmp during anaerobic growth.....	217
The role of Hcp under anaerobic and aerobic conditions.....	219
Possible roles for the hybrid cluster protein.....	221
A linked phenotype of mutants defective in Hcp and YtfE homologues in <i>Salmonella enterica</i>	227
The role of YtfE and NarG in NO generation.....	228
Final conclusions.....	230
References.....	233

List of figures

Figure 1.1 A schematic representation of electron transfer chains in bacteria	4
Figure 1.2. Schematic representation of the NarXLQP system in <i>E. coli</i>	7
Figure 1.3. A model for asymmetry in the NarXLQP cross-regulation network.....	10
Figure 1.4. The cellular location of nitrate reductase subunits in <i>E. coli</i>	14
Figure 1.5 A schematic representation of the nitrate and nitrite reductases in <i>E. coli</i> K-12	16
Figure 1.6. A schematic diagram of the Tat signal peptide and the Tat translocase.....	20
Figure 1.7. A model of activation of <i>norWV</i> transcription by the σ^{54} -dependent activator NorR.....	27
Figure 1.8 Ribbon diagram of the Hybrid Cluster Protein.....	36
Figure 1.9 Structure of the hybrid iron-sulphur cluster of Hcp.....	37
Figure 1.10 A schematic representation of <i>E. coli</i> proteins that are implicated in the nitrosative stress response	43
Figure 2.1 The <i>lacZ</i> fusion vector, pRW50.....	52
Figure 2.2 The Hcp expression vector, pCA24n2.....	53
Figure 2.3. The Datsenko and Wanner method of chromosomal inactivation, using the method of <i>hmp::kan</i> construction as an example.....	56
Figure 2.4. PCR analysis for the presence of the <i>cat</i> or <i>kan</i> cassette in transductant candidates	60
Figure 2.5. The procedure used to generate strains containing several mutations.....	61
Figure 2.6. The apparatus required to generate nitric oxide saturated water.....	67
Figure 2.7. An example calibration curve using the Hansatech Oxytherm NO electrode	70
Figure 3.1 Schematic representation of the proteins reported to generate NO in <i>E. coli</i>	84
Figure 3.2. The transcriptional fusion <i>phcp::lacZ</i> as a reporter of cytoplasmic NO.....	87
Figure 3.3. The effect of an NsrR mutation on activity of the <i>hcp</i> promoter.....	88
Figure 3.4. Activation of the <i>hcp</i> promoter by nitrite, nitrate and NO	90
Figure 3.5. The effect of slightly increased nitrite and slightly decreased NO concentrations on activation of the <i>hcp</i> promoter	91
Figure 3.6. The effect of NO concentration on the activation of the <i>hcp</i> promoter.....	92
Figure 3.7. The effect of NO concentration on the activation of the <i>ytfE</i> promoter.....	94

Figure 3.8 Nitric oxide generation as reported by <i>hcp</i> promoter activity in bacteria defective in nitrate and nitrite reductases	96
Figure 3.9 Nitric oxide generation as reported by <i>ytfE</i> promoter activity in bacteria defective in nitrate and nitrite reductases	98
Figure 3.10. Nitric oxide generation as reported by <i>hcp</i> promoter activity in bacteria defective in a combination of nitrate and nitrite reductases.....	99
Figure 3.11 NO generation as reported by the <i>hcp</i> promoter in a <i>napA-B</i> mutant	101
Figure 3.12 NO generation as reported by the <i>hcp</i> promoter in <i>narG</i> and <i>napA-B</i> mutants	101
Figure 3.13 Response of the <i>hmp</i> promoter and a synthetic Fnr-repressed promoter to nitric oxide pulses.....	104
Figure 3.14. Activity of the synthetic Fnr repressed promoter in an <i>fnr</i> mutant and the parent	106
Figure 3.15. The effect of Fnr on activity of the <i>ytfE</i> promoter in response to nitrite	107
Figure 4.1 The effect of the concentration of bacteria on the rate of NO reduction.....	112
Figure 4.2 The effect of substrate concentration on initial rate of NO reduction.....	114
Figure 4.3. Electrode trace depicting the addition of several small additions of NOSW	115
Figure 4.4 The effect of nitrate or nitrite during growth on potential rates of NO reduction	117
Figure 4.5 The effect on NO reduction of a mutation in a single transcriptional regulator	119
Figure 4.6 Rate of NO reduction of single mutants defective in known NO reductases.....	121
Figure 4.7 Rate of NO reduction of single mutants of unknown function.....	123
Figure 4.8 Rate of NO reduction of single mutants defective in the enigmatic hybrid cluster protein, Hcp, or the di-iron protein encoded by <i>ytfE</i> that is essential for the repair of iron centres.....	125
Figure 4.9. Growth phenotype of a strain defective in both nitrite reductases and the hybrid cluster protein, Hcp.....	129
Figure 4.10. Growth phenotypes of strains defective in several NO reductases.....	131
Figure 4.11. Growth phenotype a strain defective in all four known NO reductases in minimal medium which was unsupplemented, or supplemented with nitrate or nitrite ..	132
Figure 4.12. Rate of NO reduction in NarG defective bacteria.....	134

Figure 4.13 Rate of NO reduction of strains defective in all known NO reductases with additional mutations.....	136
Figure 4.14 Growth of F2 and G4 on a titration of low nitrite.....	138
Figure 5.1. Anaerobic growth of <i>Escherichia coli</i> strains in the presence of nitrate.....	146
Figure 5.2. Anaerobic growth of <i>Escherichia coli</i> strains using nitrate as a terminal electron acceptor.....	148
Figure 5.3. Anaerobic growth of <i>Escherichia coli</i> strains in the presence of nitrate.....	149
Figure 5.4. Anaerobic growth of <i>Escherichia coli</i> strains in the presence of nitrate, DMSO and nitrite.....	152
Figure 5.5. Comparative genomic hybridisation analysis to compare LMS 4209 and its parent K-12 strain ATCC 23716.....	155
Figure 5.6. The effect of growth conditions and the regulator Fnr on <i>ytfE</i> transcription.....	161
Figure 5.7. The promoter region of <i>ytfE</i>	163
Figure 5.8. Effect of NarL and NarP on transcription of the <i>ytfE</i> promoter.....	165
Figure 5.9. The effect of Fis on transcription of the <i>ytfE</i> promoter.....	166
Figure 5.10. The effect of NsrR and Fnr on transcription of the <i>ytfE</i> promoter.....	168
Figure 5.11. Anaerobic growth and β -galactosidase activity of JCB 387 transformed with pCV01 in response to NO shock.....	169
Figure 5.12 The effect of NrfAB on anaerobic growth of <i>E. coli</i> and transcription of <i>pytfE</i>	172
Figure 5.13. The effect of Hmp on anaerobic growth of <i>E. coli</i> and transcription of <i>pytfE</i>	173
Figure 6.1. Growth of <i>E. coli</i> strains in the presence of a titration of nitrate and nitrite concentrations.....	178
Figure 6.2. Growth phenotype of the <i>hcp</i> derivative of the quadruple mutant strain that is defective in all characterised NO reductases.....	182
Figure 6.3. The aerobic growth phenotype of a strain defective in all characterised NO reductases and the hybrid cluster protein, Hcp.....	183
Figure 6.4. Growth and SDS protein gel of the <i>hcp</i> derivative of the quadruple mutant transformed with a plasmid encoding Hcp.....	185
Figure 6.5. The accumulation of nitrite in cultures supplemented with sodium nitrate.....	186

Figure 6.6. Removal of nitrite by <i>E. coli</i> mutants that are deficient in nitrite reductases and other proteins involved in nitrosative stress defence	187
Figure 6.7. A model for the role of the hybrid cluster protein, Hcp	189
Figure 6.8. Growth phenotype of <i>ygbA</i> , <i>yeaR</i> and <i>yibIH</i> derivatives of the mutant strain, JCB 5253, which is defective in all characterised NO reductases and the hybrid cluster protein, Hcp	191
Figure 6.9. Growth phenotype strain of strain JCB 5260, which is deficient in all characterised NO reductases as well as the hybrid cluster protein, Hcp and YtfE	192
Figure 6.10. The effect of nitrate and nitrite on growth of Hcp ⁻ and YtfE ⁻ derivatives of the quadruple mutant defective in all characterised NO reductases	193
Figure 6.11. Rate of NO reduction of strains defective in all known NO reductases and the repair protein, YtfE	197
Figure 6.12. The effect of nitrate and nitrite concentration on the growth of a strain defective in both Hcp and YtfE	198
Figure 6.13. The effect of the nitrate reductases, NarGHJI and NarZ, on growth of the <i>hcp</i> derivative of the quadruple mutant strain	200
Figure 6.14. The effect of NarGHJI and NarZ on growth of strains defective in proteins that protect <i>E. coli</i> against nitrosative stress	201
Figure 6.15. Growth phenotype a strain defective in Hcp, YtfE, NarG-I and NarZ over a range of nitrite concentrations	202
Figure 7.1 Apparatus used to collect gas bubbles	213
Figure 7.2. The reaction of DAF-FM with NO to generate a fluorescent product	220
Figure 7.3 The effect of iron on growth of <i>hcp</i> mutants	223
Figure 7.4 Growth of the quadruple mutant and the <i>hcp</i> derivative in the presence of glucose, a fermentable carbon source	226
Figure 7.5. Models for the involvement of YtfE and Hcp in linked repair pathways in <i>E. coli</i>	229
Figure 7.6. Proteins in <i>E. coli</i> that are implicated in nitrate and nitrite metabolism, and protection against the consequences of the use of these terminal electron acceptors	232

List of Tables

Table 1.1. Table of oxido-reductases from the respiratory chain of <i>E. coli</i>	3
Table 1.2. The effect of using a non-physiological pH on K_m and V_{max} of Hcp for hydroxylamine.....	33
Table 1.3. Microarray studies that have indentified sources of nitrosative stress that induce the expression of the genes encoding proteins of unknown function.....	40
Table 2.1. Concentrations, solvents and storage conditions for antibiotics used in this work.....	45
Table 2.2. Buffers and solutions used in this work.....	46
Table 2.3. <i>E. coli</i> K-12 strains used in this study.....	48
Table 2.4. Plasmids used in this work.....	51
Table 2.5. Strains with multiple mutations made by bacteriophage P1 transduction for this work.....	62
Table 2.6. Oligonucleotide primers used in this study.....	74
Table 2.7. PCR protocols used in this work.....	77
Table 4.1. The rate of NO reduction, following growth in the presence of nitrate, by strains defective in several NO reductases.....	127
Table 4.2 The rate of NO reduction, following growth in the presence of nitrite, by strains defective in several NO reductases.....	128
Table 4.3. Reported kinetic parameters for NO reductase activity by <i>E. coli</i> proteins.....	141
Table 5.1. Doubling times of <i>ytfE</i> strains grown on minimal medium supplemented with a range of terminal electron acceptors.....	151
Table 5.2. Genes deleted in LMS 4209, as revealed by comparative genomic hybridisation.....	156
Table 6.1 Strains defective in genes implicated in the nitrosative stress response discussed in this chapter.....	177
Table 7.1. Fnr-activated genes that are downregulated by NO addition anaerobically, and the other regulators that control these operons.....	209
Table 7.2. Rates of NO reduction of <i>hcp</i> mutants grown on minimal medium supplemented with nitrate.....	222

List of abbreviations

AAA+	<u>A</u> TPase <u>a</u> ssociated with various cellular <u>a</u> ctivities
ABC	ATP binding cassette
Amp	Ampicillin
APS	Ammonium persulphate
ATP	Adenosine triphosphate
Carb	Carbenicillin
Cat	Chloramphenicol acetyl transferase
Chlor	Chloramphenicol
CIAP	Calf intestinal alkaline phosphatase
CoA	Coenzyme A
C-terminal	Carboxyl terminal
DAF	2',7'-diaminofluorescein
DAN	2,3-diaminonaphthalene
DH	Dehydrogenase
DMSO	Dimethylsulfoxide
DNA	Deoxyribonucleic acid
DNIC	Di-nitrosyl iron complex
dNTP	Deoxynucleoside triphosphate
<i>E. coli</i>	<i>Escherichia coli</i>
EDTA	Ethylene diamine tetra acetic acid
EMSA	Electromobility shift assay
EPR	Electro paramagnetic resonance
Fis	Factor for inversion stimulation
Fnr	Regulator of fumarate and nitrite reduction
FRT	Flp recombinase target
GAF	c <u>G</u> MP phosphodiesterase <u>a</u> denylate cyclase <u>F</u> hlA
GSNO	S-nitrosoglutathione
HAMP	Histidine kinase, <u>a</u> denyl cyclase, <u>m</u> ethyl accepting chemotaxis protein and <u>p</u> hosphatase
Hcp	Hybrid cluster protein
HPLC	High pressure liquid chromatography

IHF	Integration host factor
IPTG	Isopropyl- β -D-1-thiogalactopyranoside
Kan	Kanamycin
LB	Lennox broth
LB-Ca ²⁺	Lennox broth supplemented with 2 mM CaCl ₂
MS	Minimal salts
NA	Nutrient agar
NADP(H)	Nicotinamide adenine dinucleotide phosphate (reduced form)
NAD ⁺	Nicotinamide adenine dinucleotide
ND	Not determined
NO	Nitric oxide
(i)NOS	(inducible) Nitric oxide synthase
NOSW	Nitric oxide saturated water
N-terminal	Amino terminal
OD	Optical density
ONPG	Orthonitrophenyl- β -D-galactopyranoside
PCR	Polymerase chain reaction
RIC	Repair of iron centres
RNA	Ribonucleic acid
RNAP	RNA polymerase
RNS	Reactive nitrogen species
ROS	Reactive oxygen species
SDS	Sodium dodecyl sulphate
PAGE	Polyacrylamide gel electrophoresis
Tat	Twin-arginine translocase
TBE	Tris-borate-ethylene diamine tetra acetic acid
TCA	Tricarboxylic acid
TEMED	<i>N,N,N',N'</i> -Tetramethylethylenediamine
Tet	Tetracycline
TMA(O)	Trimethylamine (<i>N</i> -oxide)
UV	Ultra violet

CHAPTER 1 - INTRODUCTION

Adaptation of *Escherichia coli* to anaerobic growth

Escherichia coli is an enteric, food borne organism that colonises the mammalian gut, and also inhabits a variety of other environments. The conditions that are encountered by *E. coli*, and many other pathogenic bacteria, are not stable and in order to thrive bacteria must be able to respond quickly to transient changes in their environment. To do this, *E. coli* senses and responds to environmental oxygen, in an attempt to use the most energy-efficient metabolic processes to promote cell growth (Uden *et al.*, 1995). *E. coli* is a facultative anaerobe, and thus is able to reduce alternative terminal electron acceptors when oxygen is not available, for example, in the low oxygen environment inside the host. The alternative electron acceptors used to generate an electrochemical gradient across the cytoplasmic membrane include nitrate, nitrite, fumarate, trimethylamine-*N*-oxide (TMAO) and dimethyl sulphoxide (DMSO) (Uden and Bongaerts, 1997). *E. coli* is also able to ferment a variety of carbon sources to evolve H₂ gas, effectively using H⁺ as an electron acceptor.

Reoxidation of NADH is a critical factor during anaerobic growth because NAD⁺ is needed to maintain carbon flux through glycolysis. Pyruvate is metabolised differently when oxygen is present, and when it is unavailable. Aerobically, pyruvate is converted to acetyl CoA and CO₂, which generates NADH. Anaerobically, pyruvate is converted by pyruvate formate lyase to acetyl CoA and formate. Formate is a strong reducing agent, and provides an excellent electron donor for nitrate reduction (Cole, 1996).

This section will introduce the ways in which *E. coli* is able to adapt under anaerobic conditions to use alternative electron acceptors as well as the electron transfer components that are used for anaerobic respiration. The main transcription factors that are involved in this anaerobic switch: Fnr; NarL; and NarP will be described. Complex enzyme systems are required to reduce nitrate and nitrite. In order for such enzymes to

function in the periplasm, complex transport systems such as the twin-arginine translocation system are required and will be described in this section. DNA and protein damage that is a consequence of nitrate and nitrite reduction will be introduced, and proteins that have been previously characterised in the nitrosative stress response will be detailed. Finally, some genes of unknown function that might also be involved in the nitrosative response will be introduced, and the aims of this work will be described.

Electron transfer components during anaerobic growth

The preferred terminal electron acceptor in *E. coli* is oxygen. When available, oxygen represses the expression of alternative terminal reductases. Nitrate is the preferred alternative terminal electron acceptor. Use of oxygen as a terminal electron acceptor gives the highest release of free energy and fumarate gives the lowest (Unden and Bongaerts, 1997, Table 1.1). In some bacteria, the most electro-negative acceptor with the lowest ATP yield is preferred, which reflects adaptation to the environment, or induction of the maximal growth rate. Regulation of metabolism is governed by terminal reductase and dehydrogenase expression (Figure 1.1). Uncoupled dehydrogenases are expressed aerobically, whereas coupling dehydrogenases are expressed anaerobically. Despite the huge variability in the components described in Table 1.1, both environmental conditions and energetic constraints restrict the interactions that may occur between these components. The operons that encode the components of the *E. coli* electron transfer chains map all over the chromosome, and often include specific proteins required for cofactor production, insertion or maturation (Unden and Bongaerts, 1997).

Quinones used for electron transfer.

Some of the electron transfer enzymes are membrane associated to facilitate electron donation to quinones. Quinones function as carriers of reducing equivalents between dehydrogenases and terminal reductases or oxidases. During aerobic respiration, ubiquinone is mainly used. However, NarG receives electrons from either ubiquinone or

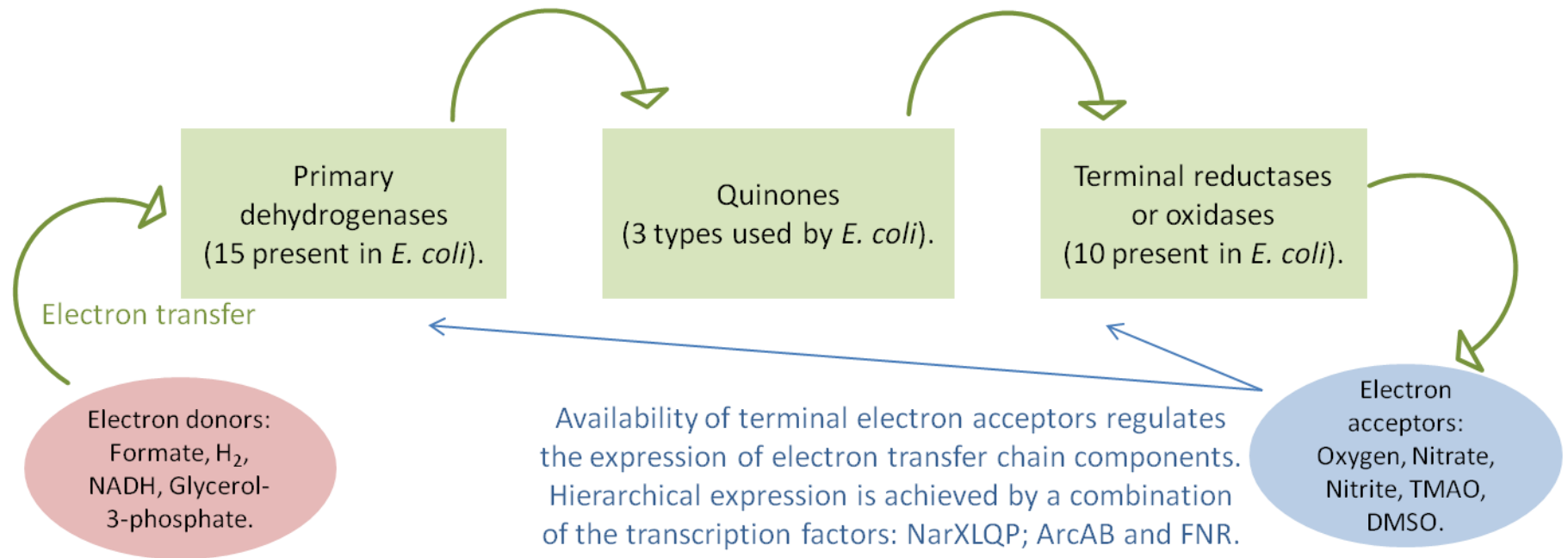
Table 1.1. Table of oxido-reductases from the respiratory chain of *E. coli*.

Enzyme	Gene	Pair	Redox couple	E'_m (V)
<u>Primary dehydrogenase (DH)</u>				
Formate dehydrogenases:				
Formate DH _N [‡]	<i>fdnGHI</i>			
Formate DH _O [‡]	<i>fdoGHI</i>	HCO ₃ ⁻ /HCO ₂ ⁻		-0.43
Formate DH _F	<i>fdhF</i>			
Hydrogenases:				
Hydrogenase 1 [‡]	<i>hyaA-F</i>			
Hydrogenase 2 [‡]	<i>hybA-G</i>	H ⁺ /H ₂		-0.42
Hydrogenase 3	<i>hycA-H</i>			
Other dehydrogenases:				
NADH DH I	<i>nuoA-N</i>	NAD ⁺ /NADH		-0.32
NADH DH II	<i>ndh</i>	NAD ⁺ /NADH		-0.32
Glycerol-3-phosphate DH _O	<i>glpD</i>	DHAP/Glycerol-3-P		-0.19
Glycerol-3-phosphate DH _N	<i>glpACB</i>	DHAP/Glycerol-3-P		-0.19
D-Lactate DH	<i>dld</i>	Pyruvate/D-Lactate		-0.19
L-Lactate DH	<i>lctD</i>	Pyruvate/L-Lactate		-0.19
D-Amino acid DH	<i>dadA</i>	2-Oxoacid + NH ₄ ⁺ /Amino acid		NR
Glucose DH	<i>gcd</i>	Glucose/Gluconate		-0.14
Succinate DH	<i>sdhCDAB</i>	Fumarate/Succinate		+0.03
<u>Terminal reductases</u>				
Quinol oxidases:				
Quinol oxidase <i>bo</i> ₃	<i>cyoABCDE</i>			
Quinol oxidase <i>bd</i>	<i>cydAB</i>	O ₂ /H ₂ O		+0.82
Quinol oxidase III	<i>appBC (cyxAB)</i>			
Nitrate reductases:				
Nitrate reductase A	<i>narGHJI</i>			
Nitrate reductase Z	<i>narZYWV</i>	NO ₃ ⁻ /NO ₂ ⁻		+0.42
Periplasmic nitrate reductase [‡]	<i>napFDAGHBC</i>			
Other reductases:				
Nitrite reductase [‡]	<i>nrfA-G</i>	NO ₂ ⁻ /NH ₄ ⁺		+0.36
DMSO reductase	<i>dmsABC</i>	DMSO/DMS		+0.16
TMAO reductase [‡]	<i>torCAD</i>	TMAO/TMA		+0.13
Fumarate reductase	<i>frdABCD</i>	Fumarate/Succinate		+0.03

The midpoint potentials (E'_m) of electron donors and acceptor in *E. coli* are listed.

[‡] signifies that the enzyme is periplasmic. NR means not reported here. Table adapted from Uden and Bongaerts, 1997.

Figure 1.1



A schematic representation of electron transfer chains in bacteria.

A multitude of dehydrogenases, quinones and terminal reductases gives variability in respiratory chains in bacteria. No cytochrome *bc*₁ complex is present in *E. coli*, so branching occurs at the level of quinone.

menaquinone (Brondijk *et al.*, 2004). TMAO, DMSO and fumarate reductases receive electrons from menaquinone or demethylmenaquinone. This variation is because ubiquinone is too electropositive to donate to these anaerobic terminal electron acceptors (Unden and Bongaerts, 1997.)

Generation of a proton motive force.

E. coli expresses conformational proton pumps that achieve charge separation by the arrangement of substrate sites on opposite sides of the membrane. Proton potential can be generated by either conventional proton pumps such as NuoA-N or CyoA-D or by redox loops, which are found in enzymes that carry the active site for substrate and quinone on opposite sides of the membrane (Table 1.1). *E. coli* expresses several dehydrogenase isoenzymes. This dehydrogenase switching is a mechanism to facilitate the most thermodynamically favourable electron donor being used first. Aerobically, dehydrogenases that are unable to conserve free energy are used, whereas during fumarate or DMSO reduction, energy-conserving dehydrogenases predominate. This is because the dehydrogenase is the only point at which proton translocation is coupled to electron transfer (Unden and Bongaerts, 1997.)

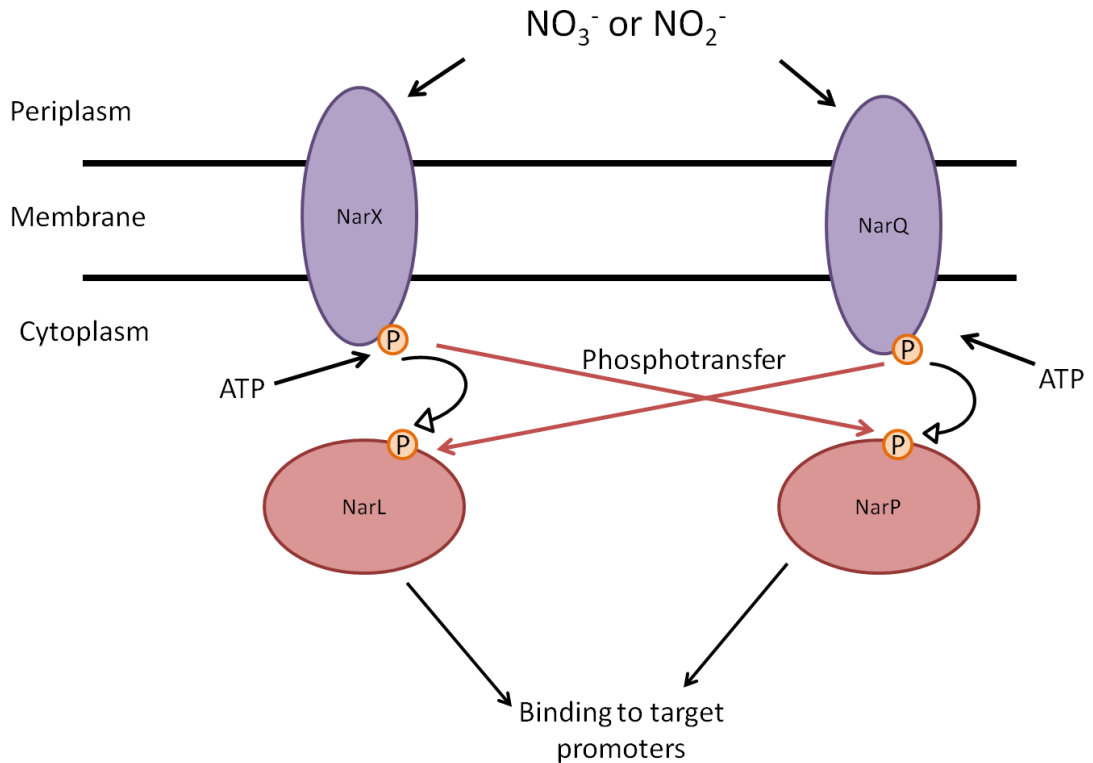
Regulation of the adaptation to anaerobic growth.

Transcription factors that are responsive to oxygen, nitrate and nitrite ensure that the bacterium uses the thermodynamically most favourable electron acceptor available, in a hierarchical manner. The regulator of fumarate and nitrite reduction (Fnr) is key in switching between aerobic and anaerobic growth. It contains a [4Fe-4S] cluster under anaerobic conditions, which promotes protein dimerisation and enhances specific DNA binding at sites that closely match the consensus sequence TTGAT-N₄-ATCAA (Jayaraman *et al.*, 1988). Once bound to the DNA, transcription is activated by RNA polymerase recruitment, or repressed by the inhibition of productive promoter-RNA polymerase interactions. In the presence of oxygen, the [4Fe-4S] cluster first disassembles to a [3Fe-4S]¹⁺ intermediate and then rearranges to form a [2Fe-2S] cluster (Khoroshilova *et al.*, 1997, Crack *et al.*, 2008a). Fnr containing a [2Fe-2S] cluster dissociates into transcriptionally inactive monomers (Lazazzera *et al.*, 1996, Sutton *et al.*, 2004a, Sutton *et al.*, 2004b).

Fnr functions in parallel with the two component system ArcAB to coordinate the response to the availability of oxygen. In two component regulatory systems, the stimulus controls sensor autophosphorylation, then phosphoryl transfer between the transmitter domain of a sensor and receiver domain of a response regulator can occur. Sensor autophosphorylation is slow relative to the rate of phosphoryl transfer to the response regulator (Noriega *et al.*, 2010). When oxygen is limiting or absent, the membrane-bound sensor kinase ArcB autophosphorylates a histidine residue, then transphosphorylates an aspartate residue in the response regulator ArcA (Kwon *et al.*, 2000). Phospho-ArcA is able to bind specifically to DNA, and activates and represses operons involved in respiratory metabolism. For example, phospho-ArcA represses the aerobic terminal oxidase, cytochrome *bo*, but activates cytochrome *bd*, which has a higher affinity for oxygen (Cotter *et al.*, 1990, Cotter *et al.*, 1997). Several ArcA responsive genes are also controlled by Fnr.

The response to nitrate and nitrite is regulated by the dual interacting two-component regulatory systems NarXL and NarQP (Rabin and Stewart, 1993). In the NarXLQP system, NarX and NarQ proteins are membrane-spanning sensor histidine kinases, which autophosphorylate a conserved histidyl residue in the presence of nitrate and nitrite. The phosphate group is then transferred by phosphorelay to a conserved aspartyl residue in the receiver domain of the response regulators NarL and NarP (Stewart, 2003, Figure 1.2). When phosphorylated, NarL and NarP have a higher affinity for their specific binding sites; upon binding they activate and repress the expression of various operons important for nitrite and nitrate respiration (Stewart, 1993, Stewart and Bledsoe, 2003, Constantinidou *et al.*, 2006). The consensus sequence for binding is the heptamer TACYNKT, where Y represents C or T and K can be A or C, (Tyson *et al.*, 1994, Darwin *et al.*, 1997). NarP binding requires an inverted repeat of this heptamer sequence separated by 2 nucleotides (a '7-2-7' arrangement), while NarL is able to bind to a single heptamer, direct repeats and inverted repeats of the sequence (Darwin *et al.*, 1997).

Figure 1.2.



Schematic representation of the NarXLQP system in *E. coli*

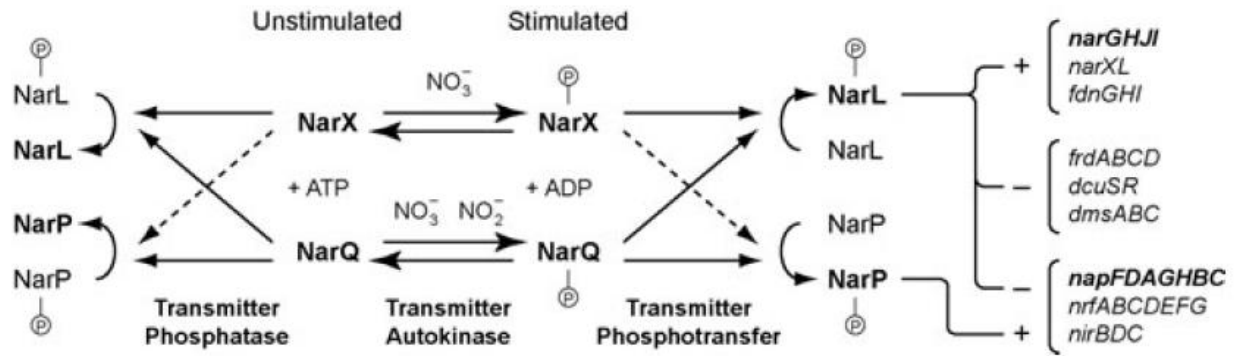
The sensor kinases, NarX and NarQ (purple), sense the presence of nitrate or nitrite in the environment. The binding of nitrate or nitrite causes a conformational change in the sensor, which brings the kinase active site close to a conserved histidine residue, which is phosphorylated using cytoplasmic ATP as a substrate. The cytoplasmic phosphate group is then transferred to the response regulators, NarL and NarP (red). The cognate phosphotransfer between NarX and NarL, and NarQ and NarP, is represented by a black arrow. However, each sensor kinase is also able to phosphorylate the alternative response regulator, as represented by red arrows. This system is complex, and has been significantly simplified in this Figure. Cross-talk, and the phosphatase roles of the sensor kinases are discussed in Figure 1.3.

The sensors NarX and NarQ have a modular structure, composed of an N-terminal sensory domain, a central section containing a HAMP (histidine kinase, adenyl cyclase, methyl accepting chemotaxis protein and phosphatase) domain and a C-terminal transmitter module (Appleman *et al.*, 2003, Stewart *et al.*, 2003). The HAMP domain is thought to transmit a signal to the output domain to convey that ligand is bound to the sensor (Appleman *et al.*, 2003). Although superficially similar in some ways, there are several important differences between the functions of the dual sensor kinases NarX and NarQ. NarX responds preferentially to nitrate, whereas NarQ responds to both nitrate and nitrite (Rabin and Stewart, 1993, Wang *et al.*, 1999, Noriega *et al.*, 2010). Finally, NarQ, but not NarX, controls gene expression in response to culture aeration as well as the presence of nitrate and nitrite (Stewart *et al.*, 2003).

The presence of an unphosphorylated sensor domain can stimulate the removal of a phosphoryl group from the response regulator. Therefore, phospho-response regulators levels are determined through the relative rates of transmitter autokinase and transmitter phosphatase activity (Noriega *et al.*, 2010). In the presence of nitrite, NarX functions mainly as a NarL-phosphate phosphatase, as opposed to a NarL kinase (Rabin and Stewart, 1993, Stewart and Bledsoe, 2003). Although NarX still has some NarL kinase activity in the presence of nitrite, much of the NarL-phosphate formed by NarQ in response to nitrite will be dephosphorylated by NarX (Rabin and Stewart, 1993, Stewart and Bledsoe, 2003).

A recent study has further highlighted the asymmetry in this cross-regulation network. NarQ interacts similarly with both NarL and NarP, whereas NarX interacts preferentially with NarL (Figure 1.3, Noriega *et al.*, 2010). In addition to the functional differences that have been determined *in vitro*, the regulation of *narXL* and *narQP*

Figure 1.3.



A model for asymmetry in the NarXLQP cross-regulation network.

Dashed arrows represent relatively slow reactions. The NarX and NarQ sensor populations are hypothesized to be in a two-state equilibrium determined by the presence of the nitrate or nitrite stimulus and ligand binding. Phospho-sensors catalyse response regulator phosphorylation, whereas dephospho-sensors catalyse regulator dephosphorylation. Phospho-regulators that activate (+) or repress (-) transcription of representative target operons are shown. Taken from Noriega *et al.*, 2010.

expression differs *in vivo* (Darwin and Stewart, 1995). The *narXL* operon is positively autoregulated, while expression of *narQP* is unregulated (Darwin and Stewart, 1995). As a result of this variation in regulation, the concentration of each protein might vary in the cell; this would lead to a difference in the relative reaction rates (Noriega *et al.*, 2010). Cross-talk between the 30 different two component regulatory systems in *E. coli* can occur, but only a weak effect is observed in the absence of mutations. In wild type bacteria, this cross-talk has a negligible effect on signal transduction, due to the fact that cognate sensor-regulator pairs exhibit strong kinetic preference over non-cognate reactions, governed by specificity determinants within both the transmitter and receiver domains (Skerker *et al.*, 2008). In addition to this, phosphatase activity at the transmitter counteracts receiver phosphorylation that arises from cross-talk. However, some cross-regulation is useful to coordinate responses from environmental cues (Noriega *et al.*, 2010). NarXLQP are thought to interact in order to fine-tune respiratory enzyme synthesis in response to variable nitrate or nitrite concentrations. NarX is specialised to respond to nitrate whereas NarQ responds to nitrate and nitrite. Only NarX is sufficient to control NarP-dependent expression. However, either sensor, NarX or NarQ, is sufficient to control NarL dependent operons (Egan and Stewart, 1990, Chiang *et al.*, 1992, Rabin and Stewart, 1992).

The factor for inversion stimulation, Fis.

Unlike eukaryotic histones, bacterial nucleoid associated proteins form unstable complexes with DNA. The associations profoundly affect both local and global chromosome organisation. All nucleoid associated proteins bind DNA non-specifically with physiologically relevant affinities, but also preferentially bind to various sequences. Fis binds to a 15 bp degenerate sequence GNtTAaWWWtTRaNC, where N

can be any nucleotide and W is A or T. Despite this consensus, Fis can contact up to 27 bp depending upon the flexibility of the flanking sequences. The most common action of Fis is to bind at the recognition site for RNAP, thereby occluding the promoter by steric hindrance. However, Fis-regulated promoters often have several binding sites both upstream and downstream of the transcription start point (McLoed and Johnson, 2001).

Nitrate reductases in *E. coli*.

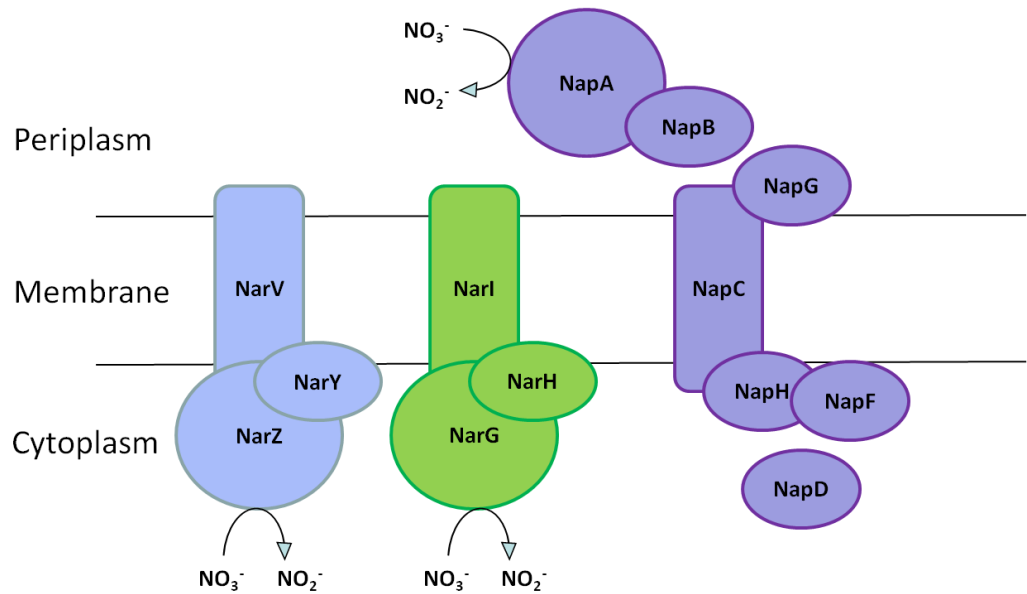
Two sets of nitrate reductase genes, *narGHJI* and *narZYWV*, which encode two membrane bound protein complexes, are present in the cytoplasm of *E. coli* (Forget, 1974, Enoch and Lester, 1975, Chaudhry and Macgregor, 1983, Blasco *et al.*, 1990, Iobbi-Nivol *et al.*, 1990). The *narGHJI* operon is activated by NarL in the presence of nitrate, whereas the *narZYWV* operon is poorly expressed under most conditions. A third nitrate reductase, encoded by *nap*, is located in the periplasm of *E. coli* (Grove *et al.*, 1996, Brondijk *et al.*, 2004). When nitrate is abundant, the NADH-dependent nitrite reductase, NirB, in the cytoplasm works with the respiratory nitrate reductase NarG on the cytoplasmic side of the membrane. Under alternative conditions, when nitrate is scarce but nitrite is abundant, Nrf is active and functions with Nap in the periplasm. NarZ is now known to be important during stationary phase (Spector *et al.*, 1999, Iobbi-Nivol *et al.*, 1990, Iobbi *et al.*, 1987.) Although these anaerobically expressed genes are subject to transcriptional control, they are never totally repressed, so the bacteria can be ready for a change in environment, for example if oxygen becomes less available, or if nitrate becomes available. The complexity in these nitrate reduction systems is not a sign of redundancy, rather it is essential for surviving environmental transitions. Each of

the enzymes is regulated in a slightly different way, facilitating adaptation to a changing environment or an appropriate stress response (Cole, 1996).

Bacteria use the same ATP synthase during aerobic and anaerobic respiratory growth: the difference is that bacteria have evolved the ability to replace oxygen with other terminal electron acceptors to release energy. The most widely used alternative to oxygen is nitrate, and nitrate reduction to nitrite can proceed using a short electron transfer chain, in which electrons flow from the quinone pool via the *b*-type cytochrome NarI and the iron-sulphur protein NarH to the molybdoprotein NarG, which is the active reductase (Richardson and Sawers, 2002). NarJ is essential for complex formation (Palmer *et al.*, 1996). The nitrate reductase complexes are membrane associated, where they reduce nitrate to nitrite, and the energy released is used to drive ATP synthesis or nutrient uptake (Figure 1.4). Transcriptional control is essential to ensure that toxic intermediates are not generated when not necessary, as well as to ensure that terminal electron acceptors are utilised in a hierarchical manner. To deal with nitrite toxicity, *E. coli* either ejects nitrite, transported by NirC or NarK, or reduces nitrite in the cytoplasm catalysed by NirBD (Clegg *et al.*, 2002, Jia *et al.*, 2009).

Genes essential for a third, periplasmic nitrate reductase (the *nap* operon) and cytochrome *c* synthesis and maturation (*ccm* operon) were found downstream of the '*aeg46.5*' operon of anaerobically expressed genes at minute 47 on the *E. coli* chromosome (Grove *et al.*, 1996). In contrast to the NarG system for nitrate reduction, the Nap proteins are expressed under nitrate limiting conditions. Nap operons in many bacteria often contain the *napDABC* genes, but *E. coli* also contains the non-essential *napFGH* genes. NapH is an integral membrane protein with 4 transmembrane helices, however both the N- and C- termini and two non-haem iron-sulphur centres are

Figure 1.4.



The cellular location of nitrate reductase subunits in *E. coli*.

In this schematic diagram, the membrane associated NarZYV complex is shaded blue, and the membrane associated NarGHI complex is shaded green. For simplicity, the chaperone components of these complexes have been omitted. The periplasmic Nap complex is shaded purple.

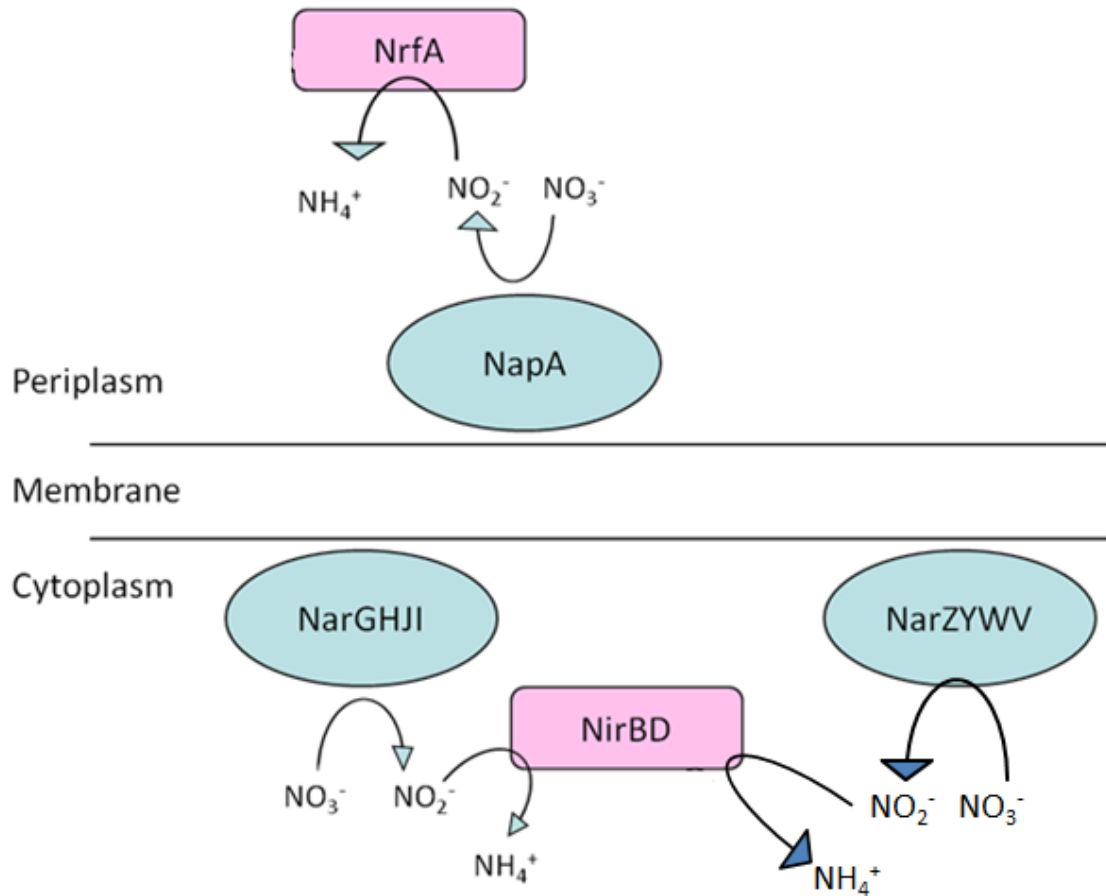
cytoplasmic (Brondijk *et al.*, 2004). NapG is secreted into the periplasm by the twin-arginine translocase (Tat) pathway (Weiner *et al.*, 1998, Berks *et al.*, 2000, Sargent, 2007). The Tat pathway will be discussed in a subsequent section. The physiological role of NapGH is to facilitate electron transfer from reduced ubiquinone, but not reduced menaquinone, to NapC. NapC is located in the cytoplasmic membrane, where it functions as a quinol dehydrogenase, as well as interacting with NapH either in the cytoplasm or at the cytoplasmic face of the membrane. Nitrate is reduced at NapA and the role of NapB is to donate electrons to NapA. NapD is located in cytoplasm and functions in NapA maturation (Brondijk *et al.*, 2004, Figure 1.4.)

Nitrite reductases in *E. coli*

E. coli has two distinct nitrite reductases that reduce nitrite to ammonia. They are encoded by the *nrfA* and *nirB* operons (Figure 1.5, Darwin *et al.*, 1993a, Darwin *et al.*, 1993b, Hussain *et al.*, 1994, Jackson *et al.*, 1981a, Jackson *et al.*, 1981b, Tyson *et al.*, 1997b). The periplasmic cytochrome *c* nitrite reductase NrfA uses formate as an electron donor and nitrite as a terminal electron acceptor. Nrf activity is strongly repressed by nitrate, because of the fact that nitrate is a more powerful oxidising agent and when available, it is the preferred source of energy.

Regulation of the *nrf* operon is very complex (Wang and Gunsalus, 2000, Browning *et al.*, 2005, Browning *et al.*, 2010). Regulation at this promoter is governed by three major factors, anaerobiosis, the availability of nitrate and nitrite and catabolite repression (Tyson *et al.*, 1997a). Under anaerobic conditions, expression of the *nrf* operon is dependent on activation by Fnr by binding at a position centred between 41 and 42 bases upstream of the transcription start site (+1). Activation is enhanced by NarL or NarP binding to an inverted repeat of a heptamer consensus sequence separated

Figure 1.5



A schematic representation of the nitrate and nitrite reductases in *E. coli* K-12.

E. coli contains three protein complexes that are able to reduce nitrate to nitrite (blue ovals), which are regulated differently. The *narGHJI* operon and the *narZYWV* operon encode cytoplasmic reductases, whereas the third nitrate reductase, encoded by *nap*, is located in the periplasm. *E. coli* has two distinct nitrite reductases that reduce nitrite to ammonia, encoded by the *nrfAB* and *nirBDC* operons (pink rectangles). The periplasmic cytochrome *c* nitrite reductase NrfA uses nitrite as a terminal electron acceptor to generate a proton gradient and NirB is a cytoplasmic enzyme that functions primarily to detoxify nitrite and does not generate a proton gradient (Wang and Gunsalus, 2000).

by 2 nucleotides, a characteristic '7-2-7' site, positioned at -74.5. Expression of *nrf* is repressed by two nucleoid associated proteins, IHF and Fis. The activity of Fis is regulated principally by its level in the cell, and the cellular concentration of Fis increases sharply during aerobic or anaerobic growth in rich medium. Higher concentrations of Fis lead to an increase in *nrf* repression (Browning *et al.*, 2005). NarL enhances activation by counteracting IHF binding at -54, a position which overlaps both the Fnr binding site and the 7-2-7 NarL and NarP binding site. However, NarL is unable to alter repression by Fis, which binds at -15, therefore overlapping the -10 element of the promoter. Fis repression can override activation by Fnr, NarL or NarP. The transcriptional repressor, NsrR, also recognises a target in the *nrf* promoter region, at a position centred at -63. NsrR responds to the presence of nitric oxide, and is thought to modulate expression, rather than totally repress expression of Nrf, so that it is available to reduce nitric oxide when required (Browning *et al.*, 2010). The high energy yield when nitrate is abundant leads to repression of Nrf, whereas a low concentration of nitrate leads to Nrf activation.

NirB is a cytoplasmic enzyme that functions primarily to detoxify nitrite and does not generate a proton gradient (Wang and Gunsalus, 2000). The structural genes for the cytoplasmic, NADH dependent nitrite reductase are *nirBD*, and *nirC* in the same operon is a nitrite transport protein (Jia *et al.*, 2009, Clegg *et al.*, 2002). Sirohaem is an essential cofactor for NirB, and synthesis of this prosthetic group by methylation and oxidation of uroporphyrinogen III is encoded in the same operon by *cysG*. Nitrite accumulates inside bacteria only when they are reducing nitrate, and even this accumulation should be minimised by NarK efflux (Cole, 1996.) The *nir* operon is regulated co-ordinately with nitrate reductase (NarGHJI) synthesis to ensure that any nitrite that does accumulate is detoxified. Expression of the *nir* operon is induced by

anaerobiosis and by the presence of nitrate or nitrite ions. Fnr activates expression by binding at a site centred at -41.5 with respect to the transcription start site (Browning *et al.*, 2005). NarL and NarP are able to bind to a '7-2-7' site positioned at -69.5; NirB expression is strongly activated by phosphorylated NarP (Jayaraman *et al.*, 1989, Tyson *et al.*, 1993). Fnr-dependent activation is repressed by IHF binding at -88 as well as by Fis binding at -142. Either NarL or NarP are able to displace IHF, and override repression. Expression from the *nir* operon is repressed in a nutrient-poor medium, an effect that is mediated by Cra binding at -16.5. In contrast to the effects seen at the *nrf* promoter, Cra repression can not be overridden by other activators (Tyson *et al.*, 1997a).

TMAO and DMSO reductases.

E. coli contains a periplasmic, molybdenum-containing TMAO reductase, encoded by *torA*, which is highly specific for *N*-oxides (Méjean *et al.*, 1994). TorC is a penta-haem *c* type cytochrome that is anchored to the membrane by one N-terminal transmembrane helix. The majority of TorC is a globular protein on the periplasmic face of the membrane and connects TorA to the quinone pool (McCrindle *et al.*, 2005). Despite responding to anaerobiosis, the *torCAD* operon is unusual in that it is not regulated by Fnr or ArcA. A sensor histidine kinase TorS, and the response regulator TorR activate the *torCAD* operon when the oxygen tension is low and *N*- or *S*-oxides are present (McCrindle *et al.*, 2005). TMAO is the effector molecule for TorR. Expression of the *tor* operon is almost totally dependent on TMAO (Simon *et al.*, 1994). TorD interacts with TorA prior to molybdenum insertion, and maintains the TorA apoprotein in a conformation that is suitable for cofactor binding (Ilbert *et al.*, 2004, Genest *et al.*, 2006). A further TMAO reductase is encoded by the *torYZ* genes, and has a constitutively low level of expression (Gon *et al.*, 2000). This alternative TMAO

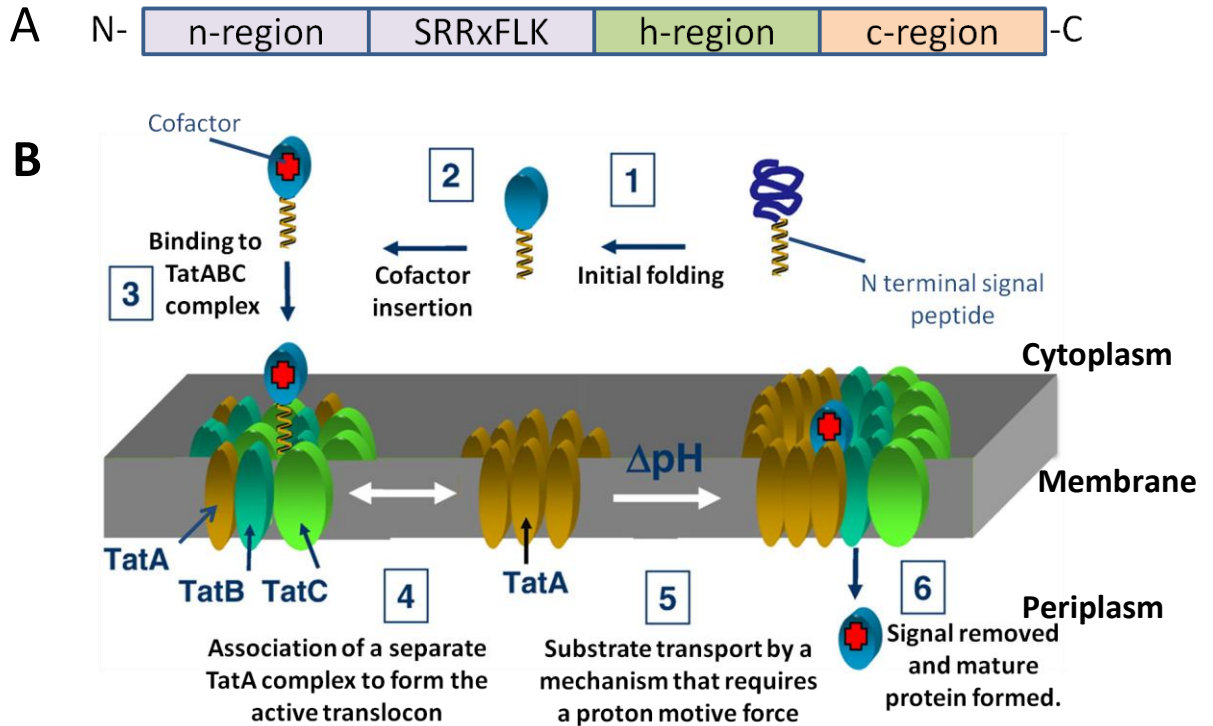
reductase is not induced by substrates nor in stationary phase, in contrast to the alternative nitrate reductase NarZ.

The *dmsABC* operon encodes a DMSO reductase, which is also able to reduce TMAO (McC Crindle *et al.*, 2005). The DmsC subunit contains 8 transmembrane helices, and anchors the heterotrimeric enzyme complex to the membrane. The polyferredoxin DmsB subunit contains 4 [4Fe4S] clusters and is involved in electron transport to the catalytic subunit, DmsA (McC Crindle *et al.*, 2005). DmsA contains a molybdenum cofactor and has been shown to face the periplasm (Stanley *et al.*, 2002). This DMSO reductase, unlike the TMAO reductase in *E. coli*, is able to reduce a variety of *S*- and *N*-oxides (McC Crindle *et al.*, 2005). An additional protein, DmsD, functions in a chaperone role, and interacts with the Tat leader sequence of apoDmsA (Ray *et al.*, 2003). The *dmsABC* operon is activated by both Fnr and ModE (McC Crindle *et al.*, 2005). In the presence of nitrate, NarL represses expression of *dmsABC* (Cotter and Gunsalus, 1989).

The twin-arginine transport system

Bacterial respiration, as described in the previous sections, requires an array of complex, multi-subunit, cofactor-containing respiratory enzymes. They are situated in the periplasm, or embedded within or on one face of the cytoplasmic membrane. The plasma membrane in *E. coli* is tightly sealed so to deliver proteins with their cofactors to the periplasm or to insert into the membrane, a specialised system is required. To transport these complexes, proteins are often synthesised with a distinctive N-terminal signal sequence that bears the ‘twin-arginine’ amino acid motif SRRxFLK (Berks, 1996, Figure 1.6). Alternatively, proteins are complexed with ‘partner proteins’ that bear

Figure 1.6.



A schematic diagram of the Tat signal peptide and the Tat translocase.

Panel A: The structure of the Tat signal peptide is shown schematically. The n-region is the N-terminal region of variable length that often contains polar amino acids. The h-region is moderately hydrophobic and contains 12 to 20 amino acids. The c-region is the C-terminal region that often contains basic residues (Sargent, 2007). Common conserved features mean that algorithms can be generated to predict proteins that would use the Tat pathway. *E. coli* is predicted to contain 26 such proteins (Berks 2005).

Panel B: An apoprotein with an N terminal twin-arginine signal peptide folds, and the cofactor is inserted. The cofactor-bound protein binds to the TatABC complex, in which the cytoplasmic amphipathic helices of TatB and C are thought to form a ‘basket’ structure to accept the substrate. The TatABC complex is thought to complex with a separate TatA complex to form the mature translocon, then the substrate is transported in a manner dependent upon a proton motive force. The signal peptide is removed and the mature protein is formed in the periplasm. Adapted from Robinson *et al.*, 2011.

the twin-arginine motif. All proteins bearing a twin-arginine signal are transported by the twin-arginine transport (Tat) system (Palmer and Berks, 2003, Sargent *et al.*, 1998). The Tat translocase is a membrane-bound nanomachine that translocates fully folded proteins across the cytoplasmic membrane. In *E. coli*, three proteins are important in the transport process; each protein is an integral membrane protein. TatA and TatB comprise a very short N-terminal section in the periplasmic space, a single transmembrane helix, and a short hinge region and an amphipathic helix on the cytoplasmic side of the membrane (Lee *et al.*, 2006, Robinson *et al.*, 2011). TatC contains six transmembrane helices and both the C- and N-termini of the protein are situated on the cytoplasmic side of the membrane (Drew *et al.*, 2002).

Two Tat complexes are thought to form in the membrane. The first of these is a heteromeric TatABC complex, in which the TatB and TatC components are thought to be involved in substrate binding (Tarry *et al.*, 2009). Secondly, TatA proteins form multimers of variable diameter that are consistent with a role as a translocation pore (Figure 1.6, Gohlke *et al.*, 2005). The full translocon is thought to form when a TatABC complex associates with a separate TatA supercomplex (Robinson *et al.*, 2011).

***E. coli* encounters oxidative and nitrosative stress.**

In order to be a successful pathogen, *E. coli* must be able to invade its host and adapt to the conditions it encounters therein, in terms of oxygen and nutrient availability. It must be able to survive exposure to reactive oxygen species (ROS) and reactive nitrogen species (RNS) that damage bacterial proteins, lipids and DNA. Superoxide radicals are generated in phagocytic cells by the NADPH phagocyte oxidase and might be converted subsequently to numerous other ROS, such as hydrogen peroxide (Fang, 2004). Nitric oxide (NO) and RNS are encountered as products of *E. coli* metabolism as a by-product of nitrite reduction, but it is unclear exactly which enzyme is responsible for this NO generation. It has been reported that NirB is the major source of NO during nitrate or

nitrite metabolism (Weiss, 2006), and conversely that NrfA is largely responsible for NO generation (Corker and Poole, 2003). Conversely, the *narGHJI* operon has been implicated as a major contributor to nitrosation in *E. coli* (Metheringham and Cole, 1997, Taverna and Sedgwick, 1996, Ralt *et al.*, 1988, Calmels *et al.*, 1988, Ji and Hollocher, 1988). NO is produced by host defence mechanisms such as neutrophils and activated macrophages (Fang, 2004). Nitric oxide synthase (NOS) functions constitutively to catalyse the conversion of arginine to NO and citrulline, whilst an inducible nitric oxide synthase (iNOS) produces large amounts of NO during inflammation or infection (Lundberg *et al.*, 2004, Poole and Hughes, 2000). Activated macrophages are able to produce extracellular NO at a concentration of up to 10 μM (Raines *et al.*, 2006).

Environments where the carbon to NO_3^- ratio is low tend to be dominated by denitrifying bacteria, which produce NO as an obligate metabolic intermediate (de Vries and Schröder, 2002, Zumft, 1997, Watmough *et al.*, 1999). However, denitrifying bacteria are rarely found in the gastrointestinal tract, where the carbon to NO_3^- ratio is very high (Forsythe and Cole, 1987). Instead, *E. coli* present in this niche reduce NO_2^- to ammonia (Corker and Poole, 2003, Weiss, 2006, Jackson *et al.*, 1981a, Ji and Hollocher, 1988).

Protein damage caused by nitrosative stress.

NO is a dangerous molecule within bacteria; it inactivates TCA cycle enzymes such as aconitase, as well as terminal respiratory oxidases (Stevanin *et al.* 2000, Gardner and Gardner 2002). NO reacts rapidly with many targets within the cellular environment. These include iron centres and reactive oxygen species such as superoxide to generate peroxynitrite, ONOO^- (Poole and Hughes, 2000). Peroxynitrite is extremely toxic, and reacts mainly with carbon dioxide to generate ONOOCO_2^- , which in turn decomposes to give NO_2 and the carbonate radical anion (Hughes, 1999). Peroxynitrite can also nitrate

tyrosine residues in proteins to form 3-nitrotyrosine: this can occur in either bacterial or host proteins in some pathological conditions (Rankin *et al.*, 2008). Tyrosine nitration can lead to loss or perturbation of enzyme activity. It seems that nitration can contribute to killing activity of bacteria in phagocytes but this has not been explicitly proven. Either peroxynitrite reductases or the ability to repair damage caused by peroxynitrite may be an important factor for pathogens to avoid killing in phagocytes. However, this is not a role that has yet been identified in *E. coli* (Rankin *et al.*, 2008).

Nitrosative stress can cause two types of damage. Where NO binds to a metal centre, the damage is termed nitrosylation. However, when new C-N or S-N bonds are formed, damage is referred to as nitrosation (Hill *et al.*, 2010). Nitrosation in bacterial cultures can be measured by monitoring fluorescent triazole formation from 2,3-diaminonaphthalene (Ji and Hollocher, 1988.) Nitrosation in *E. coli* cultures was decreased when cultures are sparged with an inert gas, which implies that nitrosation relies on the generation of a gaseous product (Ji and Hollocher, 1988). NO production from nitrite is inhibited by nitrate, presumably because of the preference of NarG to metabolise nitrate over nitrite while available. NO generated from nitrite in the study by Ji and Hollocher (1988) study never exceeded 300 μM , despite large excesses of both nitrite and formate. Synthesis of NO appeared to be self-limiting. A strong role for N_2O_3 and N_2O_4 in nitrosation was suggested. These are both species that arise from NO reacting with oxygen.

Nitrosation of a model substrate, 2,3-diaminonaphthalene (DAN), can be monitored experimentally (Metheringham *et al.*, 1997, Weiss, 2006.) Nitrosation of DAN occurs in two stages, the enzymic reduction of nitrite to NO, followed by a series of chemical reactions involving oxygen in which O_2 is thought to form the nitrosylating species N_2O_3 and N_2O_4 . In aerobic cultures treated with nitrite, no nitrosation was measured. However, nitrosation was measured in anaerobic cultures treated with nitrite.

The presence of nitrate inhibited nitrosation. Formate and lactate were both efficient electron donors for this reaction, but maximal nitrosation occurred during growth on glycerol with fumarate, but not glucose (Metheringham *et al.*, 1997). The NarGHJI complex was implicated as a major contributor to nitrosating activity but the NarZYWV complex was not. Nitrosation by bacteria in the gastrointestinal tract can cause gastric cancer. Enteric bacteria have a 10-fold lower nitrosation activity than denitrifiers, but enteric bacteria have the highest population and are the most relevant in the human body, as denitrifiers are rarely found. It has been suggested that an Fnr-activated molybdoprotein is responsible for nitrosation activity. Nitrate in the reaction mixture inhibits *in vitro* nitrosation (Calmels *et al.*, 1988). However, when bacteria are grown in the presence of sodium nitrate, then washed before assay, there is no inhibition effect. Rates of nitrosation are much lower in rich medium than in minimal medium. The nitrite reductase, Nir, is not responsible for nitrosation, and the rate of nitrosation in a *nir nrf* double mutant is similar to that of the parent. In chlorate resistant mutants, that lack all molybdoproteins due to their inability to synthesise molybdopterin cofactor, there is no nitrosation activity (Metheringham *et al.*, 1997).

DNA damage caused by nitrosative stress.

NO does not react directly with DNA, but can become a potent DNA damaging agent once it has been oxidised to N_2O_3 , a powerful nitrosating agent (Spek *et al.*, 2001). N_2O_3 reacts with exocyclic amino groups to deaminate adenine, cytosine and guanine to form hypoxanthine, uracil and xanthine. Each of these damaged bases are mutagenic if not repaired. If NO reacts with superoxide to form peroxynitrite, it can cause oxidation and nitration of DNA bases, especially guanine to generate 8-oxo-guanine, and 8-nitro-guanine. Recombinatorial repair is essential for defence against this NO toxicity (Spek *et al.*, 2001).

During nitrate or nitrite metabolism, mutagenic reactive nitrogen oxides HNO_2 and $\text{NO}\cdot$ are formed (Weiss, 2006). When DNA is exposed in vitro to HNO_2 and $\text{NO}\cdot$, the exocyclic amines of nucleotides can form unstable N-nitroso ($-\text{N}=\text{O}$) derivatives, that are subsequently deaminated. These deaminated bases mispair, causing mutagenesis. Nitrosation of cellular secondary amines and amides produces alkylating agents that cause mutagenic lesions at many sites in DNA. Nitrosative mutagenesis occurs especially when bacteria are shifted from nitrate-dependent to oxygen-dependent respiration, during which accumulated $\text{NO}\cdot$ might be oxidised to N_2O_3 . N_2O_3 is a nitrosating agent that can produce mutagenic lesions (Weiss, 2006).

Detoxification of NO in *E. coli*

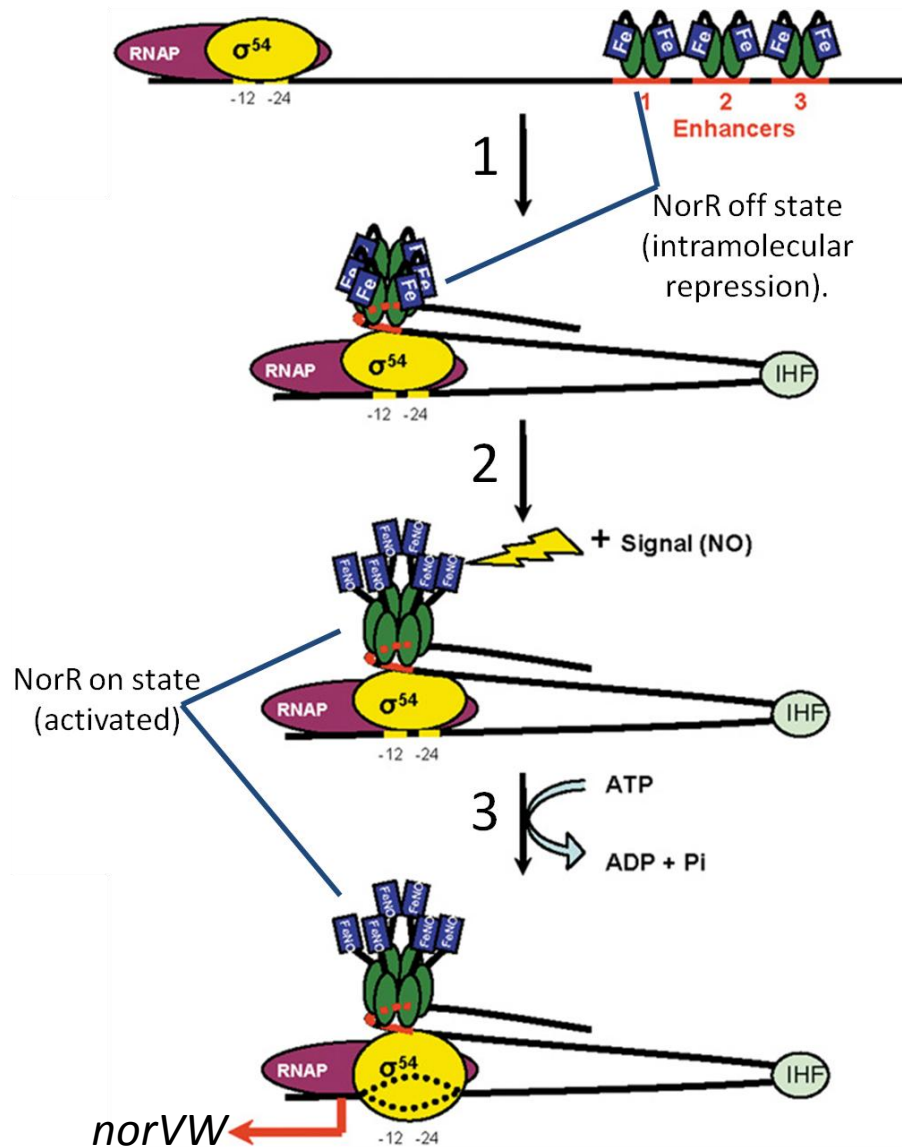
Three genes, *hmp*, *nrfA* and *norV*, have been identified in *E. coli* that encode proteins that detoxify NO. Under aerobic conditions, the flavohaemoglobin Hmp detoxifies NO through oxidation to nitrate, while under anaerobic conditions Hmp is able to reduce NO to N_2O (Gardner and Gardner, 2002, Hausladen *et al.*, 1998, Kim *et al.*, 1999). However, the anaerobic activity of Hmp is likely to be negligible under physiological conditions, in comparison to the highly effective aerobic protection afforded by this enzyme (Gardner and Gardner, 2002). Hmp belongs to a family of flavohaemoglobins, and consists of an N-terminal haem binding domain coupled to a flavin binding domain that is able to reduce NO.

The cytochrome *c* periplasmic nitrite reductase NrfA is able reduce hydroxylamine and NO, in addition to its primary function in respiratory reduction of nitrite (Poock *et al.*, 2002, van Wonderen *et al.*, 2008). This reaction occurs at the same active site as nitrite reduction. It has been proposed that NrfA in the periplasm should be effective in maintaining low levels of NO, such that any that does diffuse into the

cytoplasm can be effectively removed by flavorubredoxin, encoded by *norV* (van Wonderen *et al.*, 2008). Single iron atoms coordinated by four sulphurs donated from cysteines in the polypeptide chain are referred to as rubredoxin centres, and are the most simple forms of Fe-S cluster.

NorR is a transcription factor of the σ^{54} -dependent family of transcriptional activators, which is exclusively responsive to NO (Hutchings *et al.*, 2002). The σ^{54} factor differs in both structure and function from all other σ factors. σ^{54} proteins recognise promoter motifs located at positions -24 and -12, and are totally dependent on the ATPase activity of transcriptional activators, such as NorR, to initiate transcription (Barrios *et al.*, 1999, Shingler, 2011). NorR contains a C-terminal helix-turn-helix domain that binds DNA, a central AAA+ (ATPase associated with various cellular activities) domain, and an N-terminal iron containing GAF (cGMP phosphodiesterase adenylate cyclase FhlA) domain (D'Autréaux *et al.*, 2005). The mono-nuclear iron centre present in the GAF domain acts as a ligand for NO, which binds reversibly to the protein. When bound to NO, the conformation of the protein changes to relieve intramolecular repression of ATPase activity and DNA binding (Figure 1.7). Relief of repression stimulates ATPase activity of the central domain and consequently enables transcription activation, by coupling ATP hydrolysis to promoter DNA melting (D'Autréaux *et al.*, 2005). Under microaerobic or anaerobic conditions in the presence of NO, NorR upregulates the *E. coli* flavorubredoxin, NorV, and its associated oxidoreductase, NorW, which function to reduce NO to N₂O (D'Autréaux *et al.*, 2005, Tucker *et al.*, 2005). The NorVW protein complex is a dedicated nitric oxide reductase that contains a non-haem di-iron centre (Gomes *et al.*, 2002).

Figure 1.7.



A model of activation of *norVW* transcription by the σ^{54} -dependent activator NorR. NorR is depicted as a green oval (AAA+ and C-terminal domains) and a blue square (mononuclear iron-containing GAF domain) that binds as a dimer to three enhancer sites upstream of the *norVW* promoter. The core polymerase (purple) and σ^{54} (yellow) bind to the -12 and -24 elements of the *norVW* promoter. Step 1: The integration host factor, IHF, mediates DNA looping to allow σ^{54} to interact with the NorR oligomers. Step 2: NO binds to the GAF domain of NorR to relieve intramolecular repression. Step 3: NorR catalyzes ATP hydrolysis to induce promoter DNA melting (black dotted lines) and transcription of *norVW* (Figure adapted from Tucker *et al.*, 2005.)

The aerobic respiratory chain of *E. coli* has two terminal quinol oxidases, cytochromes *bo* and *bd*. Cytochrome *bd* confers NO resistance to *E. coli* (Mason *et al.*, 2009). These proteins couple oxidation of ubiquinol-8 to the reduction of oxygen to water. Simultaneously, a transmembrane potential is generated that drives ATP synthesis. Cytochrome *bd* was originally thought to facilitate microaerobic respiration, but it is also overexpressed under conditions of NO stress and was subsequently shown to be crucial for protecting against NO induced growth inhibition (Pullan *et al.*, 2007, Mason *et al.*, 2009). Several oxygen binding haem proteins can also bind NO, but as an inhibitory gas ligand. Growth-inhibition of a *cydAB* mutant (defective in cytochrome *bd*) was significantly greater than the wild type at high NO concentrations, but there was no significant difference in between the parent and a *cyo* mutant (defective in cytochrome *bo*).

Sensors of NO.

In *E. coli*, SoxR is the main sensor of superoxide, while OxyR coordinates the response to hydrogen peroxide (Mukhopadhyay *et al.*, 2004). Both proteins might also play a minor role in sensing nitrosative stress (Ding and Demple, 2000, Hausladen *et al.*, 1996, Cruz-Ramos *et al.*, 2002). The ferric uptake regulator (Fur) is an iron-dependent transcription regulator that typically controls the expression of genes involved in iron utilisation and acquisition (Spiro, 2007). Under iron-limited conditions, derepression of at least one Fur regulated promoter has been induced by an NO donor (D'Autréaux *et al.*, 2002). All three of these proteins might be termed 'secondary' sensors of NO, in that they principally sense alternative signals, but their activity might also be modulated by NO (Spiro, 2007). In contrast, NorR is a dedicated sensor of NO, that upregulates transcription of *norVW*, as described in the previous section (Figure 1.7).

In a study by Mukhopadhyay *et al.* (2004), some *E. coli* genes were shown to be induced by GSNO and acidified nitrite in a *fur*, *oxyR*, *soxRS*, *metR* and *norR* background, suggesting that additional nitrosative-stress-modulated regulators must exist. This novel regulator was further predicted to exist by Rodionov *et al.* (2005), and was confirmed to be the product of the *nsrR* gene from transposon insertion experiments investigating the regulation of *ytfE* expression (Bodenmiller and Spiro, 2006). NsrR is a transcriptional repressor of the Rrf2 family of regulatory proteins in a variety of bacteria, including *Nitrosomonas europaea*, where it was first identified (Beaumont *et al.*, 2004.) NsrR is a specific sensor of NO, and contains an NO-sensitive [2Fe-2S] cluster that is required for DNA binding activity (Tucker *et al.*, 2008, Tucker *et al.*, 2010.) In the presence of NO, the cluster is nitrosylated, and transcriptional repression is relieved to allow transcription of genes involved in the nitrosative stress response. NsrR has now been shown to negatively regulate the expression of several genes implicated in the nitrosative stress response: *ytfE*; *hmp*; *ygbA*; *nrfA*; *hcp-hcr*; and *yeaR-yoaG* (Bodenmiller and Spiro, 2006, Filenko *et al.*, 2007). This transcriptional repressor has been shown to bind to an inverted repeat sequence (GATG N₁₁ CATC) that overlaps the -10 element of promoters (Bodenmiller and Spiro, 2006). Transcription of several NsrR-regulated promoters, *phmp*, *pytfE* and *pygbA*, responds to iron limitation as shown by experiments with 2'2'dipyridyl. NsrR must be, directly or indirectly, inactivated by iron limitation; perhaps iron starvation leads to an inactive apo-protein being formed (Bodenmiller and Spiro, 2006).

The role of the di-iron protein, YtfE, in resisting nitrosative stress.

The di-iron protein YtfE has been shown to be critical for the repair of iron-sulphur centres damaged by nitrosative stress conditions (Justino *et al.* 2006, Justino *et al.* 2007,

Todorovic *et al.*, 2008, Overton *et al.*, 2008). This important role in the nitrosative stress response was further implied by the fact that several microarrays have highlighted *ytfE* as a gene that responds to nitrosative stress. However, recombinant YtfE did not reduce NO (Justino *et al.* 2006). It is important to note that the literature on mechanisms involved in resisting nitrosative stress gives results of experiments using a wide variety of sources of NO and the redox related species NO^+ and NO^- , including S-nitrosothiols, sodium nitroprusside, acidified nitrite and NO-saturated water (Poole, 2005). In a chemostat experiment S-nitrosoglutathione (GSNO) has recently been shown to induce a different transcriptional response to the NO donor compounds ‘NOC-5’ and ‘NOC-7’: previously such sources have been used interchangeably as nitrosating agents (Pullan *et al.*, 2007). By using S-nitrosothiols and sodium nitroprusside to generate nitrosative stress, secondary effects are revealed, instead of elucidating the primary roles of NO. Pullan *et al.*, (2007) showed a 19-fold anaerobic induction and a 2-fold aerobic induction of *ytfE* in response to NO, while Justino *et al.* (2005) reported that *ytfE* has the highest transcriptional activation among all genes studied. Experiments completed aerobically in rich medium revealed 38-fold and 50-fold induction of *ytfE* in response to 0.1 mM GSNO and 1 mM NaNO_2 , respectively (Mukhopadhyay *et al.*, 2004). Regulation of *ytfE* transcription has been shown to be dependent on NsrR and not the NarXLQP system, as activation by nitrate requires nitrate reduction to be functional, presumably to generate the NO that is sensed by NsrR (Bodenmiller and Spiro, 2006). As well as the suggested role from several studies of anaerobic protection against NO, YtfE was in a small group of proteins, including HmpA, NorV and NorW that fitted the gene profile of *E. coli* exposed to NO donors in an aerobic environment (Justino *et al.*, 2005).

YtfE is a cytoplasmic protein that is conserved in all enterobacteria (Justino *et al.*, 2006). A *ytfE* mutant grew very poorly anaerobically, and mutation of *ytfE* increased the sensitivity of *E. coli* to iron starvation, which will be examined in detail in the results section. YtfE confers protection against oxidative stress, as well as nitrosative stress (Justino *et al.*, 2007). A novel biosynthetic role for YtfE was proposed in the repair of iron centres as opposed to protection from destruction. One possibility is that YtfE is involved in the enzymic process to recruit and integrate the ferrous iron into clusters (Justino *et al.*, 2006, Justino *et al.*, 2007.)

Another study into YtfE orthologues in other species found that NO is reduced at the same rate both in the gonococcal parent and a *dnrN* mutant that is defective in the YtfE orthologue (Overton *et al.*, 2008). However, DnrN is critical in both oxidative and nitrosative stress protection. Damage to transcription factors is repaired more rapidly in the parent than in a *dnrN* mutant. The activities of iron-sulphur containing enzymes, such as fumarase, are lower in a Staphylococcal *scdA* mutant than the parent.

Identification of *E. coli* genes of unknown function implicated in the response to nitrosative stress.

In a microarray study by Constantinidou *et al.* (2006), several genes of unknown function were identified as candidates for a role in resisting nitrosative stress. These were selected due to similarities to known defence mechanisms in their anaerobic regulation by Fnr, NarXL, NarQP, nitrate or nitrite. Out of the candidates identified, the following showed some of the highest differences in expression levels between the stated growth condition (aerobic, anaerobic, presence or absence of nitrate or nitrite) or strain (wild type or *fnr*, *narXL*, *narXLP*, *narP* mutants) and a pool of RNA from the anaerobically grown parental strain; *yibIH*, *ygbA*, *hcp* and *yeaR-yoaG*. An objective of

this project is to investigate the role in NO reduction or nitrosative stress defence of the proteins encoded by these genes of unknown function.

The hybrid cluster protein, Hcp.

The hybrid cluster protein, encoded by *hcp*, contains two types of iron-sulphur clusters; a [4Fe-4S] cubane cluster and a novel [4Fe-2S-2O] hybrid cluster (van den Berg *et al.*, 2000). The *hcp* gene in *E. coli* and other facultative anaerobes occurs in a small operon with *hcr* that encodes an NADH oxidoreductase. In obligate anaerobes, *hcr* is not present in an operon with *hcp* (Filenko *et al.*, 2005). Hcr catalyses the reduction of Hcp using NADH as an electron donor. Electrons derived from NADH oxidation are transferred via the [2Fe-2S] centre of Hcr to the conventional cluster of Hcp, then to the hybrid cluster (van den Berg *et al.*, 2000). The Hcp protein has been studied extensively (by several different groups, as described below) but its physiological function is still not yet clear, though it is thought to be linked to managing nitrosative stress. Hcp has been reported to reduce hydroxylamine, but this occurs with optimal V_{\max} and K_m at pH 9.0 (Wolfe *et al.*, 2002, Table 1.2). As Hcp is able to reduce hydroxylamine, but at a rate that is not physiologically relevant, it might be that the cognate substrate of the enzyme is in fact a related species that has some homology to hydroxylamine. Such a substrate might be a hydroxamate, perhaps produced as an intermediate during the repair of NO-adducts formed under nitrosative stress conditions. Hcp did not mediate resistance to hydroxylamine stress in *Wolinella succinogenes* (Kern *et al.*, 2011.) The presence of hydroxylamine in the growth medium did not induce expression of *hcp* in *E. coli* (Squire, PhD Thesis, 2009). In another study, it was suggested that *hcp* is induced by H₂O₂ in an OxyR dependent manner (Almeida *et al.*, 2006). In this study, bacteria were not grown under conditions that promote anaerobic

Table 1.2. The effect of using a non-physiological pH on K_m and V_{max} of Hcp for hydroxylamine.

pH	K_m for NH_2OH / mM	V_{max} / mole of NH_2OH reduced min^{-1} mg protein ⁻¹
7.5	38.9	92
9.0	2.5	458

Values are taken from Wolfe *et al.*, 2000.

respiration, only fermentative conditions are used. Although the K_m is within the range expected for a peroxidase, the reported V_{max} is too low to allow the firm conclusion that Hcp is a physiologically relevant peroxidase.

Expression of *hcp* is optimal under anaerobic conditions in the presence of nitrate or nitrite (van den Berg *et al.*, 2000). Experiments completed in a chemostat using defined medium revealed that the *hcp* gene is upregulated anaerobically, but not aerobically by NO (Pullan *et al.*, 2007). Upregulation of *hcp* in response to GSNO under both aerobic and anaerobic conditions has also been reported (Flatley *et al.*, 2005.) The *hcp* promoter is regulated similarly to *nirB* and the *narGHJI* operon (Filenko *et al.*, 2007). Expression from the *Escherichia coli* *hcp* promoter is optimally induced during anaerobic conditions in the presence of nitrite. However, an extensive mutagenic analysis of the *hcp* promoter revealed that the DNA site for NarL and NarP, centred at position -104.5, plays only a minor role in regulation (Chismon *et al.*, 2010). When the *nirB* and *narGHJI* operons are active, nitrosative stress is generated. As *hcp* is co-ordinately regulated with these two genes, it might function to repair the damage caused when the operons are active. In a study by Rodionov *et al.* (2005), *hcp* was predicted to be regulated by the nitrite responsive regulator, NsrR. Filenko *et al.* (2007) confirmed experimentally that *hcp* is repressed 15-fold by NsrR, and it has been shown that NsrR binding to a DNA target centred at position +6 plays a major role in regulation of the *hcp* promoter (Chismon *et al.*, 2010.) Fnr is a transcriptional activator that binds to a target centred at position -72.5 upstream of the transcript start site (Chismon *et al.*, 2010.)

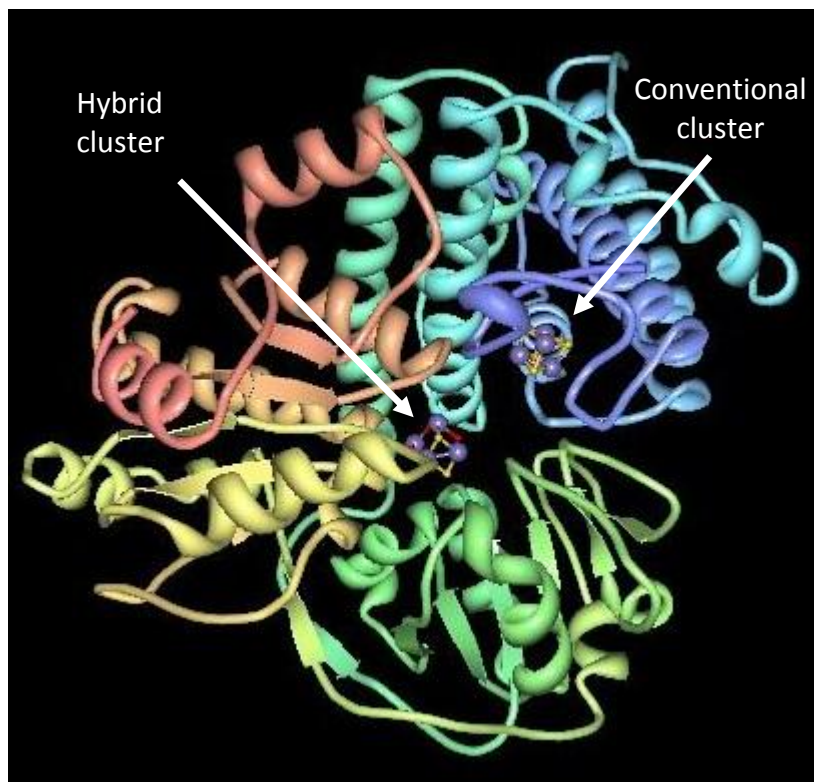
Several structures of the hybrid cluster protein from different organisms and at different resolutions have been solved. It was reported that Hcp from *Desulfovibrio*

vulgaris contains three domains, domain one from amino acid 1-222, domain two from amino acid 223-375 and domain 3 from amino acid 376-553 (Arendsen *et al.*, 1998). Another early reference refers to the hybrid cluster protein purified from *E. coli* as a fuscaredoxin (Pereira *et al.*, 1999), and reported that the conventional Fe-S cluster can transfer a single electron, whereas the hybrid cluster can accept multiple electrons and be stabilised in at least 4 oxidation states.

Domain 1 comprises two three-helix-bundles that are joined by a nine amino acid linker that loops around the conventional cluster (Figure 1.8, Figure 1.9, Cooper *et al.*, 2000). Domain 2 consists of a mixed structure, of a central beta sheet, surrounded by alpha helices in an $\alpha\beta$ -Rossmann fold-like geometry (Aragão *et al.*, 2008). Domain 3 is organised similarly, although it contains more α -helices. The polypeptide binding motif that coordinates the conventional cluster is similar to that normally expected for a 4Fe4S cluster. At 10.9 Å, the distance between the two clusters is within the distance needed for electron transfer. The presence of cavities within the polypeptide structure that would allow substrate access to the active sites reinforces the idea that Hcp is an enzyme with its activity centred around the hybrid cluster (Cooper *et al.*, 2000).

Hcp is found in several anaerobic and facultatively anaerobic bacteria, in which the cysteine residues that coordinate the hybrid cluster, near the geometric centre of the protein, are always conserved (van den Berg *et al.*, 2000). The cysteine ligands towards the N-terminal of the polypeptide that coordinate the conventional iron-sulphur cluster are also conserved. Hcp is not found in *Bacillus subtilis*, or in several bacteria with small genomes, such as *Mycobacterium sp.* and *Haemophilus influenzae*.

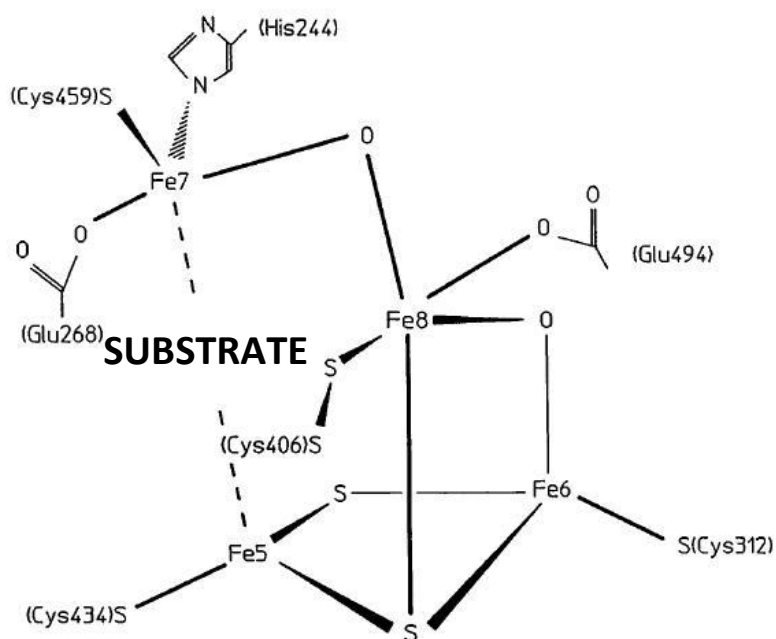
Figure 1.8



Ribbon diagram of the Hybrid Cluster Protein.

The X-Ray structure of the hybrid cluster protein from *Desulfovibrio vulgaris* at 1.35 Å resolution was downloaded from the RCSB protein data bank (ID 1W9M) using the simple viewer (Moreland *et al.*, 2005, Aragão *et al.*, 2008.) The protein backbone has been shaded using a rainbow spectrum from the N-terminus (blue) to C-terminus (red). The iron-sulphur clusters have been highlighted using white arrows.

Figure 1.9



Structure of the hybrid iron-sulphur cluster of Hcp.

The iron atoms in the hybrid cluster are bridged by both S and O atoms. For simplicity, where amino acid side chains donate a ligand to the cluster, only the key atoms involved are depicted. Diagram adapted from Arendsen *et al.*, 1998.

YgbA

The gene of unknown function, *ygbA*, was found to be co-ordinately regulated with *hmpA* and *ytfE*, in that transcription appears to be repressed by Fnr and NsrR and strongly induced by nitrate and nitrite (Constantinidou *et al.*, 2006). The binding of Fnr to the promoter was confirmed by chromatin immunoprecipitation experiments (Constantinidou *et al.*, 2006). The NsrR repression effect was further validated by the fact that the promoter is constitutively active in an *nsrR* background (Bodenmiller and Spiro, 2006). The fact that *ygbA* expression is induced by very low concentrations of both GSNO and NaNO₂ in primer extension experiments carried out using cultures grown aerobically in a rich medium suggests a role for YgbA in nitrosative stress (Mukhopadhyay *et al.*, 2004). In a separate study, a two-fold induction of *ygbA* was observed anaerobically, but not aerobically, in response to NO (Pullan *et al.*, 2007).

YeaR and YoaG.

The *yeaR-yoaG* operon has been found in *E. coli* as well as in the closely related species *Shigella*, *Salmonella* and *Citrobacter*. The protein is often found as a YeaR domain fused to TehB, a protein needed for tellurite resistance in more distantly related species such as *Streptococcus pneumoniae* or *Yersinia pseudotuberculosis*. YoaG is less broadly distributed, and is largely confined to enterobacteriaceae (Lin *et al.*, 2007). Expression of the operon in *E. coli* has been shown to be induced particularly strongly by nitrite in the absence of Fnr, such as when nitrosative stress is so severe that Fnr can no longer function (Constantinidou *et al.*, 2006). The expression of *yeaR* was also shown to be upregulated almost 3-fold in anaerobically grown cultures treated with NO, further suggesting a role in the nitrosative stress response (Justino *et al.*, 2005).

Most previously characterised genes, with the exception of *ogt*, activated by the NarXLQP system also require activation by Fnr (Squire *et al.*, 2009). A novel mechanism has been shown to activate *yeaR-yoaG*, in that phospho-NarL is able to activate transcription independently of Fnr (Constantinidou *et al.*, 2006, Lin *et al.*, 2007). The operon is repressed by NsrR, as shown by both repressor titration and mutational analyses (Filenko *et al.*, 2007, Lin *et al.*, 2007). NarL-dependent activation of *yeaR* is decreased in rich medium, and this depends on the nucleoid associated protein Fis (factor for inversion stimulation, Squire *et al.*, 2009). The promoter architecture consists of two Fis sites centred at -55 and -31 with respect to the transcription start site, that overlap the 7-2-7 NarL site centred at -43.5; Fis represses the *yeaR* promoter by displacing NarL (Squire *et al.*, 2009).

YibI and YibH.

The genes encoding the putative proteins YibI and YibH are thought to be expressed in an operon (Constantinidou *et al.*, 2006). Expression of *yibIH* appears to be highest under anaerobic conditions, in the presence of nitrite in an Fnr mutant (Constantinidou *et al.*, 2006). Under extreme nitrosative stress, Fnr becomes damaged and inactivated by NO. A possible role for the proteins encoded by *yibIH* is to function as part of a nitrosative stress response when Fnr has become inactivated. The operon is also induced by NO₃⁻ in a *narXL* background, in a similar manner to other genes implicated in the nitrosative stress response in *E. coli* (Constantinidou *et al.*, 2006). Several independent microarrays have revealed that the aforementioned genes of unknown function are upregulated by various sources of nitrosative stress; some of the findings have been summarised in Table 1.3.

Ogt.

RNS can cause lysine side chains in proteins and in some free amino acids to become potent DNA-methylating agents. Amide nitrosation is a source of agents

Table 1.3. Microarray studies that have indentified sources of nitrosative stress that induce the expression of the genes encoding proteins of unknown function.

Gene	<u>Microarray study to identify induction by</u>			
	NO	GSNO	Nitrate	Nitrite
<i>hcp</i>	Pullan <i>et al.</i> , 2007	Flatley <i>et al.</i> , 2005	van den Berg <i>et al.</i> , 2000	van den Berg <i>et al.</i> , 2000
			Constantinidou <i>et al.</i> , 2006	Constantinidou <i>et al.</i> , 2006
<i>ygbA</i>	Pullan <i>et al.</i> , 2007	Mukhopadhyay <i>et al.</i> , 2004	Constantinidou <i>et al.</i> , 2006	Mukhopadhyay <i>et al.</i> , 2004
				Constantinidou <i>et al.</i> , 2006
<i>ytfE</i>	Pullan <i>et al.</i> , 2007	Mukhopadhyay <i>et al.</i> , 2004	Constantinidou <i>et al.</i> , 2006	Mukhopadhyay <i>et al.</i> , 2004
	Justino <i>et al.</i> , 2005			Constantinidou <i>et al.</i> , 2006
	Bodenmiller and Spiro, 2006			
<i>yeaR</i>	Justino <i>et al.</i> , 2005		Constantinidou <i>et al.</i> , 2006	Constantinidou <i>et al.</i> , 2006
<i>ogt</i>			Constantinidou <i>et al.</i> , 2006	Constantinidou <i>et al.</i> , 2006
<i>yibIH</i>			Constantinidou <i>et al.</i> , 2006	Constantinidou <i>et al.</i> , 2006

that can methylate oxygen atoms and therefore form mutagenic O⁶-methylguanine in DNA. Both Ogt and Ada are O⁶-methylguanine-DNA methyltransferases and are therefore able to repair these DNA lesions. Overexpression of either Ada or Ogt proteins does not decrease the rate of spontaneous mutagenesis in *E. coli*, which suggests that the wild type levels of these proteins are sufficient to prevent mutagenesis (Taverna and Sedgewick, 1996). Single *ogt* or *ada* mutants displayed no more mutagenesis than the parent; each protein is able to compensate for the loss of function of the other (Taverna and Sedgewick, 1996). However, *ada ogt* double mutants are totally deficient in O⁶-methylguanine-DNA methyltransferases, and have an increased spontaneous mutation rate. O⁶-methylguanine pairs with T, thus causing GC to AT transition mutations. Ada and Ogt transfer the methyl group to a cysteine residue of their own polypeptide chain, and act as suicide enzymes; Ada and Ogt become inactivated during the process. Ada is inducible in response to exposure to DNA-methylating agents such as *N*-methyl-*N'*-nitro-*N*-nitrosoguanidine. Expression of *ogt* was increased at least 7-fold by the presence of nitrate or nitrite in the growth medium, even in the absence of Fnr (Constantinidou *et al.*, 2006). It was later confirmed that the DNA repair function of Ogt was induced by nitrate ions; this regulation will be discussed in detail in subsequent sections (Squire *et al.*, 2009).

Possible roles for the genes of unknown function

As little is known about the genes of unknown function so far, any common factors in nitrosative stress response proteins might be of help in designing appropriate experiments to elucidate their function. One such similarity is the fact that iron is frequently found among proteins responsive to nitrosative stress. Indeed, YtfE and the flavorubredoxin encoded by *norV* contain di-iron centres. NorR contains a mono-

nuclear iron centre, Fnr, NsrR and Hcp contain iron-sulphur clusters, NrfA and NrfB are penta-haem proteins (Clarke *et al.*, 2007), *hmp* encodes a flavohaemoglobin and the ferric uptake regulator protein (Fur) uses Fe^{2+} as a cofactor (D'Autréaux *et al.*, 2002). A group of di-iron proteins involved in nitrosative damage repair have been found in diverse pathogenic bacteria. These include ScdA from *Staphylococcus aureus*, DnrN in pathogenic Neisseria and YtfE from *E. coli* (Overton *et al.*, 2008). It is possible that these proteins or the y-gene products highlighted above might be involved in the removal of damaged iron atoms from bacterial proteins, or indeed the reinsertion of iron once damage has been rectified (Overton *et al.*, 2008).

Aims of this work.

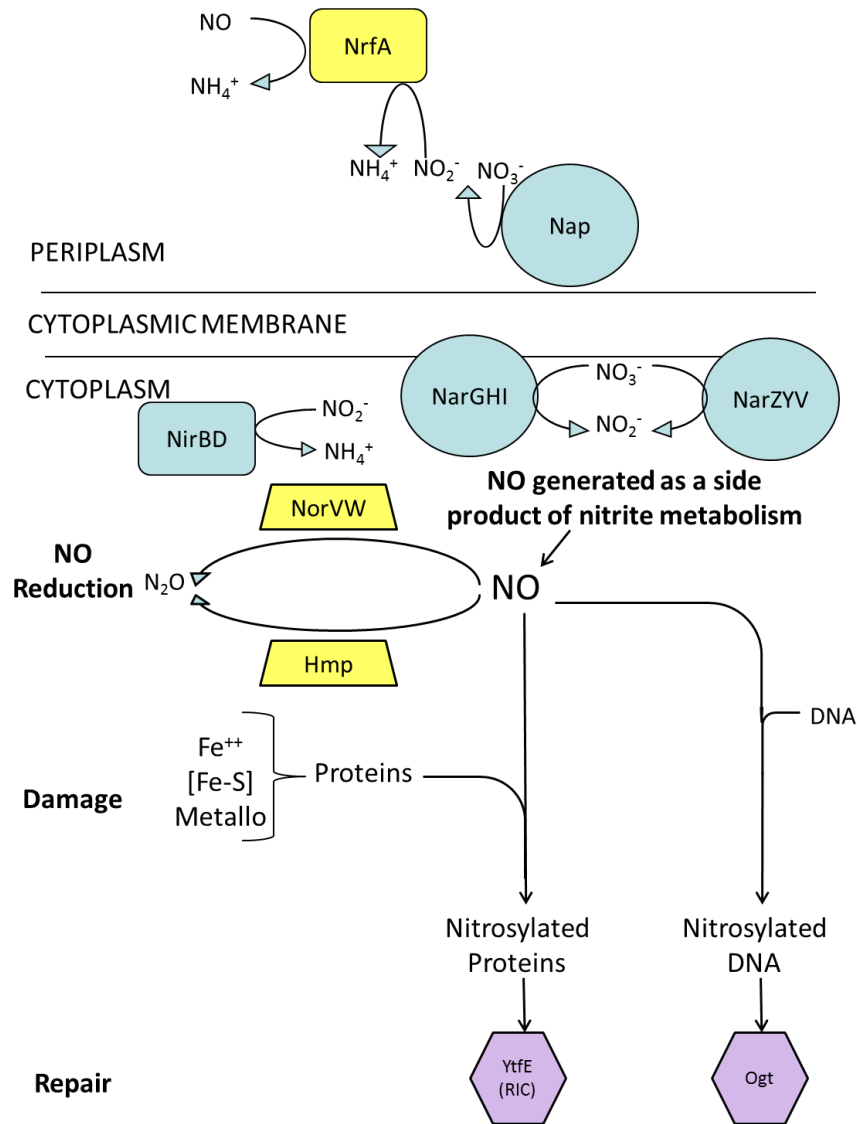
Several studies have reported that either NarG, NirB or NrfA is responsible for the generation of intracellular NO during nitrate and nitrite reduction. An initial aim of this work is to resolve this controversy, using a single method. The previous reports have not compared all three hypotheses using a systematic mutagenic approach. In order to investigate this problem, it will be necessary to develop a method to detect the formation of NO in the cytoplasm. It has been assumed, that as NO is a small, uncharged molecule, that the concentration of NO outside the cell will always be equal to that inside the cytoplasm, but there is not yet any direct evidence to prove this assumption.

Several proteins have been identified in *E. coli* that are able to reduce NO to NH_4^+ or N_2O . A further aim of this work is to validate an assay for NO reduction by washed *E. coli*, using a method that is suitable for laboratory K-12 strains. The effect of nitrate and nitrite in the growth medium, as well as various transcription factors will be investigated. The effect of mutations in known NO reductases on the rate of NO

reduction will also be determined. An objective of the project is to investigate the function and regulation of additional proteins that might reduce NO. A possible role for these genes of unknown function might be as an additional NO reductase. The complex system used by *E. coli* to combat nitrosative stress is summarised in Figure 1.10.

It has recently been reported that a mutant defective in YtfE, which is required for the repair of iron centres in proteins, grows very poorly anaerobically. Experiments will be completed to determine whether mutants defective in the genes of unknown function that are regulated similarly to YtfE might also have a growth defective phenotype, and thus might function similarly. Several studies have used reverse transcription PCR, microarray analysis and promoter-*lacZ* fusions to investigate the regulation of *ytfE* transcription. However, a comprehensive study in mutant strains defective in key regulators in an isogenic background has not been completed, so an aim of this work is to construct and assay a *ytfE::lacZ* fusion plasmid. YtfE has been characterised as a protein that repairs iron centres that are damaged by oxidative and nitrosative damage. A final aim of the project is to investigate the function of both YtfE and Hcp in the repair of nitrosative damage.

Figure 1.10.



A schematic representation of *E. coli* proteins that are implicated in the nitrosative stress response.

The location of proteins implicated in the nitrosative stress response in *E. coli* are depicted schematically. Those involved in nitrate and nitrite reduction, with the exception of NrfA, are coloured blue, and those implicated in NO reduction are coloured yellow. Proteins involved in damage repair are depicted in purple.

CHAPTER 2 - MATERIALS AND METHODS

MATERIALS.

Media.

Solid and liquid media were prepared by dissolving the appropriate amount of solid in distilled water, followed by sterilisation by autoclaving at 121°C for 15 min, or by filter sterilisation using a 0.2 µm pore filter. Lennox broth (LB) contained 20 gL⁻¹ tryptone, 10 gL⁻¹ yeast extract and 10 gL⁻¹ NaCl. Minimal salts medium (MS) contained 4.5 gL⁻¹ KH₂PO₄, 10.5 gL⁻¹ K₂HPO₄, 1 gL⁻¹ NH₄SO₄, 0.05 gL⁻¹ MgCl₂, 1 µM ammonium molybdate, 1 µM sodium selenate and *E. coli* sulphur free salts (1 mL per L). *E. coli* sulphur free salts contained 82 gL⁻¹ MgCl₂.7H₂O, 10 gL⁻¹ MnCl₂.4H₂O, 4 gL⁻¹ FeCl₂.6H₂O, 1 gL⁻¹ CaCl₂.6H₂O and concentrated HCl (20 mL per L). SOC medium contained 20 gL⁻¹ tryptone, 5 gL⁻¹ yeast extract, 0.58 gL⁻¹ NaCl, 0.185 gL⁻¹ KCl, 2.03 gL⁻¹ MgCl₂.6H₂O, 2.46 gL⁻¹ MgSO₄.7H₂O and 3.6 gL⁻¹ glucose. MacConkey lactose agar (50 gL⁻¹) was supplied by BD (Becton, Dickinson and Company). Nutrient agar (NA, 28 gL⁻¹) was supplied by Oxoid, Hampshire, UK.

Antibiotics.

The appropriate amount of each antibiotic was stirred into solvent, the solution was sterilised by filtration and stored at 4°C or -20°C (Table 2.1).

Buffers.

Buffers and solutions used in this study are described in Table 2.2.

BACTERIAL METHODS.

Bacterial strains.

The stains used in this study are listed in Table 2.3 and Table 2.5.

Preparing bacteria for long term storage.

LB (1 mL) was inoculated with a single colony of the strain to be stored, and aerated at 37°C until the optical density at 650 nm had reached 0.7 to 0.8. The culture

Table 2.1. Concentrations, solvents and storage conditions for antibiotics used in this work.

Antibiotic	Stock concentration (mgmL ⁻¹)	Working concentration (µgmL ⁻¹)	Solvent	Storage (°C)
Carbenicillin	100	100	Water	4
Kanamycin	100	25	Water	4
Chloramphenicol	50	15 or 30	Ethanol	-20
Tetracycline	10	35	50% Ethanol	-20
Streptomycin	10	10	Water	4
Spectinomycin	10	20	Water	4

Table 2.2. Buffers and solutions used in this work

Name	Composition
General buffers.	
Tris-EDTA buffer (TE, pH 8.0).	10 mM Tris-HCl and 1 mM EDTA.
Phosphate buffer (50 mM, pH 7.5).	7.26 gL ⁻¹ K ₂ HPO ₄ and 1.13 gL ⁻¹ KH ₂ PO ₄ .
Buffers for making competent <i>E. coli</i> cells.	
TFB 1.	100 mM RbCl, 50 mM MnCl ₂ , 30 mM potassium acetate, 10 mM CaCl ₂ and 15% (v/v) glycerol.
Buffers for agarose gel electrophoresis.	
5xTBE.	0.445 M Tris-HCl, 0.445 M boric acid and 0.01 M EDTA (pH 8).
Sample buffer.	TE supplemented with 0.025% w/v bromophenol blue and 10% v/v glycerol.
1% agarose solution.	1g Agarose in 10 mL 1xTBE buffer.
Buffers and solutions for β-galactosidase assays.	
Z buffer.	0.75 gL ⁻¹ KCl, 0.25 gL ⁻¹ MgSO ₄ ·7H ₂ O, 8.55 gL ⁻¹ Na ₂ HPO ₄ , 4.87 gL ⁻¹ NaH ₂ PO ₄ ·2H ₂ O and β-mercaptoethanol (2.7 mL per L).
1xA, Potassium phosphate buffer (0.1M, pH 7.0).	11.6 gL ⁻¹ K ₂ HPO ₄ and 4.54 gL ⁻¹ KH ₂ PO ₄ .
Sodium deoxycholate (1%).	1g Sodium deoxycholate in 100 mL distilled water.
ortho-Nitrophenyl β-D-galactopyranoside (ONPG, 13 mM).	0.032g ONPG in 1 x A (10 mL).
Buffers for NO electrode assays.	
Assay buffer.	Phosphate buffer (50 mM, pH 7.5), supplemented with 50 μM EDTA, and 0.4% v/v glycerol.
Electrolyte.	17.5 g KCl in 100 mL distilled water.

Buffers for polyacrylamide gel electrophoresis.

30% acrylamide solution.

30% (w/v) acrylamide/methylene bisacrylamide solution (37.5:1 ratio).
Purchased as 'Protogel', National Diagnostics.

Stock resolving gel buffer. 0.75 M Tris/HCl, pH 8.3.

90.86 gL⁻¹ Tris hydroxymethyl methylamine, pH to 8.3.

Stock stacking gel buffer. 1.25 M Tris/HCl, pH 6.8.

151.46 gL⁻¹ Tris hydroxymethyl methylamine, pH to 6.8.

20% Sodium dodecyl sulphate (SDS)

20 g SDS in 100 mL distilled water.

Sample buffer

0.125 M Tris/HCl, pH 6.8 supplemented with 20 gL⁻¹ SDS, 50 mgL⁻¹ bromophenol blue and 20% (v/v) glycerol. Supplement each 1 mL with 87 µL β-mercaptoethanol immediately before use.

Stock electrode buffer

150 gL⁻¹ glycine and 30 gL⁻¹ Tris hydroxymethyl methylamine.

Working electrode buffer

1:10 dilution of stock electrode buffer supplemented with 0.1% SDS.

0.2% Coomassie brilliant blue

2 gL⁻¹ Coomassie brilliant blue dissolved in 400 mL distilled water, 500 mL methanol and 100 mL glacial acetic acid.

Fast destain

40% methanol, 10% acetic acid, 50% distilled water.

Slow destain

10% methanol, 10% acetic acid, 80% distilled water.

Shrink solution

45% methanol, 2% glycerol, 50% distilled water.

Table 2.3. *E. coli* K-12 strains used in this study.

Strain	Description	Source
JCB 387	RV <i>nir lac</i>	Page <i>et al.</i> , 1990
JCB 3871	JCB 387 <i>fis985</i> (str/spc ^R)	Wu <i>et al.</i> , 1998
JCB 3875	JCB 387 <i>narP253::Tn10d</i> (Cm)	Tyson <i>et al.</i> , 1994
JCB 3883	JCB 387 <i>narL</i>	Tyson <i>et al.</i> , 1993
JCB 3884	JCB 387 <i>narL narP253::Tn10d</i> (Cm)	Tyson <i>et al.</i> , 1994
JCB 3901	JCB 387 Δ <i>nsrR::kan</i>	Squire, PhD Thesis, 2009
JCB 3902	JCB 387 Δ <i>fnr::cat</i> Δ <i>nsrR::kan</i>	Squire, PhD Thesis, 2009
JCB 3911	JCB 387 Δ <i>fnr::cat</i>	Squire <i>et al.</i> , 2009
JCB 4011	RK4353 Δ <i>napA-B</i> Δ <i>narZ::</i> Ω	Potter <i>et al.</i> , 1999
JCB 4022	RK4353 Δ <i>narG::ery</i> Δ <i>napA-B</i>	Potter <i>et al.</i> , 1999
JCB 4031	RK4353 Δ <i>narZ::</i> Ω <i>narG-I</i>	Potter <i>et al.</i> , 1999
JCB 4053	JCB 4031 <i>narL::Tn10</i> Δ <i>napGH</i> Δ <i>nrfAB::cat</i>	Constructed by H. Brondijk, University of Birmingham
JCB 4081a	JCB 4031 <i>narL::Tn10</i> Δ <i>nrfAB</i> Δ <i>nirBDC::kan</i>	Constructed by H. Brondijk, University of Birmingham
JCB 4999	RK4353 Δ <i>hcp::cat</i>	Fileenko, PhD Thesis, 2005
JCB 5100	RK4353 Δ <i>yeaRyoaG::cat</i>	Squire, PhD Thesis, 2009
JCB 5201	<i>ytfE:: cat</i>	K-12 ATCC 23716 transduced with P1 propagated on RK4353 Δ <i>ytfE</i>

JCB 5202	<i>ytfE::cat</i>	K-12 ATCC 23716 transduced with P1 propagated on LMS 4209
JCB 5203	<i>ytfE::cat</i>	K-12 ATCC 23716 transduced with P1 propagated on RK4353 Δ ytfE
JCB 5204	<i>ytfE::cat</i>	K-12 ATCC 23716 transduced with P1 propagated on LMS 4209
JCB 5205	Δ nirBDC:: <i>kan</i>	RK4353 transduced with P1 propagated on JCB 4081a
JCB 5206	Δ nrfAB:: <i>cat</i>	RK4353 transduced with P1 propagated on JCB 4053
JCB 5207	RK4353 Δ ygbA:: <i>cat</i>	Constructed by L. Griffiths for this work
JCB 5208	RK4353 Δ yibIH:: <i>cat</i>	Constructed by L. Griffiths for this work
JCB 5215	RK4353 Δ narL:: <i>cat</i>	This work
JCB 5217	RK4353 Δ norVW:: <i>cat</i>	RK4353 transduced with P1 propagated on LMS 2710 prior to this work
JCB 5219	RK4353 Δ hmp:: <i>kan</i>	This work
JCB 5222	RK4353 Δ nsrR:: <i>kan</i>	RK4353 transduced with P1 propagated on JCB 3901
K-12 ATCC 23716	Parental strain	ATCC
LMS 2710	K-12 ATCC 23716 Δ norVW:: <i>cat</i>	Justino <i>et al.</i> , 2005
LMS 4209	<i>ytfE::cat</i>	Justino <i>et al.</i> , 2005
RK4353	<i>lacU169 araD139 rpsL gyrA non</i>	Stewart and McGregor, 1982
RK4353 Δ ytfE	RK4353 Δ ytfE:: <i>cat</i>	RK4353 transduced with P1 propagated on LMS 4209

(0.7 mL) and 0.3 mL sterile glycerol (50% v/v) were added to a sterile screw-top 2 mL tube, and the contents were vortexed to mix. The tube was snap frozen by submerging for a few seconds in liquid nitrogen and was stored at -80°C.

Plasmids.

Plasmids were isolated by small scale DNA purification using a QIAprep Spin Miniprep kit as described by the manufacturer. Plasmids used in this work are shown in Table 2.4.

Preparation of competent *E. coli* cells.

A single colony was used to inoculate LB (1 mL) supplemented with any relevant antibiotics, and the culture was aerated at 37°C overnight. The overnight culture (200 µL) was used to inoculate LB (20 mL) containing any relevant antibiotics, then the culture was aerated at 37°C for around 2 hours until the optical density at 650 nm had reached 0.5. The bacteria were collected by centrifugation (4000 g, 3 minutes), the supernatant was discarded and the bacteria were resuspended in TFB1 buffer (Table 2.2) and were incubated on ice for 90 minutes. The bacteria were collected by centrifugation (4000 g, 3 minutes), the supernatant was discarded and the bacteria were resuspended in 0.1 M CaCl₂ supplemented with 15% (v/v) glycerol. Aliquots (100 µL) were snap-frozen by submerging in liquid nitrogen for a few seconds and were stored at -80°C.

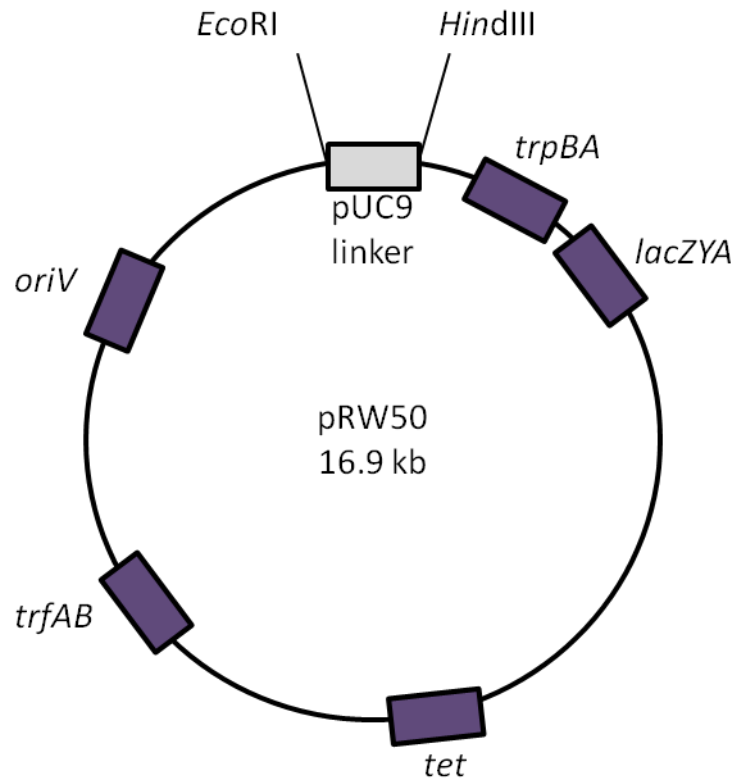
Transformation of *E. coli* with plasmid DNA.

Plasmid DNA (5 to 50 ng) was mixed with competent cells (50 µL), and the mixture was incubated on ice for 40 minutes. The bacteria were heat-shocked at 42°C for 2 minutes then incubated on ice for 2 minutes. The bacteria were resuspended in LB or SOC broth (1 mL) and were transferred to a sterile test tube. The culture was aerated at 37°C for 1 hour to allow bacteria to recover and to express the antibiotic resistance proteins. An aliquot (100 µL) was plated onto selective agar and incubated at 37 °C overnight.

Table 2.4. **Plasmids used in this work.**

Plasmid	Description	Reference or source
FF gal Δ 4	A synthetic Fnr repressed promoter fused to <i>lacZ</i> in pRW50.	Williams <i>et al.</i> , 1998
pCA24n2	The His-tagged <i>hcp</i> gene is cloned under the control of an IPTG-inducible promoter. (Figure 2.2)	Kitagawa <i>et al.</i> , 2005
pCL775	A high copy number λ -promoter expression vector carrying <i>hmp</i> . Amp ^R .	Love <i>et al.</i> , 1996
pCP20	Expresses the Flp recombinase gene (<i>exo</i>) under the control of a heat sensitive promoter (active at 30°C). Chlor ^R and Carb ^R .	Datsenko and Wanner, 2000
pCV01	<i>pytjE</i> cloned into the <i>EcoR</i> 1/ <i>Hind</i> III restriction sites of pRW50. Tet ^R .	This work
pKD3	To be used as a PCR template to create replacement of genes with a chloramphenicol resistance cassette. Can only be maintained in <i>E. coli</i> BW25141. Chlor ^R and Carb ^R .	Datsenko and Wanner, 2000
pKD4	To be used as a PCR template to create replacement of genes with a kanamycin resistance cassette. Can only be maintained in <i>E. coli</i> BW25141. Kan ^R and Carb ^R .	Datsenko and Wanner, 2000
pKD46	Expresses λ red, γ , β , and <i>exo</i> genes under the control of the <i>araB</i> promoter. Has a temperature sensitive origin of replication (active at 30°C), Carb ^R .	Datsenko and Wanner, 2000
pNF383	The <i>hcp</i> regulatory region cloned into pPRW50 to give an <i>hcp:lacZ</i> fusion. Tet ^R .	Fileenko <i>et al.</i> , 2007
pPL341	pBR322 carrying <i>hmp</i> under its own promoter. Amp ^R .	Vasudevan <i>et al.</i> , 1991
pRW50	<i>lacZ</i> fusion vector for cloning promoters as <i>EcoR</i> 1/ <i>Hind</i> III fragments for β -galactosidase assays. Contains the RK2 origin of replication. Tet ^R . (Figure 2.1).	Lodge <i>et al.</i> , 1992
pSP01	<i>phmp</i> cloned into the <i>EcoR</i> 1/ <i>Hind</i> III restriction sites of pRW50. Tet ^R .	This work

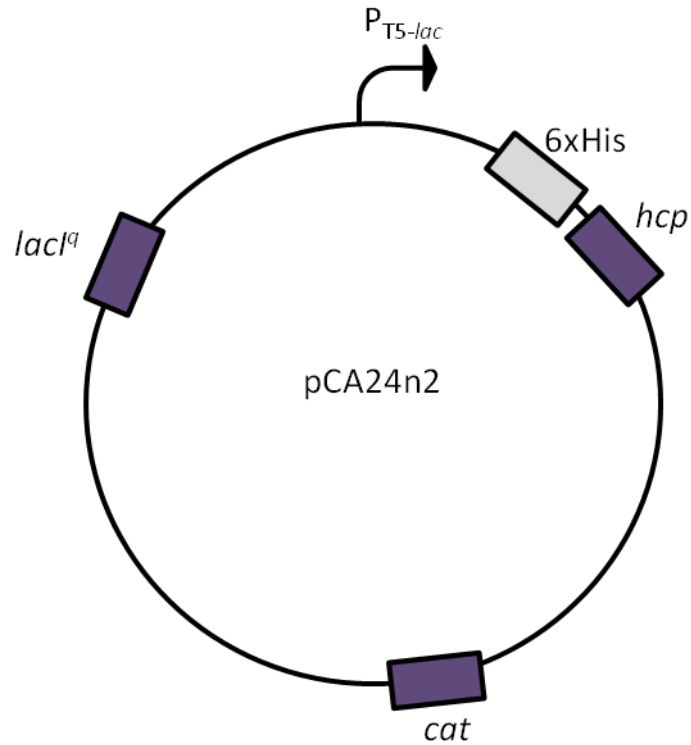
Figure 2.1



The *lacZ* fusion vector, pRW50.

In pRW50, *EcoRI/HindIII* promoter fragments are cloned into the pUC9 linker (grey) as transcriptional fusions to the *trpBA* and *lacZYA* operons, such that expression of the *lac* genes is dependent on the cloned promoter. Also depicted are the origin of replication (*oriV*), plasmid replication genes (*trfAB*) and the tetracycline resistance gene (*tet*).

Figure 2.2



The Hcp expression vector, pCA24n2.

pCA24n2 is a high copy number plasmid (a ColE1 derivative) that originated from the commercially available expression vector pQE30. Expression of *hcp* is directed by the IPTG inducible promoter, P_{T5-lac} , and is repressed by $lacI^q$. A histidine tag is attached to the N terminal end of the *hcp* gene (shaded grey); the two are separated by seven spacer amino acids. The plasmid encodes chloramphenicol resistance (*cat*).

P1 transduction.

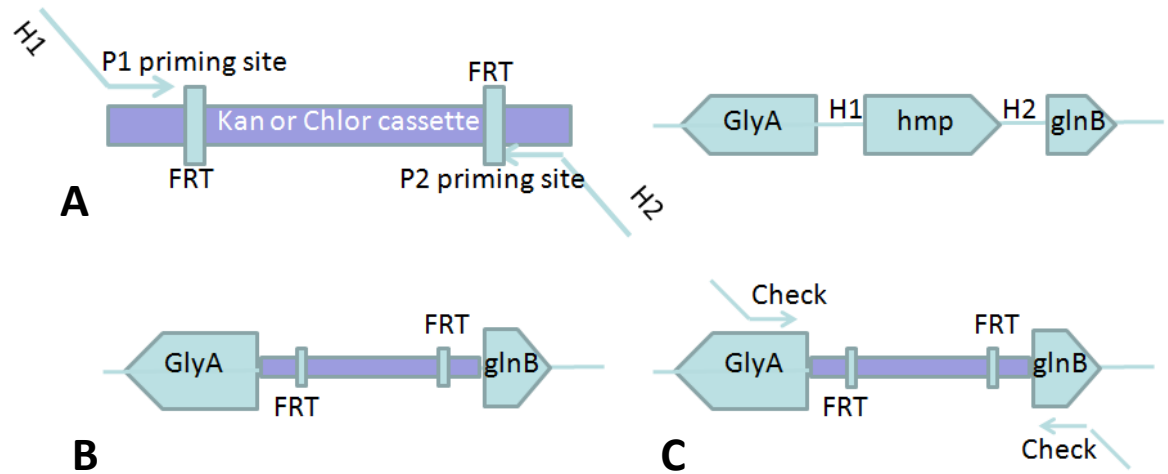
Antibiotic resistant donor strains were grown in LB supplemented with 2 mM CaCl_2 (LB- Ca^{2+}) until the optical density at 650 nm had reached 0.7 to 0.8. The stock of bacteriophage P1 was serially diluted in LB- Ca^{2+} to give a range from a 10^{-1} dilution to 10^{-6} . LB was autoclaved with 1.25% bacteriological agar to give Lennox agar (LA). Lennox agar was supplemented with 0.2% glucose and 2 mM CaCl_2 and 1 mL aliquots were transferred to 6 sterile test tubes containing 2 mL LB- Ca^{2+} at 45°C. Donor culture (0.1 mL) and a dilution of bacteriophage (0.1 mL) were added to each tube of soft agar and after mixing the whole contents of the tube were poured over a supplemented LA plate. The plates were incubated at 37°C overnight. LB- Ca^{2+} (2 mL) was added to plates with a 'lacey' pattern of plaque formation, where plaques were very close together, but did not show zones of confluent lysis. The soft agar was broken up with a dry glass spreader and homogenised with 1 mL chloroform. The mixture was centrifuged (8000 g, 15 min), and the clear supernatant containing the phage was stored in 1 mL chloroform at 4°C. Recipient strains were grown in 20 mL LB- Ca^{2+} until the optical density at 650 nm had reached 0.7 to 0.8. The bacteria were collected in three separate aliquots by centrifugation (3600 g, 3 min) and each cell pellet was resuspended in 0.5 mL LB- Ca^{2+} . The bacteriophage propagated on the donor bacterium was diluted 1:10 using LB- Ca^{2+} . Concentrated P1 (0.1 mL) was added to the first tube, diluted P1 (0.1 mL) was added to the second tube and the third tube was left as a no P1 control. All three tubes were incubated statically at 37°C for 18 min, just under the time for a single cycle of phage replication. MS (1 mL) was added to each tube then the bacteria were collected by centrifugation (3600 g, 3 min). The supernatant was discarded, and the bacteria were resuspended in 4 mL MS. The bacteria were collected by centrifugation

(3600 g, 3 min) and washed three further times to remove excess P1. The final cell pellet was resuspended in 1 mL LB and aerated at 37°C for 2 hours to allow the bacteria to recover, and antibiotic resistance proteins to be expressed. Bacteria (0.1 mL) were plated onto selective plates and incubated at 37°C overnight.

Generation of *hmp* and *narL* deletion mutants.

The method of Datsenko and Wanner (2000) was used in this work. This involves the replacement of the gene of interest with a chloramphenicol or kanamycin resistance cassette (Figure 2.3). RK4353 cells were transformed with pKD46, a plasmid that has a temperature sensitive origin of replication that is active at 30°C. PCR was used to amplify the chloramphenicol resistance cassette from pKD3 using the primers DW NarL forward and DW NarL reverse (Table 2.4) to introduce flanking regions homologous to the *narL* locus in *E. coli* RK4353. PCR was also used to amplify the kanamycin resistance cassette from pKD4 using the primers DWhmpF and DWhmpR (Table 2.6) to introduce flanking regions homologous to the *hmp* locus in RK4353. In both cases, six PCR reactions were set up in parallel to generate a high concentration of linear DNA. Each PCR reaction was purified using a QIAquick PCR purification kit then digested overnight with *DpnI* (1 U). The PCR products were concentrated by using a single QIAquick PCR purification column to purify three digests, and eluting the DNA in 30 µL EB (10 mM Tris-HCl, pH 8.5). A single colony of RK4353 transformed with pKD46 was used to inoculate 1 mL LB supplemented with carbenicillin and the culture was aerated at 30°C overnight. The overnight culture (200 µL) was used to inoculate 10 mL LB, which was aerated at 30°C until the optical density at 650 nm had reached 0.3. The bacteria were collected in 1.4 mL aliquots by centrifugation (13000 g, 2 min) and 0.35% (w/v) arabinose was added to three of the tubes. The final tube was

Figure 2.3.



The Datsenko and Wanner method of chromosomal inactivation, using the method of *hmp::kan* construction as an example.

PCR primers provide the homology to the targeted gene (denoted H1 and H2 in panel A), and are used to amplify a kanamycin or chloramphenicol resistance cassette from the plasmid pKD4 or pKD3, respectively. The linear PCR product is electroporated into wild type *Escherichia coli* cells then recombines onto the chromosome, mediated by the phage λ red recombinase that is synthesised under the control of an arabinose inducible promoter from plasmid pKD46. This recombinase includes the *gam* (γ), *bet* (β) and *exo* gene products, which prevents degradation of linear DNA by inhibiting the host RecBDC exonuclease V, protects single stranded overhangs and assists recombination, and generates single stranded overhangs on introduced linear DNA by 5' to 3' exonuclease activity, respectively. The result of the procedure is a chromosomal antibiotic resistance cassette, flanked by two FLP recognition target sites, in place of the gene of interest (FRT sites, panel B). The presence or absence of the cassette can be checked by colony PCR, using primers which anneal to sequences either side of the gene of interest (panel C). The resistance gene can be eliminated by using the helper plasmid pCP20 that encodes FLP recombinase.

left as a no arabinose control. All tubes were aerated at 37°C for 1 hour to stop the replication of pKD46. The bacteria were collected by centrifugation (13000 g, 2 min) and the supernatant was discarded and the bacteria were resuspended in 1 mL ice cold sterile glycerol (10% v/v). The bacteria were collected by centrifugation (13000 g, 2 min) and were washed in ice cold glycerol 3 further times. The final cell pellet was resuspended in 200 µL ice cold glycerol (10% v/v). PCR product (200 ng) was added the electrocompetent bacteria in one tube, and gently mixed by pipetting. The mixture was transferred to an electroporation cuvette, and a 1.8 kV pulse was applied. Prewarmed SOC medium (1 mL) was added to the cells immediately, and the resuspended bacteria were transferred to a sterile test tube. The electroporation procedure was repeated with a second tube then electroporation was completed for a no DNA control and the no arabinose control. All cultures were aerated at 37°C for 2 hours to allow the bacteria to recover and the antibiotic resistance proteins to be expressed. The recovery mixture (0.5 mL) was plated onto selective agar plates and incubated at 37°C, or longer, until colonies appeared. The chromosomal replacements were checked by PCR using primers which flank the gene of interest, in combination with the primers KD3_{C1}, KD3_{C2}, KD4_{K1} and KD4_{K2}, which anneal to the chloramphenicol and kanamycin resistance cassettes respectively. Strains JCB 5215 (*narL::cat*) and JCB 5219 (*hmp::kan*) had been successfully constructed.

Removal of the antibiotic resistance cassette using FRT sites.

Plasmid DNA (5 ng, pCP20) was mixed with 50 µL of the kanamycin or chloramphenicol resistant competent cells from which the antibiotic resistance cassette was to be removed, then the mixture was incubated on ice for 40 minutes. The bacteria were heat-shocked at 42°C for 2 minutes then incubated on ice for 2 minutes. The

bacteria were resuspended in 1 mL LB then were transferred to a sterile test tube. The culture was aerated at 30°C for 1 hour to allow bacteria to recover and express the antibiotic resistance proteins. An aliquot (100 µL) was plated onto NA supplemented with carbenicillin and the plate was incubated at 30°C overnight. Individual transformants were purified on nutrient agar, and the plates were incubated at 42°C overnight so that the temperature sensitive plasmid pCP20 would not be replicated. Single colonies were then ‘patch’ plated onto three plates; unsupplemented nutrient agar, nutrient agar supplemented with carbenicillin and nutrient agar supplemented with kanamycin or chloramphenicol. Colonies that were sensitive to both antibiotics but that grew on nutrient agar were tested by colony PCR, using primers that flank the gene of interest, for the presence of an 82 bp scar in place of the kanamycin or chloramphenicol cassette.

Construction of an isogenic set of *nirBDC* and *nrfAB* mutants.

P1 transduction was used to transfer the *nirBDC::kan* mutation from strain JCB 4081a to RK4353 and the *nrfAB::cat* mutation from strain JCB 4053 to RK4353. Colony PCR was used to check that the resultant kanamycin or chloramphenicol resistant colonies had been successfully transduced, using primers which annealed either side of the target gene, in combination with primers that anneal close to the 5' and 3' ends of antibiotic resistance cassettes. The same method of colony PCR was used in every subsequent strain construction by P1 transduction described in this chapter, using appropriate primers that anneal to the mutated loci. PCR analysis confirmed that the *nirBDC* and *nrfAB* mutations were correct (Figure 2.4). As these transductants were correct, a complete set of isogenic RK4353 mutants, JCB 5205 (*nirBDC*), JCB 5206 (*nrfAB*) and JCB 4031 (*narG-I narZ*), was available for further experiments.

Construction of an *nsrR* mutant.

The *nsrR::kan* mutation was transferred by P1 transduction from strain JCB 3901 to strain RK4353. Colony PCR confirmed that the *nsrR* mutation was correct, and that strain JCB 5222 had been successfully constructed.

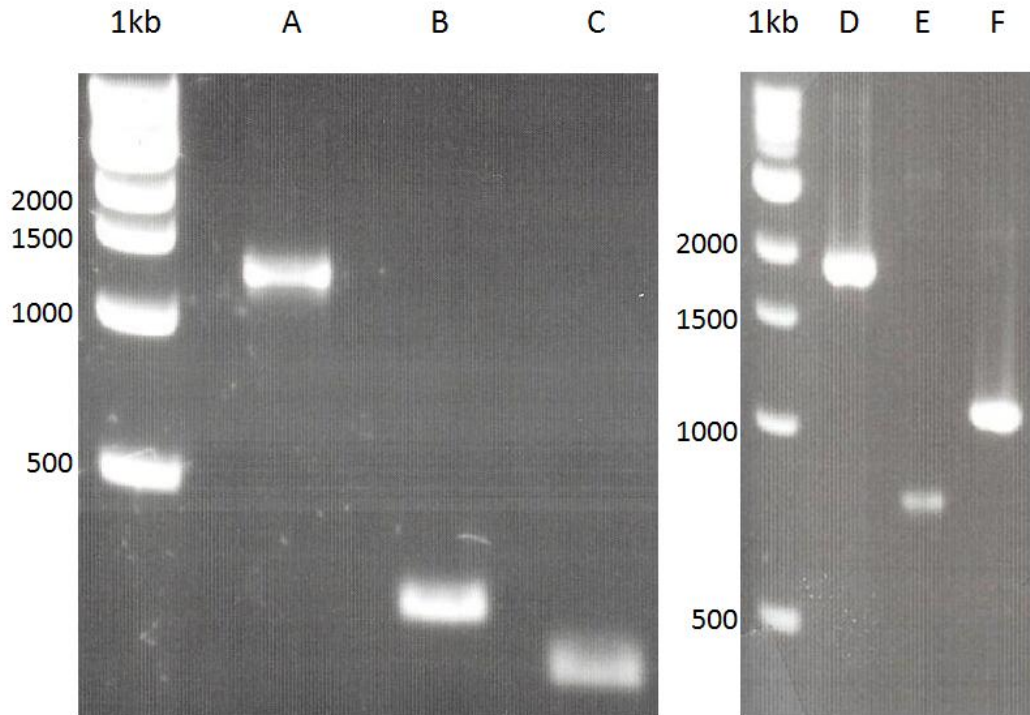
Construction of mutants defective in a combination of proteins implicated in nitrosative stress.

Based on results with the single mutant strains introduced in this chapter, it was also necessary to combine various mutations to generate strains that were defective in two to eight different proteins implicated in the nitrosative stress response. In every case, the procedure described in Figure 2.5 was used. Briefly, strains were constructed by bacteriophage P1 transduction of a deletion marked with an antibiotic resistance cassette, followed by the pCP20 mediated removal of the *kan* or *cat* cassette. Each mutated locus was checked by PCR at every stage to ensure that the correct mutation had been made. Strains with multiple mutations, and the details of the particular transduction completed are listed in Table 2.5.

Growth assays for comparison with experiments reported in Justino *et al.*, 2006.

Bacteria were grown in minimal salts medium (MS, Pope and Cole, 1984), supplemented where indicated with 0.4% glycerol, 5% LB, and either 40 mM sodium nitrate, 40 mM sodium fumarate and 5 mM sodium nitrite, or 40 mM dimethyl sulphoxide. All cultures were started with 2% inocula that had been grown at 37°C with aeration in 5 mL LB in 25 mL conical flasks overnight. Anaerobic cultures were incubated statically at 37°C either in 100 mL flasks filled with 100 mL of medium, or test tubes filled with 15 mL of medium. The optical density at 650 nm was monitored at hourly intervals, for at least 6 hours and reported results are representative of at least

Figure 2.4.

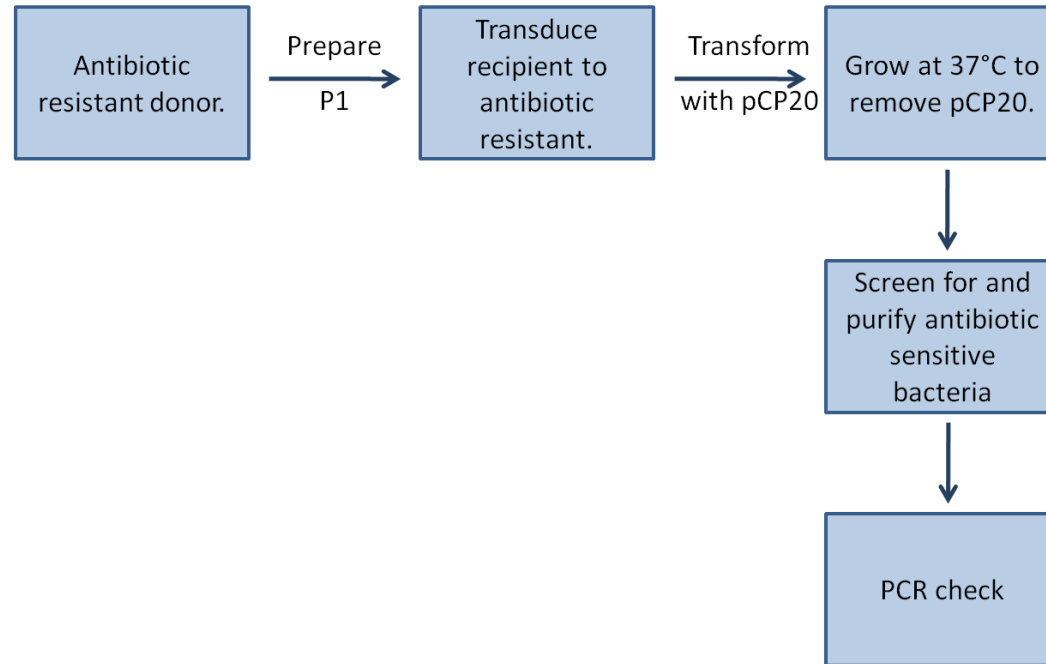


Lane	Template	Forward Primer	Reverse Primer	Expected size (bp)
A	JCB 5206	nrfA flank F	nrfB flank R	1315
B	JCB 5206	nrfA flank F	KD3 _{C1}	258
C	JCB 5206	KD3 _{C2}	nrfB flank R	183
D	JCB 5205	nirB flank F	nirC flank R	2030
E	JCB 5205	nirB flank F	KD4 _{K1}	746
F	JCB 5205	KD4 _{K2}	nirC flank R	1035

PCR analysis for the presence of the *cat* or *kan* cassette in transductant candidates.

Strains JCB 5206 and JCB 5205 were grown on agar plates and were tested by colony PCR, using the primer combinations shown in the table. PCR products were visualised using agarose gel electrophoresis. 1 kb DNA marker (New England Biolabs, band sizes (bp) are shown to the left) was used as a reference. Each new strain made by P1 transduction was checked in this manner, and this detailed analysis is given as an example.

Figure 2.5.



The procedure used to generate strains containing several mutations.

Schematic representation of the bacteriophage P1 transduction method used to generate strains defective in two to eight proteins implicated in the nitrosative stress response. It was critical that at every stage the recipient strain was sensitive to the antibiotic with which the donor mutation was marked, so pCP20 was used to remove the antibiotic resistance cassette in each newly constructed mutant to leave an unmarked 82 bp ‘scar’ in place of each target gene.

Table 2.5. Strains with multiple mutations made by bacteriophage P1 transduction for this work.

Strain	Description	Source
JCB 5210	RK4353 $\Delta nirBDC \Delta nrfAB \Delta norVW \Delta hmp::kan$	JCB 5233 transduced with P1 propagated on JCB 5219
JCB 5225	RK4353 $\Delta nirBDC::kan \Delta nrfAB::cat$	JCB 5206 transduced with P1 propagated on JCB 5205
JCB 5226	RK4353 $\Delta nirBDC \Delta nrfAB$	JCB 5207 cured of antibiotic resistance using pCP20
JCB 5230	RK4353 $\Delta nirBDC \Delta nrfAB \Delta hcp::cat$	JCB 5226 transduced with P1 propagated on JCB 4999
JCB 5231	RK4353 $\Delta nirBDC \Delta nrfAB \Delta hmp::kan$	JCB 5226 transduced with P1 propagated on JCB 5219
JCB 5232	RK4353 $\Delta nirBDC \Delta nrfAB \Delta norVW::cat$	JCB 5226 transduced with P1 propagated on JCB 5217
JCB 5233	RK4353 $\Delta nirBDC \Delta nrfAB \Delta norVW$	JCB 5232 cured of antibiotic resistance using pCP20
JCB 5234	RK4353 $\Delta nirBDC \Delta nrfAB \Delta hcp$	JCB 5230 cured of antibiotic resistance using pCP20
JCB 5235	RK4353 $\Delta narZ::\Omega \Delta narGHJI \Delta nirBDC::kan$	JCB 4031 transduced with P1 propagated on JCB 5205
JCB 5236	RK4353 $\Delta narZ::\Omega \Delta narGHJI \Delta nrfAB::cat$	JCB 4031 transduced with P1 propagated on JCB 5206
JCB 5241	RK4353 $\Delta nirBDC \Delta nrfAB \Delta hcp::cat \Delta hmp::kan$	JCB 5234 transduced with P1 propagated on JCB 5219
JCB 5242	RK4353 $\Delta nirBDC \Delta nrfAB \Delta norVW \Delta hcp::cat$	JCB 5233 transduced with P1 propagated on JCB 4999
JCB 5244	JCB 5236 $\Delta hmp::kan$	JCB 5236 transduced with P1 propagated on JCB 5219
JCB 5246	JCB 5236 Δhmp	JCB 5244 cured of antibiotic resistance using pCP20

JCB 5250	JCB 5210 $\Delta hcp::cat$	JCB 5210 transduced with P1 propagated on JCB 4999
JCB 5251	JCB 5210 $\Delta fnr::cat$	JCB 5210 transduced with P1 propagated on JCB 3911
JCB 5252	JCB 5210 $\Delta narL::cat$	JCB 5210 transduced with P1 propagated on JCB 5215
JCB 5253	JCB 5210 Δhcp	JCB 5250 cured of antibiotic resistance using pCP20
JCB 5256	JCB 5246 $\Delta norVW::cat$	JCB 5246 transduced with P1 propagated on JCB 5217
JCB 5257	JCB 5210 $\Delta ytfE::cat$	JCB 5210 transduced with P1 propagated on RK4353 $\Delta ytfE::cat$
JCB 5260	JCB 5253 $\Delta ytfE::cat$.	JCB 5253 transduced with P1 propagated on RK4353 $\Delta ytfE::cat$
JCB 5261	JCB 5253 $\Delta ygbA::cat$.	JCB 5253 transduced with P1 propagated on JCB 5207
JCB 5262	JCB 5253 $\Delta yeaR-yoaG::cat$	JCB 5253 transduced with P1 propagated on JCB 5100
JCB 5263	JCB 5253 $\Delta yibIH::cat$	JCB 5253 transduced with P1 propagated on JCB 5208
JCB 5264	JCB 5256 $\Delta nirBDC::kan$	JCB 5256 transduced with P1 propagated on JCB 5205
JCB 5265	JCB 5256 $\Delta nirBDC$	JCB 5264 cured of antibiotic resistance using pCP20
JCB 5270	JCB 5265 $\Delta hcp::cat$	JCB 5265 transduced with P1 propagated on JCB 4999
JCB 5271	JCB 5265 Δhcp	JCB 5270 cured of antibiotic resistance using pCP20
JCB 5280	JCB 5265 $\Delta hcp \Delta ytfE::cat$	JCB 5271 transduced with P1 propagated on JCB 5260

two independent assays, unless otherwise stated.

Growth assays.

For all other growth experiments, bacteria were grown in MS medium supplemented with 5% LB, 0.4% glycerol, 20 mM tri-methylamine-N-oxide (TMAO) and 20 mM sodium fumarate. This growth medium was selected for two reasons. First, in the presence of both TMAO and fumarate, an *fnr* mutant is able to grow at a similar rate to the parent strain. A microarray study of the Fnr regulon that identified genes of interest explored in this work, was completed under these conditions and hence work in this study should be consistent (Constantinidou *et al.*, 2006). Secondly, Metheringham and Cole (1997) found that in the presence of glycerol and fumarate, highest rates of nitrosation were recorded. As this work focuses on genes critical in the nitrosative stress response, such an effect is desirable. All cultures were started with 2% inocula that had been grown at 37°C with aeration in 5 mL LB in 25 mL conical flasks overnight. Anaerobic cultures were incubated statically at 37°C either in 100 mL flasks filled with 100 mL of medium, or test tubes filled with 15 mL of medium. Aerobic cultures were shaken at 100 rpm at 37 °C.

β-galactosidase assays.

For β-galactosidase assays the method described by Jayaraman *et al.*, (1987) was used. Bacteria were grown in medium as described in the previous section, supplemented with 35 μg mL⁻¹ tetracycline. Aerobic cultures were shaken at 100 rpm at 37 °C. Both aerobic and anaerobic cultures were monitored until the optical density at 650 nm had reached 0.19-0.22 or 0.6-0.7, respectively. An aliquot of culture (2 mL) was lysed using 30 μL sodium deoxycholate (1%) and 30 μL toluene, then the toluene was evaporated by aeration at 37°C for 20 minutes. The lysate (100 to 400 μL), or lysate diluted 2- to 5-fold in 1xA, was added to 1.6 to 1.9 mL Z buffer and then the total volume of 2 mL was

prewarmed at 37°C. ONPG (13 mM, 0.5 mL) was added, and the reaction was incubated at 37°C until the colour was visibly yellow. The reaction was stopped at a known incubation time with 1 mL sodium carbonate (1 M) and then the absorbance of the mixture at 420 nm was recorded. The β -galactosidase activity (nmol ONPG hydrolysed min^{-1} (mg dry mass bacteria) $^{-1}$) was calculated using Equation 2.1 below, where d represents the dilution factor of the lysate, 2.5 is the coefficient used to convert absorbance at 650 nm into mg dry mass bacteria, 3.5 represents the total reaction volume (mL), T represents the incubation time of the reaction (min), 4.5 is the molar extinction coefficient for ortho-nitrophenol and v represents the volume of lysate added (mL).

Equation 2.1.

$$\text{Activity} = \frac{A_{420}}{A_{650}} \times \frac{1000 \times d \times 2.5 \times 3.5}{T \times 4.5 \times v}$$

Unless otherwise stated, reported results are representative of at least two independent experiments, and error bars represent the standard deviation of these repeats.

Preparation of nitric oxide saturated water (NOSW).

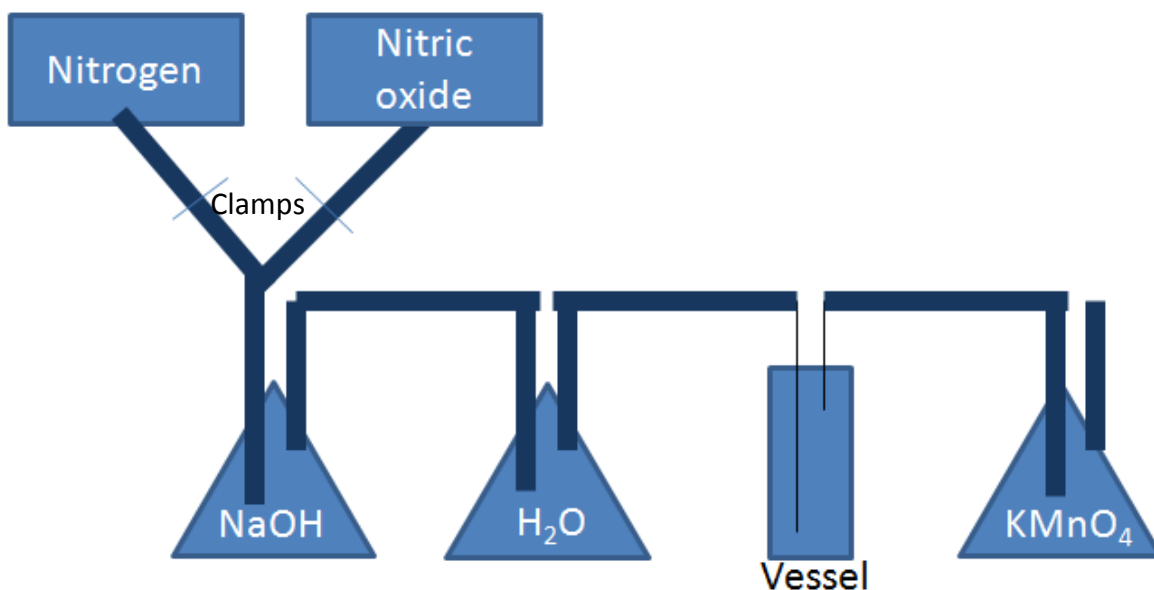
Distilled water (5 mL) was pipetted into a glass bijoux bottle, which was then closed with a turnover rubber stopper (Fisher Scientific, Leicestershire, UK). A small amount of silicone grease was applied to the rubber septum then two needles were inserted into the bottle; one to the bottom of the liquid and a shorter one into the headspace. Nitrogen and nitric oxide cylinders (BOC gases, Surrey, UK) were attached by silicone tubing, through conical flasks of distilled water and NaOH (3 M), to the needles in the vessel (Figure 2.6). The water was bubbled first with nitrogen for 30 minutes, then with nitric oxide for 30 minutes to produce water that was saturated with nitric oxide (2 mM). The needles were removed and the bottles were sealed with Parafilm sealing film to prevent

any oxygen leaking into the vessel. When required, nitric oxide saturated water (NOSW) was removed from the bottles using a syringe and needle. A similar set of equipment was used to degas assay buffer for use in the NO electrode. A glass bottle (capacity 50 mL) was filled with assay buffer, and then sealed with a turnover rubber stopper (Fisher Scientific, Leicestershire, UK). A small amount of silicone grease was applied to the rubber septum and two needles were inserted into the bottle; one to the bottom of the liquid and a shorter one into the headspace. A nitrogen cylinder (BOC gases, Surrey, UK) was attached by silicone tubing to the longer needle while the short needle was left unattached to allow gas to equilibrate out of the bottle. The buffer was bubbled with nitrogen for 30 minutes to expel oxygen and was covered with Parafilm sealing film to prevent oxygen leaking into the vessel.

Growth and β -galactosidase assays in response to the addition of nitrate, nitrite or NO.

The strain to be tested was transformed with pNF383, pSP01, pCV01 or FF gal $\Delta 4$, plasmids that encode the *hcp*, *hmp*, *ytfE*, and synthetic consensus Fnr-repressed promoter regions, respectively, fused to *lacZ* in pRW50. Purified transformants were grown anaerobically in medium supplemented 35 $\mu\text{g mL}^{-1}$ tetracycline, in duplicate test tubes filled with 15 mL medium. The optical density at 650 nm was monitored until it had reached 0.2, then one tube was left as an unsupplemented control, while the other was supplemented with 2.5 to 10 mM nitrite, 1 to 20 mM nitrate or 5 to 20 μM NOSW, as indicated in the text. NOSW was added repeatedly at 30 min. intervals under the surface of the culture using a sterile syringe and needle to avoid exposure to oxygen. A magnetic stirrer was used very briefly to ensure the supplement was distributed evenly throughout the culture, but to avoid aeration. Cultures were incubated statically at 37°C. The optical density at 650nm was monitored for at least 2 hours following the nitrite pulse, and 1 mL samples were taken every 30 minutes for 2 hours, and were lysed to be assayed for β -galactosidase activity.

Figure 2.6.



The apparatus required to generate nitric oxide saturated water.

To make the vessel of pH 3 water anaerobic, the clamp (denoted by a thin blue line perpendicular to the silicone tubing, shown in darker blue lines) to the nitric oxide cylinder was first closed and the clamp to the nitrogen cylinder was opened. The apparatus was checked for leaks then the regulator of the nitrogen cylinder was opened to allow a steady stream of bubbles to flow throughout the apparatus. This bubbling was maintained for 30 minutes, then the clamp to the nitrogen cylinder was closed and the clamp to the nitric oxide cylinder was released. The nitric oxide flow was turned on and the system was bubbled for 30 minutes with nitric oxide. The vessel was removed and the silicone tubing from the conical flask of water was connected to the conical flask of 1 M KMnO₄ (to scrub exhaust before release into fume cupboard). The apparatus was bubbled with nitrogen to a few seconds to expel nitric oxide, then both cylinders were switched off.

Effect of NO on bacterial growth.

Bacteria were grown in MS supplemented as described previously. Once the optical density at 650 nm had reached 0.15 or above, NOSW (5–100 μ M) was added under the surface of the culture using a sterile syringe and needle to avoid exposure to oxygen. A magnetic stirrer was used very briefly to ensure the NOSW was distributed evenly throughout the culture, but to avoid aeration. The cultures were reincubated statically at 37°C.

Growth and preparation of bacteria for use in the nitric oxide electrode.

Bacteria were grown in MS supplemented where indicated with 10% LB, 0.4% glycerol, 20 mM TMAO, 20 mM sodium fumarate and 2.5 mM sodium nitrite or 20 mM sodium nitrate. All cultures were started with inocula that had been grown at 37°C with aeration in 2 mL LB in a test tube for at least 2 hours. Anaerobic cultures were incubated statically overnight at 30°C in 250 mL flasks filled with 250 mL of medium. The optical density at 650 nm was monitored until it had reached 0.6 to 0.8, then the bacteria were collected by centrifugation (8000 g , 2 min, 4°C). The bacteria were resuspended in 10 mL phosphate buffer and were homogenised. The washed bacteria were collected by centrifugation (3000 g , 3 min) then resuspended in 0.5 to 1 mL phosphate buffer to give an optical density at 650 nm of 70 to 90. The bacteria were kept on ice until required.

NO electrode assays.

To measure the rate of NO reduction, an Oxytherm electrode control unit was used with an S1/MINI Clark type electrode disc and the Oxygraph Plus data acquisition software (Hansatech Instruments, Norfolk, UK). Reagents were added to the electrode chamber using Gastight High-Performance syringes (Hamilton, Bonaduz, Switzerland). The electrolyte used was 50% saturated KCl solution. To calibrate for the particular bottle of NOSW being used, the following reagents were added to the electrode chamber: 1788 μ L degassed assay buffer; 32 μ L glucose (1 M); 20 μ L glucose oxidase (0.4 U μ l⁻¹) and

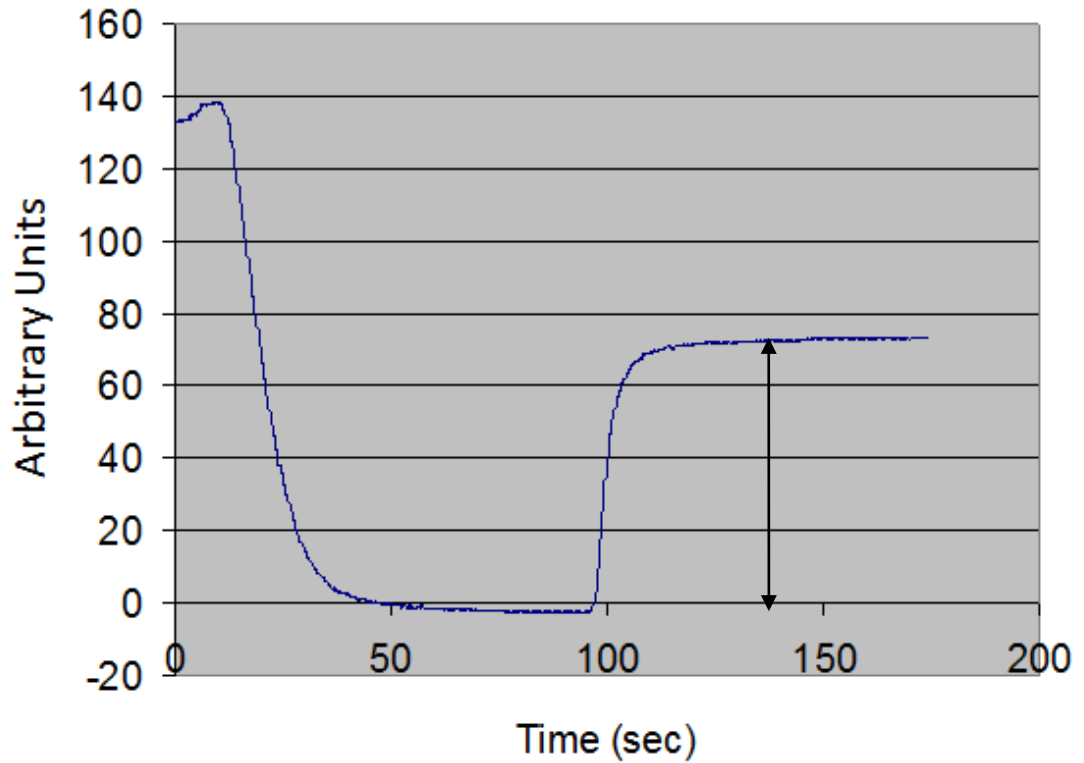
10 μL catalase ($4 \text{ U}\mu\text{L}^{-1}$). The trace was left to stabilise at zero. NOSW (2 mM, 150 μL) was added and the trace was checked carefully to ensure that the reading was in the range expected (50 to 150 units) and that there was no rate of NO reduction when bacteria were absent. The amplitude of the reading given was recorded, for use in the equation to calculate the rate of NO reduction (Figure 2.7). The electrode chamber was washed once with ethanol, and then twice with distilled water. The following experimental reagents were then added to the electrode chamber; 1688 μL degassed assay buffer; 32 μL glucose (1 M); 20 μL glucose oxidase ($0.4 \text{ U}\mu\text{l}^{-1}$); 10 μL catalase ($4 \text{ U}\mu\text{L}^{-1}$) and 100 μL bacterial suspension. The trace was left to stabilise at zero then NO reduction was started by the addition of 150 μL NOSW (2 mM). The rate of NO reduction ($\text{nmol NO reduced min}^{-1} (\text{mg dry cell mass})^{-1}$) was calculated using Equation 2.2.

Equation 2.2.

$$\text{Rate} = \frac{\text{slope} \times (\text{N/amplitude})}{(\text{V} \times 100 \times \text{OD}_{650} \times 0.4)/2}$$

The slope is the initial rate of NO reduction as given by the ‘Rate Measurement’ function of the Oxytherm electrode control unit, N represents the volume of NOSW being used (150 μL unless otherwise stated), ‘amplitude’ represents the increase in arbitrary rate caused by N μL NOSW in the electrode chamber alone (Figure 2.7), and the denominator represents the biomass of bacteria in the chamber: For the biomass value, V (mL) is the volume of cell suspension used, $100 \times \text{OD}_{650}$ is required as the OD_{650} reading taken is a 1:100 dilution, 0.4 is the coefficient to convert absorbance at 650 nm into mg dry cell mass and 2 (mL) is the total volume in the electrode chamber.

Figure 2.7.



An example calibration curve using the Hansatech Oxytherm NO electrode.

This typical electrode trace initially started at around 130 arbitrary units, as not all oxygen was removed by the degassing procedure. The reading rapidly fell to zero following the addition of glucose, glucose oxidase and catalase. Once the trace had stabilised at zero, NOSW was added, and the amplitude of the response (black arrows) was recorded for use in the rate calculation.

Qualitative determination of nitrite presence.

To determine whether or not nitrite was present in 50 μL of a culture, or in 50 μL supernatant taken from a bacterial culture, 50 μL of 1% sulphanilamide in 1M HCl and 200 μL of N-naphthylethylene diamine dihydrochloride were added. In the presence of nitrite ions a pink colour develops. If the test for nitrite is negative, Zn powder can be used to reduce nitrate into nitrite in the sample. Any subsequent formation of a pink colour can be attributed to the presence of nitrate ions in the original sample.

Determination of nitrite concentration.

Samples were taken from cultures, and bacteria were collected by centrifugation (13000 g, 2 min). The supernatant was removed immediately into a separate tube. Clean sterile test tubes were prepared, and 10 to 50 μL of each culture supernatant, 3 mL of 1% sulphanilamide in 1M HCl and 300 μL of N-naphthylethylene diamine dihydrochloride were added. The assay was calibrated in triplicate using either 10 to 50 μL of distilled water (blank) or a known 1 mM sodium nitrite solution (standard) in place of the culture supernatant. All tubes were vortexed and were left for 30 minutes before the optical density at 540 nm was determined.

Quantitative nitrite reduction assay.

Bacteria were grown in 250 mL MS supplemented with 10% LB, 0.4% glucose, 20 mM TMAO, 20 mM sodium fumarate and 2.5 mM sodium nitrite or 20 mM sodium nitrate. The optical density at 650 nm was monitored until it had reached 0.6 to 0.8, then the bacteria were collected by centrifugation (8000 g, 2 min, 4°C). The bacteria were resuspended in 10 mL phosphate buffer and were homogenised. The washed bacteria were collected by centrifugation (3000 g, 3 min) then resuspended in 0.5 to 1 mL phosphate buffer to give an optical density at 650 nm of 70 to 90. The bacteria were kept on ice until required. Bacteria (100 μL), 1M glucose (200 μL) and phosphate buffer (4680 μL) were prewarmed for 5 min at 30°C. 0.1 M sodium nitrite (20 μL) was

added, and the tube was inverted gently to mix. Samples (50 μL) were taken every 3 min, and were pipetted into a test tube containing 1% sulphanilamide in 1M HCl (3 mL). N-naphthylethylene diamine dihydrochloride (300 μL) was added, the contents of the tube were mixed, and the reaction was left to develop for 30 min before the optical density at 540 nm was measured. Standards were set up in triplicate, using 60 μL of 1 mM sodium nitrite, 3 mL of 1% sulphanilamide in 1M HCl and 300 μL of N-naphthylethylene diamine dihydrochloride. The rate of nitrite reduction ($\text{nmol nitrite reduced min}^{-1} (\text{mg dry cell mass})^{-1}$) was calculated using Equation 2.3.

Equation 2.3.

$$\text{Rate of nitrite reduction} = \frac{\Delta A_{540} \text{min}^{-1} \times 30 \times 20 \times 5}{A_{540}(\text{St}) \times 0.1 \times (A_{650}) \times 0.4}$$

In the numerator, 30 represents the concentration of nitrite in the standard (nmol), 20 is required as a conversion factor as only a 50 μL sample of the 5 mL reaction was assayed and 5 (mL) represents the total assay volume. In the denominator, $A_{540}(\text{St})$ was the average optical density at 540 nm of the nitrite standard, 0.1 (mL) was the volume of bacterial suspension used and 0.4 the coefficient to convert absorbance at 650 nm into mg dry cell mass.

DNA AND RNA TECHNIQUES

The polymerase chain reaction (PCR).

PCR is a technique used to amplify DNA between two short oligonucleotides (primers) using thermostable DNA polymerases. Primers are required to specify the portion of DNA to be amplified, and were synthesised for this study by Alta Bioscience (University of Birmingham, UK). Each primer was supplied as a dry solid, and was dissolved in sterile distilled water to a final concentration of 100 μM . The primers used in this work are listed in Table 2.6, and were diluted with sterile distilled water to a final

concentration of 10 μM for use in PCR (2 μL each primer per reaction). A mixture of *Taq* DNA polymerase and DNA polymerase from *Pyrococcus* species GB-D (22 U mL^{-1}) in Tris- SO_4 (66 mM, pH 9.1) was used in PCR supermix High Fidelity (40 μL per reaction, Invitrogen, UK). The supermix also contained 19.8 mM $(\text{NH}_4)_2\text{SO}_4$, 2.2 mM MgSO_4 and 220 μM each dNTP. Plasmid DNA or chromosomal DNA was used as a PCR template (5 to 50 ng). Chromosomal DNA was purified from an overnight culture (LB, 2 mL) using an illustra blood genomicPrep Mini Spin Kit (GE Healthcare Life Sciences, Buckinghamshire, UK). The eluted DNA was diluted 1:50 for use in PCR. Alternatively, colonies were picked into 100 μL sterile distilled water, and heated to 95°C for 10 min. Cell lysates were centrifuged (13000 g, 1 min) and 5 μL of the supernatant was used as genomic DNA. For each PCR reaction a general programme was adapted to account for the expected size of the desired fragment and the annealing temperature of the specific primers (Table 2.6, Table 2.7). It was estimated that 1 kb of DNA was polymerised per min, and the annealing temperatures of primers were calculated using Equation 2.4.

Equation 2.4.

$$\text{Annealing temperature} = 64.9 + ((\text{G+C}\%) \times 0.41) - 600/n$$

(G+C%) represents the percentage of guanine and cytosine bases and n is the total length of the primer in nucleotides. In each PCR protocol a final step of 72°C for 10 min was used to complete any partial extension reactions (Table 2.7).

pGEM®-T Easy cloning.

pGEM®-T Easy was used for cloning PCR products for amplification, as recommended by the manufacturer. T Easy is supplied by the manufacturer (Promega) as a linearized vector with a single 3'-terminal thymidine at each end. The T-overhangs at the insertion site prevent recircularisation of the vector.

Table 2.6. Oligonucleotide primers used in this study. Sequences encoding relevant restriction sites are shown in underlined text.

Primer Name	Sequence	Purpose
D10520	5' CCC TGC GGT GCC CCT CAA 3'	Anneals upstream of the <i>EcoRI</i> site in pRW50. Used for sequencing in this vector.
DW hmpF	5' TTG AGA TAC ATC AAT TAA GAT GCA AAA AAA GGA AGA CCA TTG TAG GCT GGA GCT GCT T 3'	Anneals to pKD3 and pKD4 to amplify the antibiotic resistance cassettes <i>cat</i> or <i>kan</i> flanked by sequence homologous to the <i>hmp</i> locus.
DW hmpR	5' ACC TTA TGC GGG CCA AAG CAT TCG TAA TGA ATG TTT TCC CCA TAT GAA TAT CCT CCT TAG 3'	Complimentary primer to DW hmpF.
DW NarL forward	5' ATT CCC GAA AAA ACT TTC ACA GAC GTC CAA GGA GAT ACC CTG TAG GCT GGA GCT GCT T 3'	Anneals to pKD3 and pKD4 to amplify the antibiotic resistance cassettes <i>cat</i> or <i>kan</i> flanked by sequence homologous to the <i>narL</i> locus.
DW NarL reverse	5' GCT CCT GAT GCA CCC ATA CCG CTG CTT CCA CGC GAG ACT TCC ATA TGA ATA TCC TCC TTA G 3'	Complimentary primer to DW NarL forward.
KD3 _{C1}	5' TTA TAC GCA AGG CGA CAA GG 3'	Anneals to the <i>cat</i> cassette. To be used with an upstream check primer.
KD3 _{C2}	5' GAT CTT CCG TCA CAG GTA GG 3'	Anneals to the <i>cat</i> cassette. To be used with a downstream check primer.
KD4 _{K1}	5' CAG TCA TAG CCG AAT AGC CT 3'	Anneals to the <i>kan</i> cassette. To be used with an upstream check primer.

KD4 _{K2}	5' CGG TGC CCT GAA TGA ACT GC 3'	Anneals to the <i>kan</i> cassette. To be used with a downstream check primer.
phmp forward	5' GAA CAT <u>GAA TTC</u> GCA TCT CCT GAC TCA GC 3'	Part of a primer pair to amplify the promoter region of <i>hmp</i> , incorporating an <i>EcoRI</i> site into the 5' end for sub cloning.
phmp reverse	5' TAT ACA <u>AAG CTT</u> GGC CCC GTT TCC ACC 3'	Part of a primer pair to amplify the promoter region of <i>hmp</i> , incorporating an <i>HindIII</i> site into the 3' end for sub cloning.
pytE forward	5' CAT GAT <u>GAA TTC</u> CTA TCT CGT CGC 3'	Part of a primer pair to amplify the promoter region of <i>ytE</i> , incorporating an <i>EcoRI</i> site into the 5' end for sub cloning.
pytE reverse	5' TAG TAC <u>AAG CTT</u> CAG AGC TGA AGC 3'	Part of a primer pair to amplify the promoter region of <i>ytE</i> , incorporating an <i>HindIII</i> site into the 3' end for sub cloning.
T Easy forward	5' GAC GTC GCA TGC TCC CGG 3'	Anneals upstream of the blunt-end cloning site of T-Easy for sequencing ligated fragments.
Check primers	Sequence	All anneal to the <i>E. coli</i> chromosome at the locus described.
Fnr flank A	5' TGG TTA TTG CGC CAT GAA GG 3'	Anneals upstream of <i>fnr</i> .
Fnr flank B	5' TTG TTG GTC GTC GGT AG 3'	Anneals downstream of <i>fnr</i> .
Hcp for check	5' CCA CAT CAA TGG ATT TCA CC 3'	Anneals upstream of <i>hcp</i> .

Hcp hcr rev check	5' GGC ACT AAC GGT TAA ATA GC 3'	Anneals downstream of <i>hcr</i> .
Hmp FP	5' TGT TGG TCA GCT GAG AAC CC 3'	Anneals upstream of <i>hmp</i> .
Hmp RP	5' GGG AAT TCC GCG AAG ATC TC 3'	Anneals downstream of <i>hmp</i> .
narL for check	5' TTC GCA AGC GAG TGA AGT CG 3'	Anneals upstream of <i>narL</i> .
narL rev check	5' CAA ATC CGC AGT CGT TAC GG 3'	Anneals downstream of <i>narL</i> .
nirB flank F	5' CTC ATT AAT TGC TCA TGC CGG 3'	Anneals upstream of <i>nirB</i> .
nirC flank R	5' CGG TGA ACT GTG GAA TAA ACG 3'	Anneals downstream of <i>nirC</i> .
norV lower	5' GCC CCT GAC TGA TAA CAT GG 3'	Anneals upstream of <i>norV</i> .
norV upper	5' CGG AAA AAC TCA TCT TTG CC 3'	Anneals downstream of <i>norV</i> .
nrfA flank F	5' CAT GAC AGT GTA GGT GCG GT 3'	Anneals upstream of <i>nrfA</i> .
nrfB flank R	5' ATA ACG ACT CGT CAT GCA CC 3'	Anneals downstream of <i>nrfB</i> .
yeaR F check	5' AAT CCT CCC TGA TTC TTC GC 3'	Anneals upstream of <i>yeaR</i> .
yeaR R check	5' AAG CAT AGC ACA ACA TCG GG 3'	Anneals downstream of <i>yeaG</i> .
ygbA F check	5' GGA GTT AAT CAT TTC AGG GG 3'	Anneals upstream of <i>ygbA</i> .
ygbA R check	5' CTG GGA ATT GAT AAA TCG GC 3'	Anneals downstream of <i>ygbA</i> .
yibIH F check	5' CAC CTG ATG TGA TCT ACA GC 3'	Anneals upstream of <i>yibI</i> .
yibIH R check	5' CTT ACA AGG AGC AAA GTT CC 3'	Anneals downstream of <i>yibH</i> .
yjeB forward (nsrR)	5' CTG AAA CCA TGA TTC TGC GC 3'	Anneals upstream of <i>nsrR</i> .
yjeB reverse (nsrR)	5' TCC TCC GTT GTC ATC TCT GA 3'	Anneals upstream of <i>nsrR</i> .
ytfE forward	5' ACC GAC AGT GAT TCT CC 3'	Anneals downstream of <i>ytfE</i> .
ytfE reverse	5' GTA TCG CAA ACA GCG TC 3'	Anneals downstream of <i>ytfE</i> .

Table 2.7. PCR protocols used in this work.

A – Colony PCR to check Datsenko and Wanner mutant or transductant candidates.

Denaturing	Annealing	Extension	No. of Cycles	Hold
94°C, 3 min	53°C, 1 min	72°C, 2.5 min	1	
94°C, 20 s	53°C, 1 min	72°C, 2.5 min	27	
94°C, 20 min	53°C, 1 min	72°C, 10 min	1	
				4°C

B – PCR to amplify the antibiotic resistance cassette (*cat* or *kan*) from pKD3 or pKD4 using the Datsenko and Wanner technique of chromosomal inactivation.

Denaturing	Annealing	Extension	No. of Cycles	Hold
94°C, 3 min	55°C, 1 min	68°C, 2 min	1	
94°C, 20 s	55°C, 1 min	68°C, 2 min	27	
94°C, 20 min	55°C, 1 min	68°C, 5 min	1	
				4°C

C – PCR to amplify the promoter region of *ytfE* or *hmp* to be cloned into pRW50.

Denaturing	Annealing	Extension	No. of Cycles	Hold
94°C, 3 min	35°C, 30 s	68°C, 1 min	1	
94°C, 30 s	35°C, 30 s	68°C, 1 min	10	
94°C, 20 s	54°C, 30 s	68°C, 1 min	27	
94°C, 20 min	54°C, 30 s	72°C, 10 min	1	
				4°C

Agarose gel electrophoresis.

Stock 5xTBE was diluted 1:5 to give a working solution 1xTBE. Agarose was dissolved in 1xTBE by boiling in a microwave oven or in the autoclave, then was poured onto a glass plate and allowed to set. The gel was transferred into an electrophoresis tank and covered with 1xTBE supplemented with $0.1 \mu\text{g mL}^{-1}$ ethidium bromide. DNA samples were mixed 5:1 with sample buffer and were pipetted into the wells. A DNA ladder (1kb or 100bp, New England Biolabs, Hitchin, UK) was routinely used to facilitate DNA size estimation. The products on the gel were visualised with ultraviolet light using a transilluminator.

Restriction digests.

Restriction digests contained 100 to 500 ng plasmid DNA, 10 μL restriction buffer (10x), 1 to 5 U restriction endonuclease, and sterile distilled water to make up the final reaction volume of 100 μL . The restriction reaction was incubated at the temperature and for the time optimal for the particular restriction endonuclease.

Treatment of restriction digests with calf intestinal alkaline phosphatase (CIAP).

In order to limit plasmid recircularisation following restriction digestion, CIAP was used. Plasmid DNA was incubated with 10 U CIAP for 1 h at 37°C , in the presence of restriction buffer supplied by the manufacturer.

Ligations.

T4 DNA ligase was used to ligate two pieces of digested DNA by the formation of a phosphodiester bond. DNA was incubated at 16°C for 2 h or 4°C overnight with 1 U of T4 DNA ligase in the appropriate buffer as supplied by the manufacturer.

Preparation of genomic DNA.

Cultures (20 mL) of K-12 ATCC 23716 wild type and LMS 4209 strains were grown in

LB at 37°C to an optical density at 650 nm of 1.7 to 1.8. Aliquots of the cultures (10 mL) were harvested by centrifugation (6000 g, 10 min). Genomic DNA was prepared using a Genomic DNA buffer set (QIAGEN, Crawley, UK) and Genomic Tip 500/G columns according to the manufacturer's instructions, except that the propan-2-ol precipitate was washed twice with 70% (vol/vol) cold ethanol to remove residual salts before the DNA was dried and resuspended in EB buffer (QIAGEN). Genomic DNA was sheared by repeated passage through a 23G sterile needle and quantified using a Nanodrop ND1000 microspectrophotometer (Nanodrop Technologies, Inc.). DNA purity was tested by digestion with *Hind*III, a restriction endonuclease that is sensitive to residual NaCl.

Comparative genomic hybridisation microarray experiments.

Microarrays were printed by staff in the Birmingham *E. coli* genomics unit, using an Operon Array ready 70-mer *E. coli* oligonucleotide set version 1.0 (Operon Biotechnologies, Cologne, Germany) and processed as previously described (Constantinidou *et al.*, 2006, Hobman *et al.*, 2007). Total DNA from each strain (5 µg) was labelled in a 50 µL reaction mixture with either Fluorolink Cy3 or Cy5 d-CTP (GE-Amersham, Little Chalfont, UK) in a reaction containing 60 ng random hexamers (Invitrogen, Paisley, UK)/ L; 0.1 mM dA, dG and dT NTPs; 0.04 mM dCTP (Bioline, London, UK); 50 U of Klenow exo⁻ fragment of DNA polymerase I; and 10 X EcoPol buffer (New England Biolabs, Hitchin, UK). Total DNA was mixed with random hexamers and sterile filtered high-pressure liquid chromatography (HPLC)-grade water (VWR, Lutterworth, UK) to a volume of 41.5 µL and then heated to 95°C for 5 min before rapid cooling on ice and brief centrifugation at (13000 g) in a microcentrifuge. The remaining components were added, and the reaction was incubated overnight in the

dark at 37°C. Cy dye-labelled total DNA was purified using a QIAGEN QIAquick PCR purification kit according to the manufacturer's instructions and eluted in sterile HPLC-grade water before quantification of the DNA concentration and Cy dye incorporation using a Nanodrop microspectrophotometer. Next, 80 pmol of Cy3-labelled total DNA from wild-type K-12 ATCC 23716 was cohybridized with 80 pmol of Cy5-labelled total DNA from LMS 4209 to the oligonucleotide array. Microarray slides were prehybridized, washed and scanned as previously described (Constantinidou *et al.*, 2006, Hobman *et al.*, 2007). The signal intensity from each printed feature on the array was quantified by using Genepix v5.0 software (Molecular Devices Corp. Sunnyvale, CA), and microarray data were analysed by using Genespring software (v6.1; Agilent Instruments, South Queensferry, West Lothian, UK). Intensity-dependent LOWESS normalisation was used to transform raw signal data in order to eliminate Cy dye bias, and spots with an intensity value lower than the cutoff value for the error model were filtered out.

DNA Sequencing.

All sequencing was completed using the 'Plasmid to profile' service at the Genomics and Proteomics facility, College of Life and Environmental Sciences, University of Birmingham.

Construction of plasmid pCV01.

To investigate the regulation of the *ytfE* promoter, a *ytfE::lacZ* transcriptional fusion was required. The *ytfE* promoter region between nucleotides 4428891 and 4429407 of *E. coli* K-12 strain RK4353 was isolated by PCR. The primers pytFE forward and pytFE reverse (Table 2.6) were used to amplify this 0.52 kb fragment flanked by unique *EcoRI* and *HindIII* restriction sites at the 3' and 5' ends respectively. Plasmid pCV01 was

constructed by ligating the *Eco*R1/*Hind*III digested PCR fragment into pRW50 that had been digested with the same enzymes. The recombinant plasmid was sequenced to confirm the presence of the intended *ytfE* regulatory region.

Construction of plasmid pSP01.

The *hmp* promoter region between nucleotides 2683532 and 2683912 of *E. coli* K-12 strain RK4353 was isolated by PCR. The primers phmp forward and phmp reverse (Table 2.6) were used to amplify this 0.38 kb fragment flanked by unique *Eco*RI and *Hind*III restriction sites at the 3' and 5' ends respectively. Plasmid pSP01 was constructed and the sequence confirmed as described for pCV01.

PROTEIN TECHNIQUES

SDS polyacrylamide gel electrophoresis (SDS-PAGE) of proteins.

Protein samples were separated by molecular weight using SDS-PAGE. A Mini-PROTEAN II electrophoresis cell (Bio-Rad) was used to assemble glass plates, separated by 0.75 mm. The running gel consisted of 15% acrylamide, 0.375M Tris/HCl, 0.1% SDS, 0.08% APS and 0.05% *N,N,N',N'*-Tetramethylethylenediamine (TEMED). The APS and TEMED were critical for polymerisation and so were added immediately prior to pipetting the gel between the glass plates. A layer of 0.1% SDS was applied to this layer to prevent drying, and was left for 30 min to polymerise. The stacking gel consisted of 6% acrylamide, 0.125 M Tris/HCl, 0.1% SDS, 0.08% APS and 0.05% TEMED. The layer of SDS was carefully removed into a tissue, and the stacking gel was applied, before a comb was inserted between the glass plates. The stacking gel was left to polymerise for 30 minutes. Protein samples were mixed with sample buffer according to Equation 2.5 and heated at 100°C for 10 minutes before loading on the gel.

Equation 2.5.

$$\text{Volume of sample buffer used to resuspend cell pellet } (\mu\text{L}) = \frac{0.015}{\text{OD}_{650} \text{ of 1 mL sample}}$$

The comb was removed, the gel was mounted in a vertical electrophoresis tank and wells were washed with 1x electrode buffer to remove unpolymerised acrylamide. Samples were loaded into the wells, in comparison to the Prestained Protein Marker, Broad Range (7-175 kDa, New England Biolabs). The gel was run at 120 V for 20 min, and then at 180 V for 90 minutes through the resolving gel.

Coomassie staining of SDS-PAGE gels.

The gel apparatus was disassembled, and gels were incubated for at least 30 min with shaking in 200 mL Coomassie brilliant blue, which binds to free amino groups in the side chains of amino acids. The gel was then rinsed in fast destain, then incubated in 200 mL fast destain for around 30 min. The destain solution was replaced every 30 min until the background of the gel appeared clear and the protein bands were clearly distinguishable. The gel was incubated in shrink solution for 1 h, then was mounted between two sheets of cellophane and was left to dry.

STATISTICAL ANALYSIS OF THE DATA.

Calculation of p values.

Data were analysed for statistical significance using a paired samples t-test using the SPSS Statistics 17.0 programme (IBM). P values were calculated, and results were considered statistically significant where $p \leq 0.050$.

CHAPTER 3 – RESULTS.

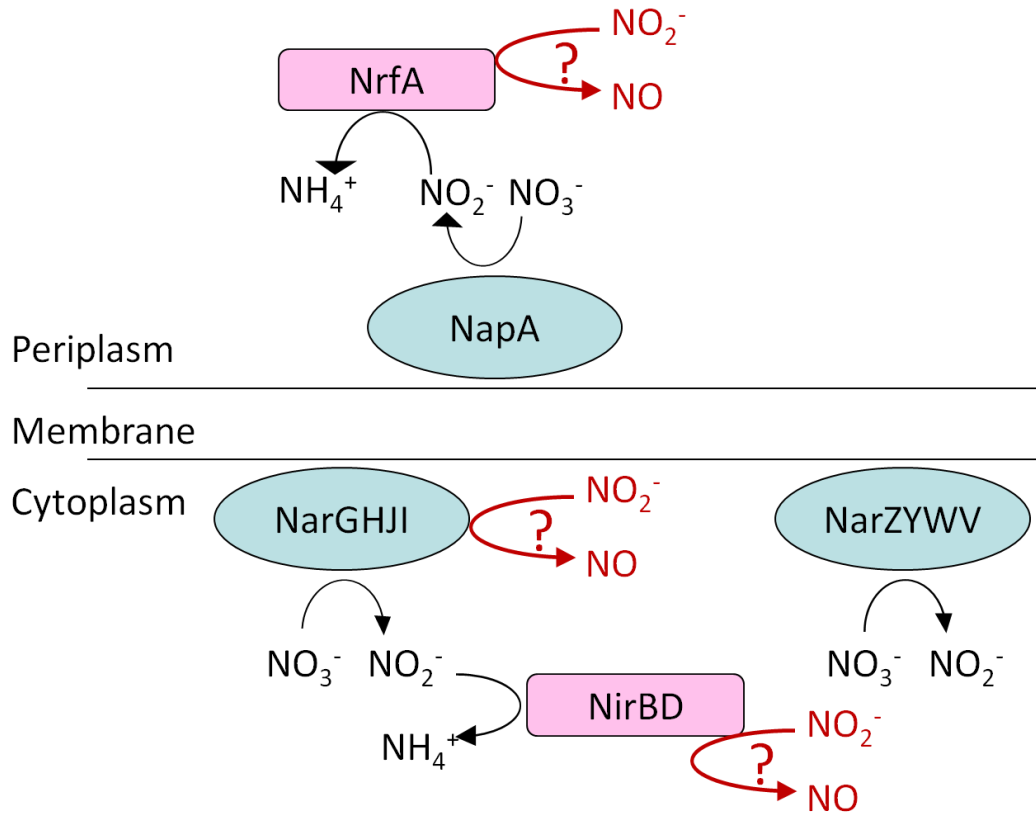
The generation of NO by *Escherichia coli*.

Introduction.

Enteric bacteria such as *E. coli* have developed several mechanisms to protect themselves from NO and other reactive nitrogen species. NO is encountered by *E. coli*, from arginine as part of the host defence, as a product of nitrite reduction by other bacteria sharing the same niche, or as a product of their own metabolism. When oxygen is not available as a terminal electron acceptor, *E. coli* is able to reduce nitrite rapidly to ammonia using either of two pathways. A cytoplasmic nitrite reductase, NirBD, is synthesised in response to a high concentration of nitrite in the cytoplasm. An alternative nitrite reductase, NrfAB, is located in the periplasm and is preferentially synthesised in response to low concentrations of nitrate.

Smith (1983) demonstrated that small quantities of NO, and subsequently N₂O, are generated during nitrite reduction. This rate of NO generation was suggested to be 100- to 1000-fold less than the maximum rate of nitrite reduction to ammonia. It was largely assumed that NO is a side product released during nitrite reduction by one or both of the nitrite reductases. Indeed, it was reported that NirB is the major source of NO during nitrate or nitrite metabolism (Weiss, 2006), although Corker and Poole (2003) concluded that NrfA is largely responsible for NO generation. It is also possible that the nitrate reductase NarG is responsible for NO generation. Several studies have implicated the nitrate reductase, NarG, as the enzyme that generates NO when nitrite is abundant, but nitrate is unavailable (Calmels *et al.*, 1988; Ralt *et al.*, 1988; Metheringham and Cole, 1997; Gilberthorpe and Poole 2008). The latter study describes experiments with *Salmonella typhimurium*, not *E. coli*. It is currently unclear exactly which enzyme is responsible for the majority of NO generation; the candidates described above are shown schematically in Figure 3.1.

Figure 3.1



Schematic representation of the proteins reported to generate NO in *E. coli*

The proteins that have been reported to generate intracellular NO are shown schematically. Reactions that are known primary functions of these enzymes are written in black text. The putative secondary reaction to generate NO from nitrite are reported in red text with question marks.

Detection of NO accumulation in the *E. coli* cytoplasm.

It is not known what concentration of NO is able to accumulate inside enteric bacteria, the precise physiological consequences of such accumulation, or how rapidly cytoplasmic NO is generated or removed. As NO is an uncharged small molecule, that is freely diffusible across membranes, it is assumed that NO generated by the nitrosative burst of the host will equilibrate with the bacterial cytoplasm. In the current literature, there is no direct evidence to prove that this assumption is correct.

One previously described method for detecting the accumulation of NO in the cytoplasm was based upon the heterologous expression of the NO-sensitive transcription factor, NNR, from *Paracoccus denitrificans* in *E. coli*. This protein was able to activate transcription from an engineered *E. coli melR* promoter (Hutchings *et al.*, 2000). A similar principle was used by Cruz-Ramos *et al.* (2002) to detect NO-induced damage to the transcription factor, Fnr, which represses transcription at the *hmp* and the synthetic FFgal Δ 4 promoters but activates expression from the synthetic FF(-71.5) promoter. An alternative method has also been described whereby the availability of free NO in the cytoplasm of *Ralstonia eutropha* is reflected by the activity of the NorR dependent promoter *pnorA* (Strube *et al.*, 2002). These studies led us to develop an assay based upon the fact that the transcription factor, NsrR, responds specifically and with very high sensitivity to NO located in the cytoplasm rather than outside the cytoplasmic membrane (Bodenmiller and Spiro, 2006; Tucker *et al.*, 2008). When NO is present in the cytoplasm, it binds to iron-sulphur clusters in the NsrR protein, and relieves repression. NsrR has been purified from *S. coelicolor*, *N. gonorrhoea* and *B. subtilis*, and *in vitro* experiments with these purified proteins have confirmed that NO binding results in DNIC formation and a consequent loss of DNA binding activity (Tucker *et al.*, 2010). As a reporter system, we used a plasmid from which β -galactosidase

synthesis is dependent upon relief of NsrR repression of the *hcp* promoter in response to cytoplasmic NO (Filenko *et al.*, 2007; Chismon *et al.*, 2010). The *hcp* promoter in *E. coli* is Fnr dependent as well as being repressed by NsrR.

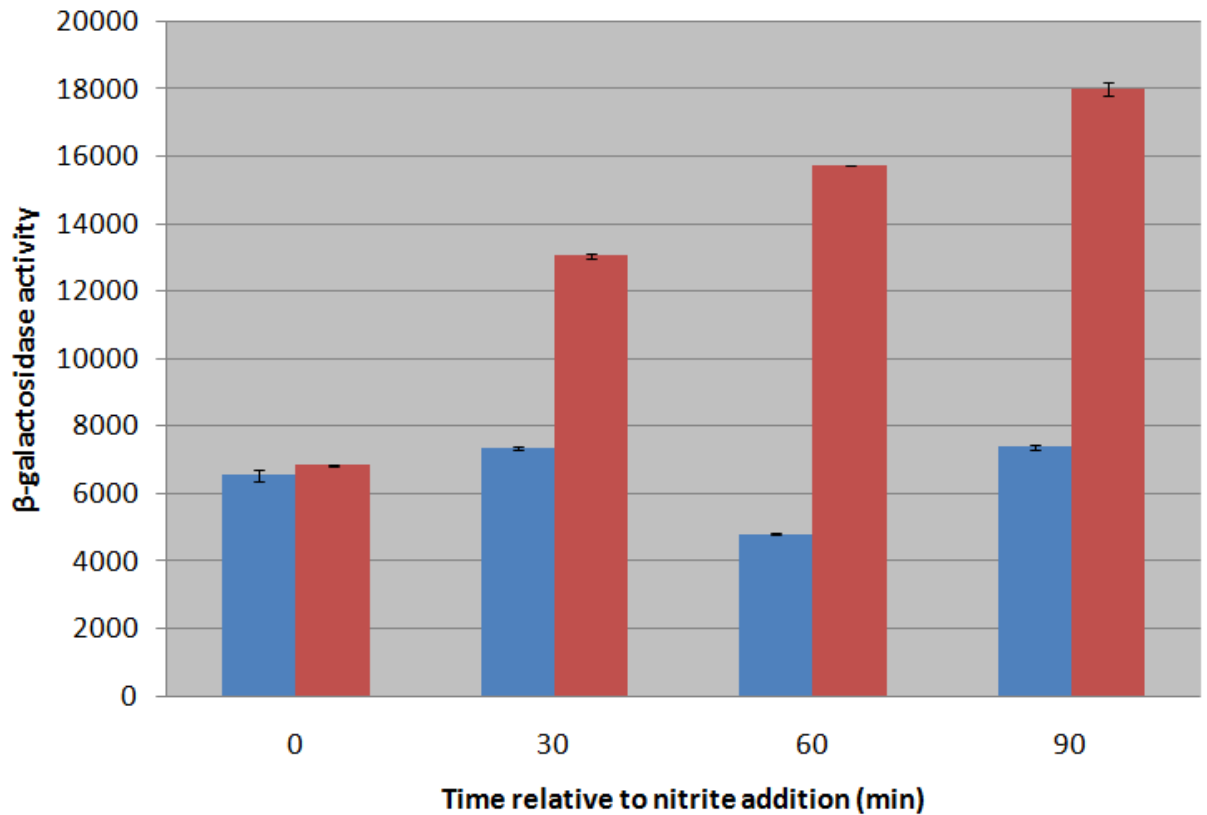
Activity of the *hcp* promoter as a reporter of NO generation.

In order to demonstrate the activity of the *hcp* promoter in response to nitrite, a single strain, RK4353, was transformed with pNF383, a plasmid that encodes the *hcp* promoter region fused to *lacZ* in pRW50. Some of the experiments in this chapter were completed with an undergraduate student, Sukhjit Purewal, under my supervision. Purified transformants were grown in duplicate anaerobically until the optical density at 650 nm had reached 0.2, then 2.5 mM nitrite was added to one culture while the other was left as an unsupplemented control. Samples (1 mL) were taken every 30 minutes for 2 hours, and were lysed to be assayed for β -galactosidase activity. The promoter activity of the culture supplemented with nitrite had increased 3-fold after 90 minutes, while the *hcp* promoter activity in the unsupplemented culture remained constant (Figure 3.2). This increase in activity is consistent with NO, which inactivates NsrR, being produced from nitrite, thus relieving repression of *phcp*. The system provides a good reporter of NO accumulation in the cytoplasm.

The effect of an *nsrR* mutation on *hcp* transcription.

The experiments were then repeated using an *nsrR* mutant as the host strain. As expected, higher activities were detected both in the presence and absence of nitrite (Figure 3.3). This confirmed that the response of the parental strain (NsrR⁺) to nitrite was dependent upon inactivation of the repressor activity of NsrR, caused by NO that had accumulated in the cytoplasm. However, the response to NO generated from nitrite was far smaller than the effect of an *nsrR* deletion mutation. This might be due to the fact that the deletion removes all NsrR protein from the *hcp* promoter, while the effect of NO is dependent upon the dose given.

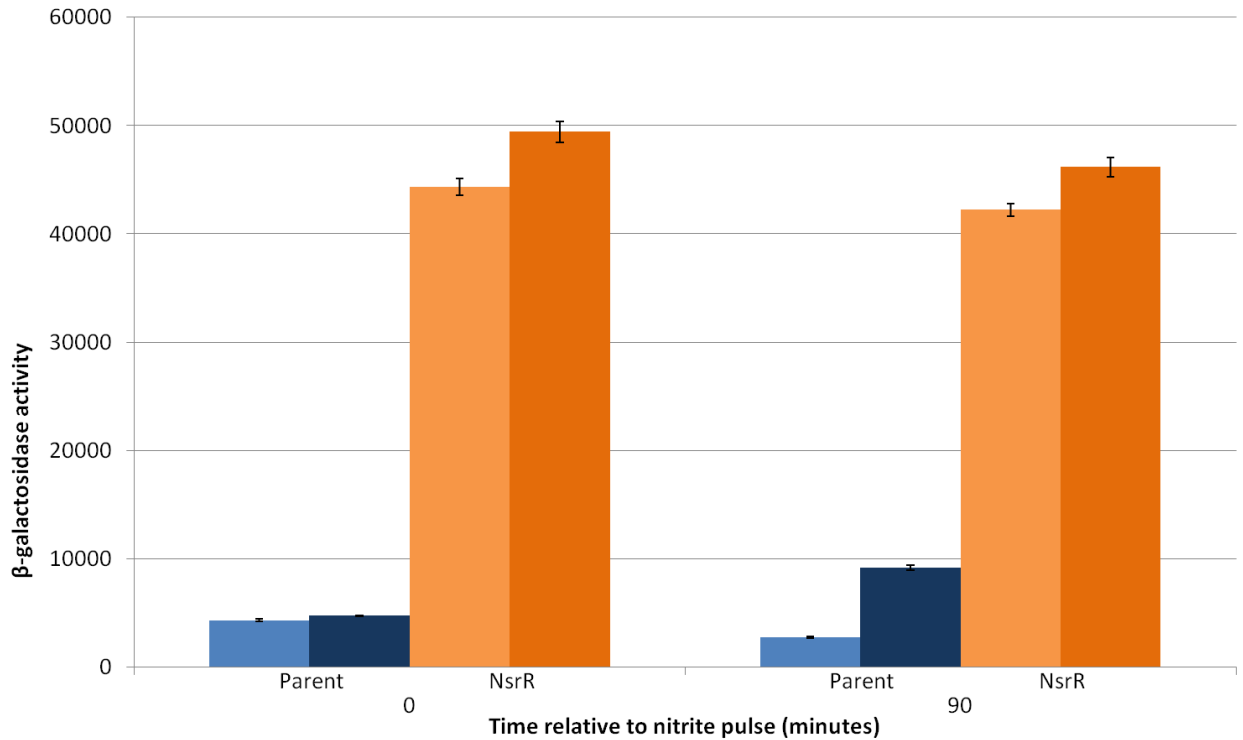
Figure 3.2.



The transcriptional fusion *phcp::lacZ* as a reporter of cytoplasmic NO.

The parental strain, RK4353, was transformed with pNF383 and purified transformants were grown anaerobically until the optical density at 650 nm had reached 0.2. One culture (red) was pulsed with 2.5 mM nitrite, while a control culture (blue) was left as an unsupplemented control. Samples (1 mL) were lysed to be assayed for β -galactosidase activity just before nitrite addition, and then every 30 minutes for 2 hours. Units of β -galactosidase activity in this and all subsequent experiments are nmol ONPG hydrolysed min^{-1} ($\text{mg dry weight}^{-1}$). Assays were repeated at least twice, from at least biological duplicate cultures. Error bars represent the standard error of all assays.

Figure 3.3.



The effect of an NsrR mutation on activity of the *hcp* promoter.

The parental strain, RK4353 (blue), and the *nsrR* strain, JCB 5222 (orange), were transformed with pNF383. The strains were grown and samples were assayed as described in Figure 3.2, then one culture of each strain (right of each coloured pair, darker bars) was pulsed with 2.5 mM nitrite, while the other was unsupplemented (left of each coloured pair, pale bars). Other details are as in Figure 3.2.

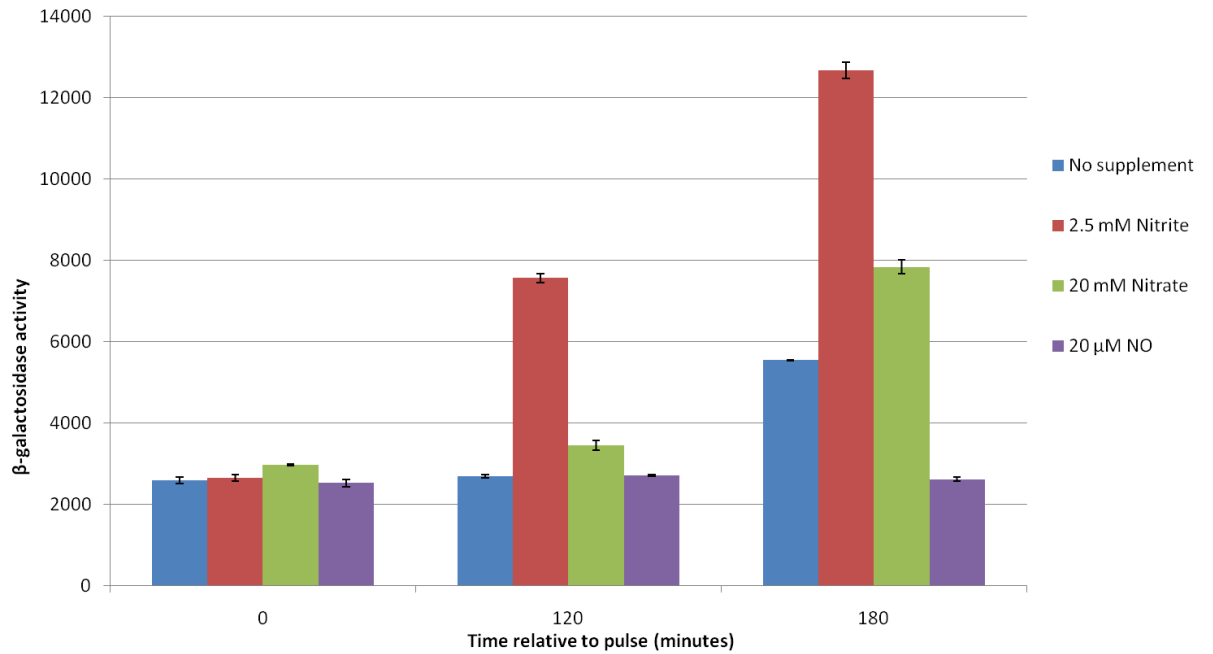
Optimal conditions for transcription activation.

To determine optimal conditions for transcription activation at the *hcp* promoter, further cultures were supplemented with either 2.5 mM sodium nitrite, 20 mM sodium nitrate or oxygen-free, NO-saturated water (NOSW) added to a final NO concentration of 20 μ M. Transcription of *hcp::lacZ* was induced far less by nitrate than by nitrite, but there was even less response to externally added NO, even when supplementation with NO was repeated at 30 min. intervals (Figure 3.4). These results not only implicated NO production from nitrite as the source of cytoplasmic NO, but also surprisingly showed that externally added NO does not equilibrate with the *E. coli* cytoplasm. In order to determine the conditions to maximally induce the *hcp* promoter, the same experiment was repeated with a higher concentration of nitrite (10 mM). In case 20 μ M NO was preventing growth of the bacteria transformed with *phcp::lacZ*, and hence the synthesis of β -galactosidase, the experiment was also repeated with a lower concentration of nitric oxide (10 μ M). This higher nitrite concentration caused a small increase in the activation of the *hcp* promoter; an induction of 17% compared with the original activity (Figure 3.5). However, the lower, and presumably less toxic, NO concentration did not induce β -galactosidase production in this strain, so overall a similar pattern was observed: externally added NOSW did not equilibrate with the *E. coli* cytoplasm (Figure 3.5).

The effect of NO concentration on the activity of NsrR regulated promoters.

In order to further investigate the small response of the *hcp* promoter to exogenous NO, an experiment was completed with varying NO concentrations added every 30 minutes for 2 h. In accordance with previous experiments, either 10 μ M or 20 μ M NOSW pulses barely induced activity of the *hcp* promoter (Figure 3.6). After 2 h, the largest induction

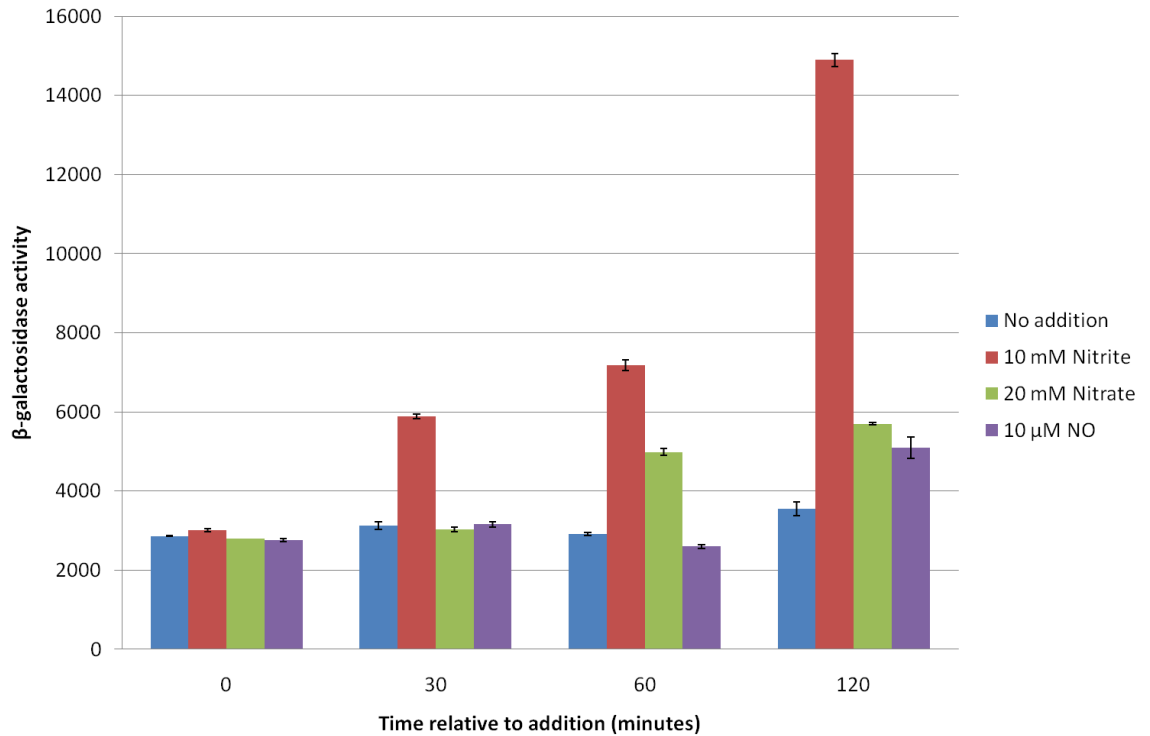
Figure 3.4.



Activation of the *hcp* promoter by nitrite, nitrate and NO

The parental strain, RK4353, was transformed with pNF383 and purified transformants were grown anaerobically until the optical density at 650 nm had reached 0.2. One culture was pulsed with 2.5 mM nitrite (red), one culture was pulsed with 20 mM nitrate (green) and one culture was pulsed every 30 minutes with 20 μ M NOSW (purple), while a control culture was left as an unsupplemented control (blue). Samples were lysed to be assayed for β -galactosidase activity just before supplement addition, and then at 120 minutes and 180 minutes post supplementation. Other details are as in Figure 3.2.

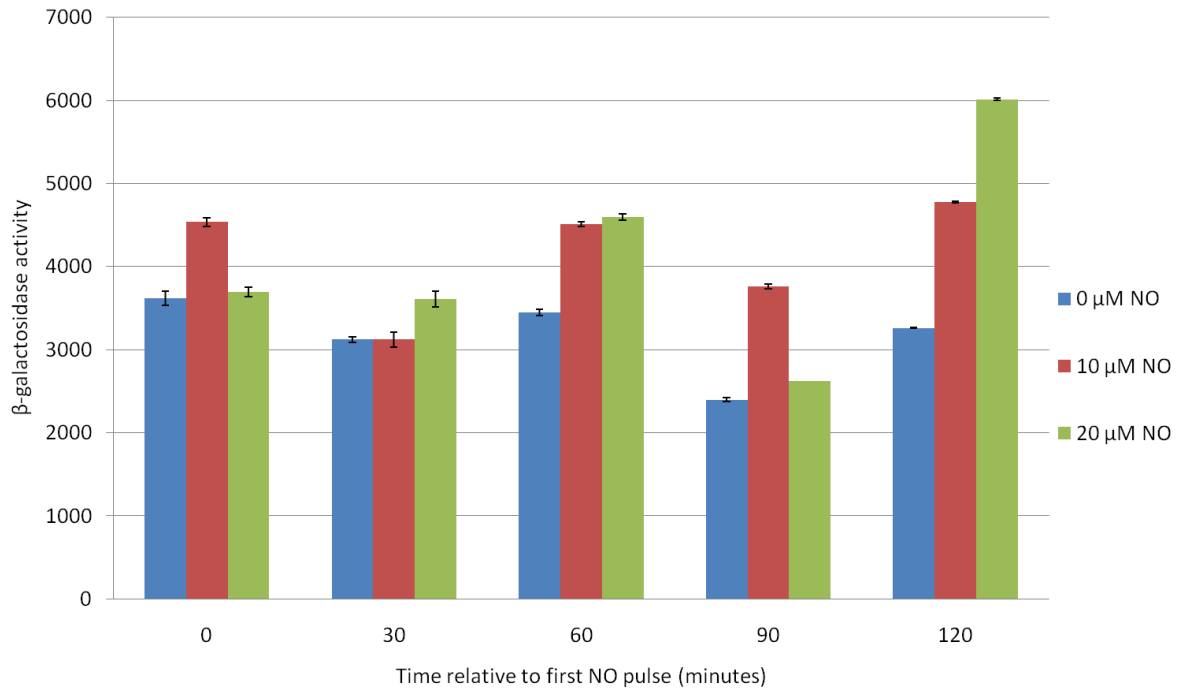
Figure 3.5.



The effect of slightly increased nitrite and slightly decreased NO concentrations on activation of the *hcp* promoter.

The parental strain, RK4353, was transformed with pNF383 and purified transformants were grown, sampled and assayed as in Figure 3.4. One culture was pulsed with nitrite (10 mM, red), one culture was pulsed with nitrate (20 mM, green) and one culture was pulsed every 30 minutes with NOSW (10 μ M, purple), while a control culture was left as an unsupplemented control (blue). Other details are as in Figure 3.2.

Figure 3.6.



The effect of NO concentration on the activation of the *hcp* promoter

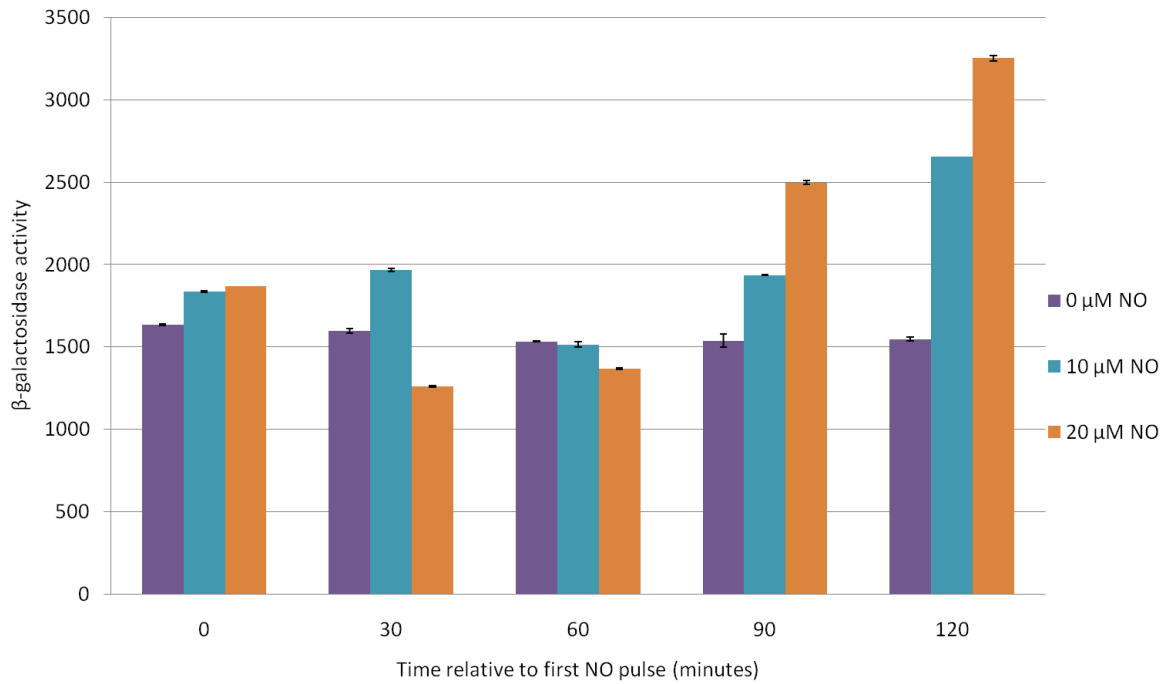
The parental strain, RK4353, was transformed with pNF383 and purified transformants were grown anaerobically until the optical density at 650 nm had reached 0.2. Two cultures were pulsed every 30 minutes with NOSW (10 μ M, red or 20 μ M, green), while one control culture was left as an unsupplemented control (blue). Samples (1 mL) were lysed to be assayed for β -galactosidase activity just before supplement addition, and every 30 minutes for 2 hours. Other details are as in Figure 3.2.

was 60% of the unsupplemented control with 20 μ M NO. In contrast, induction by 10 mM nitrite was almost 5-fold (Figure 3.6). In order to determine whether this low response was reproducible with other NsrR-regulated reporter genes, bacteria were transformed with pCV01, which contains the *ytfE* promoter fused to *lacZ* in pRW50. Cultures were grown to an optical density of 0.2, then were pulsed with NO as for the *hcp* experiment. An NO concentration of 20 μ M induced *ytfE* promoter activity by 70% compared with the unsupplemented control after 120 minutes (Figure 3.7). At both of these promoters, the induction by exogenously added NO was much lower than that of intracellular NO generated from nitrite. Reasons for this will be explored in the next chapter. NO generated from nitrite is responsible for the activation of the *hcp* and *ytfE* promoters, which is consistent with NO binding to the Fe-S clusters in NsrR and causing a structural change.

Enzymes implicated in NO production in the *E. coli* cytoplasm.

Although there is a growing consensus that NO is produced mainly as a side-product of the reduction of nitrite by NarGHI, some authors have proposed that NirBD or NrfAB are the major catalysts of NO formation. One possible explanation for the different results obtained in different laboratories is that each of these three enzymes is regulated by different combinations of transcription factors and growth conditions. The NarL-activated *narGHJI* operon is strongly induced during anaerobic growth in the presence of high concentrations of nitrate, whereas the *nrf* operon is repressed by NarL, but induced by nitrite- or nitrate-activated NarP. Synthesis of the cytoplasmic nitrite reductase, NirBD, is induced by both NarP and NarL during anaerobic growth in the presence of nitrate or nitrite. The transcription response assay was used to resolve this controversy by comparing the response of mutants defective in each of these three

Figure 3.7.



The effect of NO concentration on the activation of the *ytfE* promoter

The parental strain, RK4353, was transformed with pCV01 and purified transformants were grown, sampled and assayed as described in Figure 3.6. Two cultures were pulsed every 30 minutes with NOSW (10 μ M, blue or 20 μ M, orange), while one control culture was left as an unsupplemented control (purple). Other details are as in Figure 3.2.

enzymes with the parent strain during growth in the presence of nitrite.

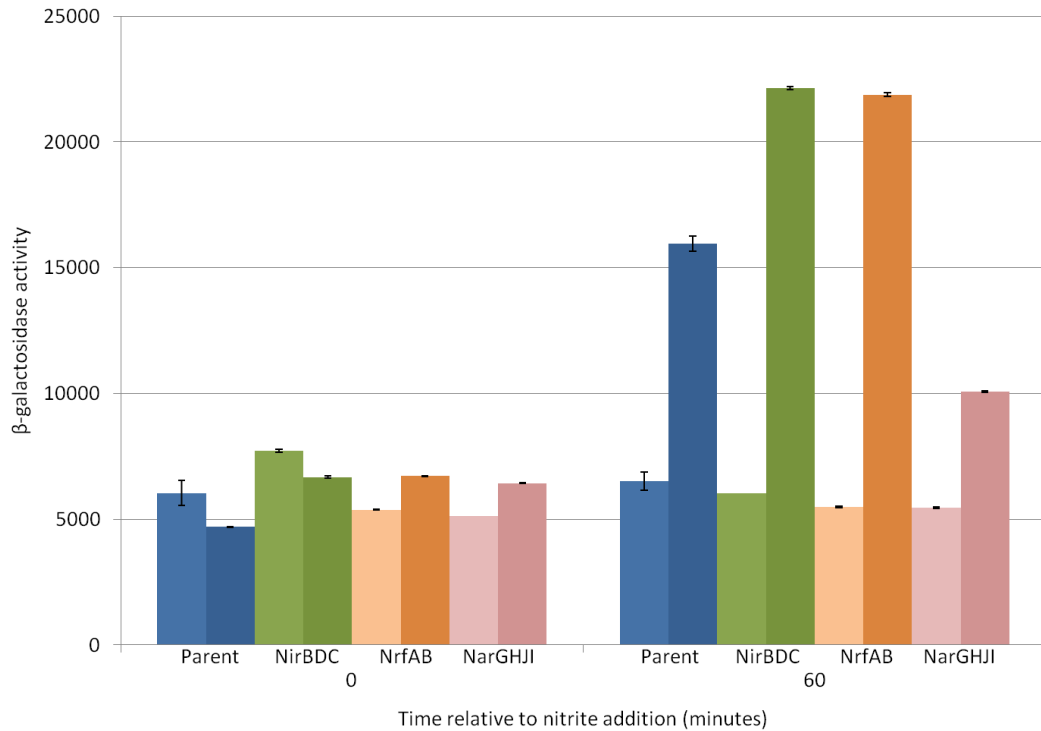
The effect of nitrite and nitrate reductases on NO accumulation in the *E. coli* cytoplasm

To investigate the effect of nitrate and nitrite reductases on NO accumulation in the cytoplasm, a *nirBDC* strain, JCB 5205, a *nrfAB* strain, JCB 5206, the *narG-I narZ::Ω* strain, JCB 4031, and the parental strain, RK4353, were transformed with pNF383. The strains were grown anaerobically and samples (1 mL) were lysed just before nitrite addition, and 60 minutes after nitrite addition to be assayed for β -galactosidase activity. The increase in β -galactosidase activity following a pulse of nitrite in *nirBDC* and *nrfAB* cultures was 40% higher than in parent cultures (Figure 3.8). This suggests that NirBDC and NrfA are not candidates for generating the majority of NO from nitrite. In fact this result confirms that both nitrite reductases are important to prevent the build up of nitrite in *E. coli*, and thus to prevent the generation of NO from nitrite. These nitrite reductases primarily decrease NO accumulation in the cytoplasm, and therefore protect bacteria against nitrosative stress (Figure 3.8). When *narGHJI narZ* bacteria were pulsed with nitrite, the consequent increase in β -galactosidase activity was 40% lower than in the parent strain (Figure 3.8). The *narG* mutant responded poorly to the addition of nitrite, confirming that nitrite reduction by NarGHI is the major source of NO in the cytoplasm. However, as nitrite still induces a response in these *narGHJI narZ* bacteria, there must be at least one secondary source of NO in *E. coli*.

Confirmation of the NsrR-based reporter system: can *ytfE::lacZ* also report NO accumulation?

To validate the use of NsrR repressed promoters to report NO generation, a similar experiment was completed with a second plasmid, pCV01, which contains the *ytfE* promoter fused to *lacZ* in pRW50. The *ytfE* promoter is not dependent upon Fnr, but is repressed by NsrR. The *nirBDC* strain, JCB5205, the *nrfAB* strain, JCB 5206, the

Figure 3.8



Nitric oxide generation as reported by *hcp* promoter activity in bacteria defective in nitrate and nitrite reductases.

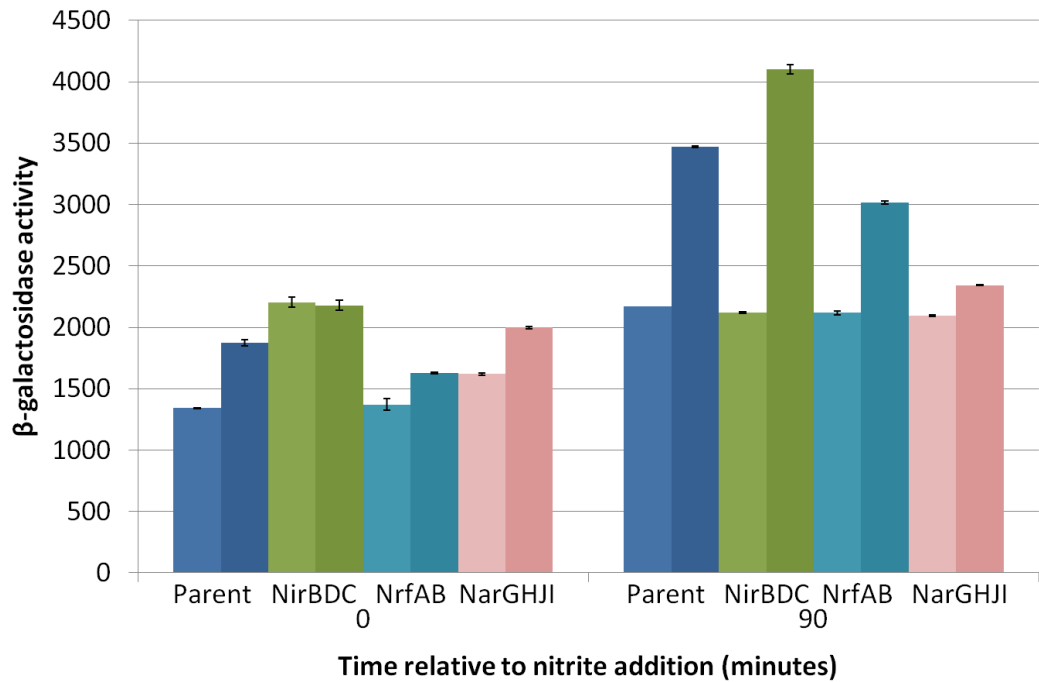
The parental strain, RK4353 (blue), a *nirBDC* strain, JCB5205 (green), a *nrfAB* strain, JCB 5206 (orange), and the *narG-I narZ* strain, JCB 4031 (pink), were transformed with pNF383. The strains were grown, sampled and assayed as described in Figure 3.2. One culture of each strain (right of each coloured pair, darker bars) was pulsed with 2.5 mM nitrite, while the other was unsupplemented (left of each coloured pair, pale bars).

narG-I narZ strain, JCB 4031, and the parental strain, RK4353, were transformed with pCV01. The strains were grown anaerobically and samples were lysed just before nitrite addition, and 90 minutes after nitrite addition. Similarly to the *hcp* data, β -galactosidase activity of the *ytfE* promoter increased in response to nitrite, although remained low in the unsupplemented control (Figure 3.9). The increase in β -galactosidase activity following a pulse of nitrite in *nirBDC* and *nrfAB* strains was similar to the response in the parent strain (Figure 3.9). When the *narGHJI narZ* strain was pulsed with nitrite, the consequent increase in β -galactosidase activity was just 20% of the parental response (Figure 3.9). The *narGHJI narZ* mutant was significantly defective in the generation of NO. This suggests that the NsrR dependent reporter system is indeed valid, and reiterates that *narGHJI* or *narZ*, a nitrate reductase, generates a significant amount of NO from nitrite.

Can a combination of deletions deplete NO generation in *E. coli* cultures supplemented with nitrite?

As there are clearly secondary enzymes responsible for generating NO in *E. coli*, further experiments were completed in strains defective in a combination of nitrite and nitrate reductases. In a double *nirBDC nrfAB* mutant, the presence of nitrite in the medium induced a greater response (54%) than that of the parent, and a slightly greater response to that of the *nirBDC* and *nrfAB* single mutants (Figure 3.10). The response of this strain is consistent with an increase in the accumulation of NO caused by the absence of both enzymes that detoxify nitrite in the *nirBDC nrfAB* strain. Both the *nrfAB narGHJI narZ* mutant and the *nirBDC narGHJI narZ* mutants show a hybrid phenotype of the constituent mutations; NO generation was decreased relative to the parent, but not to the same extent as a *narGHJI narZ* mutations alone. This hybrid phenotype is consistent

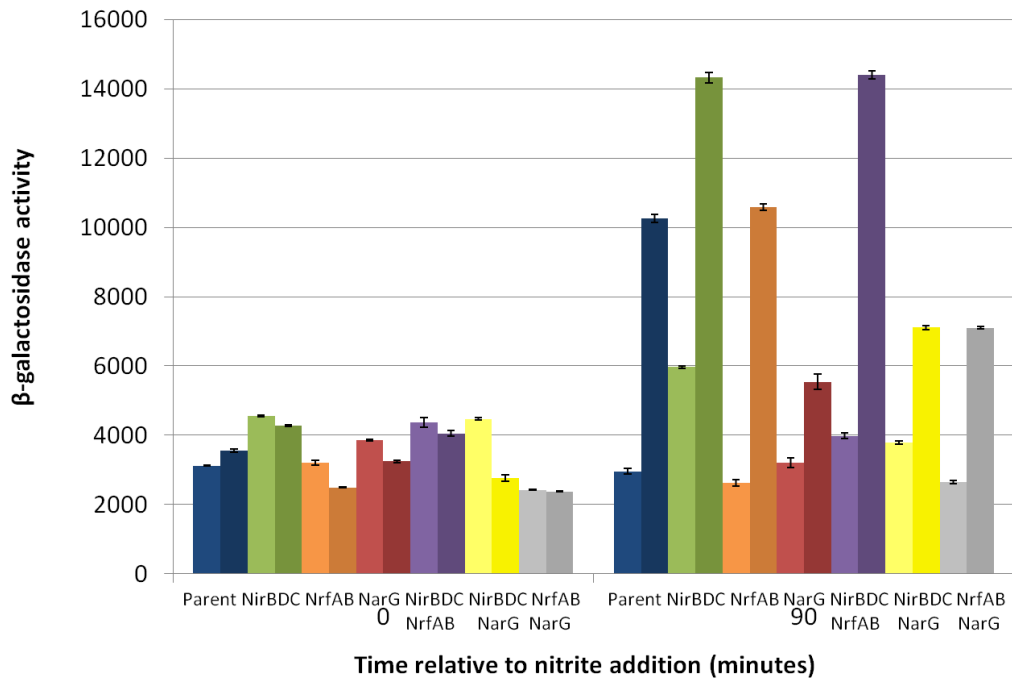
Figure 3.9



Nitric oxide generation as reported by *ytfE* promoter activity in bacteria defective in nitrate and nitrite reductases.

The parental strain, RK4353 (blue), a *nirBDC* strain, JCB5205 (green), a *nrfAB* strain, JCB 5206 (turquoise), and the *narG-I narZ:: Ω* strain, JCB 4031 (pink), were transformed with the *ytfE::lacZ* plasmid, pCV01. The strains were grown, sampled and assayed as described in Figure 3.2. One culture of each strain (right of each coloured pair, darker bars) was pulsed with 2.5 mM nitrite, while the other was unsupplemented (left of each coloured pair, pale).

Figure 3.10.



Nitric oxide generation as reported by *hcp* promoter activity in bacteria defective in a combination of nitrate and nitrite reductases.

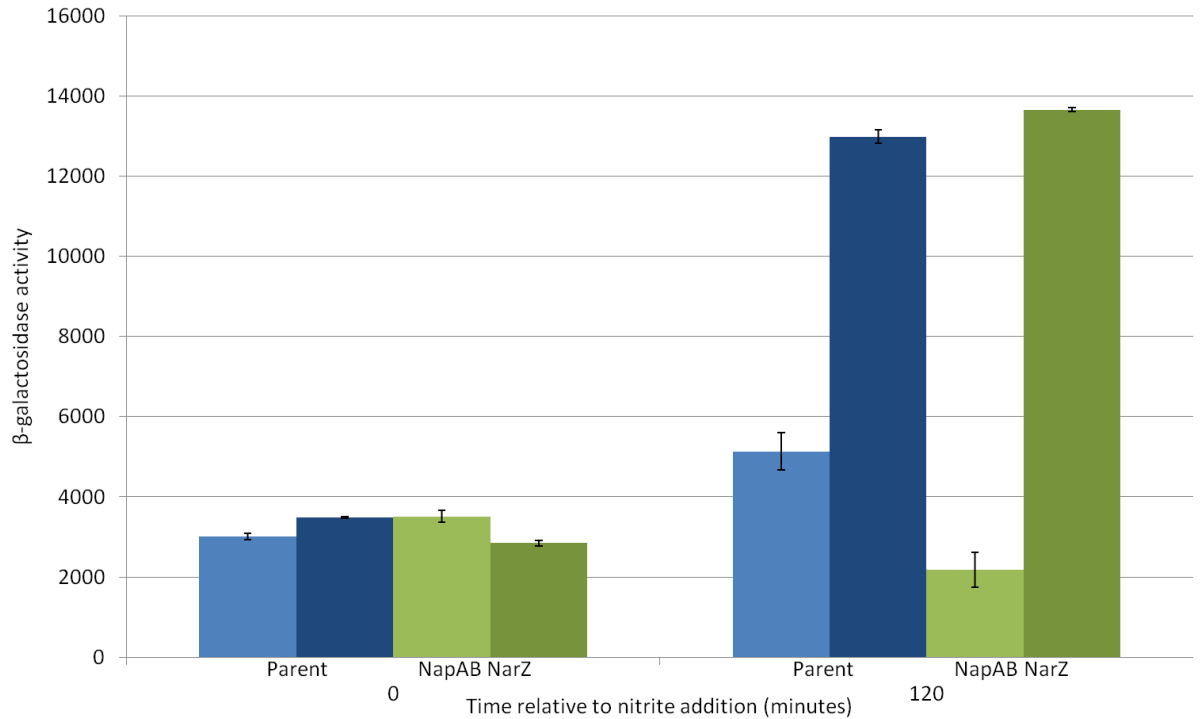
The parental strain, RK4353 (blue), the *nirBDC* strain, JCB5205 (green), the *nrfAB* strain, JCB 5206 (orange), the *narG-I narZ::Ω* strain, JCB 4031 (red), the *nirBDC nrfAB* strain, JCB 5225 (purple), the *nirBDC narG-I narZ::Ω* strain, JCB 5235 (yellow), and the *nrfAB narG-I narZ::Ω* strain, JCB 5236 (grey), were transformed with pNF383. The strains were grown, sampled and assayed as described in Figure 3.2. One culture of each strain (right of each coloured pair, darker bars) was pulsed with 2.5 mM nitrite, while the other was unsupplemented (left of each coloured pair, pale bars).

with a build up of nitrite caused by each nitrite reductase mutation, as a single protective mechanism in each case is missing. A phenotype in the *nirBDC* or *nrfAB* single mutants might have been masked by the more active NO generator NarGHJI or NarZ. However, this is clearly not the case as when the major contributor to NO generation, *narGHJI* or *narZ* is absent. In this case, a further mutation in *nirBDC* or *nrfAB* does not decrease the accumulation of NO in the cytoplasm (Figure 3.10). From these experiments, it is possible to conclude that NirBDC and NrfAB are playing a protective role, whereas the nitrate reductases NarGHJI or NarZ play a key role in generating NO from nitrite.

The effect of the periplasmic nitrate reductase, NapAB, on NO accumulation in *E. coli*

As activity of the *hcp* promoter was still induced by NO generated from nitrite in the *narGHJI narZ* strain, another source of cytoplasmic NO must be present. One candidate for this role was the periplasmic nitrate reductase, Nap. The parental strain, RK4353, and a *napA-B narZ* mutant, JCB 4011, were transformed with pNF383 and were assayed as previously described. NO accumulation reported by the *hcp* promoter fusion in this *napA-B narZ* strain was very similar to that of the parent, in which the activity of the control remained low (Figure 3.11). When NarGHJI is present to generate the majority of NO, no phenotype is apparent. However, in a further experiment, 45% less NO generation was reported in a mutant defective in both *narG* and *napA-B* than the *narGHJI narZ* mutant; this equates to just 18% of the parental induction (Figure 3.12). This suggests that *napA-B* plays a minor role in NO generation, which is masked when NarG is active. As the activity of the *hcp::lacZ* reporter is induced even in this strain in which NarG and NapA-B are absent, yet another source of intracellular NO generation must remain to be discovered.

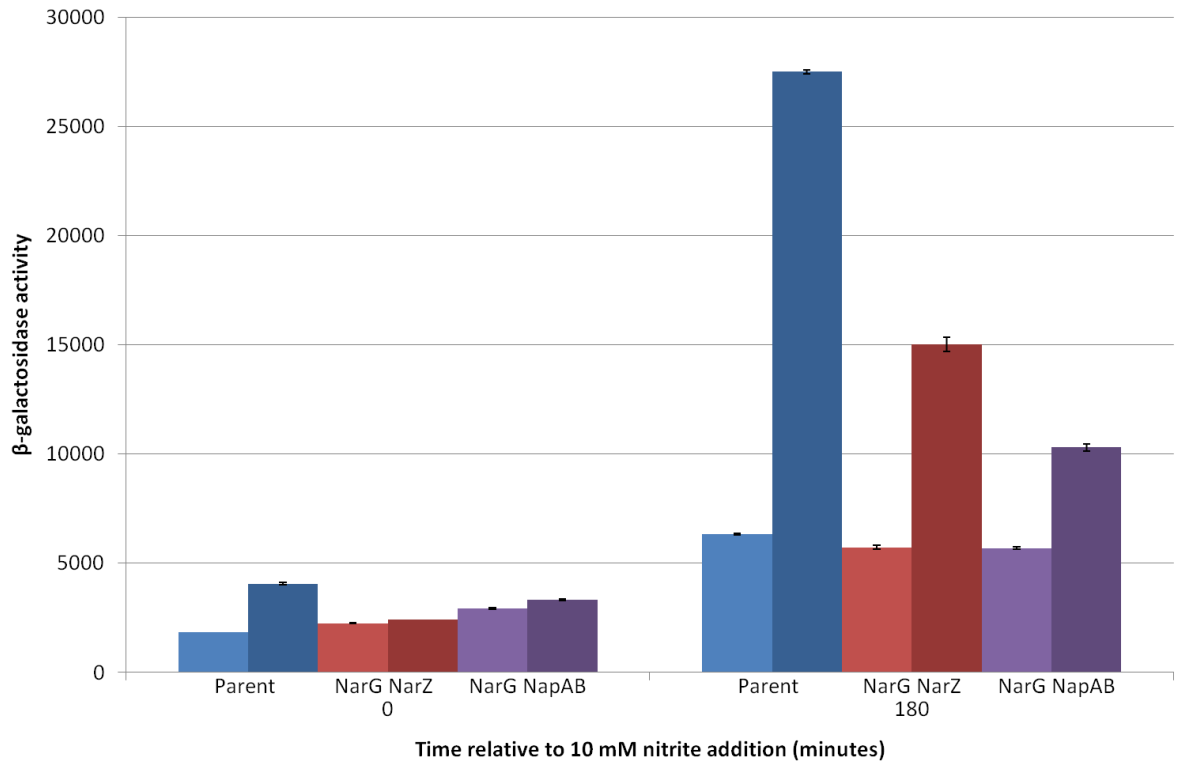
Figure 3.11



NO generation as reported by the *hcp* promoter in a *napA-B* mutant

The parental strain, RK4353 (blue), and the *napA-B narZ* mutant, JCB 4011 (green), were transformed with pNF383. The strains were grown, sampled and assayed as described in Figure 3.2. One culture of each strain (right of each coloured pair, darker bars) was pulsed with 2.5 mM nitrite, while the other was unsupplemented (left of each coloured pair, pale bars).

Figure 3.12



NO generation as reported by the *hcp* promoter in *narG* and *napA-B* mutants

The parental strain, RK4353 (blue), the *narGHJI narZ* strain, JCB 4031 (red) and the *narG napA-B* mutant, JCB 4022 (purple), were transformed with pNF383. The strains were grown, sampled and assayed as described in Figure 3.2. One culture of each strain (right of each coloured pair, darker bars) was pulsed with 10 mM nitrite, while the other was unsupplemented (left of each coloured pair, pale bars).

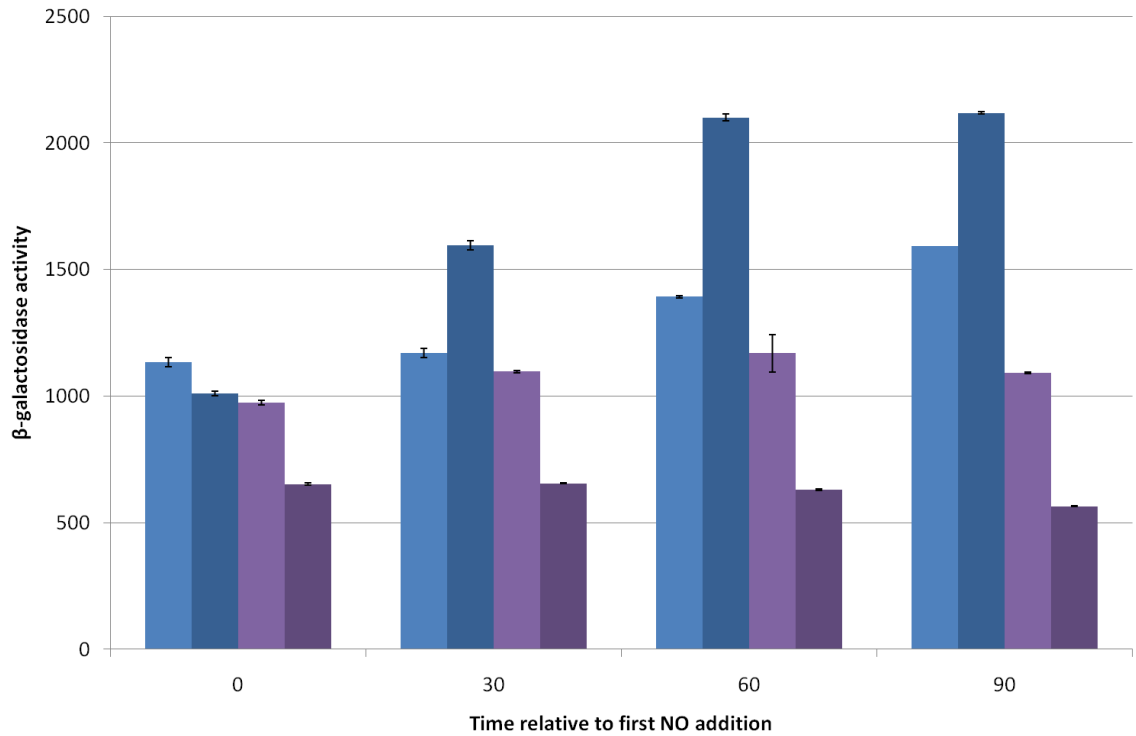
Other possibilities for this activity are other molybdoproteins. A future experiment would be to investigate the response of these promoter fusions in a *moa* mutant that is unable to incorporate molybdopterin cofactors into proteins.

Does the accumulation of NO damage the transcription factor, Fnr?

During the investigation using the *hcp* reporter system, a possible reason for the apparent lack of promoter response to exogenous NO was noticed. Cruz-Ramos *et al.* (2002) reported that high concentrations of NO can bind to the transcription factor Fnr, in order to derepress transcription at the synthetic Fnr-repressed promoter, FF*gal*Δ4, and to repress transcription at the Fnr-activated promoter, FF-71.5. It was therefore possible that failure to detect derepression of the *hcp* promoter by externally added NO was due to two opposing effects: the NO-dependent derepression of NsrR, and loss of activation by Fnr that is also caused by NO binding. Initially, the parental strain, RK4353, was transformed with two plasmids; pSP01, in which the *hmp* promoter is fused to *lacZ*, and FF*gal*Δ4, which contains a synthetic Fnr-repressed promoter fused to *lacZ*. The transformants were grown anaerobically and samples (1 mL) were lysed just before the first NO addition (10 μM, added every 30 minutes), and every 30 minutes for 2 h to be assayed for β-galactosidase activity. After 2 h, activity of the *hmp* promoter had increased by 51% relative to the unsupplemented control (Figure 3.13). The same concentration of NO had not relieved repression of the FF*gal*Δ4 promoter, even after 120 minutes. In contrast, a response (36% of the unsupplemented control) at the *hmp* promoter was apparent after just 30 minutes.

To ensure that this lack of response at the FF*gal*Δ4 promoter was indeed due to this concentration of NO (10 μM) not being sufficient to inactivate Fnr, a parental strain and an *fnr* mutant was transformed with FF*gal*Δ4. Bacteria were grown and exposed to

Figure 3.13



Response of the *hmp* promoter and a synthetic Fnr-repressed promoter to nitric oxide pulses

The parental strain, RK4353, was transformed with either pSP01 (blue bars) or FFgal Δ 4 (purple bars). Bacteria were grown anaerobically and the optical density at 650 nm was monitored until it had reached 0.2, then one culture of each transformant (right of each coloured pair, darker bars) was pulsed with 10 μ M NOSW (added every 30 minutes), while the other was unsupplemented (left of each coloured pair, pale bars).

NO as previously described. In the parent strain, activity of *FFgalΔ4::lacZ* was not changed by the addition of NO (Figure 3.14). In the Fnr mutant, activity of *FFgalΔ4::lacZ* was constitutively almost 4-fold higher than in the parent strain, as expected, and in addition did not respond to the addition of NO to the medium. It is possible to conclude that the *FFgalΔ4::lacZ* reporter does respond to Fnr inactivation, but that this inactivation is not brought about by physiologically relevant concentrations of NO damaging Fnr. Concentrations of NO that clearly derepress promoters controlled by NsrR are not sufficient to damage Fnr and thus relieve repression.

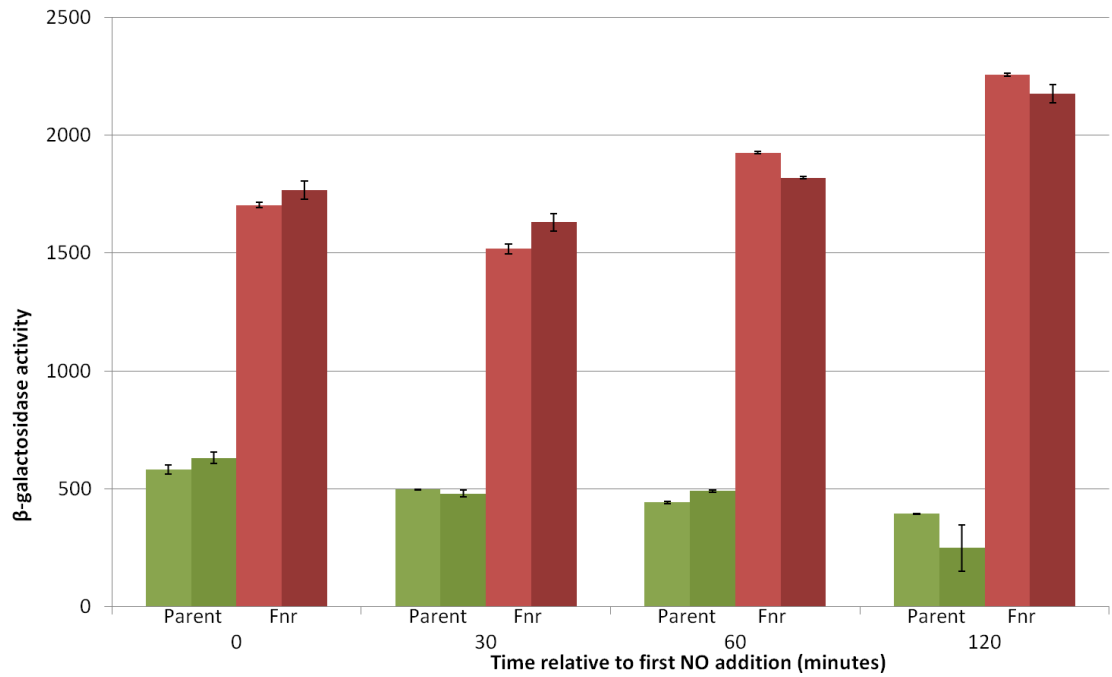
Is NO generation reliant upon Fnr?

As there was residual β -galactosidase activity in the *narG napA-B* strain, it was investigated whether deletion of *fnr* would abolish the generation of NO from nitrite in *E. coli* cultures. As the *hcp* promoter is dependent upon Fnr, another NsrR-dependent promoter, at which Fnr was not relevant, was used to report NO generation. The parent strain, RK4353 and the *fnr* strain, JCB 3911, were transformed with pCV01, which contains the *ytfE* promoter fused to *lacZ*. Transformants were grown as previously described. Samples were taken just before the addition of nitrite (10 mM) and at 120 and 180 minutes after supplementation, to be lysed and assayed for β -galactosidase activity. Activity of the *ytfE* promoter in response to nitrite addition is only slightly higher (34%) in the *fnr* strain than in the parent strain (Figure 3.15). This is consistent with the conclusion that NO generation from nitrite does not depend entirely on the function of the transcription factor Fnr.

Conclusions

By using independent reporter promoters that are repressed by NsrR, it has been confirmed that most cytoplasmic NO is formed by the interaction of the membrane-associated nitrate reductase, NarG, with nitrite. A minor contributor to NO

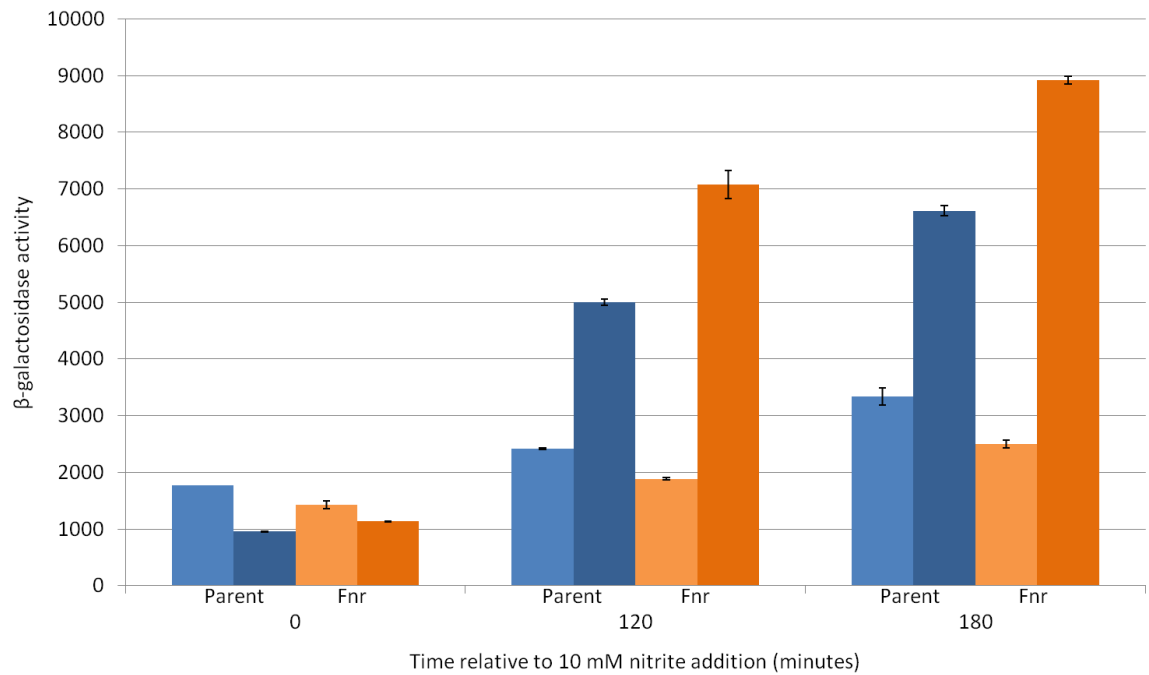
Figure 3.14.



Activity of the synthetic Fnr repressed promoter in an *fnr* mutant and the parent

The parental strain, JCB 387 (green), and the *fnr* mutant strain, JCB 3911 (red), were transformed with FF*gal**Δ4*. Bacteria were grown, sampled as assayed as described in Figure 3.2. One culture of each transformant (right of each coloured pair, darker bars) was pulsed with 5 μ M NOSW (added every 30 minutes), while the other was unsupplemented (left of each coloured pair, pale bars).

Figure 3.15.



The effect of Fnr on activity of the *ytfE* promoter in response to nitrite.

The parental strain, JCB 387 (blue), and the *fnr* mutant strain, JCB 3911 (orange), were transformed with pCV01. Bacteria were grown, sampled as assayed as described in Figure 3.2. One culture of each transformant (right of each coloured pair, darker bars) was supplemented with nitrite (10 mM), while the other was unsupplemented (left of each coloured pair, pale bars).

accumulation is the periplasmic nitrate reductase, NapA-B. It has been demonstrated that external nitrite, rather than NO, is a more effective source of intracellular NO, implying that extracellular NO does not fully equilibrate across the *E. coli* membrane with the cytoplasm. Finally, exposure to concentrations of NO that are sufficient to derepress the NsrR regulon do not cause sufficient damage to the iron-sulphur centre of the transcription factor, Fnr to provoke a physiological response.

Discussion

The development of an assay to detect the accumulation of NO in the *E. coli* cytoplasm has enabled the resolution several controversies in the nitrosative stress literature. For example, the role of the membrane-associated nitrate reductase, NarGHI, in the conversion of nitrite to NO has been confirmed. However, nitrite still induced increased expression of the *hcp* promoter, even in a *narG napA-B* double mutant, suggesting that there must be at least one more protein that catalyses the conversion of nitrite to NO. Another possibility for a role in NO production was cytochrome *bd*, a hypothesis that was ruled out by Corker and Poole (2003). However, these studies used a point mutant rather than a mutant in which the whole gene was deleted. It is possible that NO generation is a side activity of another molybdoprotein. However, nitrite reduction to ammonia by NirBD and NrfAB decreases the accumulation of NO, confirming the protective roles of these enzymes against nitrosative stress.

It is surprising that NO added externally, either at 20 μM or at 10 μM , the highest concentration that did not significantly prevent growth, failed to relieve NsrR repression. These NO concentrations are considerably higher than concentrations reported to occur physiologically *in vivo*, which are normally in the nM range and rarely exceed 1 μM (Palmer *et al.*, 1987; Cardinale and Clark, 2005). The failure of NO

to equilibrate across the *E. coli* cytoplasmic membrane to derepress NsrR controlled promoters was not due to the rapid decomposition of NO by oxygen because these experiments were completed under anaerobic conditions. Separate experiments with an electrode that is sensitive to NO confirmed that NOSW prepared using our method was stable under the conditions used. A possible explanation why other studies have readily shown a response to nitrosative stress is that alternatives to NOSW have been used as the source of NO, such as sodium nitroprusside, a lipophilic compound that freely crosses the cytoplasmic membrane and releases NO slowly within the cytoplasm (Poole, 2005). Furthermore, such studies were completed before the role of NsrR in regulating the response to nitrosative stress had been revealed (Cruz-Ramos *et al.*, 2002; Bodenmiller and Spiro, 2006). A small and delayed response of the *hcp* promoter to repeated additions of NO was observed, but this response was modest compared with the response to NO generated internally from nitrite.

Some possible explanations for the minimal response of the *hcp* promoter to external NO have been eliminated. The possibility that derepression of NsrR was counter-balanced by loss of transcription activation by Fnr, and the idea that derepression of the NsrR regulon resulted in sufficient capacity to repair nitrosative damage to Fnr as rapidly as it occurred has been disproved by control experiments with the NsrR independent promoter *FFgalΔ4*. The possibility that the capacity of the bacteria to reduce NO was sufficient to prevent its cytoplasmic accumulation has been investigated in later chapters.

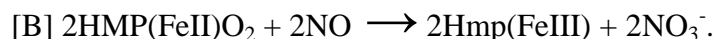
CHAPTER 4. RESULTS.

NO reduction by various strains of *E. coli*.

The mechanisms of NO detoxification in *E. coli*.

Three mechanisms by which NO is detoxified have been identified in *E. coli*. Under aerobic conditions, the flavohaemoglobin Hmp detoxifies NO through oxidation to nitrate, in a reaction that consumes NADH (Equation 4.1, Gardner and Gardner, 2002, Hausladen *et al.*, 1998). Under anaerobic conditions Hmp is able to reduce

Equation 4.1

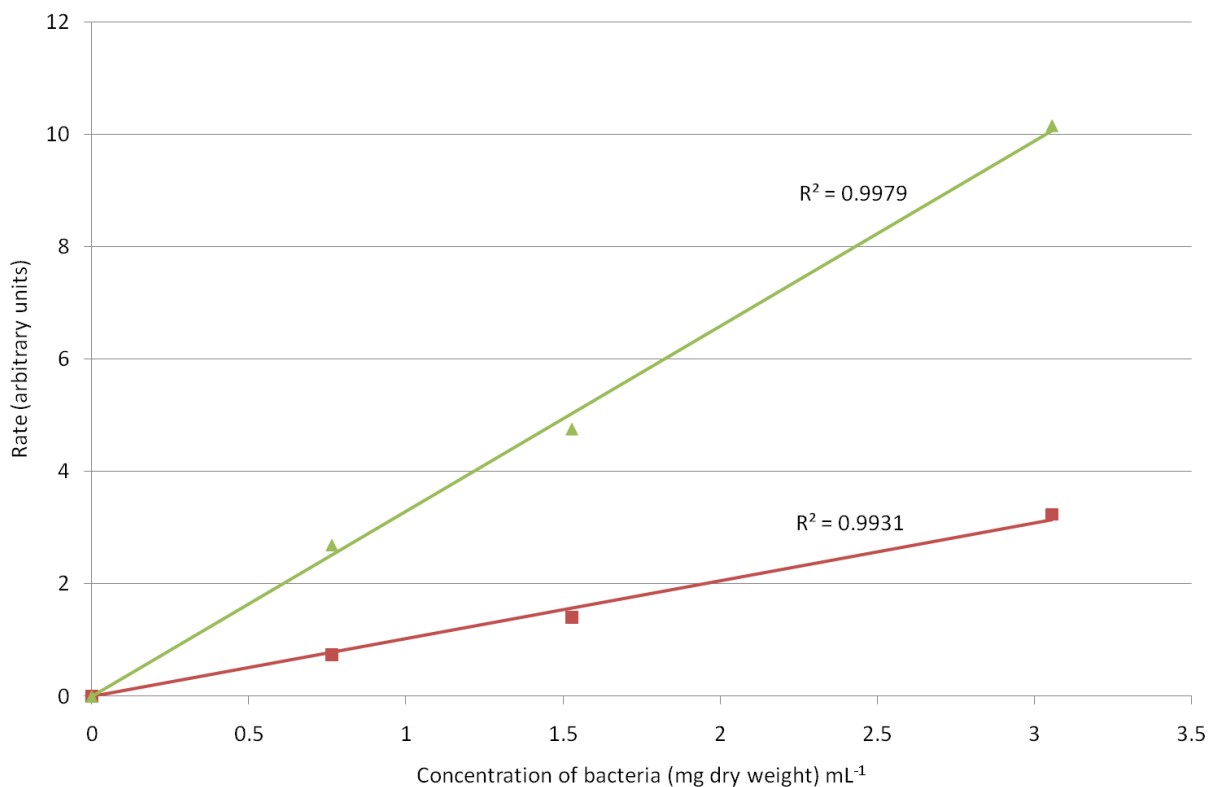


NO to N₂O (Poole and Hughes, 2000, Kim *et al.*, 1999). The cytochrome *c* periplasmic nitrite reductase NrfA is able reduce hydroxylamine and NO to NH₄⁺, in addition to its primary function in respiratory reduction of nitrite to NH₄⁺ (Costa *et al.*, 1990, Pooock *et al.*, 2002, van Wonderen *et al.*, 2008). It has been proposed that NrfA in the periplasm should be effective in maintaining low levels of NO in the cytoplasm, such that any that does diffuse into the cytoplasm can be effectively removed by flavorubredoxin, encoded by *norV* (van Wonderen *et al.*, 2008). The transcription factor NorR responds to the presence of NO (D'Autréaux *et al.*, 2005). Under anaerobic conditions NorR upregulates the synthesis of the *E. coli* flavorubredoxin, NorV, and its associated oxidoreductase, NorW, which function to reduce NO to N₂O (Tucker *et al.*, 2005). An aim of the work described in this chapter was to investigate the contribution of each of these characterised proteins to NO reduction in *E. coli*, and to investigate the function of additional proteins that might reduce NO.

Validation of the assay: use of an NO electrode to quantify the rate of NO reduction by *E. coli* suspensions.

Initially, experiments were designed to ensure that nitric oxide reduction by *E. coli* suspensions could be detected. In each case an Oxytherm electrode control unit was used with an S1/MINI Clark type electrode disc and the Oxygraph Plus data acquisition software (Hansatech Instruments, Norfolk, UK). In order to be a valid assay, the rate of NO reduction should be proportional to the concentration of enzyme (bacterial suspension) and this rate should ideally be independent of substrate concentration. However, in the case of NO, the substrate is toxic. Instead, the rate must be reproducibly dependent on substrate concentration in a non-toxic range. An experiment was designed in which the concentration of bacteria in the electrode chamber could be varied in order to test whether there was a linear relationship between the concentration of bacteria and rate of NO reduction. The parental strain, RK4353, was grown anaerobically in a medium supplemented with 20 mM sodium nitrate, harvested and washed to be assayed in the NO electrode. Experimental reagents were added to the electrode chamber, and the trace was left to stabilise until a steady state zero concentration of NO was recorded. NO was added to the desired concentration (50-800 μM), and initial rates of NO reduction were recorded. When either 50 μM or 200 μM NO was used, there was a positive correlation between the rate of NO reduction and concentration of bacteria added (Figure 4.1). This suggested that the rate of NO reduction being measured was proportional to the concentration of bacteria in the electrode chamber. However when 800 μM NO was added, there was no correlation between arbitrary rate and the concentration of bacteria in the electrode chamber. This might be due to the fact that such a high concentration of NO is toxic to the bacteria in

Figure 4.1



The effect of the concentration of bacteria on the rate of NO reduction.

The parent strain, RK4353, was grown anaerobically in medium supplemented with 20 mM sodium nitrate and bacteria were washed to be assayed in the NO electrode. The experimental reagents were added to the electrode chamber then the trace was left to stabilise at zero. NO reduction was started by the addition of NOSW: red line, NO concentration was 50 μM; green line, NO concentration was 200 μM. The initial arbitrary rate of NO reduction was recorded.

the electrode chamber. For each concentration of NO for which the rate of NO reduction was proportional to the cell density, a line of best fit representing a single NO concentration could be extrapolated back to zero (50 and 200 μM NO) and the R^2 value of the line of best fit was 1 ± 0.01 . Clearly, however, non-saturating substrate concentrations were used in these experiments; and higher concentrations were toxic to the bacteria. Nevertheless, these initial experiments defined conditions under which rates of NO reduction by different cultures could be compared. In subsequent experiments, the cell density was typically 2 to 3 (mg dry weight) mL^{-1} , and the NO concentration was between 50 and 200 μM .

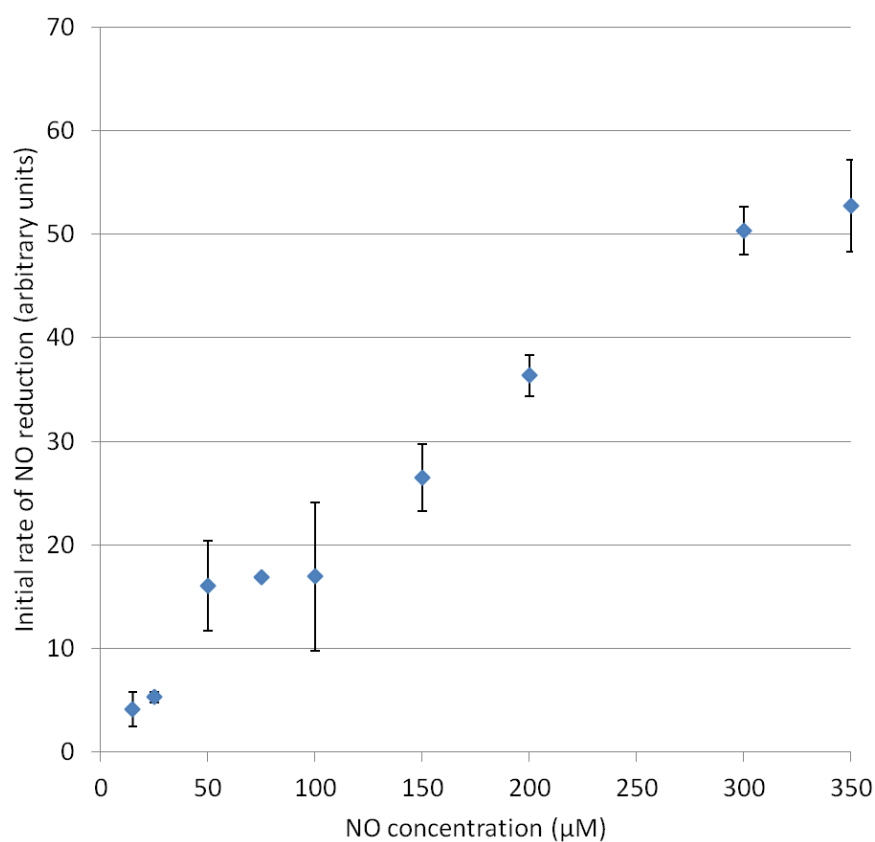
The effect of substrate concentration on the rate of NO reduction.

In order to investigate whether the rate of NO reduction correlated with substrate concentration, the parental strain, RK4353, was grown anaerobically in medium supplemented with 20 mM sodium nitrate, washed and assayed in the NO electrode. NO reduction was started by the addition of NOSW (50-350 μM) and the initial rate of NO reduction was recorded. As substrate concentration increased, rate of NO reduction also increased (Figure 4.2). As there is a positive correlation between substrate concentration and rate of NO reduction, it seems that the NO electrode is a good system for measuring the rate of NO reduction by *E. coli* suspensions.

Response of bacteria in the electrode chamber to multiple pulses of NO.

To investigate whether the bacteria in the electrode were able to turnover NO in an enzyme-like manner, NO reduction was started by the addition of a low concentration of NO (25 μM) (Figure 4.3). Once this first pulse of NO had been reduced, another bolus was added (25 μM), followed by two further pulses added in the same manner

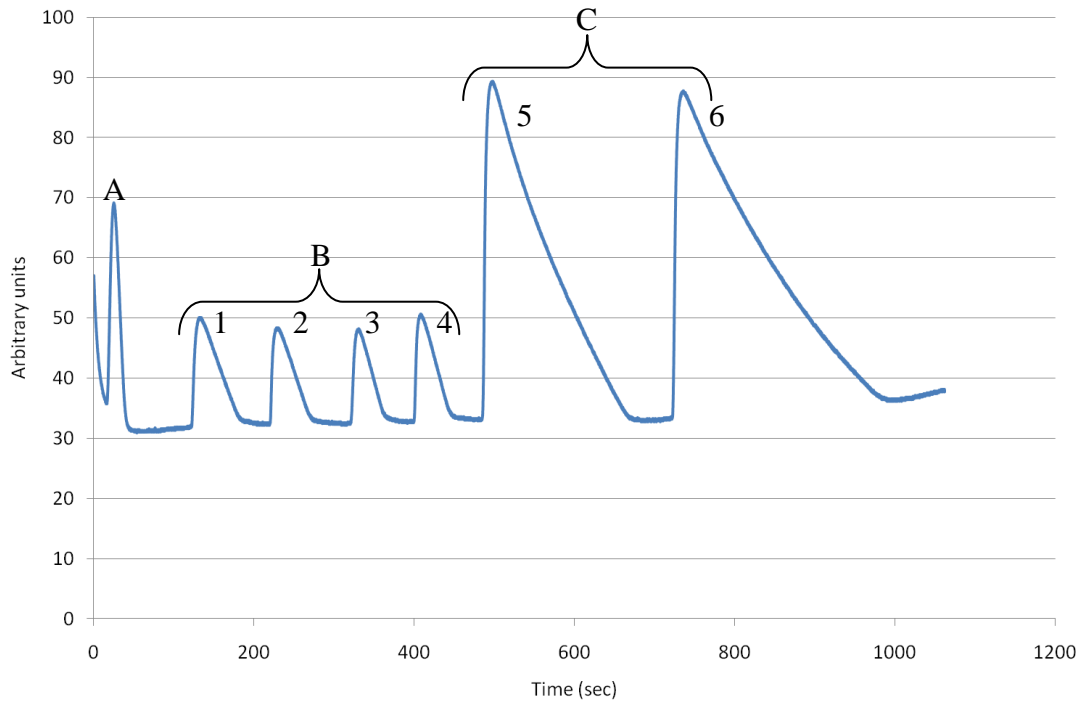
Figure 4.2



The effect of substrate concentration on initial rate of NO reduction.

The parent strain, RK4353, was grown anaerobically in medium supplemented with 20 mM sodium nitrate and bacteria were washed to be assayed in the NO electrode. The experimental reagents were added to the electrode chamber then the trace was left to stabilise at zero. NO reduction was started by the addition of NOSW (50-300 µM). The initial rate of NO reduction was recorded. Each assay was repeated at least twice, with at least two biological repeats. Data for the lowest NO concentrations were taken from Charlene Bradley. Error bars show the standard deviation of these repeats.

Figure 4.3.



Electrode trace depicting the addition of several small additions of NOSW.

An Oxytherm electrode control unit was used with an S1/MINI Clark type electrode disc and the Oxygraph Plus data acquisition software (Hansatech Instruments, Norfolk, UK) to generate this trace. Initially, assay buffer, glucose, glucose oxidase and catalase were added to the electrode chamber. Bacteria ($1.25 \text{ (mg dry weight) mL}^{-1}$) were also added, then peak A decreased rapidly as the bacteria, in combination with glucose and glucose oxidase, removed residual oxygen from the chamber. The steady state level of NO was allowed to stabilise, and the value on the arbitrary axis (30 units in this example) can be taken as '0'. The value of this does vary from day to day, which is why the electrode must be calibrated as explained in Figure 2.7 in the methods section. Peaks 1-4 labelled B represent the addition of $25 \mu\text{M}$ NOSW. Peaks 5 and 6 labelled C represent the addition of $100 \mu\text{M}$ NOSW.

(Figure 4.3). Following each of these additions of a low NO concentration, the initial rate of NO reduction was consistent. To investigate whether a higher concentration of NO would also be repeatedly reduced in the same manner, two additions of 100 μ M NOSW were added to the chamber (Figure 4.3). As each additional bolus was reduced sequentially, it was concluded that that bacteria in the chamber were able to continue to reduce NOSW as it was added. This is consistent with an enzyme-type reduction being measured.

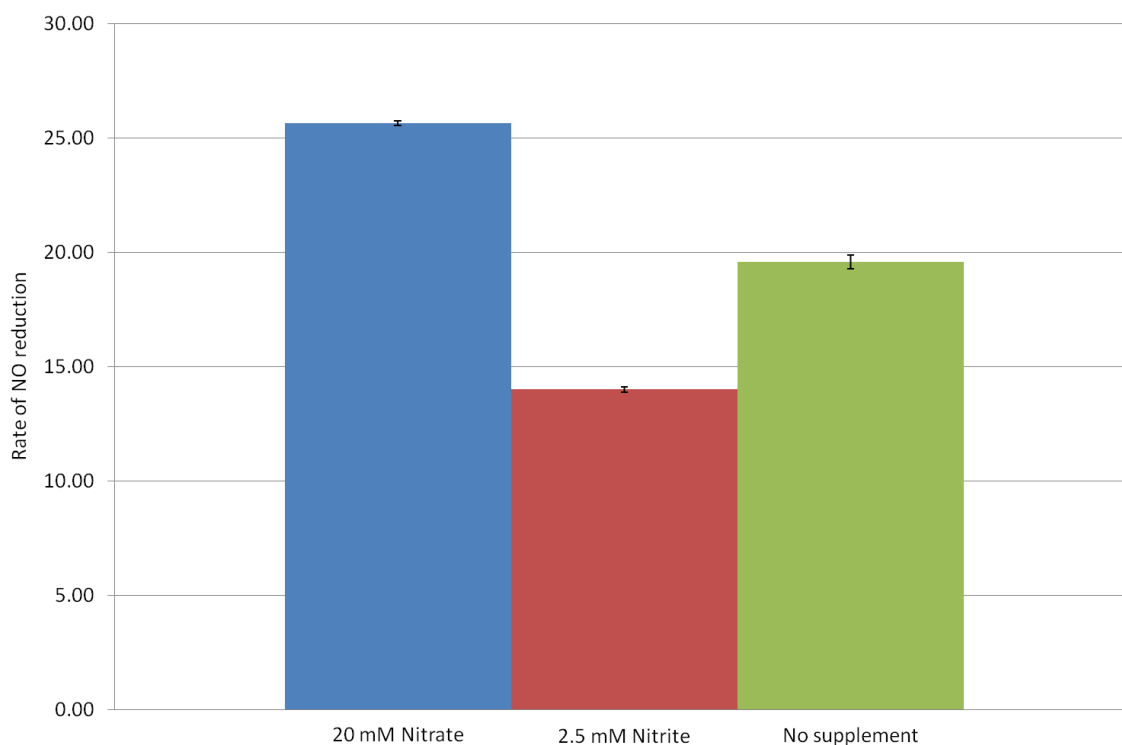
The effect of nitrate or nitrite during growth on potential rates of NO reduction.

E. coli responds according to the terminal electron acceptor available for reduction by altering the expression of proteins that are required to respire efficiently. To investigate whether the response of bacteria to these terminal electron acceptors extended to regulation of potential rates of NO reduction, bacteria were grown anaerobically with and without either sodium nitrate or sodium nitrite as a terminal electron acceptor and assayed for NO reduction as previously described. The rate of NO reduction of bacteria grown in unsupplemented medium was 20 ± 0.37 nmol NO reduced min^{-1} (mg dry cell mass) $^{-1}$. The rate of NO reduction for bacteria grown in medium supplemented with nitrite was 14 ± 0.12 nmol NO reduced min^{-1} (mg dry cell mass) $^{-1}$ and for cultures grown in the presence of nitrate was 27 ± 0.13 nmol NO reduced min^{-1} (mg dry cell mass) $^{-1}$ (Figure 4.4). The difference between the NO reduction rates recorded for bacteria grown in nitrite- or nitrate-supplemented medium was statistically significant ($p < 0.001$). This result suggested that the rate of NO reduction was regulated in *E. coli*.

The effect of a single NarL or NsrR mutation on the rate of NO reduction.

Candidates for transcription factors that might regulate these differences in rate in response to nitrate or nitrite were NarL and NsrR. NarL regulates the response to nitrate

Figure 4.4



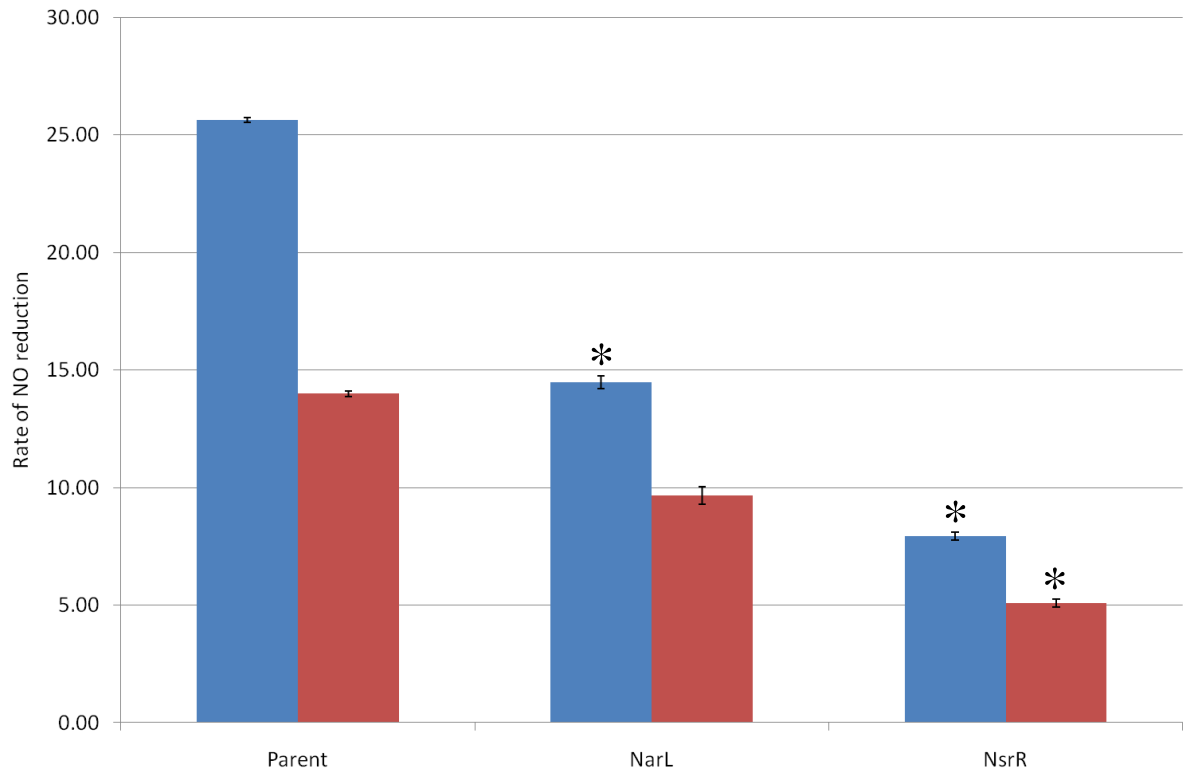
The effect of nitrate or nitrite during growth on potential rates of NO reduction.

The parental strain, RK4353, was grown anaerobically in medium that was either unsupplemented (green), or supplemented with 20 mM sodium nitrate (blue) or 2.5 mM sodium nitrite (red). The bacteria were washed and assayed in the NO electrode. The rate of NO reduction in this and all subsequent assays was nmol NO reduced min⁻¹ (mg dry cell mass)⁻¹. Each assay in this and all subsequent experiments was completed in triplicate, and with at least two biological repeats. Error bars represent the standard error of these 6 or more repeats.

and nitrite in *E. coli* (Rabin and Stewart, 1993). NsrR is a member of the Rrf2 family of transcription repressors, and is a global repressor of the bacterial nitrosative stress response (Bodenmiller and Spiro, 2006, Tucker *et al.*, 2010). To investigate the effect of NarL and NsrR on NO reduction, the *narL* strain, JCB 5215, the *nsrR* strain, JCB 5222 and the parent strain, RK4353, were grown anaerobically and assayed for NO reduction as previously described. When the *narL* strain was grown in medium supplemented with nitrate, the rate of NO reduction was 46% lower than the parent strain, RK4353; this difference was statistically significant ($p=0.003$) (Figure 4.5). When the *narL* strain was grown in medium supplemented with nitrite, the rate of NO reduction was 31% lower than the parental rate, this difference was not quite statistically significant ($p=0.053$), but if further repeats of the experiment were completed it is likely that the p value might fall below the threshold of 0.050. In this *narL* strain, there was still a statistically significant induction when nitrate was added to the medium relative to the rate when bacteria were grown in the presence of nitrite ($p=0.007$). NarL was therefore not entirely responsible for this nitrate induction.

When the *nsrR* strain was grown in medium supplemented with nitrate, the rate of NO reduction was 70% lower than the parent; this decrease was statistically significant ($p<0.001$) (Figure 4.5). This rate is the lowest that has yet been observed for bacterial cultures that reach an adequate optical density at 650 nm to be assayed. When the *nsrR* strain was grown in medium supplemented with nitrite, the rate of NO reduction was 64% lower than the parent; this decrease was also statistically significant ($p<0.001$). Despite these decreases in the rate of NO reduction, the presence of nitrate in the medium still induced a higher rate of NO reduction than the presence of nitrite; the difference is statistically significant ($p=0.006$). Neither NarL nor NsrR is entirely

Figure 4.5



The effect on NO reduction of a mutation in a single transcriptional regulator.

The *narL* strain, JCB 5215, the *nsrR* strain, JCB 5222 and the parent strain, RK4353, were grown anaerobically in minimal medium supplemented with 20 mM sodium nitrate (blue) or 2.5 mM sodium nitrite (red), then the bacteria were assayed for NO reduction activity as previously described. A star above a bar represents that data are significantly different from the parent strain, RK4353 (see text). Other details are as in Figure 4.4.

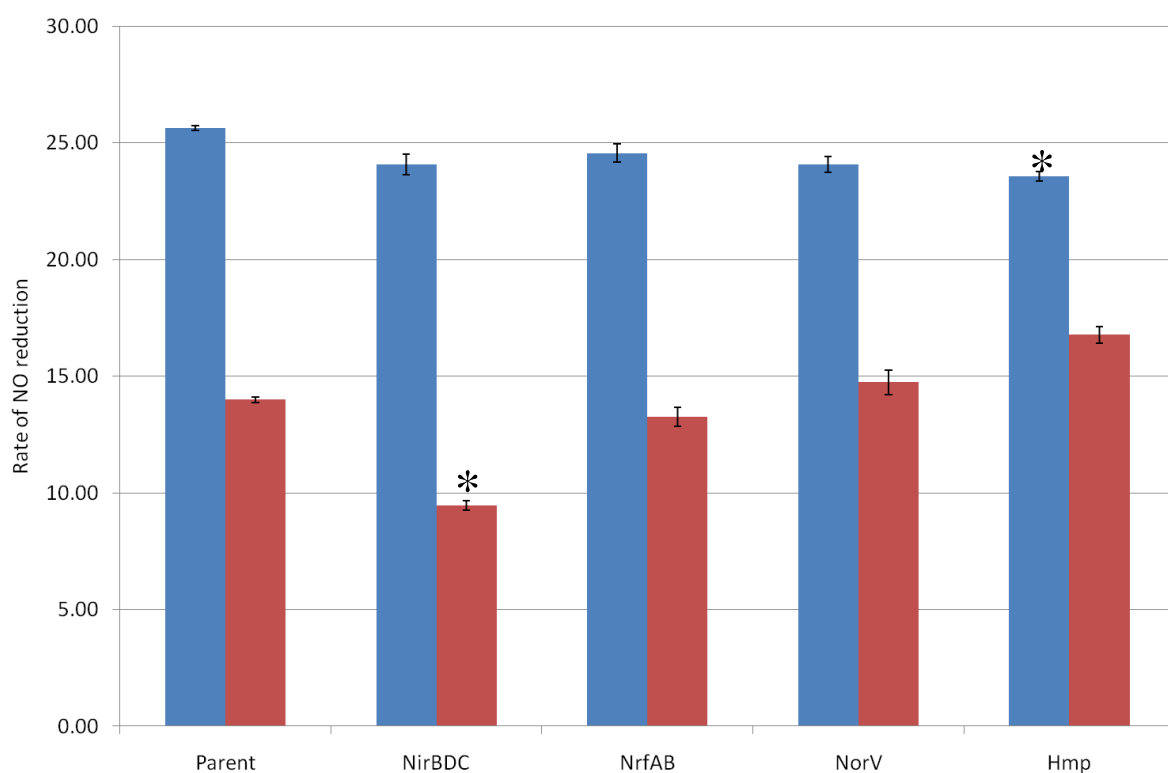
responsible for the increased rate of NO reduction due to nitrate in the growth medium.

Rate of NO reduction by single mutants defective in known NO reductases.

An isogenic set of mutants was required to investigate the effects of single mutations in genes encoding known NO reductases on the rate of NO reduction. The parental strain, RK4353, the *nirBDC* strain, JCB 5205, the *nrfAB* strain, JCB 5206, the *norVW* strain, JCB 5217, and the *hmp* strain, JCB 5219 were grown anaerobically and assayed for NO reduction as previously described. The rate of NO reduction for the parent, *nrfAB* and *norVW* strains grown in the presence of nitrite was 14 ± 0.52 nmol NO reduced min^{-1} (mg dry cell mass) $^{-1}$, while the rate of NO reduction for these bacteria grown in the presence of nitrate was 25 ± 0.33 nmol NO reduced min^{-1} (mg dry cell mass) $^{-1}$ (Figure 4.6). When the *nirBDC* strain was grown in medium supplemented with nitrate, the rate of NO reduction was not significantly different from that of the parent. However, when the *nirBDC* strain was grown in minimal medium supplemented with nitrite, the rate of NO reduction was 29% lower than the parent at 10 ± 0.20 nmol NO reduced min^{-1} (mg dry cell mass) $^{-1}$; this difference was statistically significant ($p < 0.001$). NirB has been shown to be an important enzyme to prevent the build up of cytoplasmic nitrite (Jackson *et al.*, 1981a, Macdonald and Cole, 1985). When the *hmp* mutant was grown in medium supplemented with nitrate, there was a 12% decrease in the rate of NO reduction relative to the parent, but this small difference was statistically significant ($p = 0.046$). When the *hmp* mutant was grown in medium supplemented with nitrite, there was no significant difference to the parental rate of NO reduction.

In conclusion, each mutant defective in a known NO reductase is able to reduce NO at a rate fairly similar to the parent. In every case in which the rate of NO reduction has decreased slightly, at least 70% of the NO reduction activity remains. These results suggest that no single enzyme that has been characterised so far is responsible for the

Figure 4.6



Rate of NO reduction of single mutants defective in known NO reductases

The parental strain, RK4353, the *nirBDC* strain, JCB 5205, the *nrfAB* strain, JCB 5206, the *norVW* strain, JCB 5217, and the *hmp* strain, JCB 5219, were grown anaerobically, on minimal medium supplemented with 20 mM sodium nitrate (blue) or 2.5 mM sodium nitrite (red), then the bacteria were assayed for NO reduction activity. A star above a bar represents that data are significantly different from the parent strain, RK4353 (see text). Other details are as in Figure 4.4.

majority of NO reduction in *E. coli*. It is possible that the capacity of *E. coli* to reduce NO is sufficient that the loss of one enzyme can be fully compensated for by the function of a parallel protein. Another possibility is that the main source of NO reduction activity in *E. coli* remains to be identified; either one or both of these suggestions might be correct.

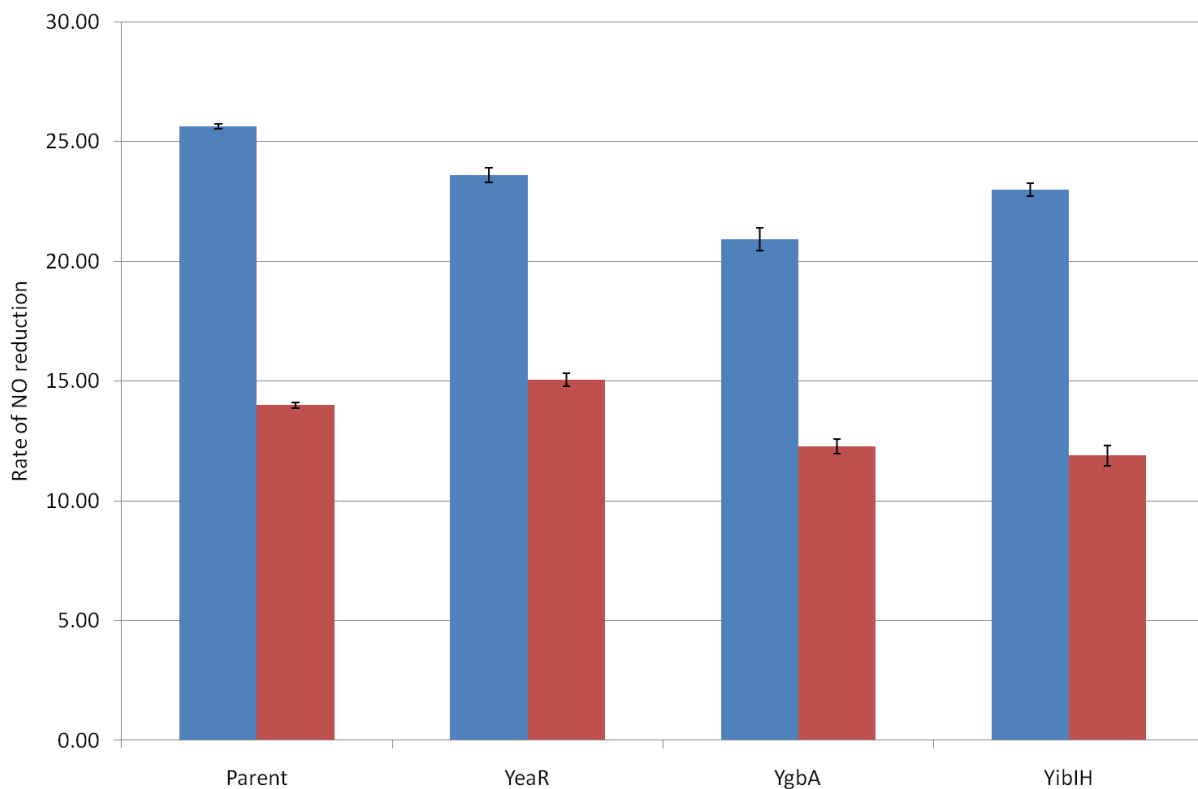
NO reduction rate of single mutants defective in proteins of unknown function.

As no single enzyme known to function as an NO reductase was responsible for the majority of NO reduction, it is apparent that other major systems for NO reduction remain uncharacterised. The possibility that genes encoding products of unknown function, which are induced by nitrosative stress, might catalyse nitric oxide reduction was therefore investigated. Single mutants defective in these proteins were assayed. The *yeaR-yeaG* strain, JCB 5100, the *yibIH* strain, JCB 5208, the *ygbA* strain, JCB 5207, and a parental strain, RK4353, were grown and assayed for NO reduction as previously described. The rate in each case for bacteria grown in the presence of nitrite was 13.5 ± 1.43 nmol NO reduced min^{-1} (mg dry cell mass) $^{-1}$, while the rate for bacteria grown in the presence of nitrate was 23 ± 0.48 nmol NO reduced min^{-1} (mg dry cell mass) $^{-1}$ (Figure 4.7). These rates were similar to those of the parent. This result suggests that none of these proteins is responsible for the majority of NO reduction in *E. coli*.

The contribution of a repair protein, YtfE, and the hybrid cluster protein, Hcp, to the rate of NO reduction.

The currently unknown pathways of NO reduction are not minor; they are adequate to sustain almost optimal rates of NO reduction, and hence potentially provide significant protection against nitrosative stress. One possibility is that NO reduction is a two-step process involving first non-specific nitrosation of metalloproteins followed by reductive

Figure 4.7



Rate of NO reduction of single mutants of unknown function

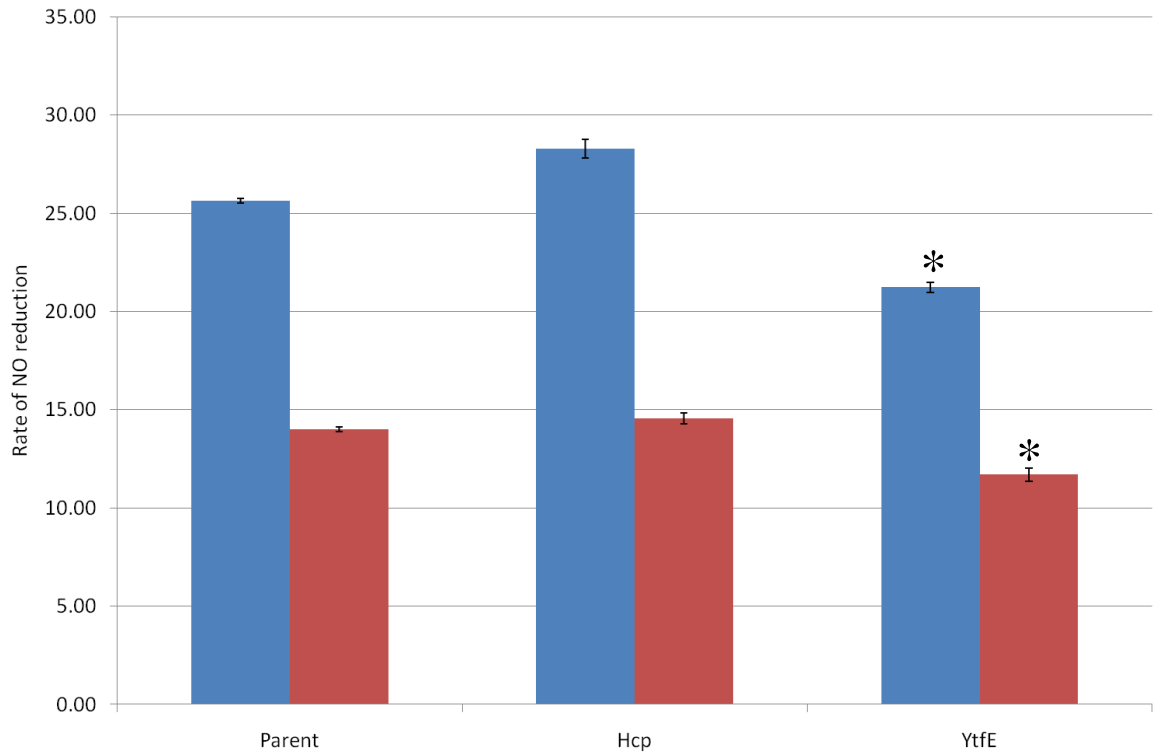
The parental strain, RK4353, the *yeaR-yaog* strain, JCB 5100, the *yibIH* strain, JCB 5208, and the *ygbA* strain, JCB 5207, were grown anaerobically, on minimal medium supplemented with 20 mM sodium nitrate (blue) or 2.5 mM sodium nitrite (red), then bacteria were assayed for NO reduction activity. Other details are as in Figure 4.4.

repair. The YtfE protein has been implicated in the repair of damaged iron centres (Justino *et al.*, 2005, Justino *et al.*, 2006, Justino *et al.*, 2007, Overton *et al.*, 2008, Vine *et al.*, 2010). Another protein, Hcp, is annotated to reduce hydroxylamine, but with very poor catalytic efficiency (Wolfe *et al.*, 2002). A possible alternative role for Hcp was in NO reduction. In order to investigate these ideas, the parent strain, RK4353, the *hcp* strain, JCB 4999 and the *ytfE* strain, RK4353 $\Delta ytfE::cat$, were grown and assayed as previously described. The rate of NO reduction measured for the *hcp* strain grown in the presence of nitrite was 14.6 ± 0.34 nmol NO reduced min^{-1} (mg dry cell mass) $^{-1}$, while the rate of NO reduction for bacteria grown in the presence of nitrate was 28.3 ± 0.46 nmol NO reduced min^{-1} (mg dry cell mass) $^{-1}$ (Figure 4.7). In each case the rate of NO reduction was similar to that of the parent. The rate of NO reduction for *ytfE* strain grown in medium supplemented with nitrate was 21% lower than that of the parent ($p=0.010$). The rate of NO reduction for the *ytfE* strain grown in medium supplemented with nitrite was 16% lower than the parent ($p=0.041$). Although the differences between a *ytfE* mutant and the parent are statistically significant, in each case 75% of the parental rate remains, so neither Hcp nor YtfE account for the majority of NO reduction in anaerobically grown *E. coli*.

Rate of NO reduction of mutants defective in several known NO reductases.

It is possible that the single mutants tested still reduced NO rapidly because each enzyme has a high capacity to reduce NO, and that the loss of a single enzyme is compensated for by an alternative reductase. In order to decrease the capacity of *E. coli* to reduce NO, mutants defective in various combinations of NO reductases were therefore constructed. The *nirBDC nrfAB* strain, JCB 5225, the *nirBDC nrfAB hcp* strain, JCB 5230, the *nirBDC nrfAB norV* strain, JCB 5232, the *nirBDC nrfAB hmp*

Figure 4.8



Rate of NO reduction of single mutants defective in the hybrid cluster protein, Hcp, or the di-iron protein encoded by *ytfE* that is essential for the repair of iron centres.

The *hcp* strain, JCB 4999, a *ytfE* strain, RK4353 $\Delta ytfE::cat$, and a parental strain, RK4353, were grown anaerobically in minimal medium supplemented with 20 mM sodium nitrate (blue) or 2.5 mM sodium nitrite (red), then the bacteria were assayed for NO reduction activity. A star above a bar represents that data are significantly different from the parent strain, RK4353 (see text). Other details are as in Figure 4.4.

strain, JCB 5231, and the quadruple *nirBDC nrfAB norV hmp* strain, JCB 5210, were used. Cultures were grown and assayed for NO reduction as previously described.

When the growth medium was supplemented with nitrate, even strains defective in more than one characterised NO reductase reduced NO at a rate similar to that of the parent (Table 4.1). A major exception to this was the quadruple mutant strain, JCB 5210, which reduced NO at a rate 48% lower than that of the parent strain, RK4353 (Table 4.1). The nomenclature ‘quadruple’ will subsequently be used to refer to this *nirBDC nrfAB norV hmp* strain, JCB 5210. The mutations in all known NO reductases decreased the NO reduction capacity of *E. coli* to only 52% of the parent. Therefore, other uncharacterised mechanisms of NO reduction remain active in *E. coli*.

When cultures were grown in the presence of sodium nitrite, strains defective in more than one known NO reductase still reduced NO at over 69% of the rate of the parent (Table 4.2). When the *nirBDC nrfAB hcp* strain was grown in medium supplemented with nitrite, the rate of NO reduction measured was actually 50% higher than the rate measured for the parent. To investigate whether the bacteria were stressed under these conditions, a growth experiment was completed. Cultures were grown in minimal medium that was either unsupplemented, or supplemented with 20 mM sodium nitrate or 2.5 mM sodium nitrite. The optical density at 650 nm was monitored for 8 hours. When the growth medium was supplemented with 20 mM nitrate, growth of the parent was stimulated, but only slight growth acceleration was observed in the *nirBDC nrfAB hcp* mutant (Figure 4.9). In the presence of nitrite, growth of parental cultures was stimulated, but growth of the *nirBDC nrfAB hcp* culture was suppressed. The poor growth could be due to a toxic metabolite building up when the combination of these protective proteins are not functional. A higher rate of NO reduction is induced in these stressed

Table 4.1. The rate of NO reduction, following growth in the presence of nitrate, by strains defective in several NO reductases.

Strain number	Mutations	Functional proteins retained	Rate of NO reduction	St Error	% Parental rate of NO reduction	P value relative to parent
JCB 5210	<i>nirBDC nrfAB norV hmp</i>		13.8	± 0.24	52	<0.001
JCB 5225	<i>nirBDC nrfAB</i>	Hmp ⁺ NorV ⁺	26.2	± 0.45	98	0.898
JCB 5230	<i>nirBDC nrfAB hcp</i>	Hmp ⁺ NorV ⁺	25.4	± 0.36	95	0.612
JCB 5231	<i>nirBDC nrfAB hmp</i>	NorV ⁺	22.9	± 0.43	86	0.173
JCB 5232	<i>nirBDC nrfAB norV</i>	Hmp ⁺	21.6	± 0.02	81	0.121
JCB 5251 [‡]	<i>nirBDC nrfAB norV hmp fnr</i>		16.7	± 0.26	63	<0.001
JCB 5252 [‡]	<i>nirBDC nrfAB norV hmp narL</i>		11.8	± 0.17	44	<0.001

Full information on strain construction or the source of these strains can be found in Table 2.3 in the methods section. P values all refer to the difference from the parent strain, RK4353.

[‡]Data are also depicted in Figure 4.13 but are included here for completeness.

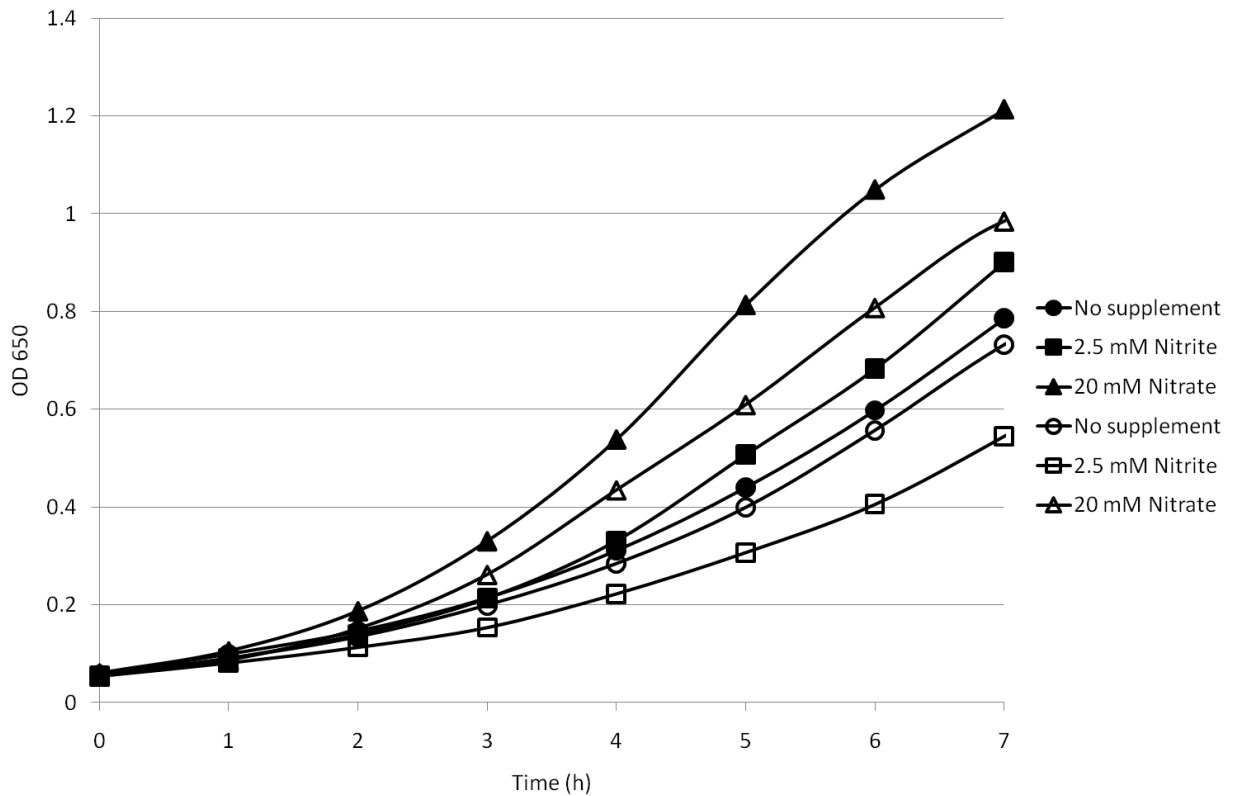
Table 4.2 The rate of NO reduction, following growth in the presence of nitrite, by strains defective in several NO reductases.

Strain number	Mutations	Functional proteins retained	Rate of NO reduction	St Error	% Parental rate of NO reduction	P value relative to parent
JCB 5210	<i>nirBDC nrfAB norV hmp</i>		10.9	± 0.31	78	0.173
JCB 5225	<i>nirBDC nrfAB</i>	Hmp ⁺ NorV ⁺	13.8	± 0.42	99	0.897
JCB 5230	<i>nirBDC nrfAB hcp</i>	Hmp ⁺ NorV ⁺	21.3	± 0.53	152	0.014
JCB 5231	<i>nirBDC nrfAB hmp</i>	NorV ⁺	9.60	± 0.21	69	0.012
JCB 5232	<i>nirBDC nrfAB norV</i>	Hmp ⁺	18.4	± 0.37	131	0.011
JCB 5251 [‡]	<i>nirBDC nrfAB norV hmp fnr</i>		ND	ND	ND	ND
JCB 5252 [‡]	<i>nirBDC nrfAB norV hmp narL</i>		7.89	± 0.18	56	<0.001

ND signifies that the rate was not determined.

[‡]Data are also depicted in Figure 4.13 but are included here for completeness.

Figure 4.9.



Growth phenotype of a strain defective in both nitrite reductases and the hybrid cluster protein, Hcp.

The parental strain, RK4353 (closed symbols), and the *nirBDC nrfAB hcp* strain, JCB 5230 (open symbols), were grown anaerobically in medium that was either unsupplemented (●○), or supplemented with 2.5 mM sodium nitrite (■□) or 20 mM sodium nitrate (▲△). Cultures were incubated statically at 37°C and samples were withdrawn at hourly intervals to be assayed spectrophotometrically for optical density at 650 nm. Growth curves were completed in at least biological duplicate and this graph represents a typical experiment.

bacteria, but the underlying mechanism can not yet be explained.

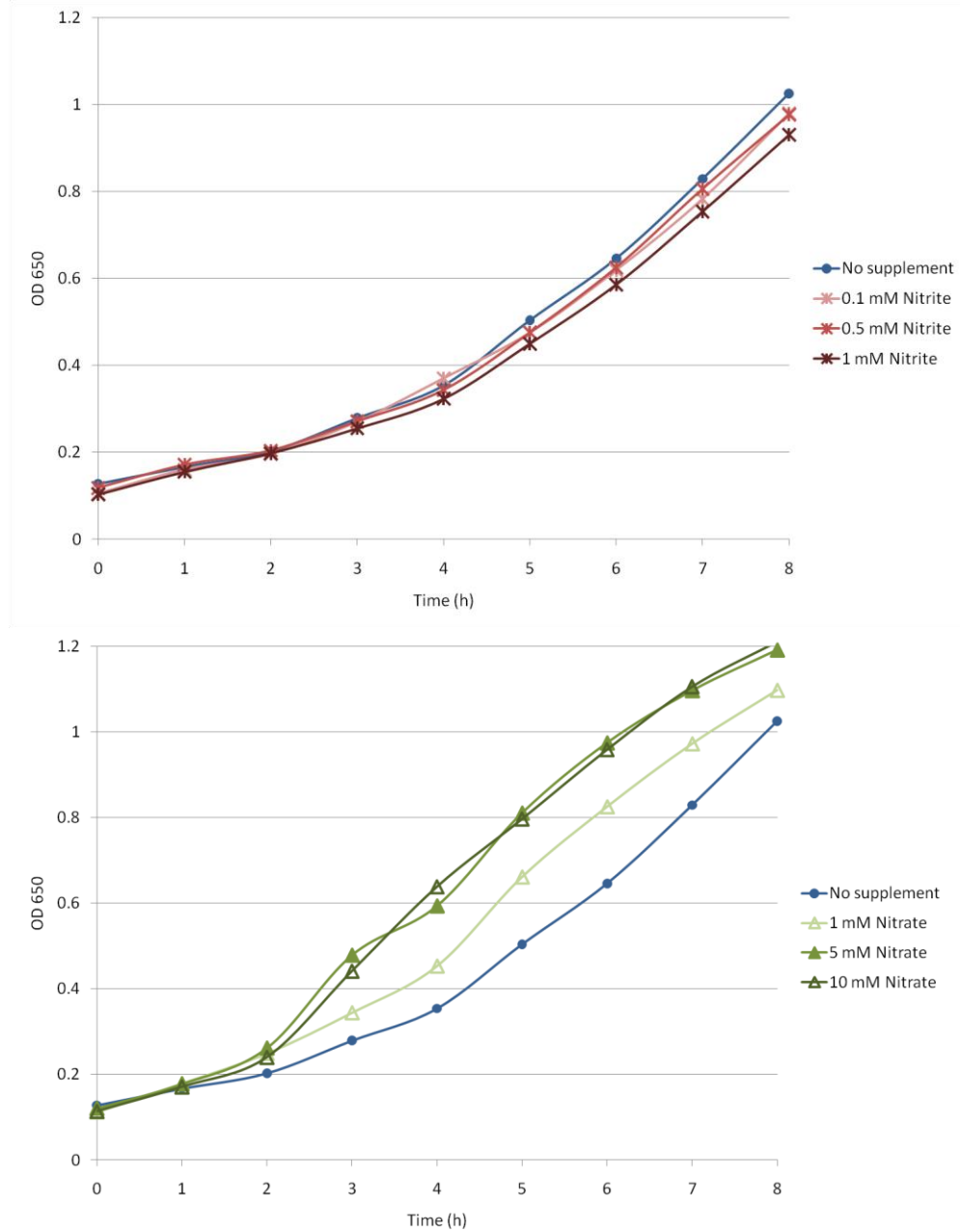
When the *nirBDC nrfAB norV* strain was grown in medium supplemented with nitrite, a similar phenotype to the *nirBDC nrfAB hcp* mutant was observed: the rate of NO reduction was 30% higher than the parental rate (Table 4.2). To investigate the sensitivity of this strain to the growth conditions used, the *nirBDC nrfAB norV* strain, JCB 5232, was grown anaerobically in medium containing 0.1 to 1 mM sodium nitrite or 1 to 10 mM sodium nitrate. Growth of the *nirBDC nrfAB norV* strain was not inhibited by addition of sodium nitrite to the medium (Figure 4.10). Growth of the *nirBDC nrfAB norV* strain did not provide any clues as to why the rate of NO reduction might be elevated.

When the quadruple mutant strain was grown in medium supplemented with sodium nitrite, the rate of NO reduction was 22% lower than the parent (Table 4.2). In the parent strain, the presence of nitrate in the medium induced a 1.9-fold increase in the rate of NO reduction relative to the rate of nitrite-grown bacteria (Figure 4.4). In the quadruple mutant strain, there was only a 1.2-fold increase (Table 4.2). However, this small induction is still statistically significant ($p=0.048$). These mutations in all known NO reductases decreased the NO reduction capacity of *E. coli* to only 50% of the parent. Therefore, this again indicated that uncharacterised mechanisms that are able to reduce NO remain active in *E. coli*.

Growth of the strain defective in all known NO reductases.

The parental strain, RK4353, and the quadruple mutant strain, JCB 5210, were used to investigate the sensitivity of the quadruple mutant to the presence of nitrate and nitrite in the growth medium. The strains were grown anaerobically in medium that was either unsupplemented, or supplemented with 2.5 mM sodium nitrite or 20 mM sodium

Figure 4.10.



Growth phenotypes of strains defective in several NO reductases

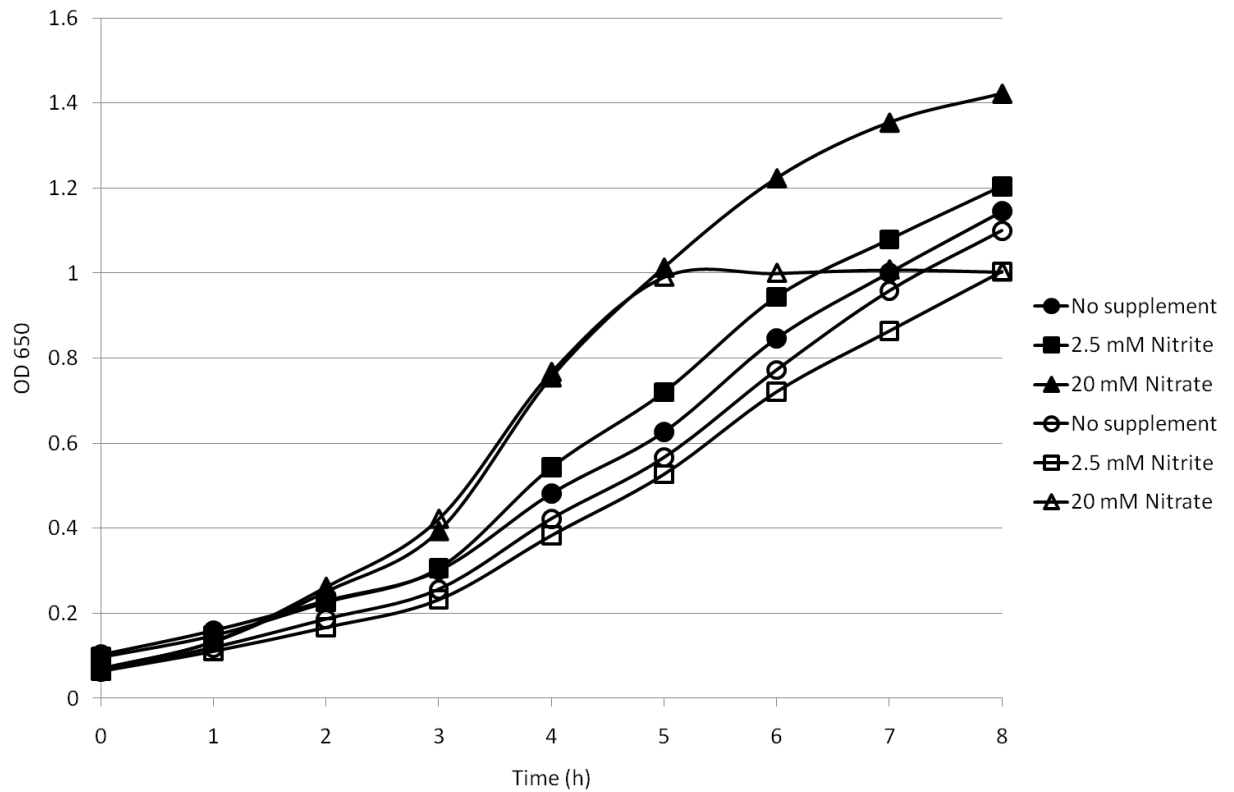
The *nirBDC nrfAB norV* strain, JCB 5232, was grown anaerobically in medium that was either unsupplemented (blue), or supplemented with 0.1-1 mM sodium nitrite (top panel, red,) or 1-10 mM sodium nitrate (bottom panel, green). In each case the palest line represents the lowest supplement concentration (see legends). Growth curves were completed in at least biological duplicate and this graph represents a typical experiment.

nitrate. When the medium was unsupplemented, the quadruple mutant strain had a similar growth phenotype to the parent strain (Figure 4.11). When the medium was supplemented with 2.5 mM nitrite, growth of the parent was slightly stimulated, but growth of the quadruple mutant was slightly inhibited relative to growth in the unsupplemented medium (Figure 4.11). In the presence of 20 mM nitrate, growth of the quadruple mutant strain was similar to the parent for the first 5 h. However, when the optical density at 650 nm had increased to 1.0, growth of the quadruple mutant stopped abruptly, whereas the parent continued to grow (Figure 4.11). The continued growth of the parent confirmed that the medium still contained nutrients required for growth.

The effect of the nitrate reductase, NarG, on the rate of NO reduction.

In chapter 3, it was concluded that NarG is a major contributor to NO generation from nitrite. To investigate whether intracellular NO generation influenced the rate of NO reduction, or influenced the induction of a higher rate in the presence of nitrate, a *narGHJI narZ* strain, JCB 4031, and a parental strain, RK4353, were grown and assayed for NO reduction as previously described. The rate of NO reduction of the *narGHJI narZ* strain grown in the presence of nitrate was 52% lower than the parental rate, while the rate of NO reduction for bacteria grown in the presence of nitrite was 37% lower than the parent (Figure 4.12). There was still a statistically significant induction of a higher rate of NO reduction caused by nitrate in the medium ($p=0.001$), relative to the rate of NO reduction in medium supplemented with nitrite. This result suggests that an active NarG is not essential for the induction of a higher rate of NO reduction by nitrate in the medium, although the absence of NarG clearly decreased the rate of NO reduction in medium supplemented with either nitrate or nitrite. This is

Figure 4.11.



Growth phenotype a strain defective in all four known NO reductases in minimal medium which was unsupplemented, or supplemented with nitrate or nitrite.

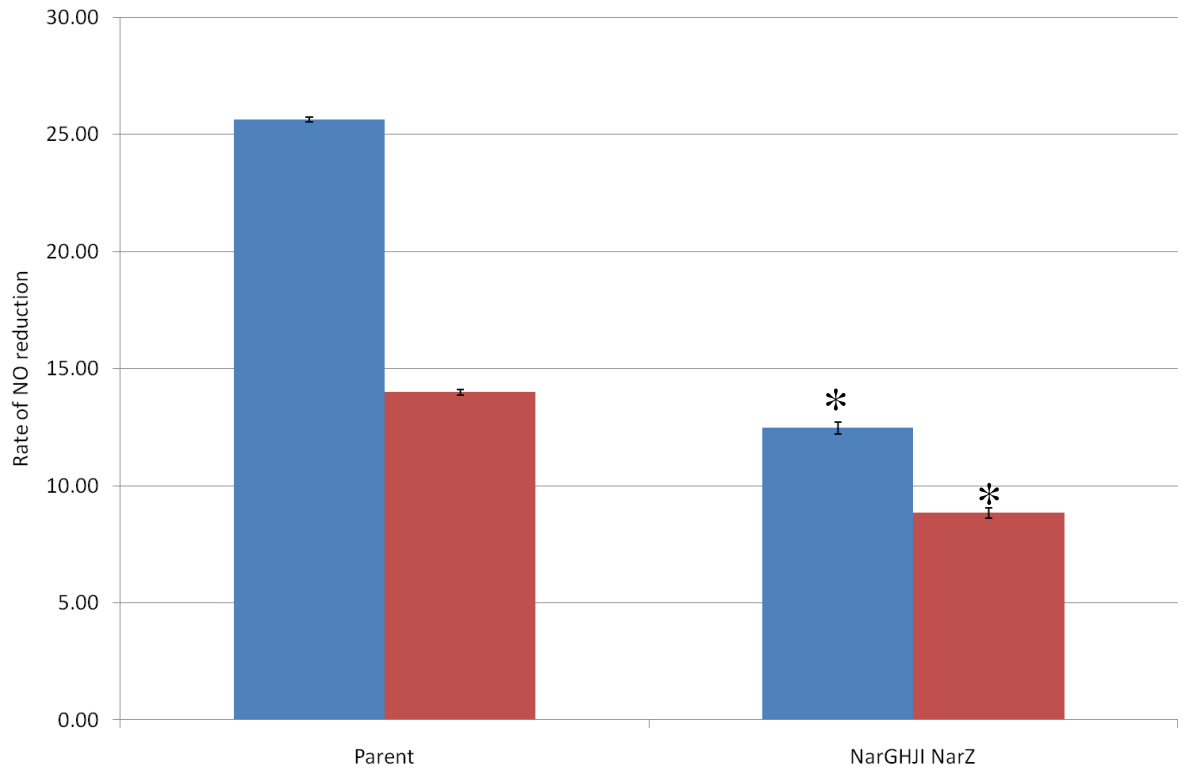
The parental strain, RK4353 (closed symbols), and the quadruple mutant strain, JCB 5210 (open symbols), were grown anaerobically in medium that was either unsupplemented (●○), or supplemented with 2.5 mM sodium nitrite (■□) or 20 mM sodium nitrate (▲△). Other details are as in Figure 4.9.

consistent with NarG being responsible for intracellular NO generation; the presence of NO in the cell would induce the activity of proteins known to reduce NO such as NorVW.

The effect of regulatory proteins on the rate of NO reduction by the quadruple mutant strain defective in all characterised NO reductases.

As the strain defective of all four known NO reductases was still able to reduce NO, it was interesting to investigate what might regulate the remaining NO reductase activity. The Fnr protein regulates the aerobic to anaerobic switch in *E. coli* and NarL regulates the response to nitrate and nitrite (Lazazzera *et al.*, 1996, Constantinidou *et al.*, 2006, Rabin and Stewart, 1993). To investigate whether these transcription factors regulate NO reduction, the quadruple mutant and its *fnr* and *narL* derivatives were grown and assayed for NO reduction as previously described (Tables 4.1 and 4.2 summarise genotypes). When bacteria were grown in medium supplemented with nitrate, the *narL* derivative reduced NO at 85% of the quadruple mutant strain, JCB 5210, but this decrease was not statistically significant ($p=0.084$) (Figure 4.13). When the *narL* derivative strain, JCB 5252, was grown in medium supplemented with nitrite, the rate of NO reduction was 72% of the parental rate; this difference was statistically significant ($p=0.021$). The remaining NO reduction activity in the strain defective in all known NO reductases was not totally NarL dependent. When the *fnr* derivative strain, JCB 5251, was grown in medium supplemented with nitrate, the rate of NO reduction was slightly higher than the parental strain (Figure 4.13). However, when the medium was supplemented with nitrite, the *fnr* derivative strain did not reach an appropriate optical density to assay. Growth of the *fnr* derivative will be explored in the next section. As Fnr induces several proteins required for anaerobic metabolism, it is unsurprising that the deletion of Fnr causes defective growth in the presence of nitrite.

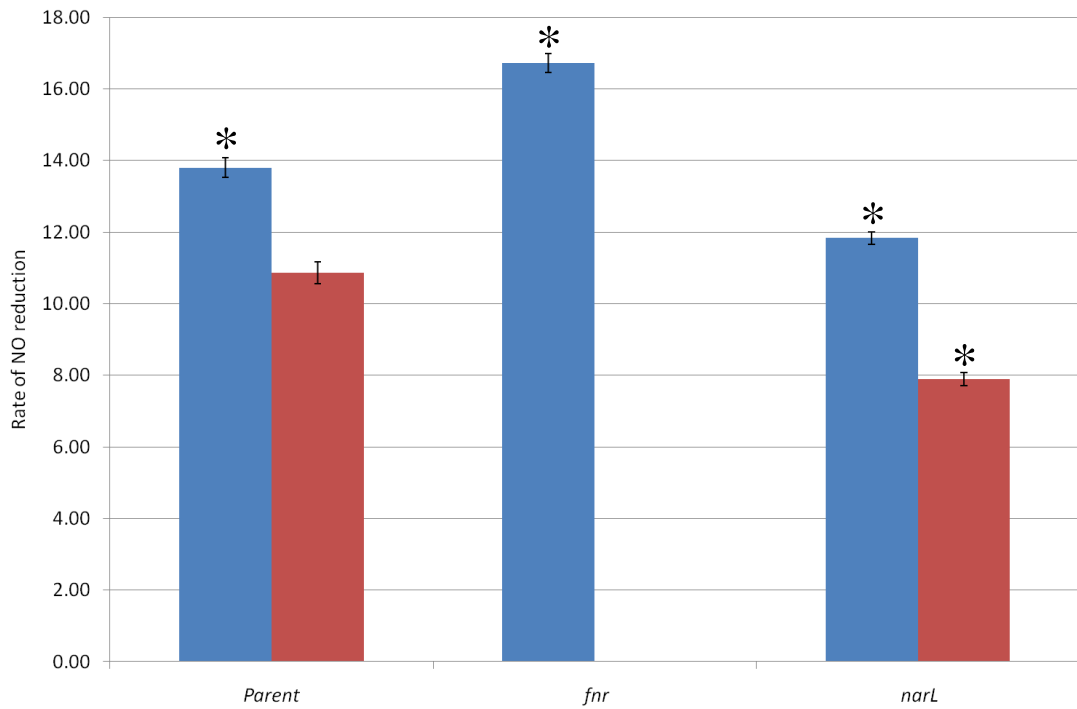
Figure 4.12.



Rate of NO reduction in NarG defective bacteria.

The *narGHJI narZ* strain, JCB 4031, and the parent strain, RK4343, were grown anaerobically in minimal medium supplemented with 20 mM sodium nitrate (blue) or 2.5 mM sodium nitrite (red), and were assayed for NO reduction activity as previously described. A star above a bar represents that data are significantly different from the parent strain, RK4353 (see text). Other details are as in Figure 4.4.

Figure 4.13



Rate of NO reduction of strains defective in all known NO reductases with additional mutations

In this experiment each strain was defective in all four known NO reductases, NirBDC NrfAB NorV and Hmp. The quadruple mutant strain, JCB 5210, the *nirBDC nrfAB norV hmp fnr* strain, JCB 5251, and the *nirBDC nrfAB norV hmp narL* strain, JCB 5252, were grown anaerobically in minimal medium supplemented with 20 mM sodium nitrate (blue) or 2.5 mM sodium nitrite (red), and were assayed for NO reduction activity as previously described. A star above a bar represents that data are significantly different from the RK4353 strain (see text). Other details are as in Figure 4.4.

Response of the *nirBDC nrfAB norV hmp fnr* strain to low nitrite concentrations.

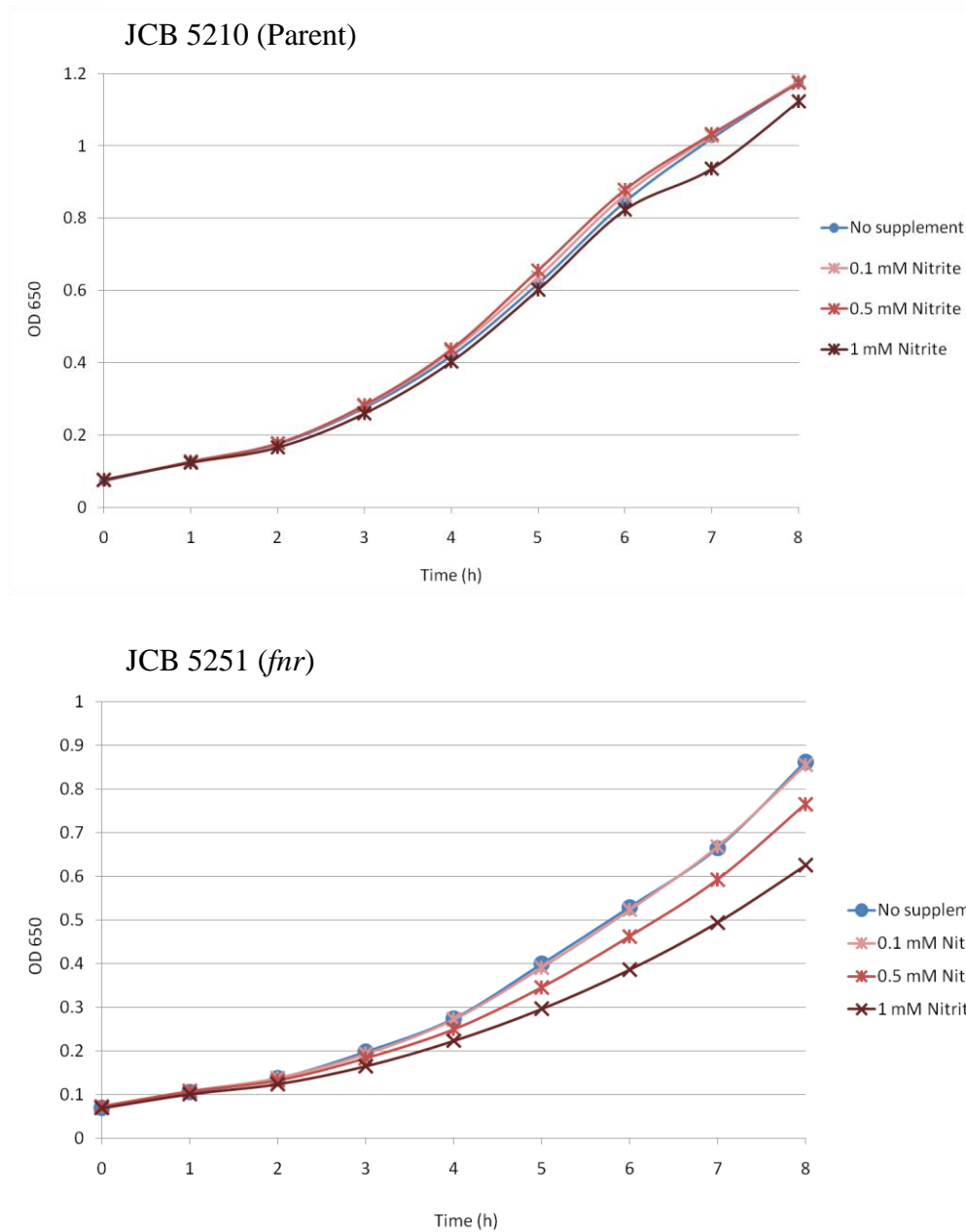
To investigate the poor growth of the *fnr* derivative strain in the presence of nitrite, the *nirBDC nrfAB norV hmp* parent strain, JCB 5210, the *nirBDC nrfAB norV hmp fnr* strain, JCB 5251, were grown in medium supplemented with a range of nitrite concentrations (0.1-1 mM sodium nitrite). The optical density at 650 nm was monitored for 8 hours. The parent strain was not sensitive to these low nitrite concentrations (Figure 4.14). However, the *fnr* derivative strain shows a clear dose-dependent sensitivity to even low concentrations of nitrite. This sensitivity to nitrite accounts for the failure of the *nirBDC nrfAB norV hmp fnr* culture to reach an adequate optical density to assay.

Discussion

Several conclusions can be drawn from the work presented in this chapter. Firstly, when *E. coli* is grown in medium that promotes anaerobic respiration using glycerol as a non-fermentable carbon source, the rate of NO reduction is around 2-fold higher following growth in the presence of nitrate than in the presence of nitrite. This induction caused by nitrate in the medium is not controlled by NarL or NsrR.

No single enzyme that is known to reduce NO *in vitro*, neither NirBDC, NrfAB, NorV nor Hmp, is responsible for the majority of NO reduction in *E. coli*. Even a strain defective in all four known NO reductases is still able to reduce NO at least 50% of the parental rate. Further mechanisms for the reduction of NO in *E. coli* during anaerobic respiration must remain uncharacterised. A similar systematic deletion experiment was completed in *Salmonella enterica* serovar Typhimurium to examine the contribution of the protective proteins NrfA, NorV and Hmp to NO reduction (Mills *et al.*, 2008). Conclusions of the study in *Salmonella* were that NrfA and NorV play a key role in

Figure 4.14



Growth of JCB 5210 and JCB 5251 in the presence of a range of nitrite concentrations

The *nirBDC nrfAB norV hmp* parent strain, JCB 5210 (top panel), and the *nirBDC nrfAB norV hmp fnr* strain, JCB 5251 (bottom panel), were grown anaerobically in medium that was either unsupplemented (blue), or supplemented with 0.1-1 mM sodium nitrite (red). The palest line represents the lowest nitrite concentration (see legends). Other details are as in Figure 4.10.

protection against killing by NO *in vivo*, but yet more NO-detoxification systems remain to be identified. Results for *E. coli* presented in this chapter do not provide strong evidence that either NrfA or NorV *in vivo* are critical for NO reduction. However, the data from *E. coli* do agree with the conclusion that further NO-detoxification systems remain to be characterised.

NorV expression increases 5-15 minutes after *in vitro* exposure to NO, and remains constant, whereas Hmp expression is induced 45 minutes after NO exposure (Justino *et al.*, 2005). In the experiments described in this chapter, both NorV and Hmp should be expressed, as intracellular NO is generated from nitrite present in the growth medium. Although *in vitro* the Hmp protein is able to reduce NO anaerobically to N₂O, the key role of Hmp is as an aerobic oxygenase (Kim *et al.*, 1999, Mills *et al.*, 2001, Gardner and Gardner, 2002). In light of this, it is unsurprising that the rate of NO reduction of an *E. coli hmp* mutant grown anaerobically in the presence of nitrate or nitrite was similar to the NO reduction rate of the parent strain. Kinetic characterisation has shown the NrfA protein to have the highest turnover number for NO reduction (Table 4.3). It has been speculated that periplasmic NrfA would detoxify the majority of NO before it reaches the cytoplasm, and that the cytoplasmic protein, NorV, would reduce any NO that enters the cytoplasm (van Wonderen *et al.*, 2008). This rationalises the low turnover number for NO of 15 for NorV (Table 4.3), which is consistent with the result in this chapter that a *norV* mutant, grown anaerobically in medium supplemented with nitrate or nitrite, reduces NO at a rate similar to the parent. However, it would have been expected that a *nrfA* mutant would reduce NO at a significantly lower rate than its parent, but this was not the case. The kinetics of NirB as an NO reductase have not been characterised, so there are no data to compare to our *in vivo* experiments. The toxicity of nitrite accumulation in the cytoplasm of bacteria

lacking the protective NirBDC proteins could contribute towards the lower rate of NO reduction in the *nirBDC* strain.

No gene of unknown function tested, neither YeaR-YoaG, YgbA, Hcp nor YibIH was responsible for the majority of NO reduction in *E. coli*. The repair protein, YtfE, might be indirectly important in resisting nitrosative stress by repairing iron centres that are important for NO reduction. Perhaps the slight decrease in the rate of NO reduction for a *ytfE* mutant, relative to the parent, is consistent with the importance of YtfE to repair iron centres. Several proteins required to resist nitrosative stress contain iron cofactors; the transcription factors NsrR, Fur and Fnr contain iron, as does the flavorubredoxin NorV. It is possible that currently uncharacterised NO reductases might also require a functional iron centre. Despite this slight effect, YtfE is not responsible for the majority of NO reduction in *E. coli*.

The lowest rate of NO reduction measured in this study was by a strain defective in the transcription factor NsrR. This suggests that a gene activated by NsrR might be an important uncharacterised mechanism for NO reduction. NsrR has been characterised mainly as a repressor of genes involved in the nitrosative stress response (Bodenmiller and Spiro, 2006, Filenko *et al.*, 2007). However, at least one other transcription factor in the Rrf2 family, IscR, can function both as a repressor and an activator. Microarray data suggest that the *ydbC* promoter is activated by NsrR (Filenko *et al.*, 2007). It is possible that YdbC is responsible for the residual NO reduction in the *nirBDC nrfAB norV hmp* strain. Further experiments must assay a *ydbC* mutant, and involve the construction and assay of a *nirBDC nrfAB norV hmp ydbC* strain.

Although the rate of NO reduction for mutants defective in a combination of NO reductases was similar to the parent, growth inhibition became apparent. After 5 h of

Table 4.3. Reported kinetic parameters for NO reductase activity by *E. coli* proteins.

Protein	Estimated turnover number for NO (s⁻¹)	Reported K_m Value (μM)	Relevant information	Reference
NrfA	840	300		van Wonderen <i>et al.</i> , 2008
NrfA	390	NR		Poock <i>et al.</i> , 2002
NrfA	27	NR	Estimated if NO concentration was 10 μM	van Wonderen <i>et al.</i> , 2008
Hmp	0.013	NR	Anaerobic estimated	Kim <i>et al.</i> , 1999
Hmp	0.24	NR	Anaerobic measured	Kim <i>et al.</i> , 1999
Hmp	670	NR	Aerobic	Gardner and Gardner, 2002
Hmp	0.02	NR	Anaerobic	Gardner and Gardner, 2002
Hmp	1/100 of Aerobic rate	NR	Anaerobic	Mills <i>et al.</i> , 2001
NorV	15	0.4		van Wonderen <i>et al.</i> , 2008

This table summarises the predicted turnover numbers and K_m values for NO of various proteins involved in NO detoxification. The column ‘relevant information’ gives important parameters of the experiment described, where relevant. The data were taken from several different studies. NR means that a K_m value was not reported in the reference cited.

growth in the presence of nitrate, the concentration of nitrate in the medium had decreased. In chapter 3, it was confirmed that at a low nitrate concentration, NarG starts to reduce nitrite to NO (Figure 3.8). When all four known protective proteins are absent, the accumulation of NO in the cytoplasm would become toxic. This is consistent with the growth cessation observed in late exponential phase. From both the NO reduction and growth data, these characterised systems clearly contribute to protection against nitrosative stress, but are not the sole protective mechanism. This raised the question: how do bacteria protect themselves from nitrosative damage? In chapter 6, data will be presented from multiple mutant strains that are defective in a combination of NO reductases as well as characterised repair proteins and proteins of unknown function that might be involved in the repair of nitrosative damage.

CHAPTER 5. RESULTS.

Repair of nitrosative damage: regulation of *PytfE* transcription and phenotypes of *ytfE* mutants.

Introduction.

Reactive nitrogen species (RNS), such as nitric oxide, are able to bind to and damage bacterial proteins, lipids, and DNA. Iron-sulphur cofactors in proteins are particularly susceptible to damage, and several di-iron proteins in different species have recently been shown to be important for repair (Overton *et al.*, 2008). RNS can cause lysine sidechains in proteins to become potent DNA methylating agents (Taverna and Sedgwick, 1996, Weiss, 2006, Squire *et al.*, 2009). The O⁶-methylguanine DNA methyltransferase, Ogt, is induced by nitrate to repair methylated DNA adducts, and therefore prevents mutagenesis during anaerobic growth in the presence of nitrate (Squire *et al.*, 2009). An aim of the work presented in this chapter was to investigate links between known and uncharacterised repair proteins, their regulation, and the importance of repair pathways to anaerobic growth of *E. coli*.

The role of the di-iron protein, YtfE, in resisting nitrosative stress.

A microarray paper first identified YtfE as a candidate for conferring anaerobic resistance to NO (Justino *et al.*, 2005). YtfE is cytoplasmic protein that is conserved in all enterobacteria (Justino *et al.*, 2006). A *ytfE* mutant grew poorly anaerobically, under a range of conditions, and this phenomenon will be examined in detail in this chapter. All examined iron-sulphur proteins had decreased specific activities in a *ytfE* mutant, and mutation of *ytfE* increased the sensitivity of *E. coli* to iron starvation. Recombinant YtfE did not reduce nitric oxide (Justino *et al.*, 2006). Analysis of the protein sequence

identified conserved carboxylate and histidine residues that would coordinate a non-haem iron centre, which was a candidate for an active site for NO chemistry. YtfE was shown by UV-visible and EPR spectroscopy to be a binuclear non-haem iron protein. A novel biosynthetic role in the formation of iron-sulphur clusters was proposed (Justino *et al.*, 2006). YtfE confers protection against both oxidative stress and nitrosative stress (Justino *et al.*, 2007). In a *ytfE* mutant, intracellular free iron levels increase. YtfE does not protect iron centres from destruction, instead performing a repair role, perhaps in the enzymatic process to recruit and integrate ferrous iron into clusters (Justino *et al.*, 2007).

Similarities between the regulation of *ytfE* and several genes encoding proteins of unknown function, *hcp*, *yeaR-yoaG*, *ygbA* and *yibIH* were reported in a microarray paper (Constantinidou *et al.*, 2006). As such a distinct phenotype was revealed for a *ytfE* mutant from the work by Justino and colleagues (2005 and 2006), it was interesting to compare the growth phenotype of a *ytfE* mutant with strains mutated in these genes of unknown function. Proteins that are expressed under similar conditions, or are regulated by similar transcription factors often function in related roles. The regulation of the *ytfE* promoter was compared to the recently published regulation of the *yeaR-yoaG* and *ogt* promoters (Squire *et al.*, 2009).

Construction of a new *ytfE* mutation in strain RK4353.

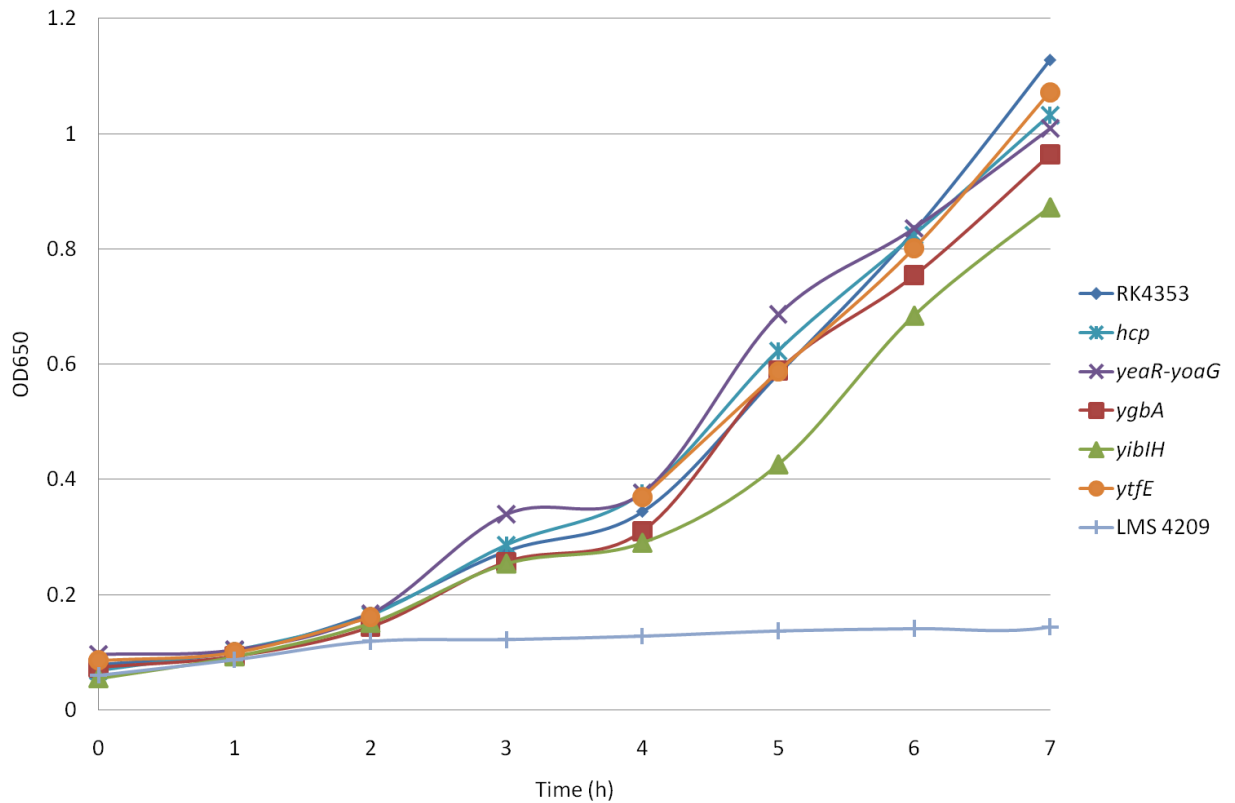
It has been shown that the growth of a *ytfE* mutant is particularly inhibited during anaerobic growth, especially in minimal salts medium supplemented with glycerol as the main carbon source and nitrate as a terminal electron acceptor (Justino *et al.*, 2006). Experiments were completed to investigate whether *yibIH*, *ygbA*, *hcp*, and *yeaR-yoaG*

mutants have a similar growth-defective phenotype and thus might function in a related role. In order to compare the anaerobic growth phenotype of *E. coli* RK4353 mutant strains to that of a K-12 *ytfE* mutant, an isogenic set of mutants was required. P1 transduction was used to transfer the *ytfE* mutation from strain LMS 4209 into wild type RK4353. Colony PCR was used to confirm that the resultant chloramphenicol resistant colonies contained the chloramphenicol resistance cassette (*cat*) in place of the *ytfE* gene, and thus had been successfully transduced.

Anaerobic growth of RK4353 mutants in medium supplemented with nitrate.

In order to investigate whether a deficiency in genes of unknown function gave a similar growth-defective phenotype to the *ytfE* strain, LMS 4209, the parent strain, RK4353, the *hcp* strain, JCB 4999, the *yeaR-yoaG* strain, JCB 5100, the *ygbA* strain, JCB 5207, the *yibiH* strain, JCB 5208, and the *ytfE* strains, RK4353 $\Delta ytfE::cat$ and LMS 4209, were grown anaerobically in minimal medium supplemented with nitrate, as described by Justino *et al.*, (2006). The optical density at 650 nm of each culture was measured at hourly intervals for 8 hours. The growth rate and final optical density of each new mutant, including unexpectedly the strain RK4353 $\Delta ytfE::cat$, was similar to the RK4353 parent (Figure 5.1). LMS 4209 had a severe growth deficient phenotype under these conditions (Figure 5.1). It is possible to conclude that the set of genes encoding proteins of unknown function do not play the same critical role as is suggested for YtfE by strain LMS 4209. However, the fact that the RK4353 $\Delta ytfE::cat$ strain is not deficient in growth required further investigation. It was possible that the phenotype of strain LMS 4209 was not due to the *ytfE* mutation alone.

Figure 5.1.



Anaerobic growth of *Escherichia coli* strains in the presence of nitrate.

The parent strain, RK4353 (dark blue), the *hcp* strain, JCB 4999 (turquoise), the *yeaR-yoaG* strain, JCB 5100 (purple), the *ygbA* strain, JCB 5207 (red), the *yibIH* strain, JCB 5208 (green), and the *ytfE* strains, RK4353 $\Delta ytfE::cat$ (orange) and LMS 4209 (pale blue), were used. Bacteria were grown anaerobically, in minimal medium that was supplemented with nitrate, as described by Justino *et al.*, (2006). The optical density at 650 nm of each culture was measured at hourly intervals for 8 hours. The growth experiment was completed at least in duplicate and this graph represents a typical result.

Reconstruction and growth of *Escherichia coli* K-12 ATCC 26176 *ytfE*.

To investigate whether the different growth phenotypes of the *ytfE* strains, LMS 4209 and RK4353 $\Delta ytfE::cat$, were due to differences between the parent strains, RK4353 and K-12 ATCC 23716, the *ytfE* mutation was transduced from RK4353 *ytfE::cat* into the original parental strain K-12 ATCC 23716, to make strain JCB 5201. PCR was used to confirm the presence of the *cat* cassette in JCB 5201. The *ytfE* strains, JCB 5201, LMS 4209 and RK4353 $\Delta ytfE::cat$, and the parent strains, RK4353 and K-12 ATCC 23716, were grown anaerobically in the presence of nitrate as described previously. Growth of both new *ytfE* mutants closely matched those of both of the wild type strains, RK4353 and K-12 ATCC 23716 (Figure 5.2). The original *ytfE* strain, LMS 4209, was severely growth deficient. The rapid growth of RK4353 $\Delta ytfE::cat$ relative to LMS 4209 was not due to the fact that it was an RK4353 derivative.

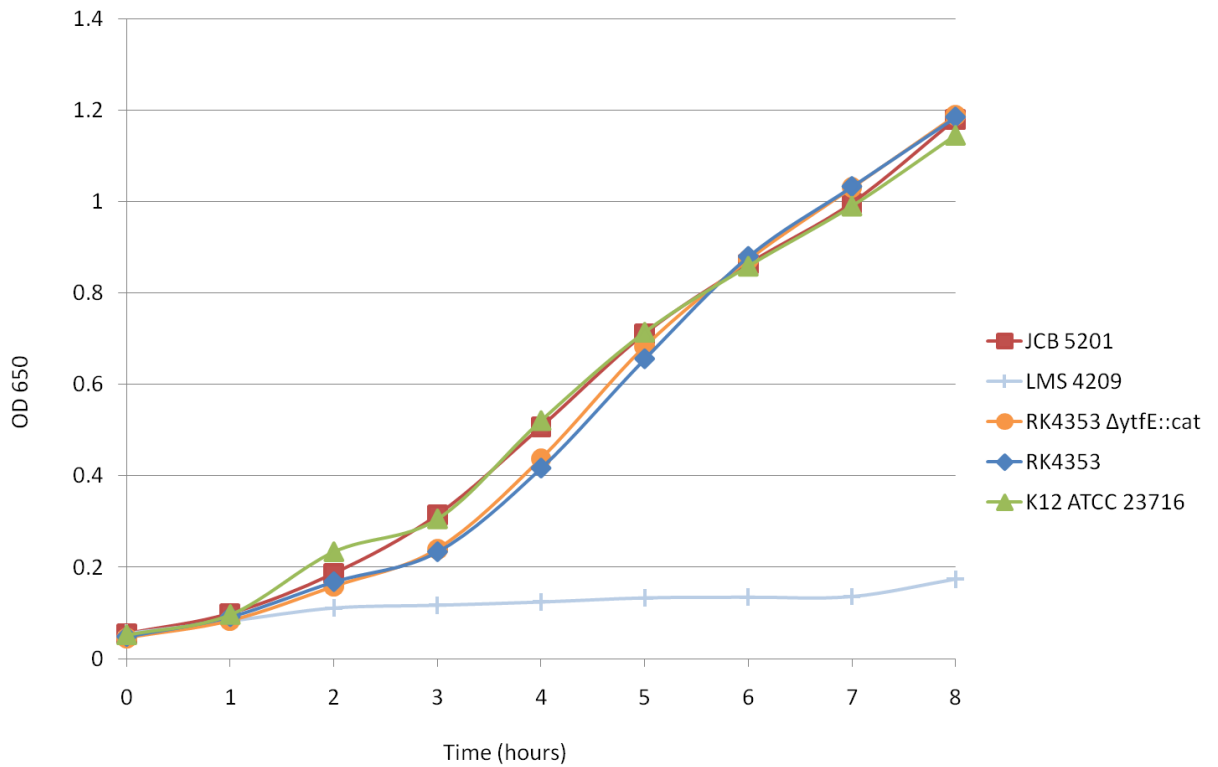
Reconstruction of the *ytfE* mutation in *E. coli* K-12 ATCC 23716.

In separate experiments, several *ytfE* derivatives of K-12 ATCC 23716 were constructed by P1 transduction to generate strains JCB 5202, JCB 5203 and JCB 5204. The *ytfE* strains, JCB 5201, JCB 5202, JCB 5203, JCB 5204 and LMS 4209, and the parent strain, K12 ATCC 23716, were used. Anaerobic growth of all transductants in medium supplemented with nitrate was not deficient relative to the parental strain and strain LMS 4209 was deficient in growth (Figure 5.3). In comparison to several other *ytfE* strains, LMS 4209 is unique in the inability to grow anaerobically in medium supplemented with sodium nitrate.

Growth of K-12 ATCC 23716 *ytfE* mutants in the presence of DMSO, fumarate or nitrite.

To determine whether the unique growth deficiency of strain LMS 4209 extended to

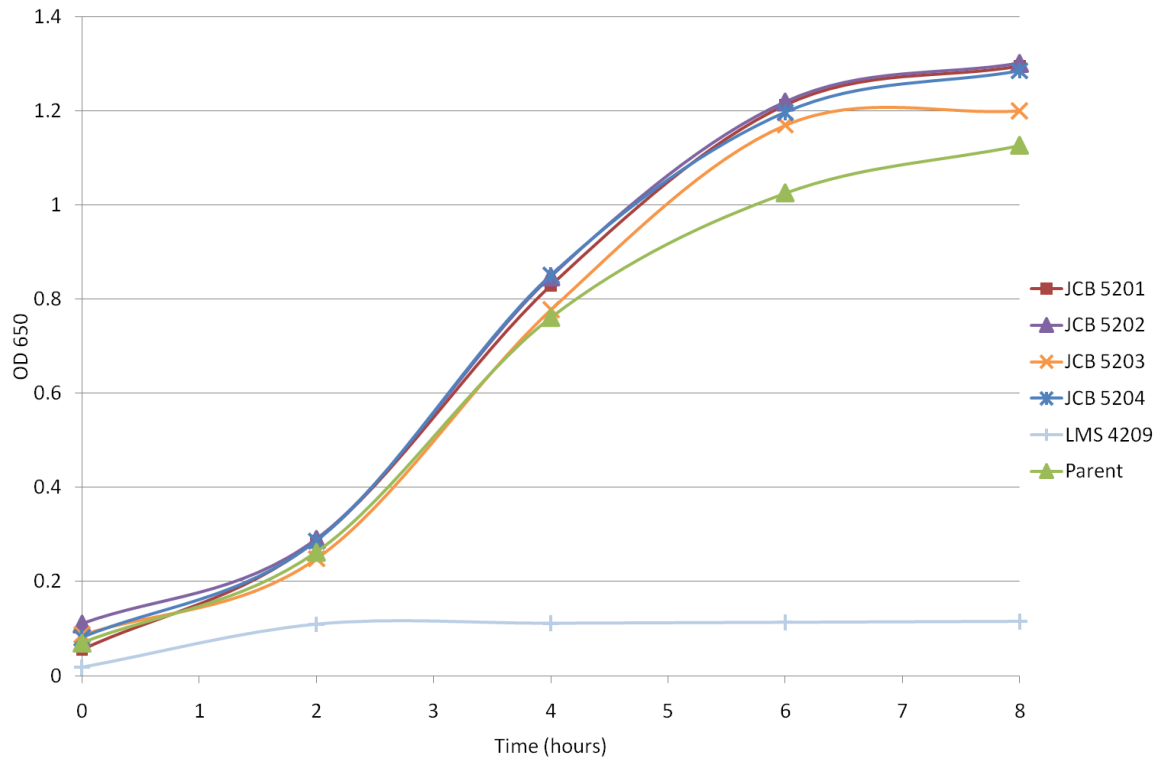
Figure 5.2.



Anaerobic growth of *Escherichia coli* strains using nitrate as a terminal electron acceptor.

The *ytfE* strains, JCB 5201 (red), LMS 4209 (pale blue) and RK4353 $\Delta ytfE::cat$ (orange), and the parent strains, RK4353 (dark blue) and K12 ATCC 23716 (green), were used. Bacteria were grown anaerobically, in minimal medium that was supplemented with nitrate, as described by Justino *et al.*, (2006). Other details were as in Figure 5.1.

Figure 5.3.



Anaerobic growth of *Escherichia coli* strains in the presence of nitrate.

The *ytfE* strains, JCB 5201 (red), JCB 5202 (purple), JCB 5203 (orange), JCB 5204 (dark blue) and LMS 4209 (pale blue), and the parent strain, K12 ATCC 23716 (green), were used. Bacteria were grown anaerobically, in minimal medium that was supplemented with nitrate, as described by Justino *et al.*, (2006). Other details were as in Figure 5.1.

growth in the presence of other terminal electron acceptors, several growth experiments were completed with the *ytfE* strains, LMS 4209, JCB 5201 and JCB 5202, and the parent strain, K-12 ATCC 23716. The optical density at 650 nm was measured at hourly intervals, and the doubling time for each strain and condition was calculated (Table 5.1). Anaerobic growth of both JCB 5201 and JCB 5202 was similar to that of the parental strain when the minimal medium was supplemented with 40 mM fumarate, 40 mM DMSO or 40 mM fumarate and 5 mM nitrite. In each case, the growth of LMS 4209 was perturbed (Figure 5.4). The results of these assays suggested that growth defect of LMS 4209 might have been due to a secondary mutation, rather than the *ytfE* deletion itself.

Comparative genomic hybridisation to locate any secondary mutations.

The introduction of secondary mutations, such as unintended deletions, following use of the chromosomal gene inactivation method of Datsenko and Wanner (2000) has been described previously (Hobman *et al.*, 2007). To identify the cause of the inability of strain LMS 4209 to grow rapidly anaerobically, genomic DNA from both the mutant and K-12 ATCC 23716 parent strain was prepared, and used in a comparative genomic hybridisation assay. Total DNA was hybridised to an *E. coli* K-12 oligonucleotide microarray based on the published sequence of the strain MG1655. The hybridisation was completed by Mala Patel and Dr Chrystala Constantinidou in the *E. coli* genomics unit at the University of Birmingham. The initial results were analysed by Dr Chrystala Constantinidou and have been summarised in Figure 5.5 and Table 5.2. One hundred and twenty six genes, including *ytfE*, had been deleted from strain LMS 4209 (Vine *et al.*, 2010). The remaining 125 genes were deleted from a separate locus, from position 782389 to 914128 on the chromosome and included, crucially, genes essential for

Table 5.1. Doubling times of *ytfE* strains grown on minimal medium supplemented with a range of terminal electron acceptors.

Terminal electron acceptor	K-12 ATCC 23716 Parent strain	LMS 4209 (<i>ytfE</i>)	JCB 5201 (<i>ytfE</i>)	JCB 5202 (<i>ytfE</i>)
Nitrate	78±8	317±10	76±7	81±9
Fumarate and 5 mM Nitrite	151±16	240±25	162±17	155±17
Fumarate	125±15	240±24	162±17	155±16
DMSO	203±7	450±30	243±23	229±19

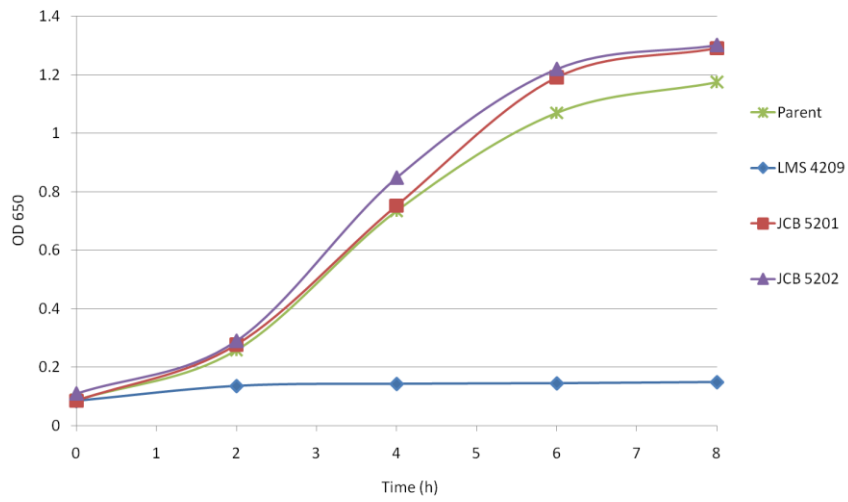
Doubling times (min) of *Escherichia coli* strains are tabulated. Bacteria were grown in minimal medium, supplemented with 0.4% glycerol and 40 mM each terminal electron acceptor unless otherwise stated. Growth experiments were completed at least in biological duplicate, and the error noted is the standard deviation of these repeats.

Figure 5.4.

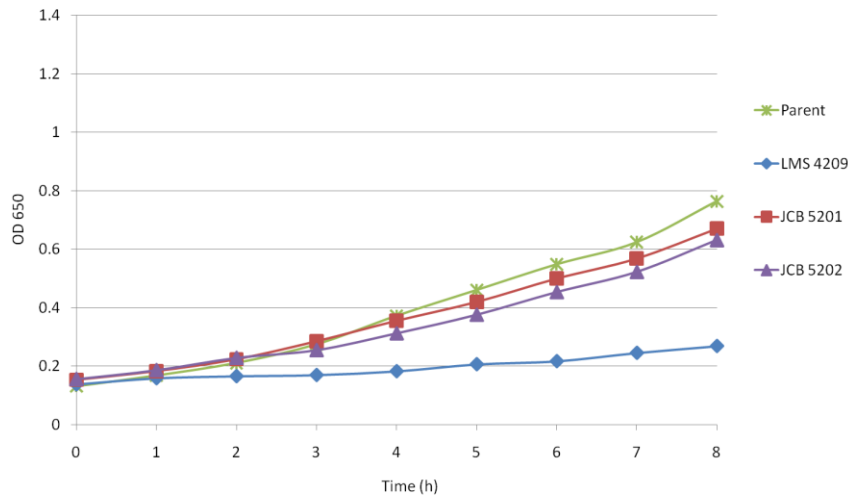
Anaerobic growth of *Escherichia coli* strains in the presence of nitrate, DMSO and nitrite.

The parent strain, K12 ATCC 23716 (green) and the *ytfE* strains, JCB 5201 (red), JCB 5202 (purple) and LMS 4209 (blue), were used. Bacteria were grown anaerobically, in minimal medium that was supplemented with either 40 mM nitrate (Panel A), 40 mM DMSO (Panel B) or 40 mM fumarate and 5 mM nitrite (Panel C), as described by Justino *et al.*, (2006). Other details were as in Figure 5.1

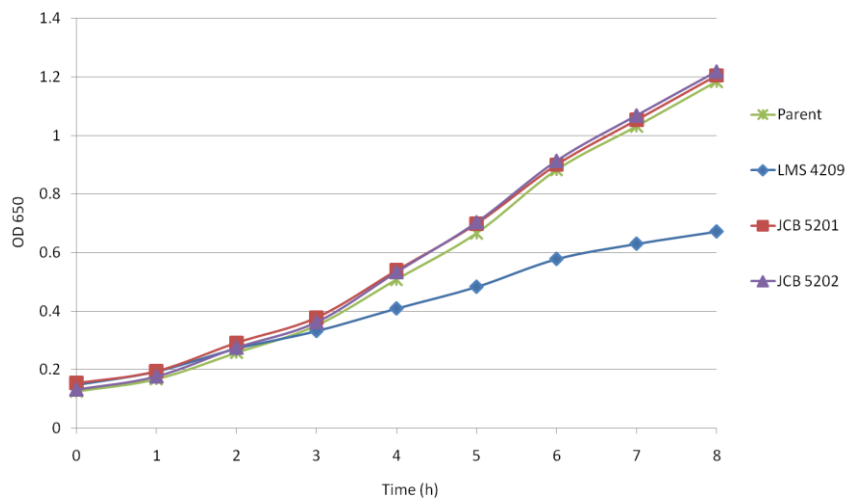
A. Nitrate



B. DMSO



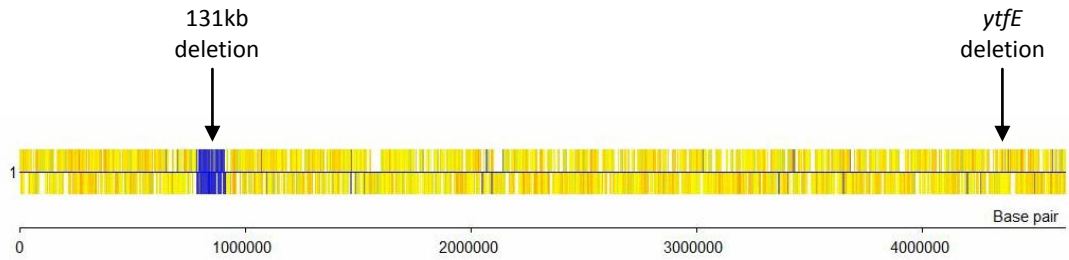
C. Fumarate and nitrite



molybdopterin biosynthesis. These include genes from the *mod*, *moa* and *moe* operons, which are required for molybdate transport and molybdopterin synthesis. Proteins involved in anaerobic respiration in *E. coli* that require a molybdopterin cofactor include DMSO reductase, TMAO reductase, nitrate reductase (*narGHI* and *narZYW*) and formate dehydrogenase (*fdnGHI* and *fdoGHI*) (Kisker *et al.*, 1997). The results suggested that pathways requiring molybdoproteins were defective in LMS 4209 but not in the parental strain K-12 ATCC 23716. This prediction matches the published growth phenotypes in Justino *et al.*, (2006), where an inability to reduce nitrate and DMSO led to a growth deficiency.

Another of the genes deleted in LMS 4209, *modE*, encodes a transcription factor which activates expression of *dmsABC* and *napFDAGHBC* (McCrindle *et al.*, 2005, McNicholas and Gunsalus, 2002). Another protein deleted, ModC, induces *narGHJI* transcription (McNicholas *et al.*, 1998). Deletion of these activators would decrease transcription of the operons that encode a DMSO reductase and a nitrate reductase in *E. coli*. This further supports the reasoning that the secondary deletion identified in this study causes growth deficiency of LMS 4209 when using DMSO or nitrate as a terminal electron acceptor. It has been reported that a *ytfE* mutant has an increased sensitivity to iron starvation (Justino *et al.*, 2007). Comparative genomic hybridisation revealed that LMS 4209 lacks the iron storage protein encoded by *dps*. This protein has been reported to be important in sequestering iron and thus avoiding oxidative damage mediated by Fenton Chemistry (Fang, 2004, Zhao *et al.*, 2002). It has also been reported that higher intracellular iron concentrations are found in the strain LMS 4209 (Justino *et al.*, 2007). The removal of the iron storage protein encoded by *dps* might be a contributory factor to this observation.

Figure 5.5.



Comparative genomic hybridisation analysis to compare LMS 4209 and its parent K-12 strain ATCC 23716.

Genomic DNA was extracted from strains LMS 4209 and K-12 ATCC 23716 and hybridised to an oligonucleotide microarray based on the published sequence of *E. coli* strain MG1655. Genes identical in the two strains are represented by yellow bars, and mismatches are represented in blue. Arrows highlight the loci at which differences were found.

Table 5.2. Genes deleted in LMS 4209, as revealed by comparative genomic hybridisation.

Gene	Gene product description
b0751 <i>pnuC</i>	nicotinamide mononucleotide transporter
b0752 <i>ybgR</i>	zinc efflux system
b0753 <i>ygbS</i>	conserved protein; putative regulator
b0754 <i>aroG</i>	3-deoxy-D-arabino-heptulosonate-7-phosphate synthase,
b0755 <i>gpmA</i>	phosphoglyceromutase 1
b0756 <i>galM</i>	galactose-1-epimerase (mutarotase)
b0757 <i>galK</i>	galactokinase
b0758 <i>galT</i>	galactose-1-phosphate uridylyltransferase
b0759 <i>galE</i>	UDP-galactose-4-epimerase
b0760 <i>modF</i>	fused molybdate transporter subunits of ABC superfamily: ATP-binding components
b0761 <i>modE</i>	DNA-binding transcriptional dual regulator
b0762 <i>b0762</i>	predicted protein; Unknown function
b0763 <i>modA</i>	molybdate transporter subunit
b0764 <i>modB</i>	molybdate transporter subunit
b0765 <i>modC</i>	molybdate transporter subunit; ATP-binding component of ABC superfamily
b0766 <i>ybhA</i>	pyridoxal phosphatase / fructose 1,6-bisphosphatase
b0767 <i>pgl</i>	6-phosphogluconolactonase
b0768 <i>ybhD</i>	predicted DNA-binding transcriptional regulator
b0769 <i>ybhH</i>	conserved protein; Unknown function
b0770 <i>ybhI</i>	predicted tricarboxylate transporter
b0771 <i>ybhJ</i>	predicted hydratase
b0772 <i>ybhC</i>	outer membrane lipoprotein
b0773 <i>ybhB</i>	predicted kinase inhibitor; Unknown function
b0774 <i>bioA</i>	7,8-diaminopelargonic acid synthase, PLP-dependent
b0775 <i>bioB</i>	biotin synthase
b0776 <i>bioF</i>	8-amino-7-oxononanoate synthase
b0777 <i>bioC</i>	predicted methyltransferase, enzyme of biotin synthesis
b0778 <i>bioD</i>	dethiobiotin synthetase
b0779 <i>uvrB</i>	DNA repair; excision nuclease subunit B
b0780 <i>ybhK</i>	predicted transferase with NAD(P)-binding Rossmann-fold domain
b0781 <i>moaA</i>	molybdopterin biosynthesis protein A
b0782 <i>moaB</i>	molybdopterin biosynthesis protein B
b0783 <i>moaC</i>	molybdopterin biosynthesis, protein C
b0784 <i>moaD</i>	molybdopterin synthase, small subunit
b0785 <i>moaE</i>	molybdopterin synthase, large subunit
b0786 <i>ybhL</i>	predicted inner membrane protein; Unknown function
b0787 <i>ybhM</i>	conserved inner membrane protein; Unknown function
b0788 <i>ybhN</i>	conserved inner membrane protein; Unknown function
b0789 <i>ybhO</i>	cardiolipin synthase 2
b0790 <i>ybhP</i>	predicted DNase; Unknown function
b0791 <i>ybhQ</i>	predicted inner membrane protein; Unknown function

b0792	<i>ybhR</i>	predicted subunit of ABC transporter; Unknown function
b0793	<i>ybhS</i>	predicted subunit of ABC transporter; Unknown function
b0794	<i>ybhF</i>	predicted subunit of ABC transporter; Unknown function
b0795	<i>ybhG</i>	predicted membrane fusion protein component of efflux pump; Unknown function
b0796	<i>ybiH</i>	predicted DNA-binding transcriptional regulator; Unknown function
b0797	<i>rhlE</i>	ATP-dependent RNA helicase
b0798	<i>ybiA</i>	conserved protein; Unknown function
b0799	<i>dinG</i>	ATP-dependent DNA helicase
b0800	<i>ybiB</i>	predicted transferase/phosphorylase; Unknown function
b0801	<i>ybiC</i>	predicted dehydrogenase; Unknown function
b0802	<i>ybiJ</i>	predicted protein; Unknown function
b0803	<i>ybiI</i>	conserved protein; Unknown function
b0804	<i>ybiX</i>	conserved protein; Unknown function
b0805	<i>fiu</i>	predicted outer membrane receptor for iron transport
b0806	<i>McbA</i>	protein involved in colanic acid production
b0807	<i>rlmF</i>	23S rRNA m6A1618 methyltransferase
b0808	<i>ybiO</i>	predicted mechanosensitive channel; Unknown function
b0809	<i>glnQ</i>	glutamine ABC transporter subunit
b0810	<i>glnP</i>	glutamine ABC transporter subunit
b0811	<i>glnH</i>	glutamine ABC transporter subunit
b0812	<i>dps</i>	Fe-binding and storage protein
b0813	<i>rhtA</i>	threonine and homoserine efflux system
b0814	<i>ompX</i>	outer membrane protein X
b0815	<i>ybiP</i>	predicted hydrolase, inner membrane; Unknown function
b0816	<i>yliL</i>	predicted protein; Unknown function
b4416	<i>rybA</i>	small RNA RybA; Unknown function
b0817	<i>mntR</i>	DNA-binding transcriptional regulator of mntH
b0818	<i>ybiR</i>	predicted transporter; Unknown function
b0819	<i>ybiS</i>	L,D-transpeptidase
b0820	<i>ybiT</i>	fused predicted transporter subunits of ABC superfamily; Unknown function
b0821	<i>ybiU</i>	predicted protein; Unknown function
b0822	<i>supH</i>	sugar phosphatase
b0823	<i>pflF</i>	predicted pyruvate formate lyase
b0824	<i>pflE</i>	predicted pyruvate formate lyase activating enzyme
b0825	<i>mipB</i>	fructose-6-phosphate aldolase 1
b0826	<i>moeB</i>	molybdopterin synthase sulphurylase
b0827	<i>moeA</i>	molybdopterin biosynthesis protein
b0828	<i>iaaA</i>	L-asparaginase
b0829	<i>gsiA</i>	subunit of gsiABCD glutathione ABC transporter
b0830	<i>gsiB</i>	subunit of gsiABCD glutathione ABC transporter
b0831	<i>gsiC</i>	subunit of gsiABCD glutathione ABC transporter
b0832	<i>gsiD</i>	subunit of gsiABCD glutathione ABC transporter
b0833	<i>yliE</i>	predicted c-di-GMP-specific phosphodiesterase
b0834	<i>yliF</i>	putative lipoprotein; Unknown function
b0835	<i>rimO</i>	ribosomal protein S12 D88 methylthiotransferase
b0836	<i>bssR</i>	regulator of biofilm through signal sretion

b0837	<i>yliI</i>	aldose sugar dehydrogenase
b0838	<i>yliJ</i>	predicted glutathione S-transferase
b0839	<i>dacC</i>	D-alanyl-D-alanine carboxypeptidase (PBP6-penicillin-binding protein 6a)
b0840	<i>deoR</i>	DeoR (Deoxyribose Regulator) transcriptional repressor
b0841	<i>bcrC</i>	undecaprenyl pyrophosphate phosphatase
b0842	<i>cmr</i>	multidrug efflux system protein
b0843	<i>ybjH</i>	predicted protein; Unknown function
b0844	<i>ybjI</i>	FMN phosphatase from haloacid dehalogenase (HAD)-like hydrolases superfamily
b0845	<i>ybjJ</i>	predicted transporter; Unknown function
b0846	<i>ybjK</i>	predicted DNA-binding transcriptional regulator; Unknown function
b4417	<i>rybB</i>	regulatory small RNA RybB
b0847	<i>ybjL</i>	predicted transporter; Unknown function
b0848	<i>ybjM</i>	predicted inner membrane protein; Unknown function
b0849	<i>grxA</i>	glutaredoxin 1, redox coenzyme for ribonucleotide reductase (RNR1a)
b0850	<i>ybjC</i>	predicted inner membrane protein; Unknown function
b0851	<i>nfsA</i>	NADPH nitroreductase A, FMN-dependent
b0852	<i>rimK</i>	ribosomal protein S6 modification protein
b0853	<i>ybjN</i>	predicted oxidoreductase; putative sensory transductin regulator
b0854	<i>potF</i>	subunit of putrescine ABC transporter PotFGHI
b0855	<i>potG</i>	subunit of putrescine ABC transporter PotFGHI
b0856	<i>potH</i>	subunit of putrescine ABC transporter PotFGHIr
b0857	<i>potI</i>	subunit of putrescine ABC transporter PotFGHI
b0858	<i>ybjO</i>	predicted inner membrane protein; Unknown function
b0859	<i>rimC</i>	23S rRNA m(5)U747 methyltransferase
b0860	<i>artJ</i>	subunit of arginine ABC transporter ArtPMQJI
b0861	<i>artM</i>	subunit of arginine ABC transporter ArtPMQJI
b0862	<i>artQ</i>	subunit of arginine ABC transporter ArtPMQJI
b0863	<i>artI</i>	subunit of arginine ABC transporter ArtPMQJI
b0864	<i>artP</i>	subunit of arginine ABC transporter ArtPMQJI
b0865	<i>ybjP</i>	predicted lipoprotein; Unknown function
b0866	<i>ybjQ</i>	conserved protein; Unknown function
b0867	<i>amiD</i>	anhydro-N-acetylmuramoyl-L-alanine amidase
b0868	<i>ybjS</i>	predicted NAD(P)H-binding oxidoreductase with NAD(P)-binding Rossmann-fold domain; Unknown function
b0869	<i>ybjT</i>	conserved protein with NAD(P)-binding Rossmann-fold domain; Unknown function
b0870	<i>ltaE</i>	L-allo-threonine aldolase, PLP-dependent
b0871	<i>poxB</i>	pyruvate dehydrogenase (pyruvate oxidase), thiamin-dependent
b0872	<i>hcr</i>	Hcp oxidoreductase, NADH-dependent
b0873	<i>hcp</i>	hybrid-cluster protein
b0874	<i>ybjE</i>	predicted transporter; Unknown function
b4209	<i>ytfE</i>	RIC, repair system for Fe-S centres damaged by oxidative or nitrosative stress

Annotations were based on information available at NCBI and Ecocyc databases

It is particularly interesting for this study that the *hcp* gene, which encodes the hybrid cluster protein, was also deleted in strain LMS 4209. The enigmatic protein, Hcp, is upregulated by nitrosative stress. Although the precise function is unknown, the deletion is likely to accentuate any growth defect caused by a lack of YtfE, particularly during growth in the presence of nitrate or nitrite. In conclusion, the strain LMS 4209 contained two mutations, the intended *ytfE* mutation, and a further, substantial deletion of many genes that are essential for anaerobic growth. Further work completed with colleagues in Portugal confirmed that the lack of 125 additional genes did not account for the phenotypes related to oxidatively damaged iron-sulphur clusters, thus confirming the role of YtfE as a Ric protein in the repair of iron-sulphur centres damaged by oxidative or nitrosative stress (Vine *et al.*, 2010).

Regulation of the *ytfE* promoter.

None of the RK4353 mutants defective in genes encoding the proteins of unknown function, YeaR-YoaG, Hcp, YgbA or YibIH, had a clear growth phenotype under the conditions tested. Indeed, even the dramatic phenotype reported for a *ytfE* mutant strain, LMS 4209, was due to a secondary mutation, not the lack of the YtfE protein. As an alternative method to investigate possible links between these proteins, the regulation of the *ytfE* promoter was compared to previously reported data. Two transcripts, *yeaR-yoaG* and *ogt*, are regulated by NarL and by the factor for inversion stimulation, Fis (Squire *et al.*, 2009, Lin *et al.*, 2007). An unusual property of the regulation at these promoters is that NarL activates transcription of both *ogt* and *yeaR*, but does not require Fnr for coactivation. NarL often enhances activation by Fnr but these are the first examples of promoters at which NarL activates transcription alone. Fis was shown to repress both promoters by displacing NarL. Fis plays a direct role in the repression of several promoters in response to nutrient abundance and rapid growth. YeaR activity

sharply decreases in rich medium, which is due to the role of Fis (Squire *et al.*, 2009). How a gene is regulated can give clues to a possible function, as genes that are regulated similarly often function in the same pathway. Experiments were completed to investigate whether the regulation of the *ytfE* promoter was similar to the regulation of the aforementioned genes.

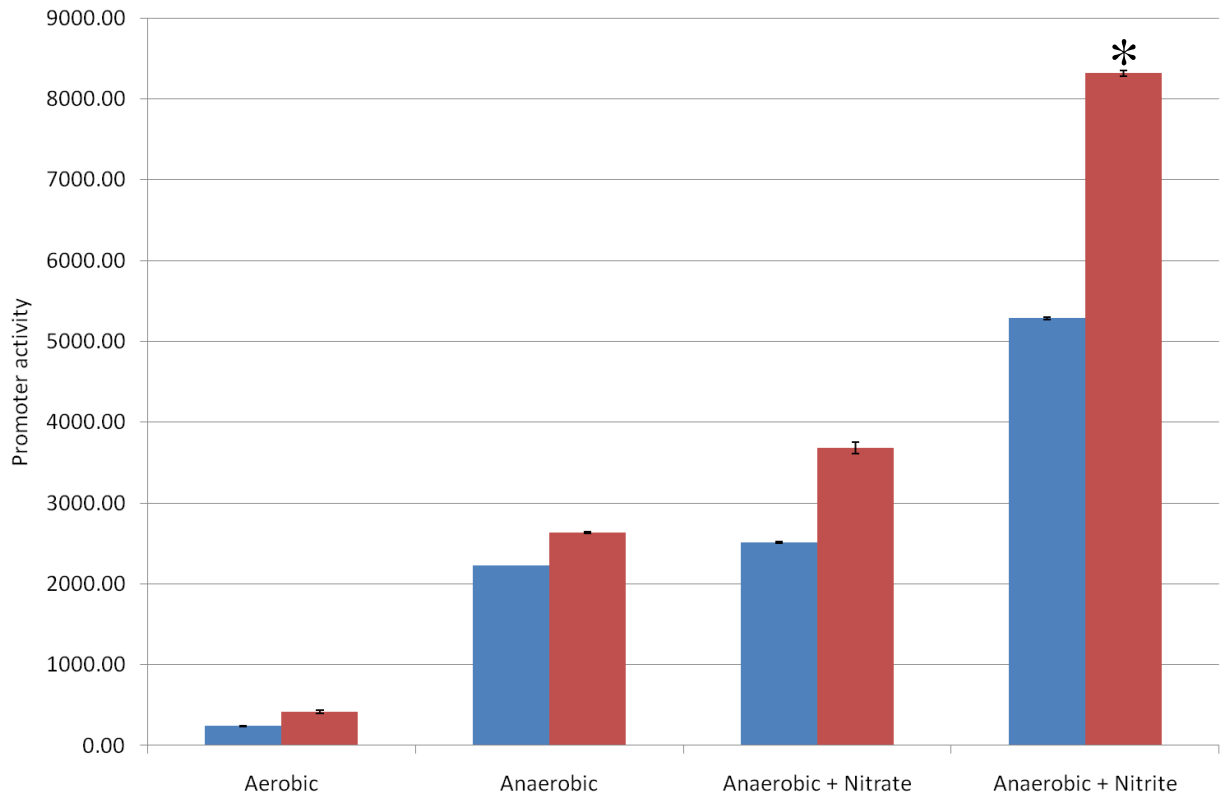
The effect of growth conditions on the regulation of the *ytfE* promoter.

To investigate regulation of the *ytfE* promoter, a plasmid, pCV01, was constructed in which *pytfE* was fused to *lacZ* in pRW50. The parent strain, JCB 387, was transformed with pCV01 and the bacteria were grown aerobically or anaerobically until the optical density at 650 nm had reached the appropriate value as described in the methods section. Samples were withdrawn and were lysed and assayed for β -galactosidase activity. The β -galactosidase activity of the *ytfE* promoter was low when bacteria were grown aerobically, and increased 4-fold when bacteria were grown under anaerobic conditions (Figure 5.6). Activity of the promoter during anaerobic growth was induced a further 2-fold by nitrite, but not by nitrate in the growth medium, relative to expression in bacteria grown anaerobically in unsupplemented medium. This upregulation under anaerobic conditions and by the presence of nitrite in the medium is consistent with a role in the repair of nitrosative damage that has been reported by Justino and colleagues (2005, 2006, 2007, 2009, Todorovic *et al.*, 2008, Overton *et al.*, 2008).

The effect of Fnr on the *ytfE* promoter.

Microarray data suggest that *ytfE* is repressed by Fnr, and is activated by the presence of nitrate and nitrite in the medium, particularly when Fnr is absent (Constantinidou *et al.*, 2006). Reverse transcription PCR analysis revealed that both Fur and Fnr repress

Figure 5.6.



The effect of growth conditions and the regulator Fnr on *ytfE* transcription.

The parental strain JCB 387 (blue) and the *fnr* mutant strain JCB 3911 (red) were transformed with pCV01, and cultures were grown aerobically, or anaerobically in the presence of 20 mM nitrate or 2.5 mM nitrite. The optical density at 650 nm of the cultures was monitored until it had reached 0.19 to 0.21 for aerobic cultures or 0.5 to 0.7 for anaerobic cultures. At this point, samples were withdrawn and were assayed for β -galactosidase activity. Units of promoter activity in this and all subsequent experiments are $\text{nmol ONPG hydrolysed min}^{-1} (\text{mg dry weight})^{-1}$. Each assay was repeated at least twice, with at least two biological repeats. Error bars represent the standard error of these repeats. A star above a bar represents that data are significantly different from the parental JCB 387 strain (see text).

transcription of *ytfE* (Justino *et al.*, 2006). To investigate whether this repression observed in the parental strain, JCB 387, was due to activation by Fnr, the *fnr* mutant strain, JCB 3911, was transformed with pCV01. The bacteria were grown aerobically or anaerobically and samples were lysed and assayed for β -galactosidase activity. The β -galactosidase activity of the *ytfE* promoter in an Fnr mutant was low when bacteria were grown aerobically, and increased 4-fold when bacteria were grown under anaerobic conditions (Figure 5.6). This indicates that the anaerobic induction of β -galactosidase activity is not dependent on Fnr. In the *fnr* mutant, β -galactosidase activity of the promoter was induced 48% by nitrate in the growth medium, relative to the unsupplemented control (Figure 5.6). This activity was not significantly different from that of the parent strain, JCB 387, when the medium was supplemented with nitrate ($p=0.060$). In the absence of Fnr, the increase in β -galactosidase activity when the medium was supplemented with nitrite was 4-fold, compared to a 2-fold increase in the parent strain (Figure 5.6). This difference was statistically significant ($p=0.023$). This activation by nitrate and extra induction by nitrite in the growth medium might be due to an accumulation of NO in the absence of proteins that are normally activated by Fnr.

The effect of NarL and NarP on the *ytfE* promoter.

It has been reported that regulation of *ytfE* transcription is not dependent on the NarXLQP system, as activation by nitrate requires nitrate reduction to be functional, presumably to generate the NO that is sensed by NsrR (Bodenmiller and Spiro, 2006). However, analysis of the *ytfE* promoter revealed a putative repeat of the TACYYMT motif in a '7-2-7' arrangement, which is centred 40.5 bp upstream of the transcription start site identified by Bodenmiller and Spiro (2006) (Figure 5.7, panel A). When the promoter regions of *yeaR*, *ogt*, and *ytfE* were aligned relative to the -10 element, the

Figure 5.7.

A CTATCTCGTCGCTTGTACTGGCTGAATACGCAAACGCCGGACTTCTCCCTTACCCTTTGGCCCCGTCCGCT
 GGTGTTTATTAGTCTGATGGTTGCGATAGCCGTGCTTTGCTCATGGGTTGGCGCACTCTGCTGGAACGTGC
 CCAGCCAGCTATTACCGACAGTGATTCTCGGGCCGCTGATTGTTTTCGAAACGCTGGCAGGTTTGCTGTAC
 ACCTTTTACTCCGCCAGCAAATGCCGCCGCTAATGACGCTGAGCGGTATCGCGCTGTTAGTGATTGGCGT
 GGTCATCGCGGTGAGAGCAAACCCAGAAAAACCTTTAACTGAATCTGTCTCAGAAAGTTGACACGCTGGC
 AGTGAGTTAAATAAGCCTCTGCTACGTAAGGGTTATAGCTTTTGCCTAAAGATGCATTTAAATACATCTT
 ATCTTATTAAGAATGAGGTATCAGCTATGGCTTATCGCGACCAACCTTT

B

AAAACCAGAAAAACCTTTAACTGAATCTGTCTCAGAAAGTTGACACGCTGG
 TTCAGCCCGCGTTGTGCGGGCTTCCCATCTATAATCCCTGATTCTT
 GGATTCCTGCAACGCTACAAACCAGACGCGAAACTGGGTACTTACTATTG
 TACYMTNNAKRR

TACYMTNNAKRRGTA

CAGTGAGTTAAATAAGCCTCTGCTACGTAAGGGTTATAGCTTTTGCCTTA
 CGCTGATATGGTGCTAAAAAGTAAACCAATAAATGGTATTTAAAATGCAA
 TTAGTCTTGCCCTATCCACTTATCTTTTTGGTGGTATGGCTGCTGATGTT
 GTA TACYMTNNAKRRGTA

-10 element

AAGATGCATTTAAATACATCTTATCTTATTAAGAATGAGGTAT ytfE
 TTATCAGGCGTACCCTGAAACGGCTGGAATAAACCGTTTTTCAGC yeoR
 GCTGGCGTGGTATCTTGTGCGTCTGCCGATAGGTCCGGGTATTT ogt

The promoter region of *ytfE*.

Panel A: This figure shows the full length promoter region of *ytfE*, from positions -453 to +63 with respect to the transcription start site. The transcription start point is designated by underlined text and a bent arrow and the translation start ATG is in bold text. The DNA sites for NarL and NsrR are identified by blue arrows and a rectangle respectively.

Panel B: The *ytfE*, *yeoR* and *ogt* promoters are aligned relative to their -10 elements (underlined text). The DNA sites for NarL are identified by underlined text shown with the consensus in red text above and below the DNA sequences. Degenerate bases in the consensus site are as follows: Y=C/T; M=A/C; K=G/T; R=A/G.

7-2-7 site also aligned in a similar region (Figure 5.7, panel B). DNA repair by Ogt is induced by nitrate, through NarL, but NarP plays little or no role at the *yeaR* or *ogt* promoters. NarL is a transcription activator of both *yeaR* and *ogt* (Squire *et al.*, 2009). To investigate whether there was a similar effect at the *ytfE* promoter, the *narL* mutant, JCB 3883, the *narP* mutant, JCB 3875, and the parent strain, JCB 387, were transformed with pCV01 and were assayed for β -galactosidase activity. The β -galactosidase activity of the *ytfE* promoter in a *narL* mutant and a *narP* mutant was similar to the parent (Figure 5.8). This indicates that the activation of *ytfE* transcription is not dependent on NarL or NarP.

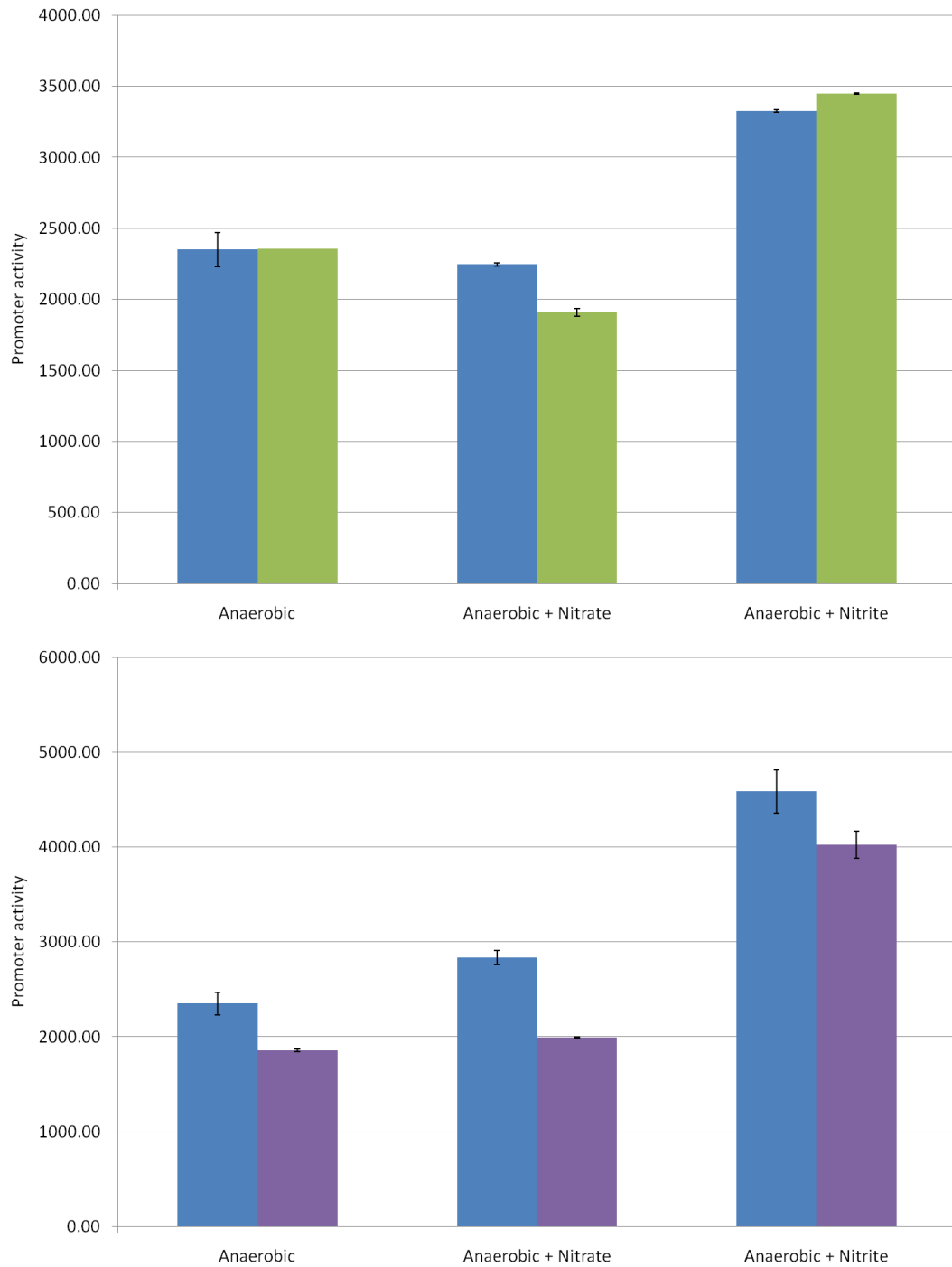
The effect of Fis on the *ytfE* promoter.

Fis is a DNA binding protein that has been extensively studied and is implicated in compaction of the *E. coli* chromosome (McLeod and Johnson, 2001). Fis represses both *yeaR* and *ogt* transcription (Squire *et al.*, 2009). To investigate whether Fis also regulates *ytfE* transcription, the *fis* mutant, JCB 3871, and a parental strain, JCB 387, were transformed with pCV01 to be assayed for β -galactosidase activity. The β -galactosidase activity of the *ytfE* promoter in a *fis* mutant was similar to the parent aerobically and anaerobically (Figure 5.9). The activity of the *ytfE* promoter was higher in the *fis* mutant than in the parent strain when the medium was supplemented with nitrite ($p=0.005$), and similar to the parent when supplemented with nitrate ($p=0.135$). This indicates that any Fis effect is not relevant to all conditions tested, and is certainly not as significant as the effect seen at the *yeaR* and *ogt* promoters (Squire *et al.*, 2009).

The effect of NsrR on the *ytfE* promoter.

In a previous study of the regulation of the *ytfE* promoter, NsrR was found by transposon mutagenesis to be a repressor of *ytfE* transcription (Bodenmiller and Spiro,

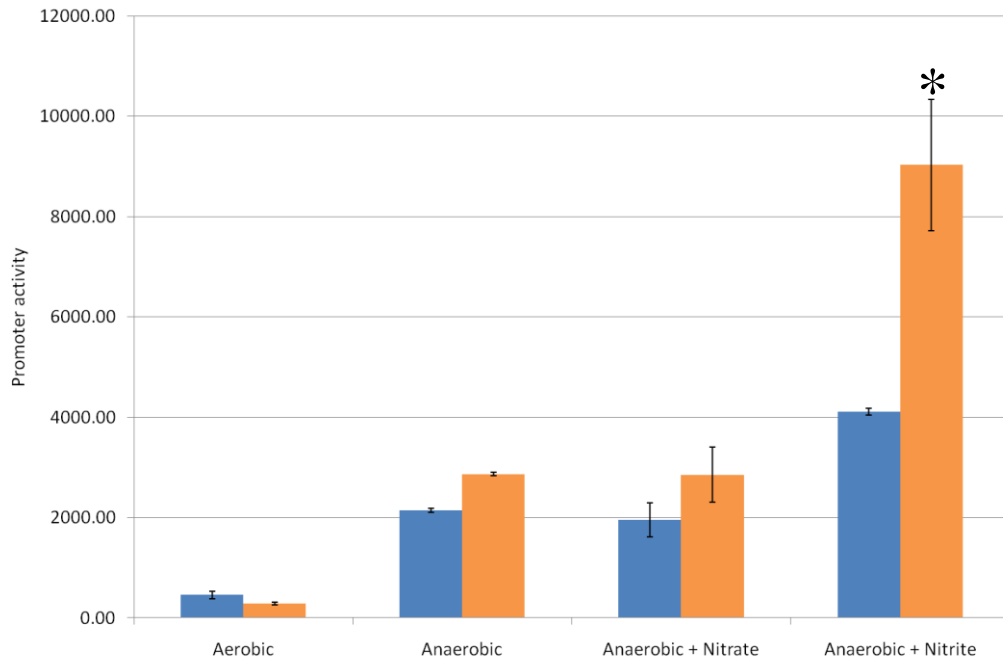
Figure 5.8.



Effect of NarL and NarP on transcription of the *yfE* promoter.

The parental strain, JCB 387 (blue bars in both graphs), a *narL* mutant, JCB 3883 (green), and a *narP* mutant, JCB 3875 (purple), were transformed with pCV01, and were assayed for β -galactosidase activity. Other details are as in Figure 5.6

Figure 5.9.



The effect of Fis on transcription of the *ytfE* promoter.

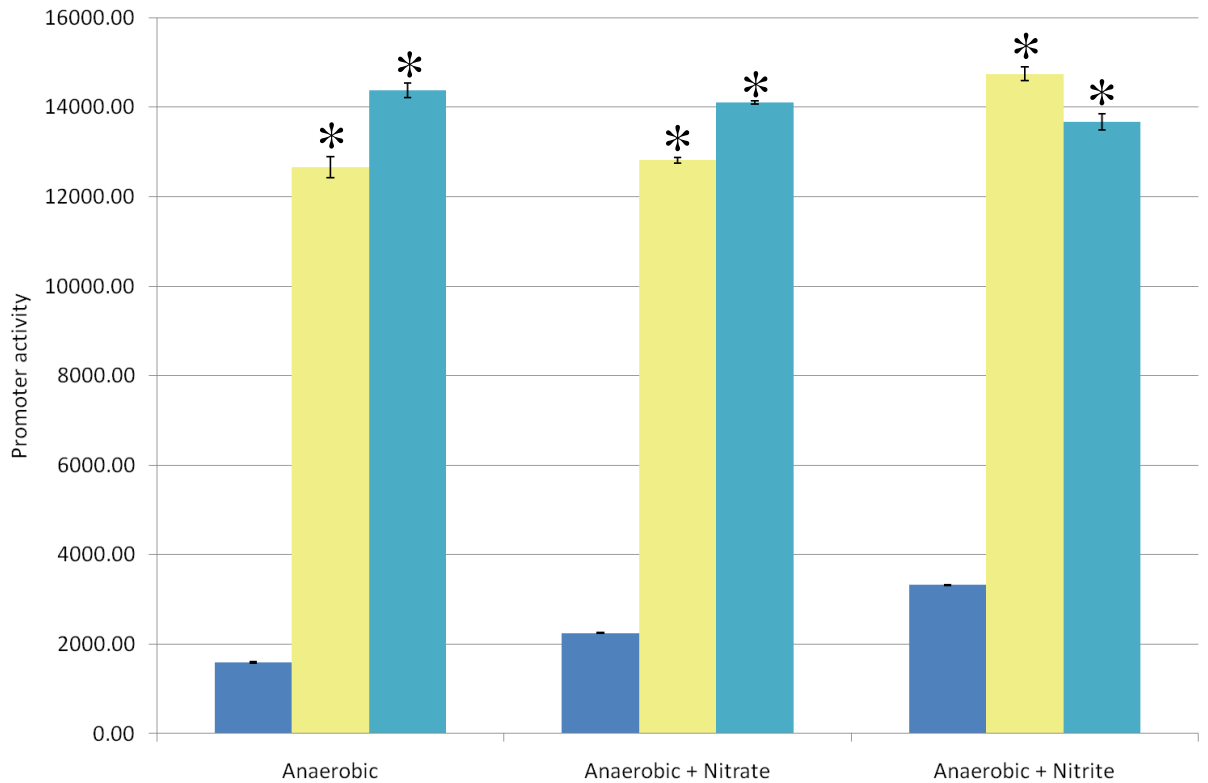
The parental strain, JCB 387 (blue bars), and the *fis* mutant, JCB 3871 (orange), were transformed with pCV01 and were assayed for β -galactosidase activity. Units of β -galactosidase activity are nmol ONPG hydrolysed min⁻¹ (mg dry weight)⁻¹. All other details are as for Figure 5.6. A star above a bar represents that data are significantly different from the JCB 387 strain (see text).

2006). It was interesting to investigate whether the Fnr repression effect was observed in the absence of NsrR repression. The parent strain, JCB 387, the *nsrR* mutant strain, JCB 3901, and the *fnr nsrR* mutant strain, JCB 3902, were transformed with pCV01 and cultures were grown anaerobically to be assayed for β -galactosidase activity. The β -galactosidase activity of the *ytfE* promoter in an *nsrR* mutant increased 7-fold relative to the parent, whether the bacteria were grown in minimal medium supplemented with nitrate ($p=0.005$) or nitrite ($p=0.011$) or if medium was unsupplemented ($p=0.017$) (Figure 5.10). There was no statistically significant difference in β -galactosidase activity in bacteria defective in both *fnr* and *nsrR*, relative to the *nsrR* parent ($p\geq 0.065$) (Figure 5.10). NsrR is certainly the major known regulator at this promoter.

The effect of exogenous NO on anaerobic growth of *E. coli* and on the *ytfE* promoter.

The addition of exogenous NOSW to the culture medium mimics the conditions that might be found in the host, as NO is generated as a defence against pathogens such as *E. coli*. To investigate the response of the *ytfE* promoter to NO shock, the parental strain, JCB 387, was transformed with pCV01. Cultures were grown anaerobically until the optical density at 650 nm had reached 0.2, then NOSW (10-20 μM NO) was added at 30 minute intervals. Samples were taken every 30 minutes and were assayed spectrophotometrically for optical density, and for β -galactosidase activity. Growth of the culture that was treated with NOSW was delayed by 1 hour (Figure 5.11). The β -galactosidase activity of the *ytfE* promoter from the culture that was shocked with NOSW was 10% higher than in the control culture. The concentration of NOSW being used was sufficient to perturb growth, but was not sufficient to induce transcription of *ytfE* in the cytoplasm.

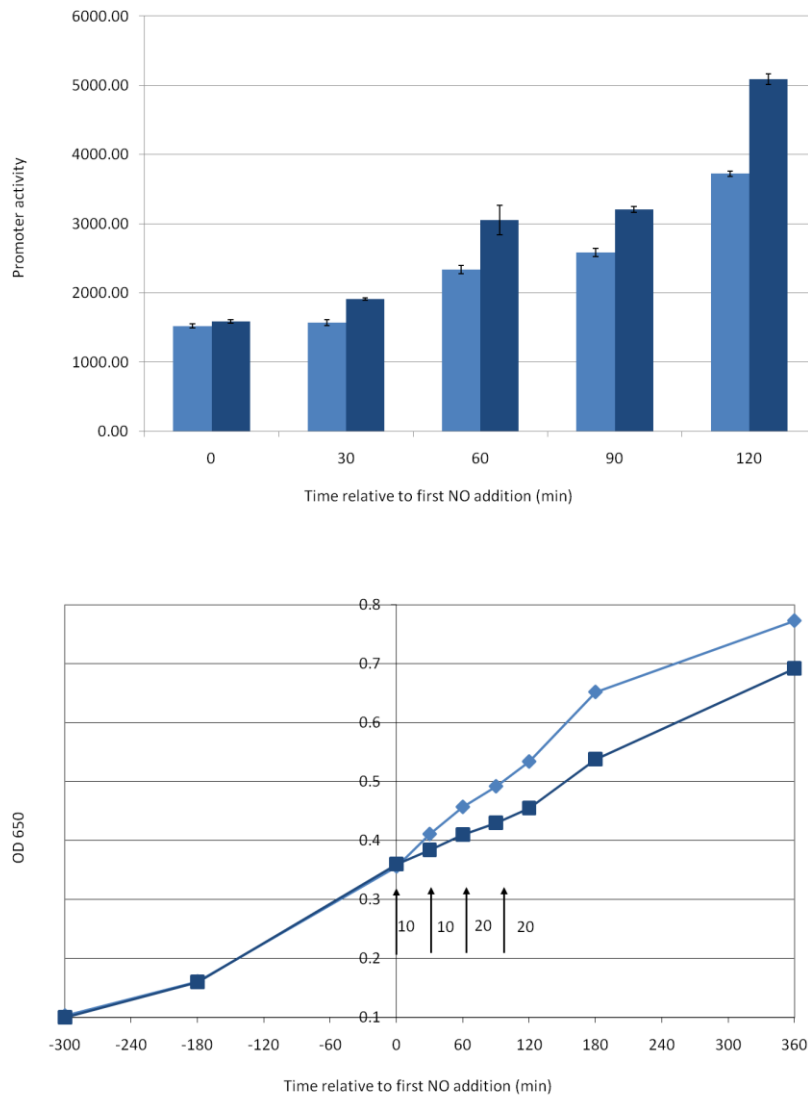
Figure 5.10.



The effect of NsrR and Fnr on transcription of the *ytfE* promoter.

The parental strain JCB 387 (blue), the *nsrR* mutant strain, JCB 3901 (yellow), and an *fnr nsrR* mutant strain, JCB 3902 (turquoise), were transformed with pCV01, and were assayed for β -galactosidase activity. Units of β -galactosidase activity are nmol ONPG hydrolysed min^{-1} ($\text{mg dry weight}^{-1}$). Other details are as for Figure 5.6. A star above a bar represents that data are significantly different from the JCB 387 parent strain (see text).

Figure 5.11.



Anaerobic growth and β -galactosidase activity of JCB 387 transformed with pCV01 in response to NO shock

The parental strain, JCB 387, was grown anaerobically. The optical density at 650 nm was monitored until it had reached 0.3, then one culture (dark) was pulsed with NOSW where indicated (μM) by black arrows, while the other (pale) was pulsed with the equivalent volume of pH 3 water (0.5 – 1 mL). Samples were taken and were assayed for β -galactosidase activity. Units of promoter activity are $\text{nmol ONPG hydrolysed min}^{-1} (\text{mg dry weight})^{-1}$. Other details are as in Figure 5.6.

Effect of exogenous NO on bacteria defective in *nrfA* in the periplasm.

In the parent strain, JCB 387, pulses of exogenous NO did have an effect on growth; however NOSW was not able to induce the expression of *ytfE* in the cytoplasm as reported by the promoter::*lacZ* fusion in plasmid pCV01. It is possible that a protective mechanism detoxifies NO before it is able to reach NsrR in the cytoplasm, and therefore derepress *ytfE* transcription. One possible explanation for the failure of externally added NO to equilibrate with the cytoplasm was that it is reduced by an active NO reductase located either in the periplasm or in the cytoplasmic membrane. An obvious candidate for such NO reductase activity is NrfAB, which reduces NO to ammonia with high catalytic efficiency (Poock *et al.*, 2002; van Wonderen *et al.*, 2008). In order to investigate the protective role of Nrf, the parent strain, RK4353, and the isogenic *nrfAB* strain, JCB 5206, were transformed with pCV01. Samples were lysed to be assayed for β -galactosidase activity, and the optical density was monitored for 6 hours after the first shock. Growth of the cultures that were supplemented with NOSW paused for 2 h, then resumed (Figure 5.12). The final optical density of each culture was 0.9 ± 0.08 after 24 h of growth. The β -galactosidase activity of the *ytfE* promoter in the *nrfAB* strain was no higher than in the parental strain. From these data, it is possible to conclude that NrfAB is not responsible for the prevention of exogenous NOSW reaching the cytoplasm.

The role of the flavohaemoglobin, Hmp, in preventing exogenous NO from activating *ytfE* expression.

Another candidate for rapid removal of NO before it reaches NsrR in the cytoplasm is the flavohaemoglobin, Hmp. To investigate this possibility, the parent strain, RK4353, and the *hmp* strain, JCB 5219, were grown anaerobically and cultures were supplemented with NO and sampled as previously described. Growth of both the parent

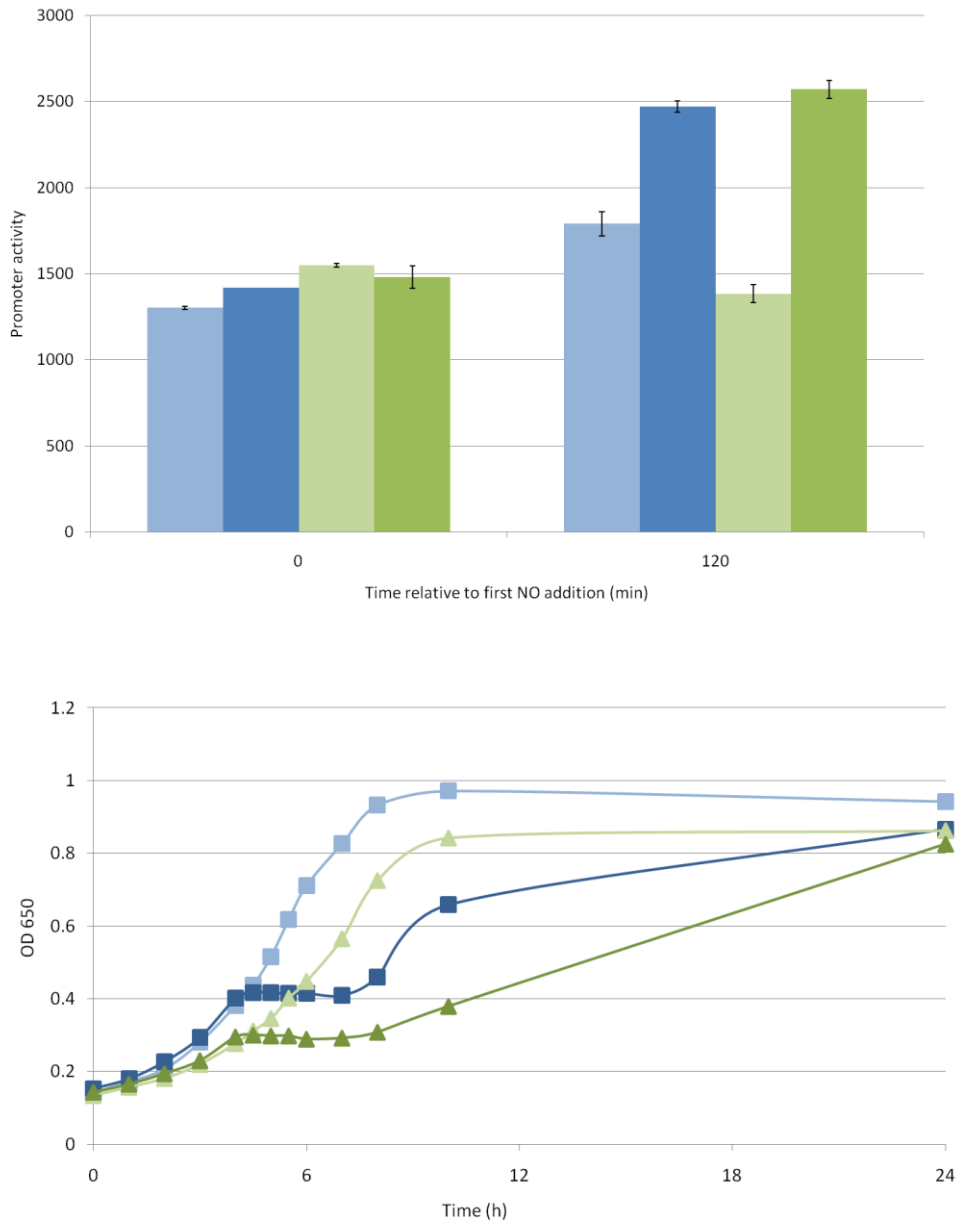
strain and the *hmp* strain was perturbed by the addition of NOSW (Figure 5.13). There was a 1 to 2 h lag in recovery of the *hmp* strain relative to the parent. The inactivation of Hmp did not influence activation of the *ytfE* promoter by NO (Figure 5.13). Neither NrfA nor Hmp was responsible for preventing exogenous NO from activating transcription of the YtfE promoter.

However, data in chapter 4 and that has been published showed that even in the absence of all currently characterised NO reductase activities, anaerobic cultures of *E. coli* still reduce NO rapidly (Vine and Cole, 2011). A significant NO reduction activity remains to be characterised. This uncharacterised activity might prevent significant damage to cytoplasmic proteins by concentrations of externally generated NO that are relevant to pathogenicity.

Discussion.

The poor anaerobic growth of the *ytfE* strain LMS 4209 that was reported by Justino *et al.*, (2006) was due to a secondary deletion of 126 genes, including those required for molybdopterin synthesis, iron storage and the enigmatic function of the hybrid cluster protein, Hcp. Experiments completed in another laboratory with the newly constructed *ytfE* strains, JCB 5201 and JCB 5202, have confirmed the role of YtfE (Ric) in the repair of iron centres (Vine *et al.*, 2010). The activities of three Fe-S cluster enzymes, aconitase, fumarase and the Entner-Doudoroff pathway 6-phosphogluconate dehydratase, Edd, were lower in the new *ytfE* mutants, JCB5201 and JCB5202, than in the parental strain. This confirms the previously proposed role of YtfE in the assembly of iron-sulphur centres (Justino *et al.*, 2006). The newly constructed *ytfE* strains, JCB 5201 and JCB 5202, as well as LMS 4209, were more sensitive to growth inhibition by hydrogen peroxide, a phenotype consistent with the loss of the repair of iron-sulphur

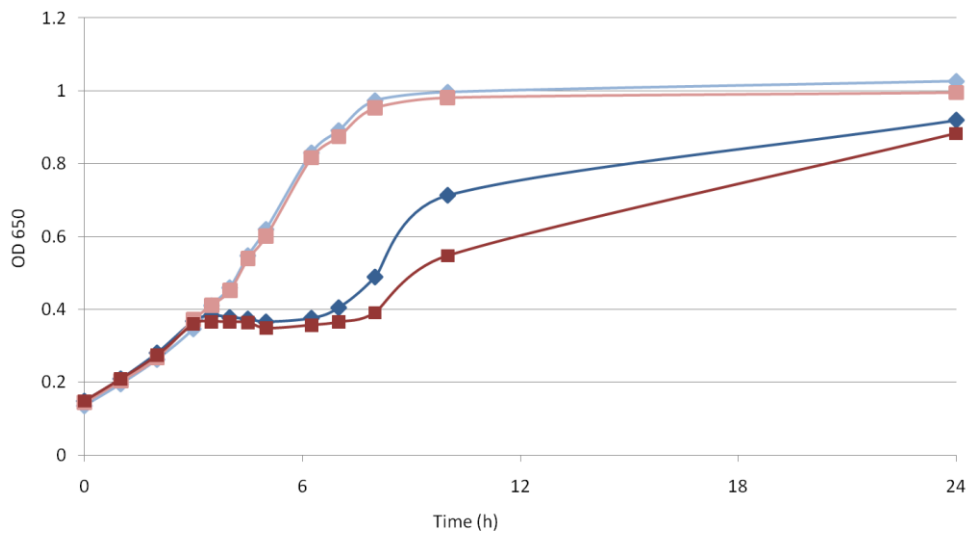
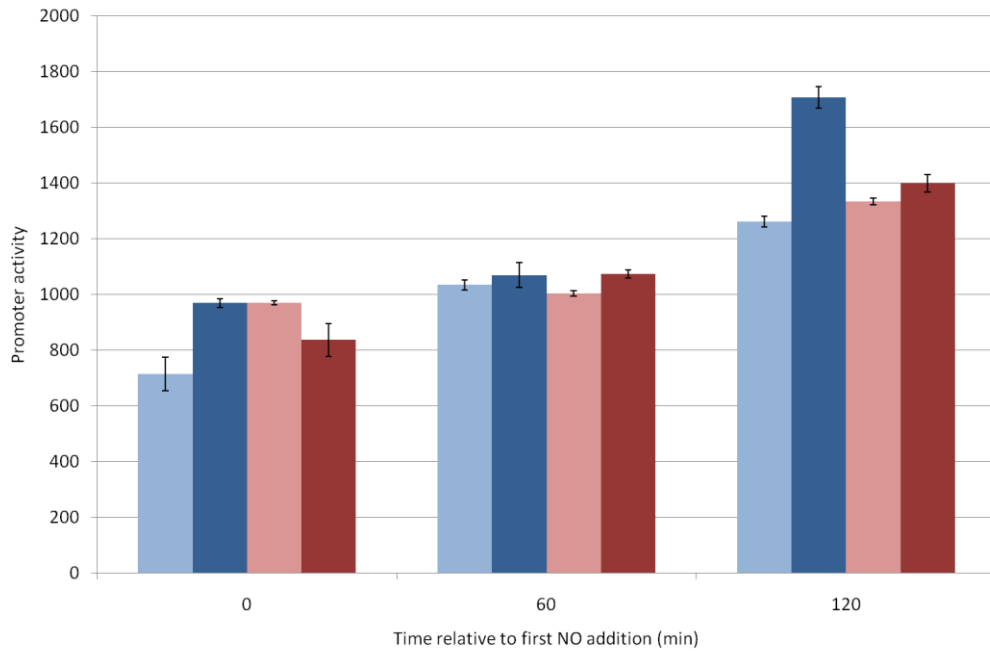
Figure 5.12.



The effect of NrfAB on anaerobic growth of *E. coli* and transcription of *pytE*.

The parental strain, RK4353 (blue), and the *nrfAB* mutant, JCB 5206 (green) were transformed with pCV01. Cultures were grown anaerobically until the optical density at 650 nm had reached 0.3, then one culture (dark bars) was pulsed with NOSW (20 μ M) every 30 minutes for 2 hours, while the other (pale bars) was pulsed with the equivalent volume of pH 3 water. Other details are as in Figure 5.11.

Figure 5.13.



The effect of Hmp on anaerobic growth of *E. coli* and transcription of *pytE*.

The parental strain, RK4353 (blue), and the *hmp* mutant, JCB 5219 (red) were transformed with pCV01. Cultures were grown anaerobically until the optical density at 650 nm had reached 0.3, then one culture (dark bars) was pulsed with NOSW (20 μ M) every 30 minutes for 2 hours, while the other (pale bars) was pulsed with the equivalent volume of pH 3 water. Other details are as in Figure 5.11.

proteins damaged by oxidative stress (Justino *et al.*, 2007). As previously observed for LMS 4209 (Justino *et al.*, 2007), the two new mutant strains JCB 5201 and JCB 5202 were unable to repair the 4Fe-4S cluster of fumarase A after exposure to oxidative damage. Furthermore, addition of purified YtfE protein to the lysates of the mutants led to the repair of the damaged centre. The newly constructed *ytfE* strain has thus revealed a clear phenotype for the *ytfE* mutant that was obscured by phenotypes due to a second site deletion in the original *ytfE* strain, LMS 4209 (Vine *et al.*, 2010).

Transcription of *ytfE* is mainly regulated by NsrR and any small effects of the regulator of fumarate and nitrite reduction, Fnr, are likely to be indirect. The fact that transcription of *ytfE* is anaerobically induced, but that this induction is not Fnr-dependent has been reported previously for a *ytfE* homologue, *nipC*, in *Salmonella enterica* serovar Typhimurium (Kim *et al.*, 2003). Results presented in this chapter show that the activity of the *ytfE* promoter was no higher in the double *nsrR fnr* mutant strain than in the single *nsrR* mutant strain (Figure 5.10). Critically, this was true in the presence of sodium nitrite; there was no significant difference between β -galactosidase activity measured for the *nsrR* strain and for the *nsrR fnr* double mutant strain. This is consistent with the idea that any effect on transcription seen in an *fnr* single mutant is indirect. NsrR has been found to be partially inactive in an *fnr* mutant (Spiro, 2007). Effects of Fnr at NsrR-repressed promoters, including *hmp* and *ytfE*, were reported to be indirect. The apparent negative regulation of *ytfE* by Fnr, described both in this chapter and by Justino *et al.* (2006) can also be explained by an indirect effect. The basis of the Fnr effect on NsrR activity is not known.

The response regulators of dual interacting two-component regulatory systems NarXL and NarQP do not regulate transcription of *ytfE*. Despite the possible similarities

suggested by bioinformatic analysis with the promoter regions of *yeaR* and *ogt*, it has not been possible to draw parallels between these three promoters. Fis is a DNA binding protein that has been extensively studied and is implicated in compaction of the *E. coli* chromosome (McLoed and Johnson, 2001). Fis abundance varies throughout bacterial growth, and this fluctuating pattern of expression can impart an additional level of transcriptional control on promoters within the Fis regulon, in accordance with environmental conditions. However, the influence of fluctuating levels of Fis at different growth stages was not investigated in this study. Nucleoid associated proteins modulate the structure of the bacterial chromosome. Perhaps in the absence of Fis, an alternative chromosome organisation persists, meaning that it is easier for NsrR repression to be relieved by NO. This would be consistent with the result that activity of the *ytfE* promoter in response to nitrite in the growth medium is elevated in a *fis* mutant strain. The transcriptional fusion *ytfE::lacZ* reports that exogenously added NO does not reach the *E. coli* cytoplasm in order to inactivate NsrR. Neither NrfA nor Hmp prevents NO from reaching NsrR.

CHAPTER 6. RESULTS.

Repair of nitrosative damage: the role of the hybrid cluster protein, flavohaemoglobin and YtfE.

Introduction

Throughout the experiments described in this chapter, a mutant that was deficient in *nirBDC nrfAB* and *norV* (JCB 5252) was used as a starting strain. This strain will subsequently be referred to as the triple mutant strain. Three of the genes that are most regulated by NsrR in *E. coli* encode: Hmp that is documented to be an NO reductase; YtfE that is defined as a protein for the repair of iron centres (Ric); and Hcp that is more likely to have a role in defence against nitrosative stress than in hydroxylamine reduction. Once the results of experiments with the triple mutant were available, further mutations were introduced to investigate the effects of these proteins implicated in the nitrosative stress response: Hmp; YtfE; and Hcp. The *hmp* derivative strain, JCB 5210, has already been referred to as the ‘quadruple mutant’ in previous chapters, and will also be discussed in this chapter. For ease of reference, these strains are summarised in Table 6.1. To follow the investigation of NO reductases reported in chapter 4, the contribution of YtfE to the rate of NO reduction in *E. coli* was explored. The role of repair proteins and genes of unknown function was investigated under conditions in which damage is allowed to accumulate, due to the absence of NO reductase proteins.

The effect of the hybrid cluster protein, Hcp, and the flavohaemoglobin, Hmp, on growth of the triple mutant.

To investigate the role of Hmp and Hcp in the growth of the triple mutant, the *hmp*⁺ *hcp*⁺ parent, JCB 5232, the *hmp* derivative strain, JCB 5210, and the *hcp* derivative strain, JCB 5242, were grown anaerobically in minimal medium that was supplemented with 1 to 10 mM sodium nitrate or 0.1 to 1 mM sodium nitrite. Recall that nitrite slightly suppressed growth of the triple mutant, but low nitrate stimulated growth (Figure 4.10, repeated in Figure 6.1 for comparison). At 3 h after inoculation, the rate of growth of the triple mutant in the presence of 5 mM nitrate decreased, but at 4 h after

Table 6.1 Strains defective in genes implicated in the nitrosative stress response discussed in this chapter.

Strain name	Phenotype*			Note
	Hmp	Hcp	YtfE	
JCB 5232	+	+	+	Triple mutant
JCB 5210	-	+	+	Quadruple mutant
JCB 5257	-	+	-	
JCB 5250	-	-	+	
JCB 5260	-	-	-	
JCB 5242	+	-	+	

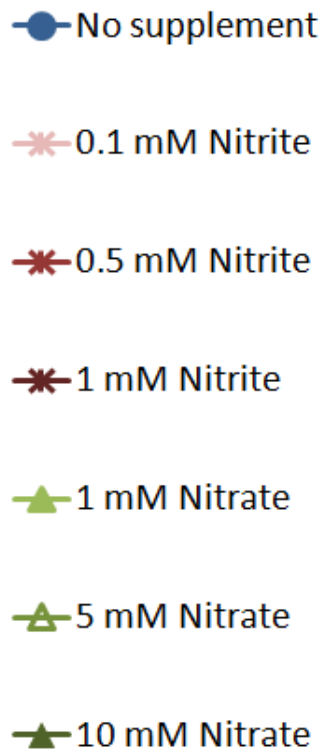
*Every strain is defective in *nirBDC nrfAB* and *norV*.

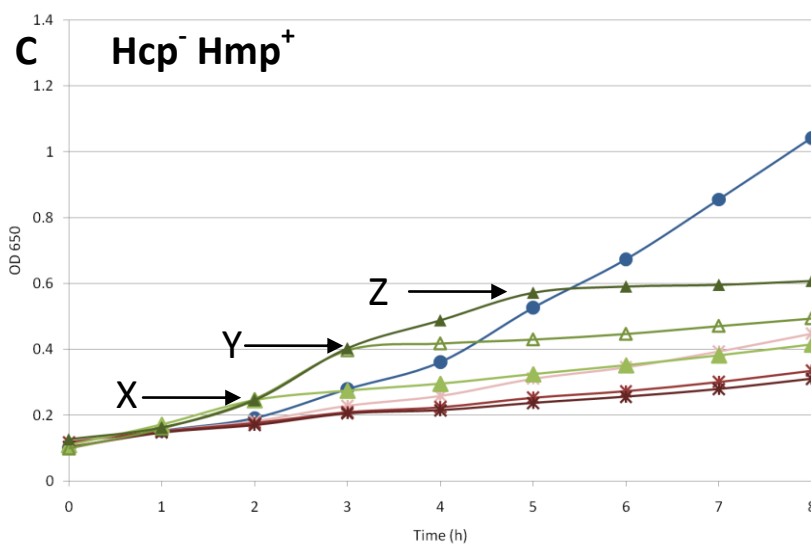
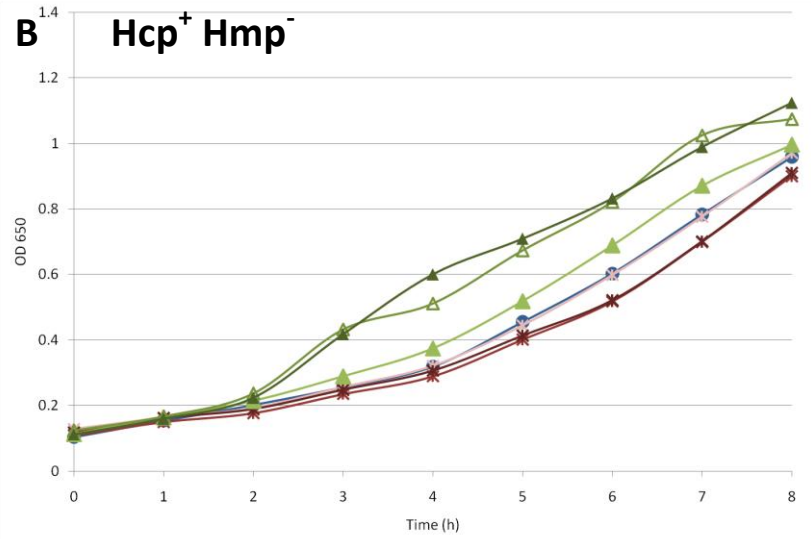
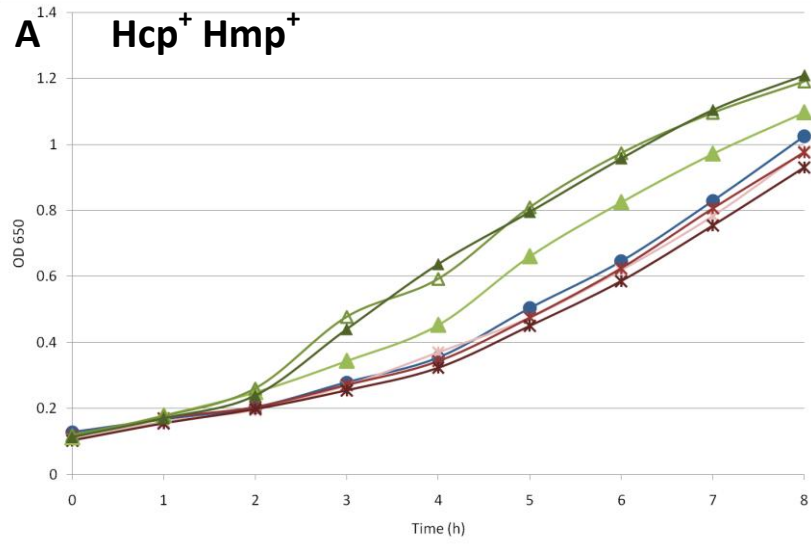
Full details of strain construction and genotypes can be found in Table 2.5.

Figure 6.1.

Growth of *E. coli* strains in the presence of a titration of nitrate and nitrite concentrations.

The parent *nirBDC nrfAB norV* strain, JCB 5232 (A), the quadruple mutant strain, JCB 5210 (B), and the *nirBDC nrfAB norV hcp* strain, JCB 5242 (C), were used. Cultures were grown anaerobically in minimal medium that was supplemented with 1 to 10 mM sodium nitrate (green) or 0.1 to 1 mM sodium nitrite (red). The palest line in each case represents the lowest concentration of supplement (see legend below). Growth curves were completed at least in biological duplicate, and these graphs represent a typical experiment. Annotations X, Y and Z with arrows refer to data during the time course that are of particular interest and are referred to in the text.





inoculation, growth resumed (Figure 6.1, A). This phenotype was highly reproducible.

The *hmp* derivative strain, JCB 5242, grew identically to the triple mutant in which Hmp is functional (Figure 6.1, B). However, when an *hcp* mutation was introduced, a very interesting phenotype was revealed. Nitrite clearly inhibited growth of the *hcp* strain in a dose dependent manner. A low concentration of sodium nitrate (1 mM) in the culture suppressed growth of the *hcp* strain 2 h after inoculation (Figure 6.1, C). However, a higher concentration of sodium nitrate (5 or 10 mM) in the medium led to growth arrest of the *hcp* strain 3 h and 5 h after inoculation, respectively. This is initially counter-intuitive, until the property of the nitrate reductase, NarG, which was confirmed in chapter 3 is considered (Figure 3.8). When the concentration of nitrate is low, NarG is able to convert nitrite in the medium into NO, which is toxic. The lowest concentration of nitrate would be depleted most rapidly, and NO would be generated by NarG earliest in the culture supplemented with 1 mM nitrate (Annotated X, Figure 6.1). The higher concentration of 5 mM nitrate would be depleted later (Annotated Y, Figure 6.1) and the highest concentration of 10 mM nitrate would be depleted last (Annotated Z, Figure 6.1). At each annotated point (X, Y or Z) in Figure 6.1, the growth phenotype is consistent with the idea that NO starts to accumulate when most of the nitrate has been reduced to nitrite, and becomes toxic to bacteria that lack the hybrid cluster protein, Hcp, for protection.

The effect of an *hcp* mutation on growth of the quadruple mutant defective in previously characterised NO reductases.

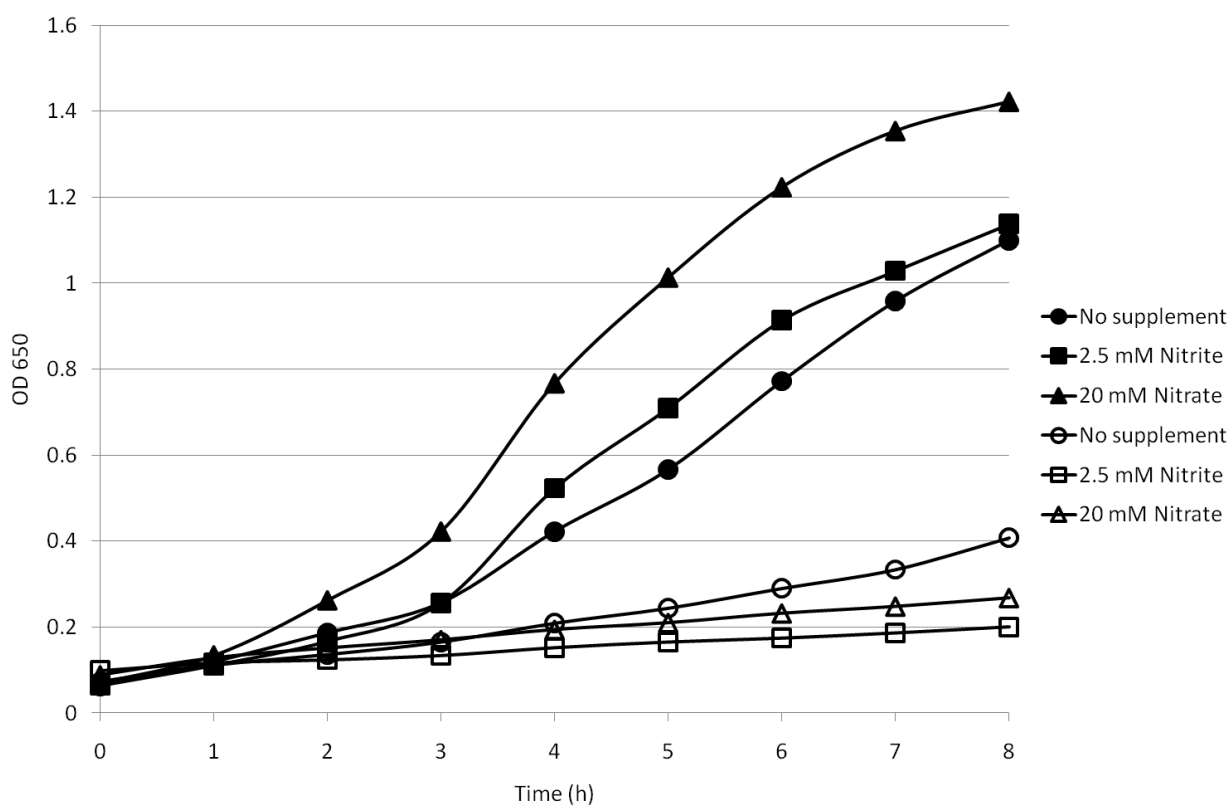
In chapter 4, it was reported that when the genes for all known reductases had been deleted, the rate of NO reduction was still at least 50% of the parental rate, whether the culture had been grown in medium supplemented with sodium nitrate or sodium nitrite

(Table 4.1 and Table 4.2). In order to investigate whether Hcp was a previously unrecognised NO reductase, the *hcp* derivative of the quadruple mutant was constructed. The quadruple mutant parent strain, JCB 5210, and the *hcp* derivative strain, JCB 5250, were grown anaerobically as previously described. Anaerobic growth of the *hcp* derivative was poor, whether the medium was unsupplemented, or supplemented with nitrate or nitrite (Figure 6.2). This is the strongest phenotype that has yet been reported for an *hcp* mutant. There is also a clear phenotype, even in the absence of nitrate or nitrite, so it is important to note that Hcp is likely to be generally important for anaerobic metabolism, but even more critical in the presence of nitrate or nitrite as suggested by previous studies and the data presented in Figure 6.1. It was not possible to determine the rate of NO reduction by the *hcp* derivative as there was insufficient biomass in the culture to assay. To determine whether aerobic growth of strain JCB 5250 was also inhibited by the *hcp* mutation, strains were grown in minimal medium supplemented as previously described with glycerol, TMAO and sodium fumarate. However, as oxygen was to be used as a terminal electron acceptor, nitrate and nitrite were not included in the medium. Aerobic growth of the parent strain, RK4353, the *nirBDC nrfAB norV hcp* strain, JCB 5242, and the *hcp* mutant strain, JCB 5250, were similar (Figure 6.3). This suggested that Hcp is critical for anaerobic growth, but not for aerobic growth.

Complementation of the *hcp* mutation using a plasmid.

It was critical to ensure that the growth phenotype observed in strain JCB 5250 was due to the *hcp* mutation and not to a secondary deletion, or a polar effect of the *hcp* mutation. Bacteria were transformed with a plasmid encoding Hcp under the control of an IPTG inducible promoter. The antibiotic sensitive *hcp* derivative strain, JCB 5253,

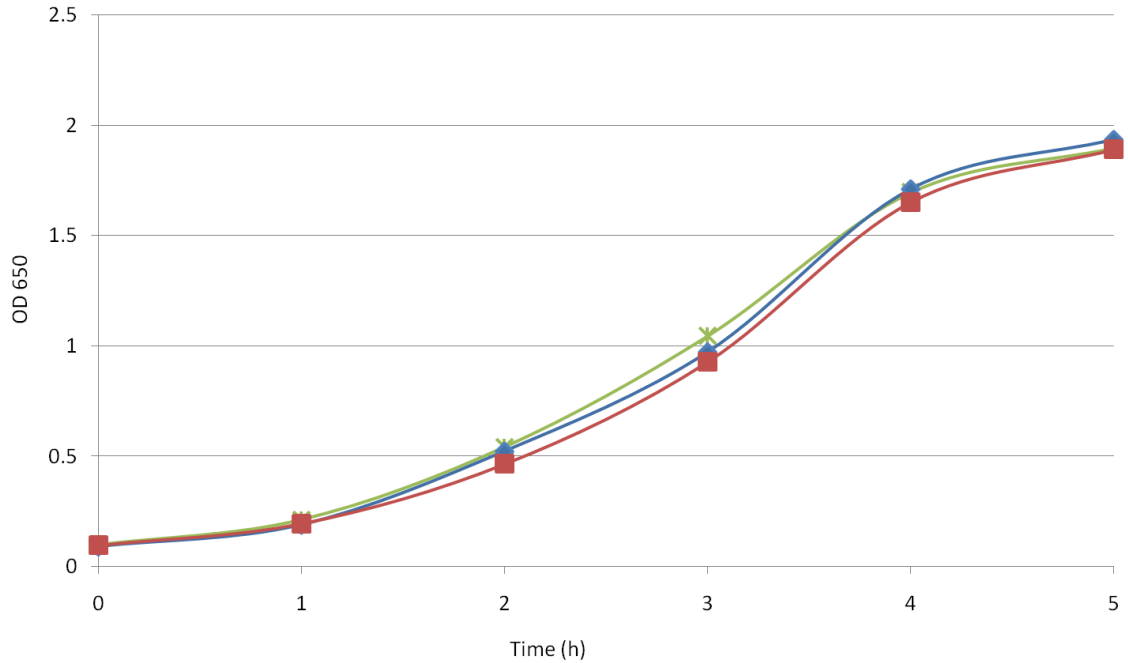
Figure 6.2.



Growth phenotype of the *hcp* derivative of the quadruple mutant strain that is defective in all characterised NO reductases.

The quadruple mutant strain, JCB 5210 (filled symbols), and its *hcp* derivative, JCB 5250 (open symbols), were grown anaerobically in medium that was either unsupplemented (●○), or supplemented with 2.5 mM sodium nitrite (■□) or 20 mM sodium nitrate (▲△). Other details were as in Figure 4.9.

Figure 6.3.



The aerobic growth phenotype of a strain defective in all characterised NO reductases and the hybrid cluster protein, Hcp.

The parent strain, RK4353 (green), the *nirBDC nrfAB norV hcp* strain, JCB 5242 (blue), and the *nirBDC nrfAB norV hmp hcp* strain, JCB 5250 (red), were grown aerobically 37°C. Other details were as in Figure 4.9.

was used because both the plasmid and the original strain, JCB 5250, encoded chloramphenicol resistance. Bacteria were grown anaerobically as previously described, and cultures in which the plasmid was present were supplemented with both chloramphenicol and IPTG. Growth of bacteria in the presence of nitrate was complemented by the plasmid (Figure 6.4). However, growth of the culture supplemented with sodium nitrite was not rescued by the plasmid. After 5 or 7 h of growth, bacteria transformed with the plasmid had accumulated a 60 kDa protein, consistent with the reported size of Hcp (Figure 6.4). In the presence of sodium nitrate, these complementation data are consistent with the growth phenotype being due to the *hcp* mutation. However, it is possible that in the presence of nitrite, damage is too severe to be rescued by expression of Hcp.

The accumulation of nitrite in growth medium supplemented with nitrate.

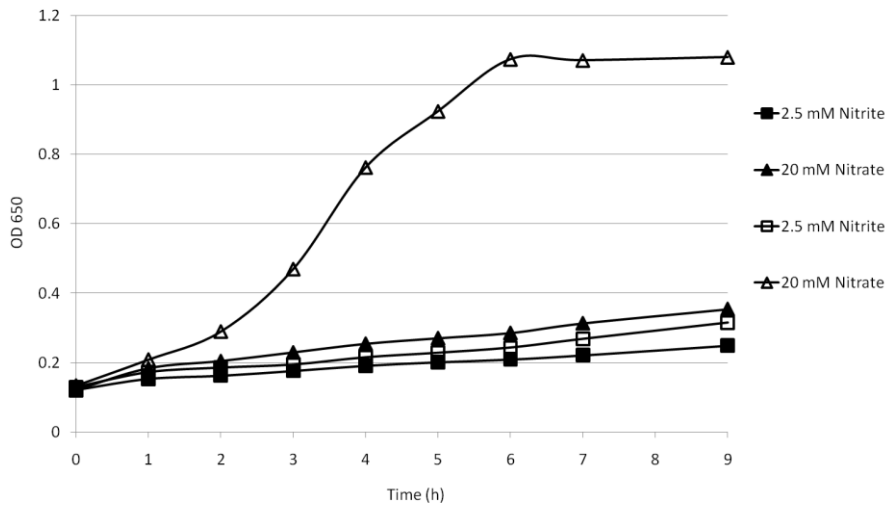
In light of the growth phenotype of the *hcp* mutant observed in Figure 6.2, it was interesting to quantify the rate of nitrite accumulation in the growth medium of strains defective in characterised nitrite and NO reductases. To investigate this, the quadruple mutant strain, JCB 5210, and the *hcp* derivative, JCB 5250, were grown anaerobically until the optical density at 650 nm had reached 0.5. Cultures were then supplemented with 1 mM nitrate. Samples were taken every 20 min, and the nitrite concentration in each sample was quantified. A concentration of 1 mM nitrate added at time 0 was converted quantitatively to 1 mM nitrite within 40 min (Figure 6.5). The nitrite concentration then decreased at a very slow rate, decreasing from 1 mM to around 0.9 mM over the next 3 h. In the absence of both nitrite reductases, this slow degradation represented the upper limit for the rate of NO generation from nitrite.

Nitrite removal in the absence of both nitrite reductases.

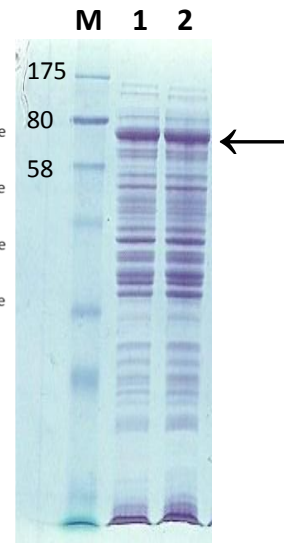
Corker and Poole (2003) reported that NO can be generated in wild-type bacteria at 10 nmol NO (mg protein)⁻¹ from 2.5 mM nitrite, and at 44 nmol NO (mg protein)⁻¹ from 25

Figure 6.4.

A



B

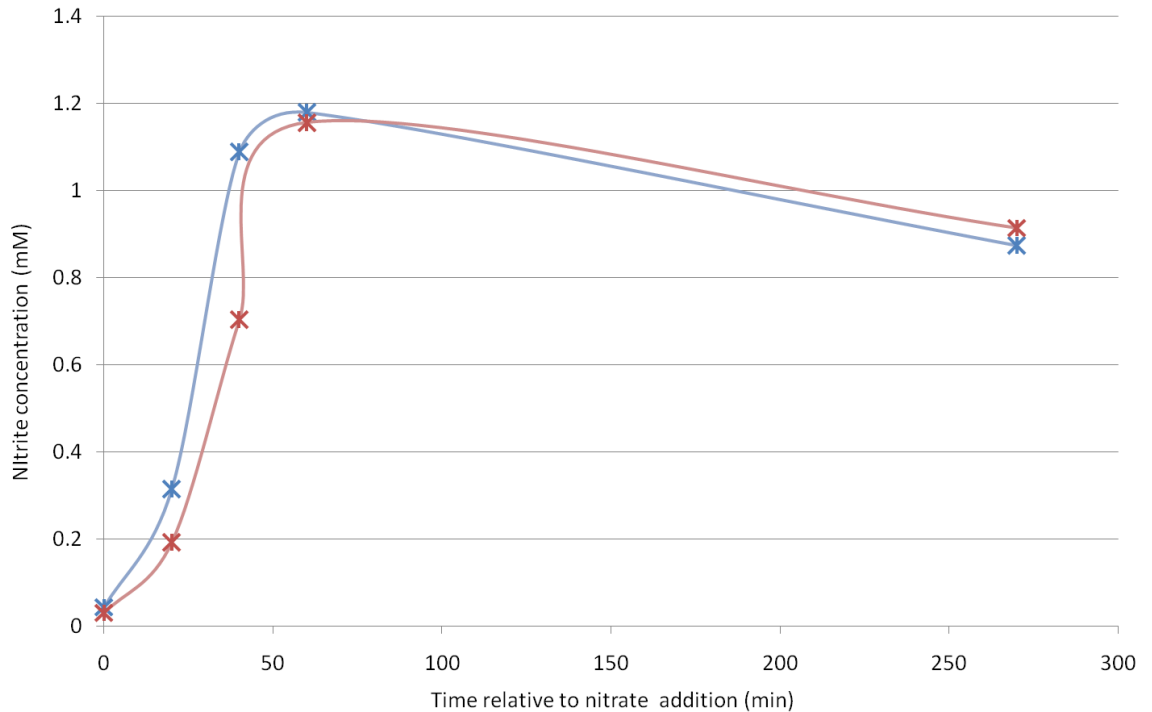


Growth and SDS protein gel of the *hcp* derivative of the quadruple mutant transformed with a plasmid encoding Hcp.

A: The *nirBDC nrfAB norV hmp hcp* strain, JCB 5253, was either transformed with a plasmid that expresses Hcp, pCA24n2 (open symbols) or was left as an untransformed control (filled symbols). Cultures were grown anaerobically in medium that was either supplemented with 2.5 mM sodium nitrite (■□) or 20 mM sodium nitrate (▲△), and where appropriate with chloramphenicol to maintain the plasmid and 100 μ M IPTG to induce the expression of Hcp. Other details were as in Figure 4.9.

B: Additional samples from bacteria grown in the presence of sodium nitrate were taken at 5h and 7h to be assayed for total protein by SDS-PAGE. Lane M: protein sizes (kDa) are indicated. Lane 1: JCB 5253 transformed with the pCA24n2 harvested at 5h. Lane 2: JCB 5253 transformed with the pCA24n2 harvested at 7h. The arrow indicates the protein band that corresponds to Hcp overexpression.

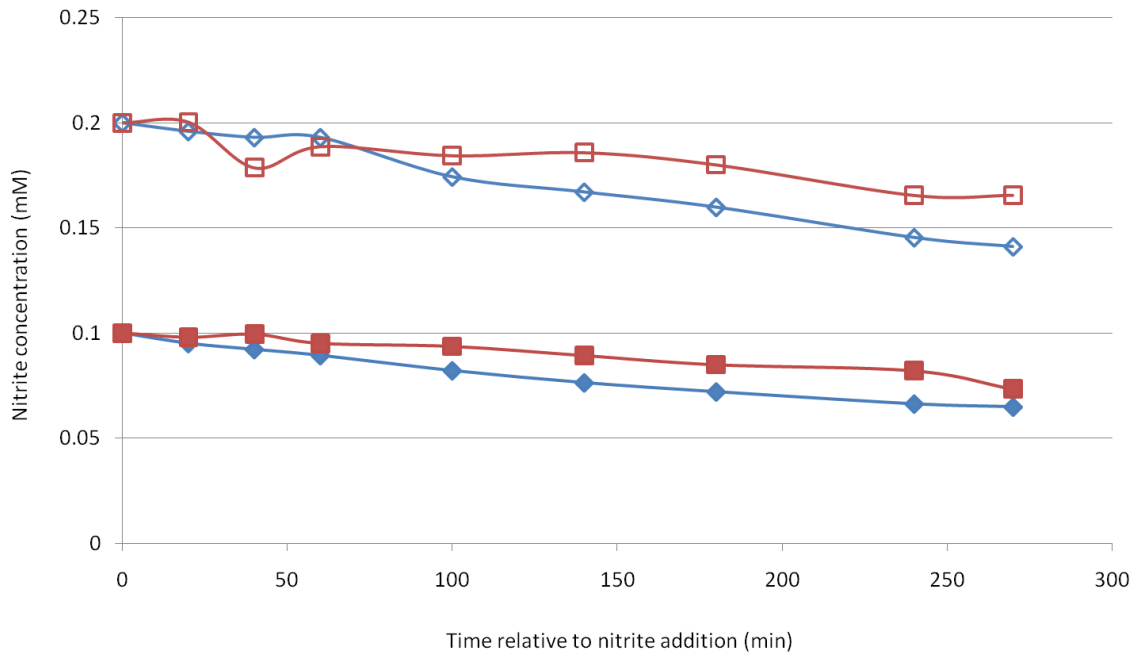
Figure 6.5.



The accumulation of nitrite in cultures supplemented with sodium nitrate.

The quadruple mutant strain, JCB 5210 (blue), and the *hcp* derivative strain, JCB 5250 (red), were grown anaerobically in minimal medium until the optical density at 650 nm had reached 0.5. At this time, cultures were supplemented with 1 mM nitrate. Samples were withdrawn every 20 min for the first hour, and at 280 min to be assayed spectrophotometrically for optical density and to determine the concentration of nitrite in the culture supernatant. Assays were completed at least in biological duplicate, and this graph shows a typical result.

Figure 6.6.



Removal of nitrite by *E. coli* mutants that are deficient in nitrite reductases and other proteins involved in nitrosative stress defence.

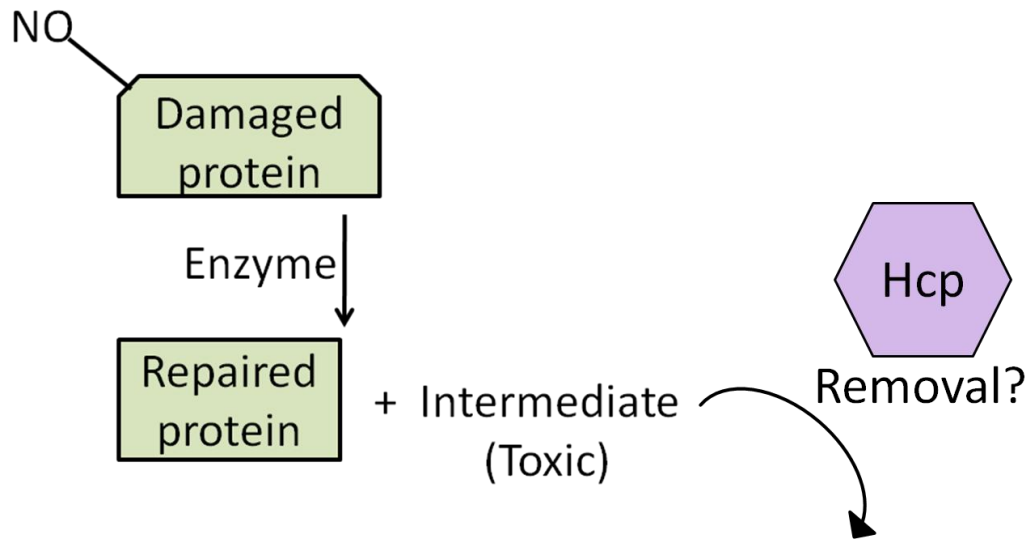
The quadruple mutant strain, JCB 5210 (blue), and the *hcp* derivative strain, JCB 5250 (red), were grown anaerobically in minimal medium until the optical density at 650 nm had reached 0.5. Cultures were then supplemented with sodium nitrite to a final concentration of 0.1 mM (filled symbols) or 0.2 mM (open symbols). Samples were withdrawn, and the concentration of nitrite in the culture supernatant was determined. Other details were as in Figure 6.5.

mM nitrite. To quantify the rate of nitrite removal by bacteria lacking both nitrite reductases, the quadruple mutant strain, JCB 5210, and the *hcp* derivative strain, JCB 5250, were grown anaerobically until the optical density at 650 nm had reached 0.5. Cultures were then supplemented with nitrite, samples were taken every 20 min and the nitrite concentration in each sample was quantified. Nitrite added at time 0 was depleted very slowly. Even 4 h after the addition, an initial concentration of 0.2 mM nitrite had decreased to only 0.15 mM nitrite, and 0.1 mM nitrite had decreased to 0.07 mM nitrite (Figure 6.6). It was possible that this nitrite removal was due to conversion of nitrite to NO by NarG. The rate of nitrite removal was slightly higher when cultures were supplemented with nitrate, which subsequently was converted to nitrite, than when the culture was supplemented with nitrite (Figure 6.5, Figure 6.6). This is consistent with the fact that expression of *narG* is nitrate-induced. In the presence of nitrate, more NarG would accumulate and thus be available for the side reaction.

A possible role for Hcp in repair of nitrosative damage.

A model was considered in which Hcp might catalyse the removal of a toxic intermediate generated by another repair enzyme (Figure 6.7). If so, mutation of the gene for the enzyme that generates the toxic intermediate should suppress the growth-defective phenotype of the *hcp* mutants. To investigate this model, additional mutations were introduced into the *hcp* derivative strain in an attempt to find a mutation that would suppress the growth defective phenotype. Candidates for the repair enzyme generating a toxic intermediate were the proteins of unknown function that are synthesised under conditions of nitrosative stress (Constantinidou *et al.*, 2006). These are YibIH, YgbA, YeaR-YoaG and YtfE, the protein for the repair of iron centres. Derivatives of the antibiotic sensitive *hcp* strain, JCB 5253, were constructed

Figure 6.7.



A model for the role of the hybrid cluster protein, Hcp.

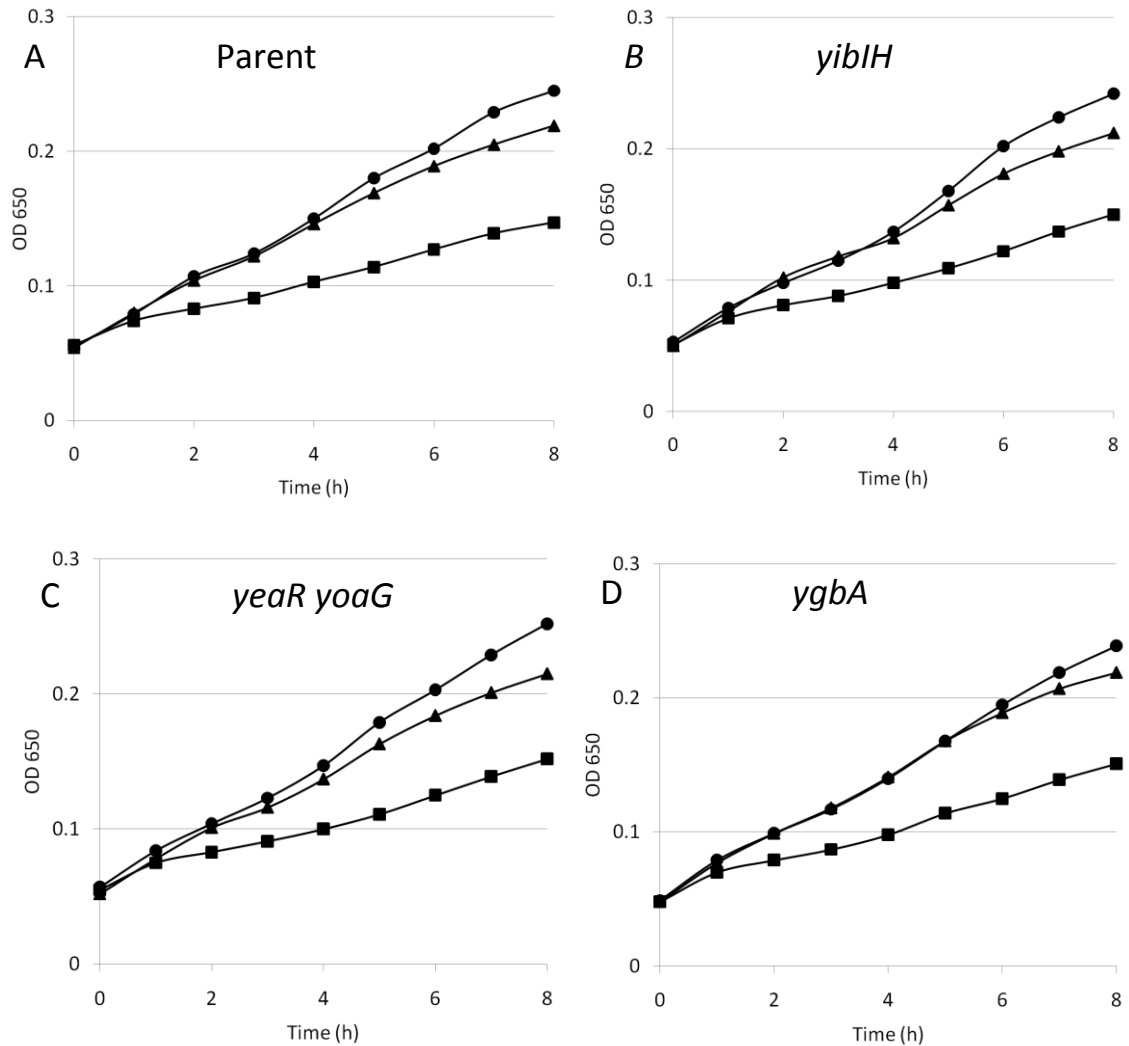
A model was considered, in which proteins are damaged by nitrosylation. A repair enzyme that remains to be identified is responsible for the repair of the nitrosylated protein, thereby generating a toxic intermediate that requires removal. The model proposes that Hcp is required for the removal and detoxification of the intermediate. If the repair enzyme is deleted, the toxic intermediate would no longer build up, and hence suppress the *hcp* mutation. The toxic intermediate might be NO, or free iron that would then induce Fenton Chemistry and consequently oxidative stress in bacteria.

The parent *hcp* strain, JCB 5253, the *ytfE* derivative strain, JCB 5260, the *ygbA* derivative strain, JCB 5261, the *yeaR* derivative strain, JCB 5262, and the *yibIH* derivative strain, JCB 5263, were grown in minimal medium that was either unsupplemented, or supplemented with 2.5 mM sodium nitrite or 20 mM sodium nitrate as previously described. In each case, the introduction of a *ygbA*, *yeaR-yoaG*, or *yibIH* mutation did not suppress the growth defective phenotype (Figure 6.8). This is consistent with the idea that the genes of unknown function do not perform an early repair role in the same pathway as Hcp. When the medium was unsupplemented, or was supplemented with 20 mM sodium nitrate, the *ytfE* mutation suppressed the growth-defective phenotype of strain JCB 5253 (Figure 6.9). This observation was consistent with YtfE and Hcp functioning in the same pathway in the cell, as shown in Figure 6.7. However, in the presence of sodium nitrite, the defective growth phenotype was not suppressed.

The role of Hcp and YtfE in strains defective in all characterised NO reductases.

An isogenic set of strains was used to confirm the roles of Hcp and YtfE in resisting nitrosative stress that were implied by the suppression genetics experiments. The set of four strains were all defective in the flavohaemoglobin, Hmp, but contained all combinations of the presence and absence of Hcp and YtfE (summarised in Table 6.1). The *hmp* strain, JCB 5210, the *hmp ytfE* strain, JCB 5257, the *hmp hcp* strain, JCB 5250 and the *hmp hcp ytfE* strain, JCB 5260, were grown anaerobically in medium that was either unsupplemented, or supplemented with 2.5 mM nitrite or 20 mM nitrate as previously described. The *hmp* strain that was *ytfE*⁺ and *hcp*⁺, JCB 5210, grew to an optical density at 650 nm of 1.1 in unsupplemented medium, and to an optical density of 1.0 in medium supplemented with sodium nitrite (Figure 6.10). This strain reached an

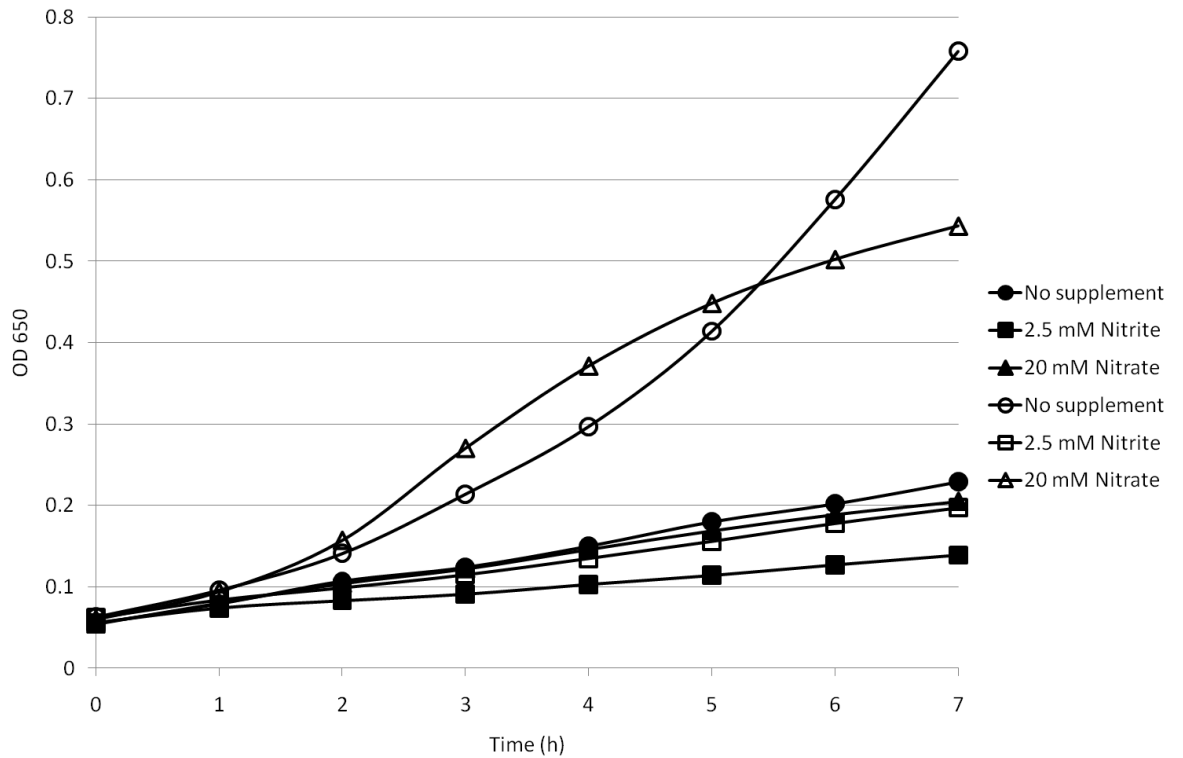
Figure 6.8.



Growth phenotype of *ygbA*, *year* and *yibIH* derivatives of the mutant strain, JCB 5253, which is defective in all characterised NO reductases and the hybrid cluster protein, Hcp.

The *nirBDC nrfAB norV hmp hcp* parent strain, JCB 5253 (A), the *yibIH* derivative, JCB 5263 (B), the *year* derivative, JCB 5262 (C), and the *ygbA* derivative, JCB 5261 (D), were grown anaerobically in medium that was either unsupplemented (●), or supplemented with 2.5 mM sodium nitrite (■) or 20 mM sodium nitrate (▲). Note that the scale of the y-axis is low (OD 650, 0 to 0.3) compared to previous graphs. Other details were as in Figure 4.9.

Figure 6.9.



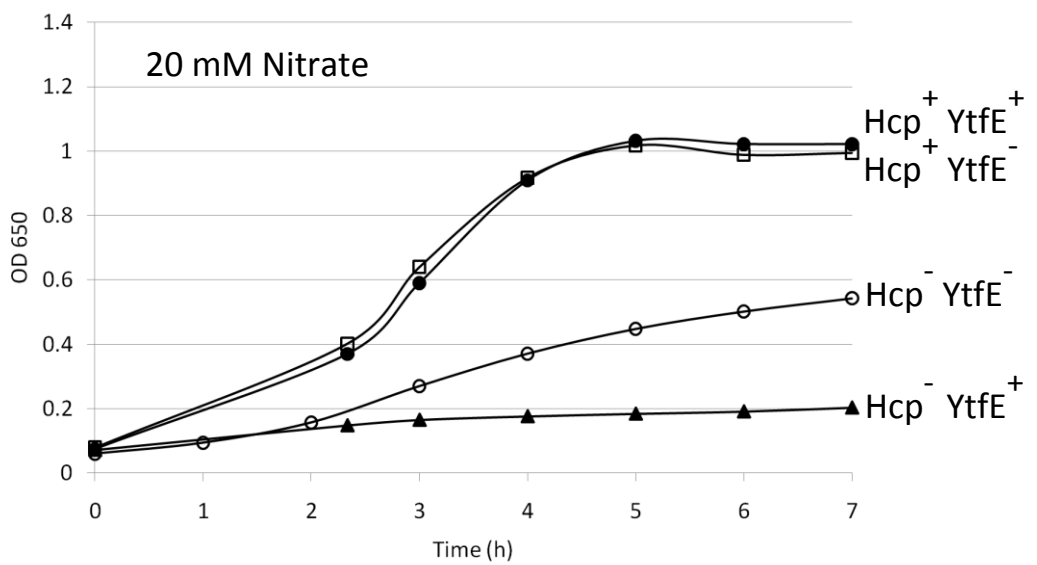
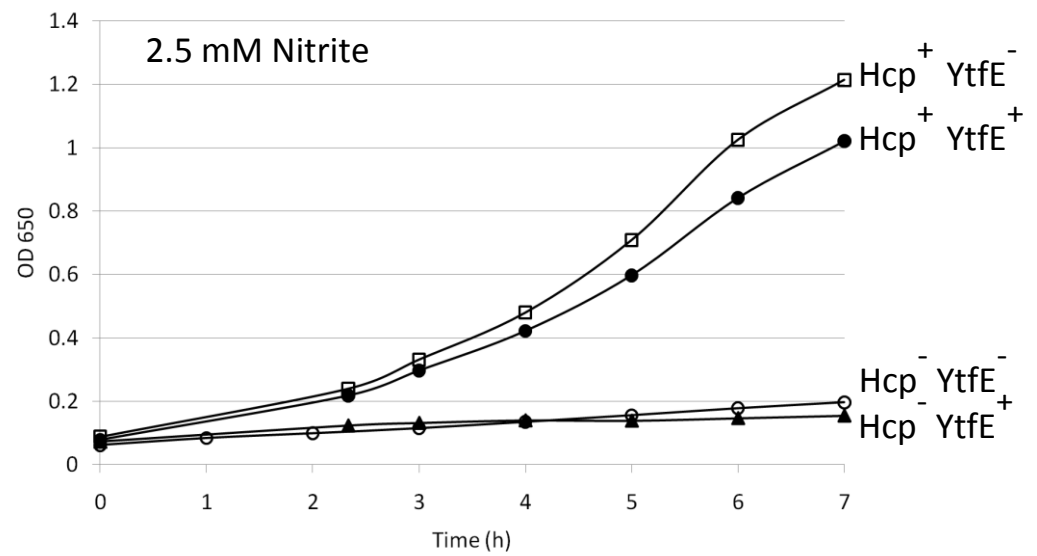
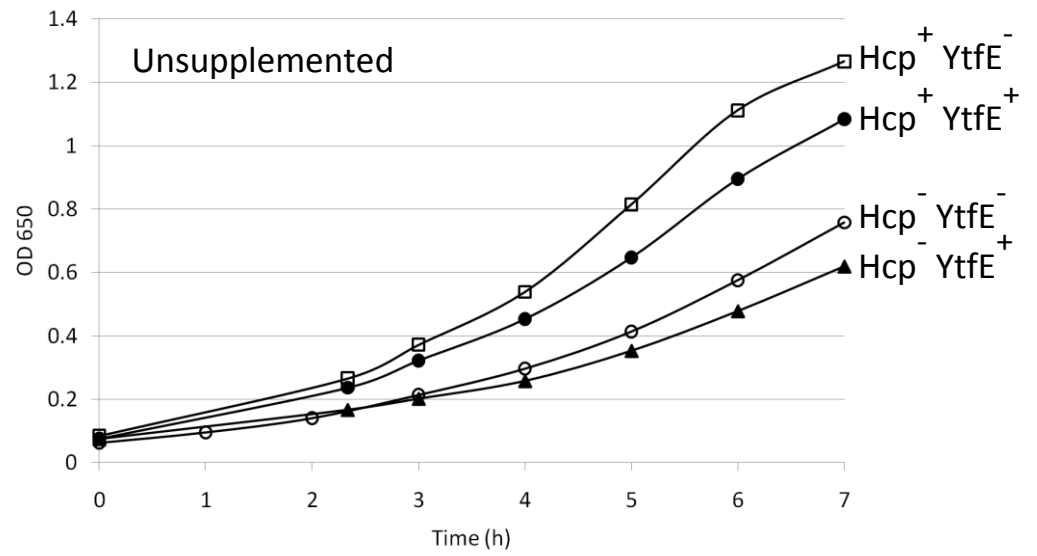
Growth phenotype strain of strain JCB 5260, which is deficient in all characterised NO reductases as well as the hybrid cluster protein, Hcp and YtfE.

The *nirBDC nrfAB norV hmp hcp* strain, JCB 5253 (filled symbols), and the *ytfE* derivative strain, JCB 5260 (open symbols), were grown anaerobically in medium that was either unsupplemented (●○), or supplemented with 2.5 mM sodium nitrite (■□) or 20 mM sodium nitrate (▲△). Other details were as in Figure 4.9.

Figure 6.10.

The effect of nitrate and nitrite on growth of Hcp⁻ and YtfE⁻ derivatives of the quadruple mutant defective in all characterised NO reductases.

All strains in this experiment were defective in *nirBDC nrfAB* and *norV* and are summarised in Table 6.1. The *hmp* strain, JCB 5210 (●), the *hmp ytfE* strain, JCB 5257 (□), the *hmp hcp* strain, JCB 5250 (▲), and the *hmp hcp ytfE* strain, JCB 5260 (○) were grown anaerobically in medium that was either unsupplemented, or supplemented with 2.5 mM sodium nitrite or 20 mM sodium nitrate. Other details were as in Figure 4.9



optical density of 1.0 at 5 h after inoculation, then the culture failed to grow any further, as observed previously (Figure 4.11). The *ytfE* derivative that was YtfE⁻ and Hcp⁺, JCB 5257, grew to a slightly higher optical density than the YtfE⁺ strain in both unsupplemented medium and in the presence of sodium nitrite. However, in the presence of sodium nitrate, there was no difference in growth between the *ytfE* mutant and the *ytfE*⁺ strain (Figure 6.10).

The *hmp hcp* strain that was Hcp⁻ and YtfE⁺, JCB 5250, grew poorly in unsupplemented medium, reaching an optical density at 650 nm of 0.6 in 7 h of growth. Growth of this strain was totally abolished in medium that was supplemented with sodium nitrite or sodium nitrate, and did not reach an optical density above 0.2. The *ytfE* derivative of this strain that was Hcp⁻ and YtfE⁻, JCB 5260, grew to a higher optical density than the *ytfE*⁺ parent in unsupplemented medium. In medium supplemented with sodium nitrite, growth of the *ytfE* derivative was very poor and was not altered relative to the YtfE⁺ strain. However, in the presence of sodium nitrate, the *ytfE* derivative grew to a higher optical density than the YtfE⁺ parent, reaching an optical density of 0.6 during 7 h of growth. The *ytfE* mutation had suppressed the growth defect of the YtfE⁺ strain (Figure 6.10).

It was important to compare the growth phenotype of the Hcp⁻YtfE⁻ strain, JCB 5260 to the Hcp⁺ YtfE⁻ strain, JCB 5257. If the hypothesis presented in Figure 6.7 was correct, it would be expected that an *hcp* mutation would be irrelevant in the absence of YtfE. Because the toxic product would not be generated in the absence of YtfE, Hcp would no longer be required to remove it. However, in every growth condition tested, the Hcp⁺ strain grew to a much higher optical density than the *hcp* mutant. The role of *hcp* is clearly still important for growth in a *ytfE* mutant, even in the absence of nitrosative stress. This raises the question of whether the proteins function in parallel pathways. Hcp is certainly not irrelevant for growth of a *ytfE* mutant (Figure 6.10).

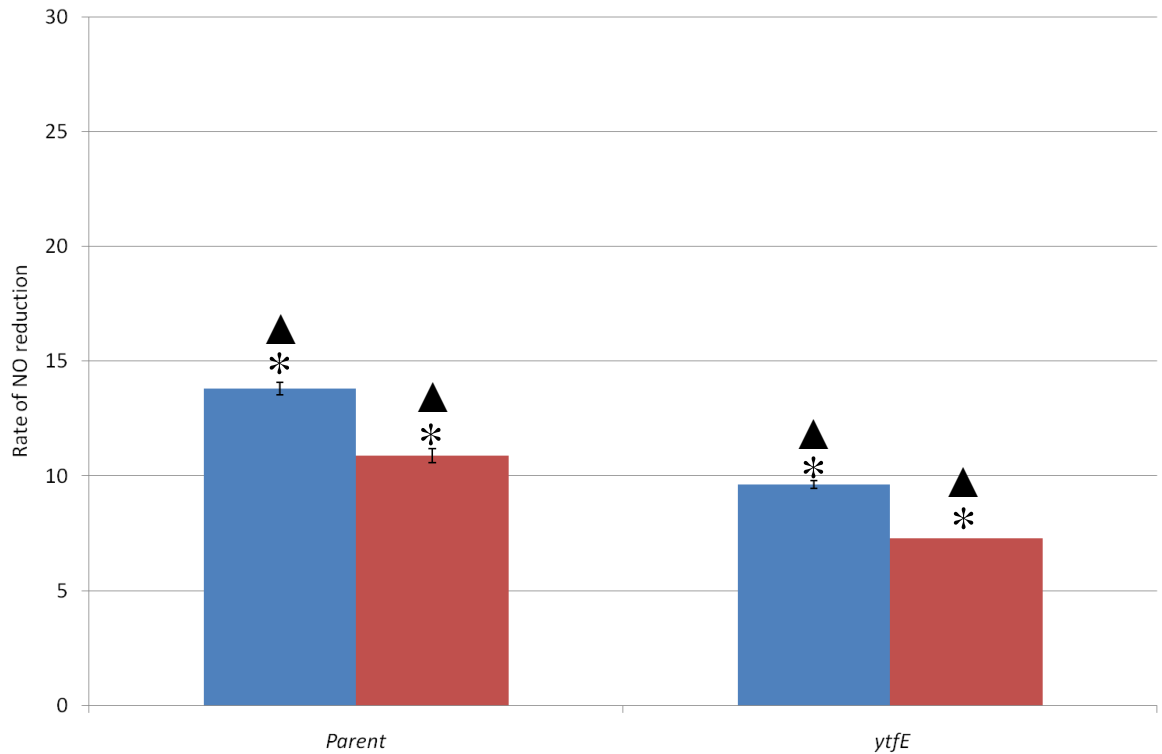
The rate of NO reduction of a *ytfE* derivative of the quadruple mutant.

The rate of NO reduction by a mutant defective in only YtfE, RK4353 $\Delta ytfE::cat$, was slightly lower than the parent after growth in medium supplemented with nitrite (Figure 4.8). It was possible that more active NO reductases were masking an effect of YtfE in the single mutant strain. To investigate the effect of mutating these NO reductases, the quadruple mutant parent strain, JCB 5210, and the *ytfE* derivative, JCB 5257, were grown and assayed for NO reduction as previously described. When that *ytfE* derivative was grown in medium supplemented with nitrate, the rate of NO reduction was 30% lower than the quadruple mutant parent. This difference was statistically significant ($p=0.016$) (Figure 6.11). After growth in medium supplemented with nitrite, the rate of NO reduction was 33% lower than the quadruple mutant parent ($p=0.020$) (Figure 6.11). In both cases, there was still a statistically significant difference between the rate of NO reduction for bacteria grown in the presence of sodium nitrate, compared to bacteria grown in the presence of sodium nitrite (Figure 6.11).

The effect of nitrate and nitrite concentration on growth of the *hcp ytfE* derivative of the quadruple mutant.

It was interesting to investigate growth of the *hcp ytfE* strain, JCB 5260, over a range of nitrite and nitrate concentrations. Cultures were grown anaerobically in minimal medium that was supplemented with either 1 to 10 mM sodium nitrate or 0.1 to 1 mM sodium nitrite. The *ytfE* mutation suppressed the growth defective phenotype of the *hcp* mutant until NO was generated in the cell (Figure 6.12). This was a similar phenotype to that observed in the YtfE⁺ Hmp⁺ strain (Figure 6.1, C). As soon as the nitrate concentration had decreased, NarG was able to convert the accumulated nitrite into NO and this is certainly toxic in the absence of all characterised NO reductases, as well as Hcp and YtfE. Note that NO accumulation was not toxic in the Hcp⁺ quadruple mutant strain (Figure 6.1, A).

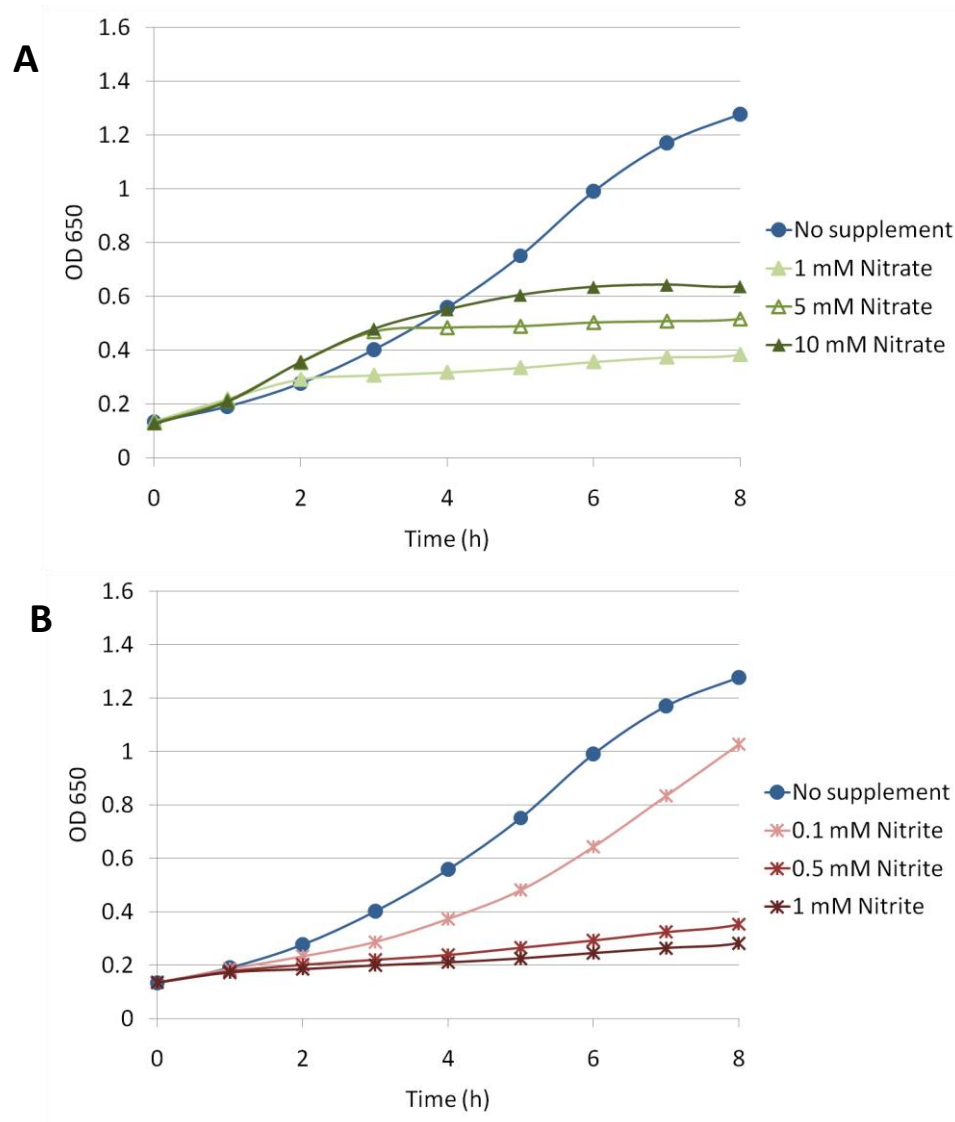
Figure 6.11.



Rate of NO reduction of strains defective in all known NO reductases and the repair protein, YtfE.

In this experiment each strain was defective in all four known NO reductases, NirBDC NrfAB NorV and Hmp. The parent strain, JCB 5210, and the *ytfE* strain, JCB 5257, were grown anaerobically in minimal medium supplemented with 20 mM sodium nitrate (blue) or 2.5 mM sodium nitrite (red), then the bacteria were assayed for NO reduction activity as previously described. A star above a bar represents that data are significantly different from the RK4353 strain (see text). A triangle above a bar represents that there is a significant difference between the rate of NO reduction for bacteria of a particular strain grown in the presence of nitrate and nitrite (see text). Other details are as in Figure 4.4.

Figure 6.12.



The effect of nitrate and nitrite concentration on the growth of a strain defective in both Hcp and YtfE.

Panel A: The *hcp ytfE* strain, JCB 5260, was grown anaerobically in minimal medium that was either unsupplemented (blue) or supplemented with 1 to 10 mM sodium nitrate (green).

Panel B: JCB 5260 was grown anaerobically in the presence of 0.1 to 1 mM sodium nitrite (red).

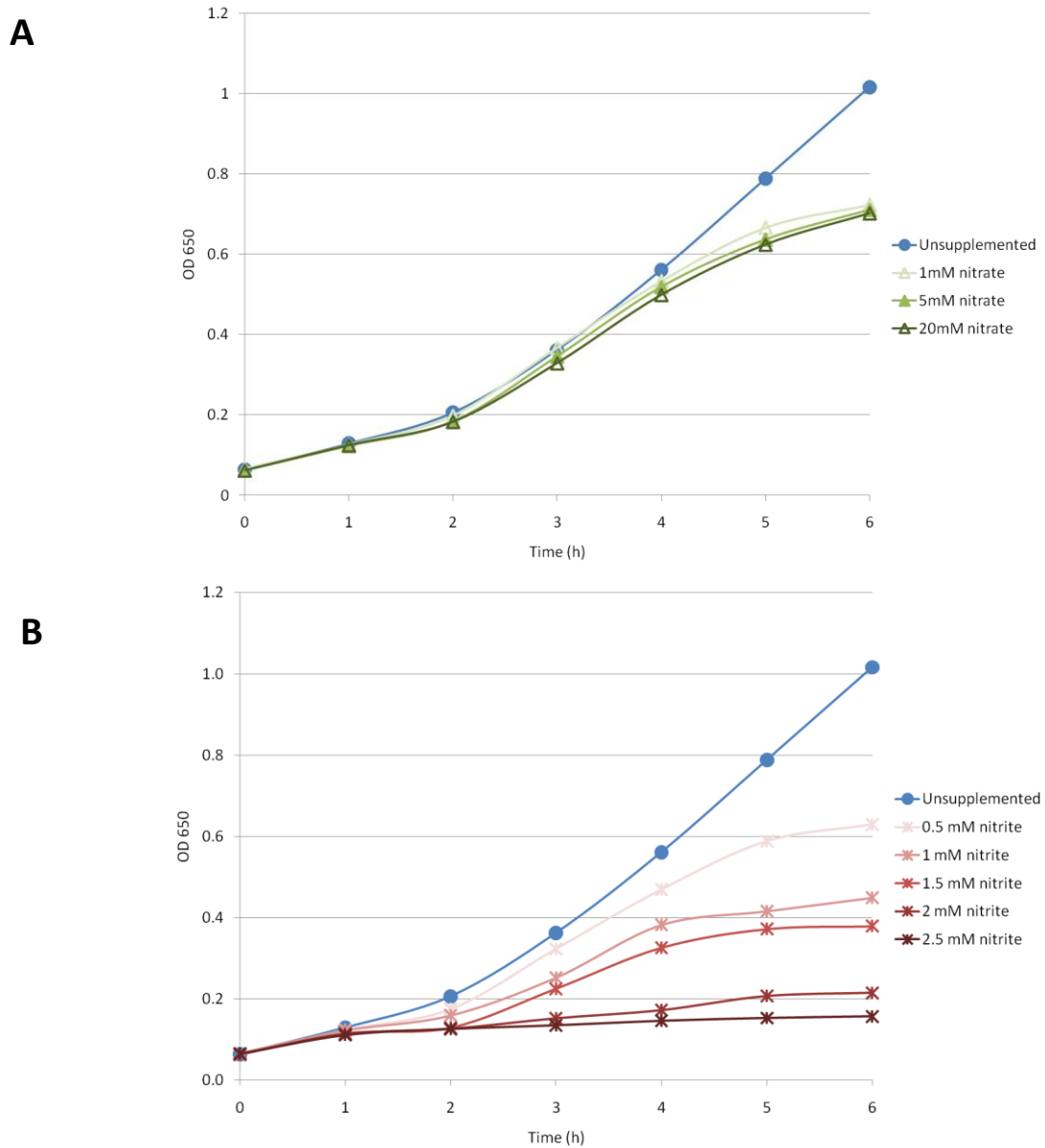
The palest line in each case represents the lowest concentration of supplement (see legend). Note that the full genotype of strain JCB 5260 was *nirBDC nrfAB norV hmp hcp ytfE*. Other details were as in Figure 4.9.

The effect of NarG on growth of the *nirBDC nrfAB norV hmp hcp* strain.

The *hcp* derivative of the quadruple mutant, JCB 5250, grew very poorly anaerobically and did not reach an optical density at 650 nm above 0.3 in the presence of nitrate or nitrite (Figure 6.2). It has also been observed in two *hcp* strains, JCB 5242 and JCB 5260, that the depletion of nitrate in the medium causes growth arrest indirectly. This is consistent with a side-reaction of the nitrate reductase, NarG, generating toxic NO. A strain defective in Hcp as well as NarG and NarZ was constructed to test whether decreased intracellular generation of NO would prevent growth inhibition in the presence of nitrate or nitrite. The *narGHJI narZ* derivative strain, JCB 5270, was grown anaerobically in the presence of a range of nitrate or nitrite concentrations as previously described, by a visiting student, Merve Yasa. Growth of strain JCB 5270 was not suppressed in the presence of low concentrations of nitrate, but was suppressed by nitrite in a dose dependent manner (Figure 6.13). This was consistent with NO being generated from nitrite by the NarG⁺ strain JCB 5253, but not in the *narGHJI narZ* derivative.

It was important to investigate the effect of NarG and NarZ on the *hcp ytfE* strain, JCB 5260, which had a complex growth phenotype in the presence of a range of nitrate or nitrite concentrations. The depletion of nitrate was coordinated with growth arrest in the *hcp ytfE* derivative of the quadruple mutant (Figure 6.12). The *narGHJI narZ* strain, JCB 5280, was constructed and grown in comparison to the isogenic NarGHJI⁺ NarZ⁺ strain, JCB 5260, in medium supplemented with a range of nitrate or nitrite concentrations as previously described. Growth of the *narGHJI narZ* derivative strain was not suppressed by low concentrations of nitrate, and this strain grew in the presence of low concentrations of nitrite, in contrast to the isogenic NarG⁺ NarZ⁺ strain (Figure 6.14). The *narGHJI narZ* bacteria reached a high optical density at 650 nm over a range of nitrate concentrations, and were sensitive to sodium nitrite in the growth medium in a dose-dependent manner (Figure 6.15). It seems that the lack of YtfE and Hcp was not critical when NO was not generated by the major source, NarG, intracellularly.

Figure 6.13.



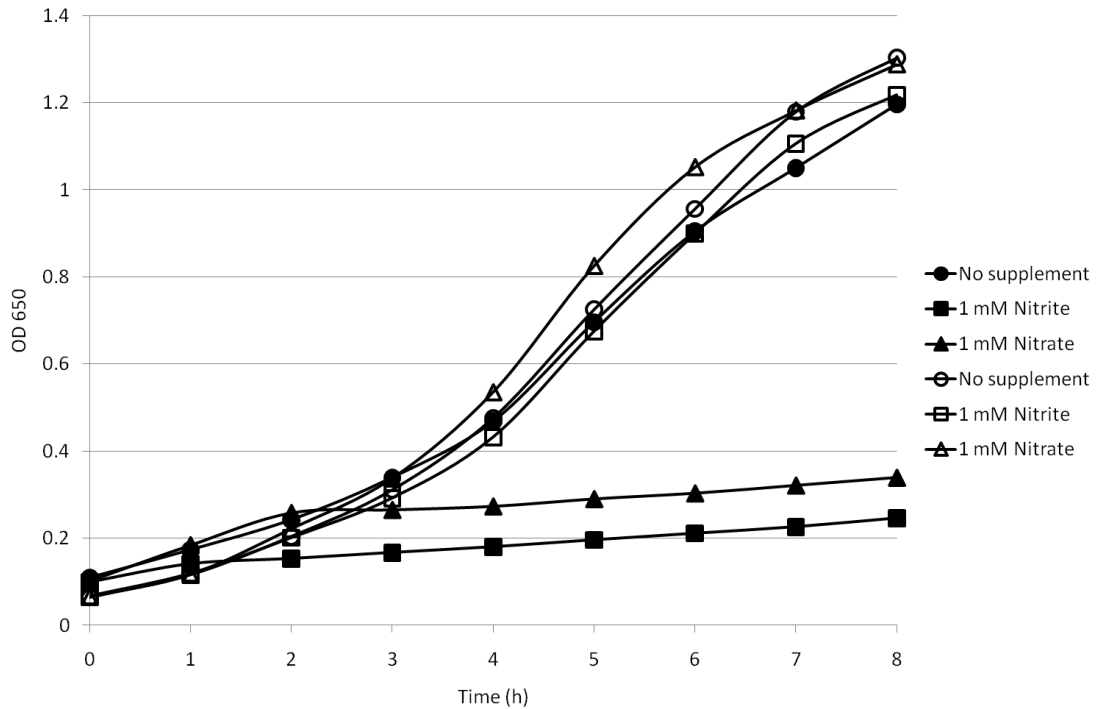
The effect of the nitrate reductases, NarGHJI and NarZ, on growth of the *hcp* derivative of the quadruple mutant strain.

Panel A: The *narGHJI narZ* strain, JCB 5270 was grown anaerobically in medium that was either unsupplemented (blue) or supplemented with either sodium 1 to 20 mM sodium nitrate (green).

Panel B: Strain JCB 5270 was grown anaerobically in medium supplemented with 0.5 to 2.5 mM sodium nitrite (red).

Note that the full genotype of strain JCB 5270 was *nirBDC nrfAB norV hmp hcp narGHJI narZ*. The experiment in this figure was completed by Merve Yasa. All other details were as in Figure 4.9.

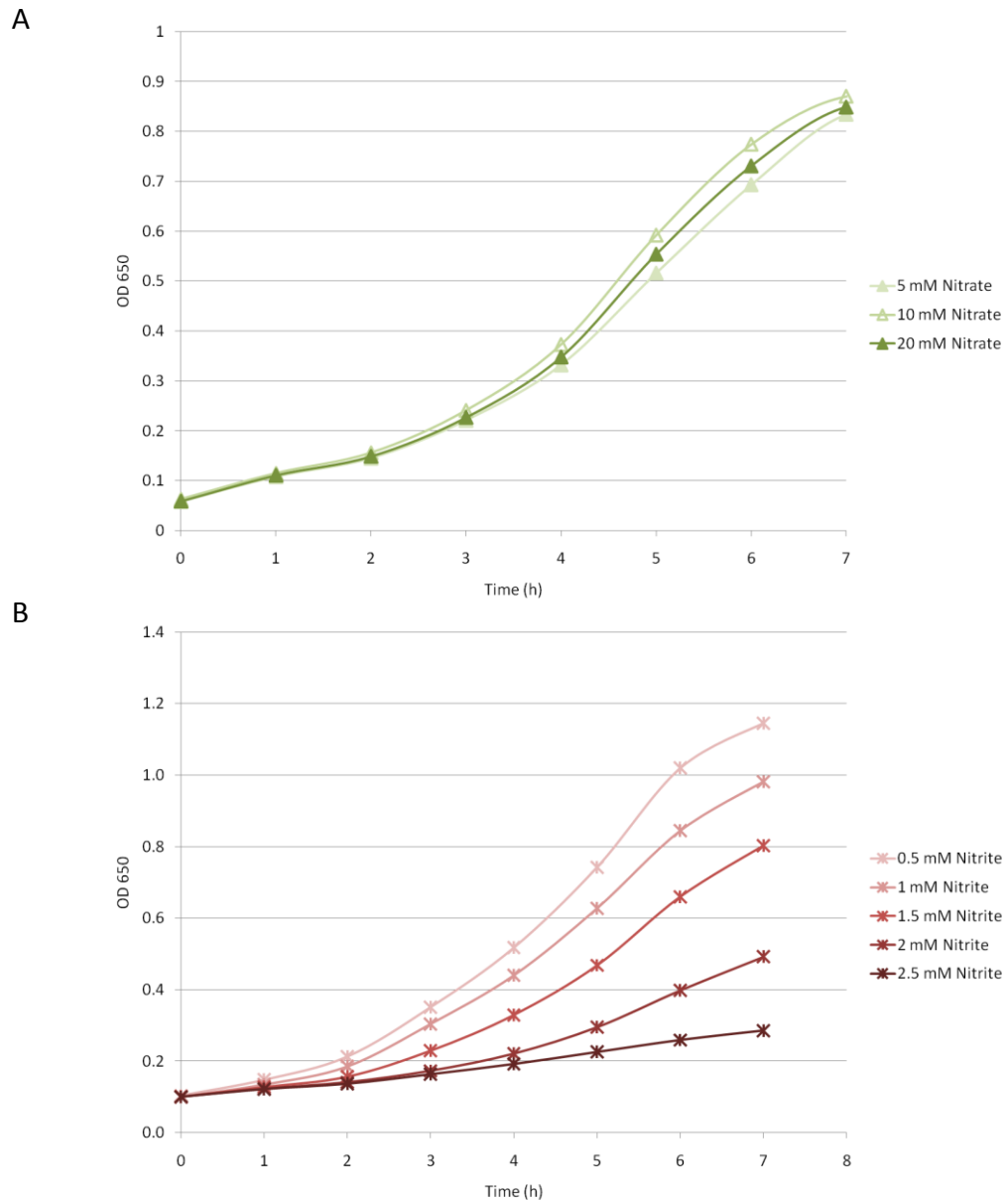
Figure 6.14.



The effect of NarGHJI and NarZ on growth of strains defective in proteins that protect *E. coli* against nitrosative stress.

The NarGHJI⁺ NarZ⁺ strain, JCB 5260 (filled symbols), and the narGHJI narZ strain, JCB 5280 (open symbols), were grown anaerobically in medium that was either unsupplemented (●○) or supplemented with either 1 mM sodium nitrate (▲△) or 1 mM sodium nitrite (■□). Note that the both strains are defective in *nirBDC nrfAB norV hmp hcp* and *ytfE*. All other details were as in Figure 4.9.

Figure 6.15.



Growth phenotype a strain defective in Hcp, YtfE, NarG-I and NarZ over a range of nitrite concentrations.

Panel A: The *narGHJI narZ ytfE* strain, JCB 5280, was grown anaerobically in medium supplemented with 5 to 20 mM sodium nitrate.

Panel B: Strain JCB 5280 was grown anaerobically in medium that was supplemented with 0.5 to 2.5 mM sodium nitrite. The palest bar represents the lowest nitrite concentration (see legend).

Note that the full genotype of strain JCB 5280 was *nirBDC nrfAB norV hmp hcp narGHJI narZ ytfE*. Other details were as in Figure 4.9.

Discussion.

Several conclusions can be drawn from the work presented in this chapter. First, the hybrid cluster protein is critical during anaerobic growth in the absence of NirBDC, NrfAB, NorV and Hmp, but it is irrelevant during aerobic growth. Hcp becomes increasingly critical for growth as nitrate is depleted and the nitrate reductase, NarG, is able to generate NO from nitrite. The rate of conversion of nitrite to NO is slow, but very low intracellular NO concentrations (in the nM range, rarely exceeding 1 μ M) are thought to be physiologically relevant (Palmer *et al.*, 1987, Cardinale and Clarke, 2005). The growth-defective phenotype of the *nirBDC nrfAB norV hmp hcp* strain is suppressed by the mutation of *ytfE* or *narG*, but not by other genes encoding proteins of unknown function: YeaR-YoaG; YgbA or YibIH. A suggestion arising from these data is that both NarG and YtfE might generate NO during growth.

In chapter 3, NarG was shown to generate NO from nitrite as a side reaction. The fact that a *ytfE* mutation suppressed the *hcp* mutant phenotype in a similar manner to the *narG* deletion suggests that YtfE might generate NO as part of its repair mechanism. However, this suppression by *ytfE* occurs only in the presence of sodium nitrate. In the presence of sodium nitrite, the growth phenotype is not suppressed. This might be due to the fact that in the presence of sodium nitrite, damage is so severe in these mutants lacking both Hcp and YtfE that no recovery is possible. Despite the conclusions that can be drawn from experiments with strains defective in several NO reductases, it is critical to note that in the parental strain in which these NO reductases are functional, the NO would likely be effectively detoxified.

Evidence is building that Hcp is involved in anaerobic metabolism, and is particularly important during nitrate, nitrite and NO metabolism, or repair of damage

caused by NO. Hcp becomes crucial when NO is allowed to accumulate, in a strain in which all characterised NO reductases have been deleted. The fact that nitrate inhibits NO production from nitrite has been reported previously (Ji and Hollocher, 1988). Results of experiments with a series of nitrate concentrations were consistent with the idea that the presence of nitrate represses NO generation from nitrite. However, at a point where the nitrate concentration becomes low, relative to the concentration of nitrite present, growth defects that correspond to an inability to deal with NO are revealed.

A very subtle growth phenotype was observed in Figure 6.1 for the triple mutant strain. When the medium was supplemented with 5 mM sodium nitrate, the growth rate decreased 3 h post-inoculation. At 4 h after inoculation, rapid growth resumed. This diauxic growth was highly reproducible, both in several repeats of the experiment with the triple mutant strain, and also in experiments with the *hmp* derivative strain. As the *hmp* strain had the same growth phenotype as the *hmp*⁺ parent, it is clear the recovery from growth suppression is not Hmp-dependent. However, it is possible that recovery at this point in growth is dependent upon Hcp, as no recovery is observed in the *hcp* derivative strain (Figure 6.1).

The role of Hcp in detoxifying NO generated when nitrate is depleted might be very relevant *in vivo*, as nitrate rarely exceeds 1 mM in the human host (Forsythe *et al.*, 1988). The nitrate concentration of 1 mM would be depleted rapidly by the nitrate reductases present in *E. coli*. However, *E. coli* also persists in environments where it might have to encounter much higher nitrate concentrations, such as in sewage plants. Therefore, the ability to survive in a range of conditions is critical.

It is possible that Hcp is required for the repair of nitrosative damage, or to metabolise an intermediate formed during the repair of nitrosative damage. However, as a phenotype is clear in the absence of nitrate or nitrite, the role of Hcp might not be limited to nitrosative damage, but Hcp becomes more important when nitrosative damage accumulates. If the function of Hcp was solely to remove an intermediate generated by YtfE, the Hcp mutation would be irrelevant in the absence of YtfE. However, this is not the case, as demonstrated by rapid growth of the Hcp⁺ strain, JCB 5257, that is defective in NirBDC, NrfAB, NorV, Hmp and YtfE (Figure 6.10). Additional models to the one presented in Figure 6.7 will be required, and discussed in the next chapter, in order to further investigate the role of Hcp.

The work presented in this chapter contributes towards the wealth of suggestions that Hcp is involved in the anaerobic nitrosative stress response. The most apparent phenotype for an *hcp* mutation was revealed in the absence of characterised NO reductases. During growth in the presence of nitrate, but not nitrite, it is clear that the phenotype of the *hcp* mutation can be complemented by the expression of Hcp from a plasmid (Figure 6.4). However, it is likely that there is a lag in the expression of Hcp from the plasmid. Perhaps by the time that Hcp has been expressed, it is too late to rescue growth of the mutant strain under nitrosative stress caused by sodium nitrite. The growth phenotype of the *hcp* strain suggested that the build-up of NO, or a consequence of NO accumulation, made the role of Hcp critical. Structural studies have revealed a hydrophilic channel in Hcp that allows access of a hypothetical substrate to the hybrid cluster, which is coordinated at the geometric centre of the protein (Cooper *et al.*, 2000). There is also a hydrophobic cavity that allows access to the hybrid cluster in the centre of Hcp (Aragão *et al.*, 2008). Hydrophobic cavities often allow gaseous substrates to

access the active site of enzymes, so NO or another nitrogen oxide gas are good candidates for the true substrate of Hcp (Kim *et al.*, 2003). It has been suggested that the true substrate might be a diatomic molecule, according to the size of the entry and efflux channels in the protein (Arendsen *et al.*, 1998).

The precise nature of the mechanism by which YtfE repairs damage to iron centres has not yet been determined. It is possible that in the quadruple mutant, in which nitrosative damage might accumulate, the repair of iron centres by YtfE contributes towards the measured rate of NO reduction. Indeed, the absence of YtfE caused a small but significant decrease in the rate of NO reduction (Figure 4.8, Figure 6.11). In this role, YtfE is important for nitrosative protection, but it is not essential due to the fact that NO reduction activity remains even in the *nirBDC nrfAB norV hmp ytfE* strain.

It is possible that YtfE releases NO, or an NO derivative, during the repair process, and that Hcp becomes critical when this repair intermediate accumulates, for example when NO reductases have been inactivated. This is consistent with the suppression effects that have been observed; a *ytfE* mutation partially suppresses the growth defect of an *hcp* mutation in the strains described in this chapter (Figure 6.9). It is interesting that YtfE and Hcp homologues have been identified in *Salmonella enterica* serovar Typhimurium as acidified nitrite-induced promoters that modulate virulence (Kim *et al.*, 2003). They have been designated *nipA* (*hcp*) and *nipC* (*ytfE*). In *S. enterica*, a mutant defective in each protein has a similar phenotype in mouse infection models; both mutants exhibited lower oral 50%-lethal doses than the wild type. In some way, the absence of these bacterial genes diminishes the ability of mice to clear infection. It was postulated that perhaps the mutant bacteria are able to escape detection by the adaptive immune response, and are able to persist to cause systemic

disease due to this early avoidance (Kim *et al.*, 2003). It is also interesting that *hcp* and *ric* co-localize in the genome of *Pelobacter propionicus*, a strictly anaerobic bacterium that encodes a nitrite reductase homologue (Justino *et al.*, 2009). This co-localization might reflect a related role that is also relevant in this *E. coli* study.

CHAPTER 7. DISCUSSION.

The role of Fnr as a physiological sensor of NO.

It has been reported that Fnr is a physiological sensor of NO. This conclusion was based upon evidence that NO generated by proline NONOate is able to bind to purified Fnr protein to produce DNICs that were measured spectroscopically. This was a reversible phenomenon, throughout which the protein structure remained native (Cruz-Ramos *et al.*, 2002, Crack *et al.*, 2008b). A five minute exposure to the NO releasing compounds, NOC 5 and NOC 7, led to the downregulation of some, but not all, operons that are activated by Fnr (for example: *narG*, *pyrD*, *yjiH*, *aroP*, and *rmuC*). Pullan *et al.*, (2007) also reported the upregulation of some Fnr-repressed genes (*ndh*, *hmp*, *gpmA*, and *lpdA*) under the same conditions. The patterns of gene expression were concluded to be consistent with NO mediated deactivation of Fnr. Consistent with the inactivation of Fnr by NO, it was generally observed in a microarray study that some Fnr-repressed genes were induced, whereas Fnr-activated genes were repressed (Justino *et al.*, 2005). However, because of overlapping transcriptional regulation, some genes failed to follow this trend. For example, transcription of the Fnr-repressed *nuo* operon was diminished by NO. Hence Fnr seems to be an NO-sensitive regulator that is involved in ‘fine-tuning’, as opposed to being a dedicated NO sensor like NorR or NsrR.

The same authors conclude from other experiments using a *norR* mutant that an increase in transcription of the *nrfA* promoter might have been due to nitrite accumulation. It was speculated that nitrite might form under anoxic conditions via metal ion-dependent oxidation of NO to NO₂, which during reaction with H₂O yields NO₂⁻ (Pullan *et al.*, 2007). However, such a scenario was not taken into account when

Table 7.1. Fnr-activated genes that are downregulated by NO addition anaerobically, and the other regulators that control these operons.

Gene	Fold regulation	Gene product or function	Other regulators
<i>ackA</i>	-3.8	Acetate kinase	ArcA(+)
<i>ansB</i>	-2.1	Asparaginase II	Crp(+) Fis(-)
<i>arcA</i>	-2.1	Response regulator of two-component system	Fnr can activate or repress
<i>caiF</i>	-3.1	Transcriptional activation of <i>cai</i> operon	Crp(+) HNS(-) NarL(-)
<i>dcuC</i>	-2.5	Anaerobic C ₄ -dicarboxylate transport	ArcA(+)
<i>dcuR</i>	-3.9	Anaerobic C ₄ -dicarboxylate transport.	NarL(-) Crp(+)
<i>dmsA</i>	-2.0	DMSO reductase subunit A	NarL(-) Fis(-) ModE(-) Ihf(-)
<i>dmsB</i>	-2.4	DMSO reductase subunit B	NarL(-) Fis(-) ModE(-) Ihf(-)
<i>fliJ</i>	-2.7	Flagellar biosynthesis	CsgD(-) FhlCD(+)
<i>frdB</i>	-2.8	Fumarate reductase subunit	DcuR(+) NarL(-)
<i>frdC</i>	-2.6	Fumarate reductase subunit	DcuR(+) NarL(-)
<i>frdD</i>	-2.2	Fumarate reductase subunit	DcuR(+) NarL(-)
<i>glpB</i>	-2.1	Glycerol-3-phosphate dehydrogenase subunit	Crp(+) Fis(+) FhlCD(+) ArcA(-) GlpR(-)
<i>napD</i>	-3.1	Essential for NapAB activity	NarP can activate or repress NarL(-) IscR(-)
<i>napF</i>	-3.7	Electron transfer from ubiquinol to NapAB	NarP can activate or repress NarL(-) IscR(-)
<i>napH</i>	-2.2	Electron transfer from ubiquinol to NapAB	NarP can activate or repress NarL(-) IscR(-)
<i>narG</i>	-2.8	Nitrate reductase subunit	ModE(+) FhlCD(+)
<i>nirC</i>	-2.2	Nitrite transporter	Crp(-) Fis(-) FruR(-) HNS(-) NarLP(+) Ihf(+)
<i>nrfA</i>	-4.9	Nitrite reductase	NarP(+) NarL(-) NsrR(-) FhlCD(+) Fis(-)
<i>nrfB</i>	-2.9	Nitrite reductase	NarP(+) NarL(-) NsrR(-) FhlCD(+) Fis(-)
<i>ydhV</i>	-3.7	Putative oxidoreductase	NarLP(-)

Adapted from Pullan *et al.*, 2007. Function and additional regulator information are taken from the Ecocyc database. Additional regulators either activate (+) or repress (-) transcription.

the authors concluded that Fnr-regulated promoters must be responding to physiologically relevant NO-sensing. It is possible that during NO treatment of an *fnr* mutant, NO also accumulates and forms nitrite in a similar manner. Some of the genes used as a clear example of NO modulating the Fnr regulon are also controlled by other transcription factors (Table 7.1). Of particular interest are the genes that are also controlled by NarL and NarP that would respond to accumulated nitrite in the medium. A review article by Spiro (2007) points out that earlier data do not support regulation of *nrfA* transcription by Fnr in response to NO.

In the work presented in chapter 3, the activity of a synthetic Fnr-repressed promoter was not changed by the addition of NO at concentrations that clearly derepressed transcription at NsrR regulated promoters (Figure 3.14). In an *fnr* mutant, the activity of the synthetic promoter was 4-fold higher than in the parent strain, as expected, and in addition did not respond to the addition of NO to the medium. It is possible to conclude that the reporter does respond to Fnr inactivation, but that physiologically relevant concentrations of NO do not sufficiently damage Fnr. In agreement with data in chapter 3, others conclude that accumulation of NO at physiologically relevant concentrations does not damage Fnr adequately to be a true sensor (Fleischhacker and Kiley, 2011).

In light of the characterisation of NsrR, several authors question whether Fnr can be physiologically relevant as a sensor of NO (Justino *et al.*, 2005, Spiro, 2007, Fleischhacker and Kiley, 2011, Vine *et al.*, 2011). Emphasis was put on Fnr controlling the response of Hmp to NO, but this is more likely to be due to NsrR regulation (Bodenmiller and Spiro, 2006). Complex regulation is apparent at several of the

promoters cited by Pullan *et al.*, (2007) (Table 7.1). The effect of NO on other transcription factors involved in regulation must be taken into consideration.

Another NO reductase must remain to be characterised.

An *E. coli* strain that is defective in NrfA, NirB, NorV and Hmp, is still able to reduce NO at least 50% of the parental rate (Table 4.1, Table 4.2). A deletion experiment was completed in *Salmonella enterica* serovar Typhimurium to examine the contribution of NrfA, NorV and Hmp to NO reduction (Mills *et al.*, 2008). Conclusions of the study in *Salmonella* were that yet more NO-detoxification systems remain to be identified. Results for *E. coli* presented in chapter 4 agree with this conclusion. However, it is clear that there are differences in the strategy used by each of these bacteria to evade nitrosative stress; NrfA and NorV are critical for survival of *Salmonella*, but a double *nrfA norV* mutant in *E. coli* is able to both survive and reduce NO rapidly.

The lowest rate of NO reduction measured in this study was by a strain defective in the transcription factor NsrR. This suggests that a gene activated by NsrR might be an important mechanism for NO reduction. NsrR has been characterised mainly as a repressor of genes involved in the nitrosative stress response (Bodenmiller and Spiro, 2006, Filenko *et al.*, 2007). No *in vitro* studies of NsrR interactions with DNA have yet been published to show a role as a transcriptional activator. However, at least one other transcription factor in the Rrf2 family, IscR, can function both as a repressor and an activator (Yeo *et al.*, 2006, Giel *et al.*, 2006). Microarray data suggest that the *ydbC* promoter is activated by NsrR (Filenko *et al.*, 2007). It is possible that YdbC is responsible for the residual NO reduction in the *nirBDC nrfAB norV hmp* strain. The protein is annotated on the Ecocyc database as a predicted oxidoreductase, and is predicted to bind NAD(P) based upon the presence of a putative binding motif. To prove whether this suggested role in NO reduction is correct or incorrect, further

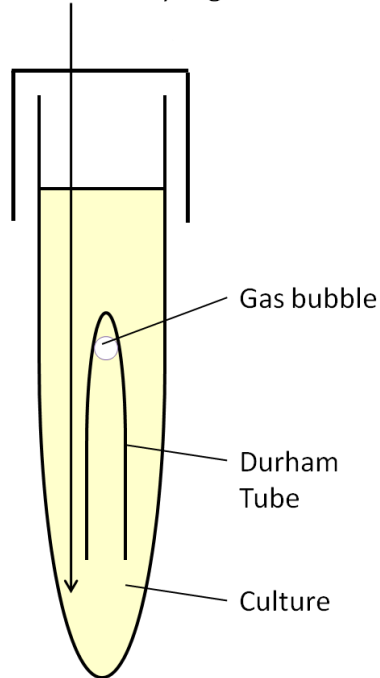
experiments must assay a *ydbC* mutant for the rate of NO reduction, and involve the construction and assay of a *nirBDC nrfAB norV hmp ydbC* strain. If the *ydbC* mutants did reduce NO at a rate significantly lower than that of the parent, it would be possible to construct a promoter fragment, cloned into a *lacZ*-fusion vector such as pRW50. The promoter fragment could then be used for β -galactosidase activity assays in a mutant defective in NsrR, to determine whether transcription activation is abolished. NsrR has not yet been reported to be a transcriptional activator, so it would be interesting to characterise the interaction of the *ydbC* promoter fragment with lysates of bacteria overexpressing NsrR protein. It has been difficult in the past to purify NsrR from *E. coli*, but electromobility shift assays (EMSAs) have been completed with cell lysates (Chismon, PhD Thesis, 2011).

Current work has not yet elucidated whether the product of the NO reduction being measured in a strain defective in all characterised NO reductases is N_2O or NH_4^+ . Experiments must be completed to analyse this. It is possible to collect gaseous products during growth using a Durham tube (Figure 7.1). If the product generated from NOSW is gaseous, it is likely to be N_2O . The identity of the collected gas could be confirmed using mass spectroscopy. If the product is not gaseous and instead is soluble, it is likely to be ammonia. It would be possible to test for ammonia in the growth medium using titration methods, before and after addition of NOSW, and to subsequently determine the concentration of ammonia produced.

In the next section, the fact that externally added NO does not equilibrate with the bacterial cytoplasm in order to derepress NsrR-regulated promoters will be discussed. One possibility to explain this apparent lack of NO 'equilibration' could be that rapid NO reduction, by an uncharacterised NO reductase, could detoxify NO before

Figure 7.1

NOSW can be administered anaerobically using a gastight Hamilton syringe.



Apparatus used to collect gas bubbles.

It is possible to collect gaseous products during metabolism using the apparatus depicted here. The growth medium can be sterilised with the upturned Durham Tube in place. Any gaseous product produced by bacteria in the culture is trapped. This system is suitable for identification, but not quantification of gaseous products.

it reaches NsrR in the cytoplasm. An active NO reductase could remove sufficient NO such that any that does reach the cytoplasm binds to other proteins for which it has a higher affinity, perhaps other protein components of the respiratory chains, such as cytochrome *bd*. Any small effect of NO binding might therefore not be reported by using a low, but still multiple, copy number plasmid. NsrR binds to several targets across the chromosome. It is possible that the affinity of NsrR binding at individual sites would be reflected in derepression at weaker affinity sites at lower concentrations of NO, and derepression at high affinity binding sites at higher concentrations of NO.

Exogenous NO does not derepress transcription of *pytfE*: is there a barrier to NO equilibration?

Exogenous NOSW is unable to derepress transcription effectively from the NsrR-regulated *ytfE* promoter, as reported by a *lacZ* fusion, despite the fact that growth is clearly inhibited by the addition. NO is an uncharged small molecule that is assumed to be freely diffusible across bacterial membranes, and should be able to pass from the culture medium into the cytoplasm. However, nitrite introduced to the culture medium that is subsequently metabolized inside the cell to NO is a more effective way to derepress transcription at the NsrR-regulated promoters: *ytfE* (Figure 3.7); *hmp* (Figure 3.13); and *hcp* (Figures 3.4 to 3.6) (Vine *et al.*, 2011).

It is possible that there is a protein detoxification mechanism that has such a high affinity for NO that NO is unable to reach NsrR and relieve repression of transcription at NsrR-regulated promoters. The most obvious candidate for protection was the periplasmic nitrite reductase, NrfA, but this possibility was excluded in chapter 5 (Figure 5.12). The flavohaemoglobin, Hmp, is also not responsible for this apparent lack of NO equilibration (Figure 5.13). A further candidate for this role is cytochrome

bd. It would be useful to construct a *cydAB* mutant in order to test the hypothesis with a β -galactosidase assay.

The role of Hcp as a hydroxylamine reductase.

Wolfe *et al.* (2002) concluded that Hcp may function as a hydroxylamine reductase, as the protein is able to reduce this substrate *in vitro*. The kinetics of this reaction proceeds with a K_m of 40 mM in physiologically relevant conditions (pH 7.4). The role as a hydroxylamine reductase was logical, as hydroxylamine is produced by NirB and NrfA as an enzyme-bound intermediate during reduction of nitrite to ammonia, and regulation of *hcp* suggests an involvement in the nitrosative stress response (Jackson *et al.*, 1981a, Jackson *et al.*, 1981b). However, just 1 mM hydroxylamine in the growth medium is sufficient to cause bacterial cell death, so the role as an hydroxylamine reductase is not likely to be physiologically relevant. Anaerobic growth of both the parent strain and an *hcp* mutant was inhibited by 500 μ M hydroxylamine for 5 h before a recovery of the parent is observed (Squire, PhD Thesis, 2009). There was a 2 h delay in the recovery of the *hcp* mutant compared to the parent following treatment. As the *hcp* mutant does eventually recover, Hcp is not essential for recovery from hydroxylamine toxicity.

Evidence has been published that 1 mM hydroxylamine allows growth of a *Rhodobacter capsulatus* parent strain, but inhibits growth of an *hcp* mutant (Cabello *et al.*, 2004). However, the *hcp* mutant used in these experiments is deficient in the whole 17 kb *hcp-nas* region, which includes the genes that encode sirohaem and molybdopterin cofactor biosynthesis as well as many other proteins involved in nitrate assimilation. A recent report of the nitrosative stress defence network of *Wolinella succinogenes* found that Hcp did not mediate resistance to hydroxylamine stress; instead NrfA played a key role in this bacterium (Kern *et al.*, 2011).

The growth phenotype of an *E. coli hcp* mutant revealed during this work was suppressed when NO was no longer generated by NarG. This suggests a role in the metabolism of NO or as a consequence of NO damage, as opposed to resisting hydroxylamine toxicity. There is currently no evidence that YtfE or NarG generate hydroxylamine as a side product, therefore neither should suppress the *hcp* mutant phenotype. It is important to note that Hcp is critical for anaerobic metabolism in the absence of characterised NO reductases, even when the growth medium is not supplemented with nitrate or nitrite. However, both regulation data from previous studies and growth curves presented in this work suggest that Hcp becomes more important in the presence of nitrosative stress, and during nitrate or nitrite reduction (Filenko *et al.*, 2007, Chismon *et al.*, 2010).

Regulation of *ytfe* transcription and function of the YtfE protein in different bacterial species.

That Fnr represses transcription of *ytfe* has been reported from both microarray studies (Constantinidou *et al.*, 2006) and following mRNA purification from an *fnr* mutant (Justino *et al.*, 2006). However, as no clear Fnr-binding site was observed in the promoter region, it was possible that this repression effect was indirect. It was confirmed using the *ytfe::lacZ* reporter in this work that expression of *ytfe* is increased in an Fnr mutant (Figure 5.6). However, in the *fnr nsrR* double mutant, no additional increase of expression was observed relative to the *nsrR* mutant strain. This suggested that any repression effect might have been indirect. In order to prove whether Fnr binds to the promoter region, it would be necessary to complete EMSAs with a radiolabelled *ytfe* promoter fragment and purified Fnr. If binding was observed, the position in which it bound could be elucidated using DNase I footprinting. Perhaps the potassium permanganate footprinting technique could be used to detect promoter opening in the

presence and absence of Fnr, and could be used to determine whether Fnr represses transcription in order to prevent open complex formation.

YtfE analogues in different species respond differently to transcription factors. For example, YtfE is Fnr-activated in *H. influenzae*, in contrast to the indirect Fnr-repression effects that have been observed in *E. coli*. The *H. influenzae* YtfE mutant was more sensitive to NO donors than the isogenic parent (Harrington *et al.*, 2009). Note that no hybrid cluster protein is encoded by *H. influenzae*. It is possible that the role of YtfE and its homologues might vary between species, especially when other proteins that might be involved in the nitrosative stress response are absent. In a denitrifying bacterium, *Ralstonia eutropha*, the YtfE orthologue NorA is co-expressed with NorB, a membrane-bound NO reductase (Strube *et al.*, 2007). Expression of this di-cistronic operon is controlled by the regulator NorR, but a role for Fnr was not investigated. NorA is a di-iron protein, that is able to bind NO as shown by optical and EPR spectroscopy. However, NorA did not turnover NO as measured during experiments using a Clark-type electrode. NorA lowered the free cytoplasmic concentration of NO in a role that was suggested to scavenge, store or transport NO. It thus functions in a different way to the proven role in the repair of iron centres in *E. coli*, *S. aureus* and *N. gonorrhoeae* (Overton *et al.*, 2008).

The role of Hmp during anaerobic growth

Corker and Poole (2003) found that anaerobic growth of the *hmp* mutant was not stimulated by nitrate, and the mutant failed to produce periplasmic cytochrome *c*. This led to the hypothesis that NO accumulation in the absence of Hmp inactivates the global anaerobic regulator Fnr by reaction with the $[4\text{Fe-4S}]^{2+}$ cluster (Corker and Poole, 2003). The physiological level of nitrate likely to be encountered by *E. coli* is around 1 mM (Forsythe *et al.*, 1988). The concentration of 100 mM nitrate used in these

experiments is high; perhaps under these conditions Fnr would be inactivated due to stress. The growth medium used in these experiments was unsupplemented LB, with no additional carbon source provided. The addition of nitrate to the growth medium stimulated rapid growth of the parent strain, but did not stimulate growth of the *hmp* mutant. However, an alternative result was obtained in the current work using a minimal medium that was supplemented with 0.4% glycerol as a carbon source, and 20 mM TMAO and 20 mM fumarate as well as 1 to 10 mM nitrate as terminal electron acceptors. The addition of nitrate to the growth medium of a *nirBDC nrfAB norV hmp* mutant did stimulate growth; 1 mM nitrate induced a slight increase in the growth rate, and 5 and 10 mM nitrate further increased the rate of growth (Figure 6.1 B). More strikingly, the growth phenotype of this *hmp* derivative was exactly the same as that of the *nirBDC nrfAB norV* parent (Figure 6.1 A,B). This result suggested that Hmp is not crucial for the anaerobic growth of bacteria in the presence of 2.5 mM nitrite or 1 to 10 mM nitrate. Under these conditions, NO would be generated intracellularly, and therefore it is implied that Hmp is not essential for anaerobic protection against NO.

It has previously been found that Hmp showed negligible anaerobic NO reductase activity and afforded no protection to an NO-sensitive aconitase or the growth of anoxic *E. coli* (Gardner and Gardner, 2002). Instead, NO detoxification by Hmp occurs most effectively via O₂-dependent NO dioxygenation (Gardner and Gardner, 2002). Mills *et al.* (2001) also suggested that Hmp activity might be compromised in anoxic environments. Accordingly, the turnover numbers for NO are consistently lower under anaerobic conditions than in the presence of oxygen (Table 4.3). It would be possible to further confirm or disprove the prediction that Hmp has little effect in protection against NO accumulation by using 4-amino-5-methylamino-2',7'-

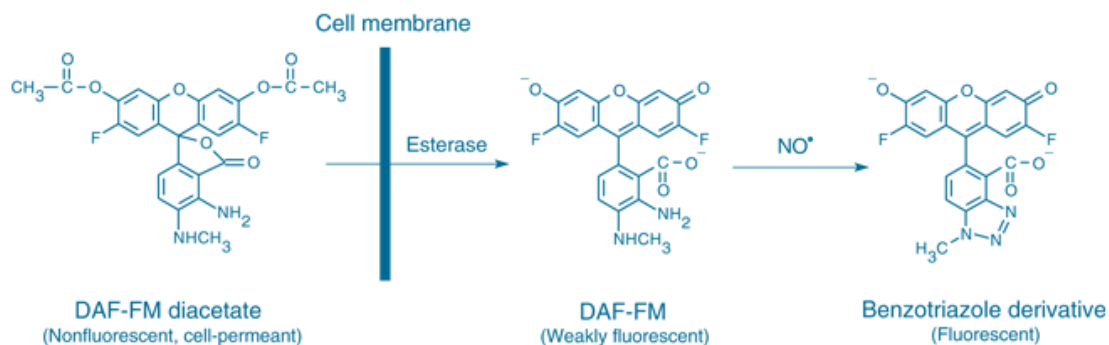
difluorofluorescein diacetate (DAF-FM diacetate, Figure 7.2). The non-fluorescent, cell-permeable NO detection dye reacts with NO with high specificity, sensitivity and accuracy, and generates a red fluorescent product (Kojima *et al.*, 1999). It is possible to use fluorescence microscopy or flow cytometry to analyse dye accumulation in bacterial populations. Bacteria that were Hmp⁺ would be expected to accumulate just as much dye as the corresponding *hmp* mutant. However, if the prediction is incorrect, and Hmp is critical for the prevention of NO accumulation, there should be more dye development.

The role of Hcp under anaerobic and aerobic conditions.

A clear anaerobic growth phenotype for an *hcp* mutant was revealed in chapter 6. Deletion of NrfAB, NirBD, NorV and Hmp did not significantly suppress growth of *E. coli*. However, when an *hcp* mutation was introduced into the same strain, anaerobic growth was abolished (Figure 6.2). When the *hcp* derivative was cultured under aerobic conditions, there was no growth difference relative to the parent strain, RK4353. This is unsurprising, as the transcription regulation of *phcp* is maximal under anaerobic conditions in the presence of sodium nitrite, suggesting a key role in the absence of oxygen (Filenko *et al.*, 2007, Chismon *et al.*, 2010).

One possibility for the critical role of Hcp under these conditions was as an additional NO reductase. However, experiments with a single *hcp* mutant, and a *nirBDC nrfAB hcp* mutant in this study gave no evidence for this hypothesis (Figure 4.1, Table 4.2). In both *hcp* mutants, the rate of NO reduction was similar to the relevant parent strain. Additional experiments completed with bacteria grown in the presence of sodium nitrate only show that other multiple *hcp* mutants reduce NO at rates that are 87% of, or higher than, the parental rate (Table 7.2). In conclusion, Hcp must have another

Figure 7.2.



The reaction of DAF-FM with NO to generate a fluorescent product.

The chemical structures of DAF-FM diacetate and its fluorescent products are shown.

Diagram taken from <http://www.invitrogen.com/site/us/en/home/References/Molecular-Probes-The-Handbook/Probes-for-Reactive-Oxygen-Species-Including-Nitric-Oxide/Probes-for-Nitric-Oxide-Research.html>

significant role in protection during anaerobic growth, but it does not function as a major NO reductase.

Possible roles for the hybrid cluster protein.

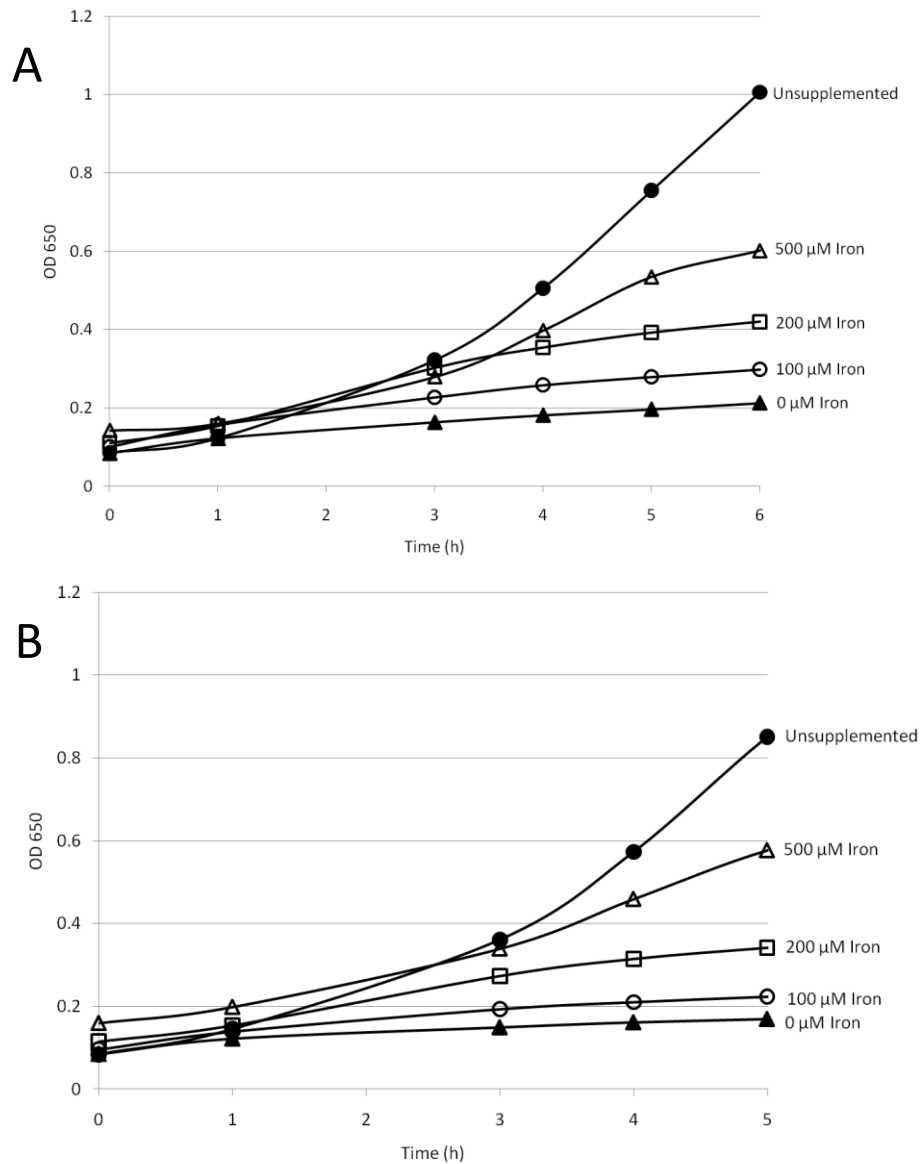
In facultative anaerobes, *hcp* is found in a dicistronic operon with a gene encoding an NADH oxidoreductase, *hcr*. However, in obligate anaerobes, *hcp* is found alone on the chromosome, and does not require Hcr as a specific electron donor (van den Berg *et al.*, 2000, Filenko *et al.*, 2004). This fact should be considered when forming models to explain Hcp function. It is also essential to consider which electron donors might replace Hcr in obligate anaerobes. Hcp is not found in bacteria with small genomes, such as *Mycobacteria* species and *Haemophilus influenzae* (van den Berg *et al.*, 2000.)

Some interesting possibilities for a role for Hcp have arisen from growth experiments completed with *hcp* mutants by a PhD student at the University of Birmingham, Charlene Bradley. The *hcp* derivatives of the triple and quadruple mutants, JCB 5242 and JCB 5250 were grown anaerobically in the presence of 0.5 mM nitrite and a range of iron concentrations (0-500 μ M). Defective growth of both *hcp* strains in the presence of 0.5 mM nitrite was suppressed, in a dose-dependent manner, by the addition of an excess of iron (200 or 500 μ M) to the growth medium (Figure 7.3). This raised the possibility for a role of Hcp, which contains a unique iron-sulphur centre, in iron metabolism or iron insertion that is necessary during anaerobic growth. The loss of iron, and therefore a requirement for the repair or synthesis of iron sulphur clusters, would be increased during nitrosative stress. This is because nitrosylation often damages vulnerable iron sulphur clusters. Further work to characterise the role of Hcp should answer the question whether excess iron suppresses the growth defect of the *hcp ytfE* derivative of the quadruple mutant strain, JCB 5260, in the presence of nitrite.

Table 7.2. Rates of NO reduction of *hcp* mutants grown on minimal medium supplemented with nitrate.

Strain	Genotype	Functional proteins remaining	Average	Standard Error	% Parent
JCB 5241	<i>nirBDC nrfAB hcp hmp</i>	NorV ⁺	23.4	1.81	87
JCB 5242	<i>nirBDC nrfAB norV hcp</i>	Hmp ⁺	23.6	0.47	87
JCB 5228	<i>hcp ytfE</i>	NirBDC ⁺ NrfAB ⁺ NorV ⁺ Hmp ⁺	27.0	0.93	100

Figure 7.3



The effect of iron on growth of *hcp* mutants

Panel A: The *hcp* derivative of the triple mutant strain, JCB 5242, was grown anaerobically in the absence (●) or presence (Δ□○▲) of 0.5 mM sodium nitrite. Cultures were supplemented with 0 to 500 μM iron as indicated.

Panel B: The *hcp* derivative of the quadruple mutant strain, JCB 5250, was used. All details are as in Panel A.

The experiment in this figure was completed by Charlene Bradley. Other details were as in Figure 4.9

The authors of one study of Hcp function concluded that transcription of *hcp* was induced by H₂O₂ in an OxyR dependent mode, based upon reverse transcriptase PCR data (Almeida *et al.*, 2006). To make a firm conclusion about *hcp* transcription, it would be possible to transform bacteria with an *hcp::lacZ* reporter plasmid, and to monitor β -galactosidase activity in the presence and absence of OxyR (as described by Chismon *et al.*, 2010). Further to this, if OxyR could be purified, it would be possible to complete EMSA and DNase I footprinting assays to confirm an *in vitro* role of this regulator at the *hcp* promoter. In the work by Almeida *et al.* (2006), bacteria had been grown aerobically, or under fermentative conditions, not under conditions that promote anaerobic respiration. As work presented in this thesis has shown that Hcp is critical during anaerobic respiration, it would be prudent to complete experiments to investigate this oxidative stress role under similar conditions to those described in this work.

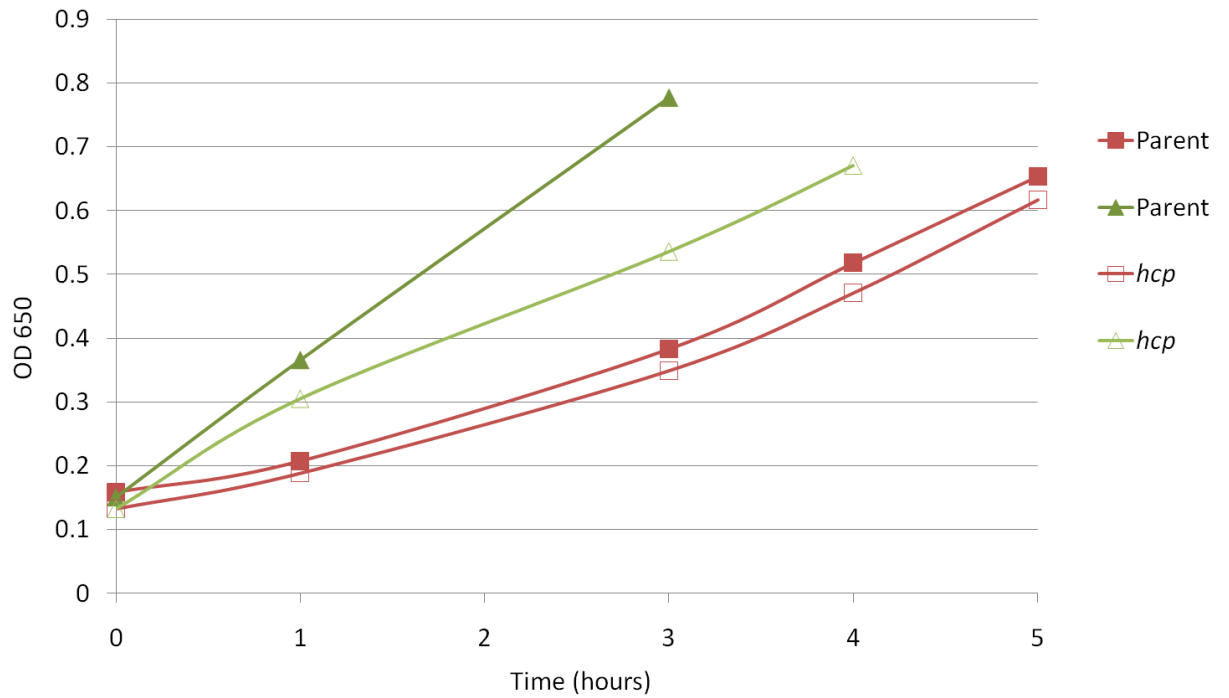
As well as exploring regulation of *hcp* transcription, the role of Hcp as a peroxidase was also assayed (Almeida *et al.*, 2006). These kinetic experiments revealed a K_m that was comparable to other reported peroxidases, but a very low V_{max} . The reasoning for this low V_{max} was attributed to the fact that Hcp was assayed in the absence of Hcr. The authors concluded that the true physiological substrate is not known, but a role as a peroxidase was proposed. In future experiments, it would be important to assay Hcp from facultative anaerobes in the presence of the proposed physiological electron donor, Hcr. The presence of Hcr is important in experiments to confirm or exclude the role as a peroxidase, and in assays to investigate an alternative function of Hcp.

During anaerobic respiration, using the non-fermentable carbon source glycerol, a clear growth phenotype for the *hcp* mutant is apparent. The growth defect is exacerbated by the presence of nitrite or nitrate in the medium. This growth phenotype

is not observed during aerobic growth. In the presence of glycerol as a carbon source, the *hcp* derivative of the quadruple mutant strain did not reach an optical density at 650 nm above 0.2. However, when using glucose as a carbon source, the growth of the *hcp* derivative was not defective (Figure 7.4). The *hcp* derivative grew similarly to the Hcp⁺ parent when fermentation was possible. It is possible that fewer reactive nitrogen species are generated during growth in the presence of glucose, such that fermentation leads to less accumulation of NO. It would be possible to test for decreased NO accumulation during fermentative growth rather than anaerobic respiration using the dye DAF-FM diacetate as described above. It might also be interesting to use the *phcp::lacZ* reporter for NO generation from nitrite that was developed in this work to analyse the differences in NO generation following fermentative growth compared to after anaerobic respiration.

A possible role for Hcp might be in fulfilling a demand for iron-sulphur clusters, which is increased during anaerobic growth, and particularly during nitrate and nitrite metabolism as NarGHI, NarZ, NapA, NapGH, NirB and NrfC all contain multiple iron sulphur clusters. Anaerobic growth using TMAO or fumarate as a terminal electron acceptor also requires iron-sulphur clusters for function of FumAB and DmsB. It has been shown that maximum nitrosation activity is observed when bacteria are grown in medium supplemented with glycerol and fumarate compared with in any other medium tested (Metheringham *et al.*, 1997). It is possible that there is more nitrosation activity in glycerol-supplemented medium, relative to the medium supplemented with glucose, giving rise to the growth difference in the presence of these alternative carbon sources.

Figure 7.4



Growth of the quadruple mutant and the *hcp* derivative in the presence of glucose, a fermentable carbon source.

The quadruple mutant parent strain, JCB 5210 (filled symbols), and the *hcp* derivative, JCB 5250 (open symbols), were grown anaerobically in medium supplemented with 0.4% glucose as a carbon source and either 2.5 mM nitrite (red) or 20 mM nitrate (green). In this experiment, bacteria were harvested at an optical density at 650 nm of 0.6-0.8, explaining the different times at which sampling was completed.

A linked phenotype of mutants defective in Hcp and YtfE homologues in *Salmonella enterica*.

A study in *Salmonella enterica* highlighted two acidified nitrite-responsive loci that have been termed *nip*, for nitrite inducible promoters (Kim *et al.*, 2003). These loci are orthologues of genes implicated in nitrosative stress in *E. coli*; *nipABC* are orthologues of *hcp*, *hcr* and *ytfE*, respectively. In light of the experiments completed in this work that suggested a possible link between the role of YtfE and Hcp, it is interesting that deletion of these genes gave rise to a linked phenotype in a study in this alternative organism. Acidified nitrite can be used to generate NO. The pH of the growth medium was varied, and *nipAB* induction was found to be maximal at pH 6.5, and *nipC* induction was highest at pH 5.5. Transcription of *nipAB* was shown to be Fnr-dependent, but a regulatory role for OxyR, NarL, SoxS, and a NorR homologue was ruled out (Kim *et al.*, 2003). Transcription of *nipC* was also regulated by oxygen tension, but not by Fnr or any of the aforementioned regulators. Transcription of *nipAB* and *nipC* was specifically upregulated in macrophages producing reactive nitrogen intermediates. There was no discernable difference in growth or survival between the *nipAB* or *nipC* mutants and the parent in various media, at differing pHs, or in the presence of various carbon sources; despite the fact that expression data suggested a role in the nitrosative stress response. Expression of *ogt* is induced in response to nitrite, and has a role in the repair of O⁶-methylguanine lesions of DNA. The *nipAB* and *nipC* mutants displayed no more sensitivity to mutagenesis by nitrite than the parent strain and both mutants survived similarly to the parent in macrophage like-cells (Kim *et al.*, 2003).

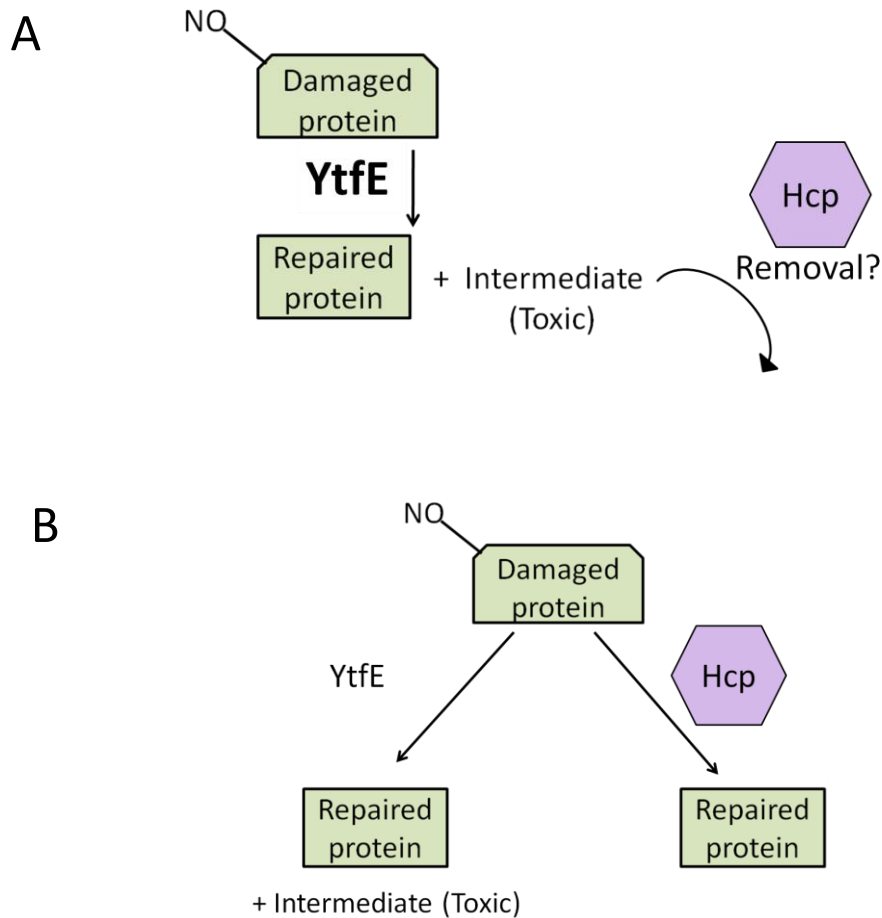
In comparison to the wild type, smaller doses of *nipAB* and *nipC* mutants were able to cause lethal infection in mice, by an unknown mechanism. It was suggested that NO might play a role in the development of adaptive responses during *S. typhimurium* infection of the mouse. Perhaps the *nipAB* and *nipC* mutants fail to metabolise NO effectively. This would lead to increased NO concentrations in mouse tissues and subsequent host damage. It is possible that bacteria escape detection due to altered RNS metabolism, and that due to this early avoidance, able are able to cause lethal infection in the mouse several days after infection.

The role of YtfE and NarG in NO generation

Deletion of both YtfE (Figure 6.9) and NarG (Figure 6.13) suppressed the growth-defective phenotype of an *hcp* derivative of the quadruple mutant strain. Experiments with a range of nitrate concentrations have shown that when nitrate has been depleted, NarG is able to convert nitrite to NO. It is clear that the deletion of NarG prevents the majority of this NO generation, and hence prevents the exacerbation of the anaerobic growth defect of the *hcp* derivative strain.

Initially, the fact that a *ytfE* mutation suppressed the growth defective phenotype of an *hcp* strain was consistent with the idea that YtfE might generate a toxic product during repair that Hcp removed (Figure 7.5, A). However, it was possible to exclude this model. If Hcp function was restored in the sequential pathway, there should be no effect on growth of a YtfE mutant. This was not the case (Figure 6.10). Restoration of Hcp function significantly improved growth, suggesting that Hcp must have an important role in the absence of YtfE. The role must extend beyond removing a toxic intermediate generated by YtfE. The data are consistent with the model presented in Figure 7.5, B. Hcp could function in a parallel repair role to YtfE. It is possible that

Figure 7.5.



Models for the involvement of YtfE and Hcp in linked repair pathways in *E. coli*.

A: This model was considered, in which proteins were damaged by nitrosation. The model proposes that YtfE is responsible for the repair of the nitrosated protein, thereby generating a toxic intermediate that required removal. Hcp was required for the removal and detoxification of the intermediate. Deletion of *ytfE* is predicted to result in the failure of the toxic intermediate to build up, and hence would suppress the *hcp* mutation. The toxic intermediate might be NO.

B: An alternative model proposes that YtfE and Hcp both catalyse repair of nitrosative damage to proteins. YtfE repairs proteins to generate a toxic intermediate, whereas Hcp repairs proteins without generating a toxic molecule. Deletion of *ytfE* is predicted to result in the failure of the toxic intermediate to accumulate. The *hcp* mutation would be suppressed.

YtfE metabolism generates a toxic intermediate, such as NO, but Hcp functions in a repair role to generate a non-toxic product such as NH_4^+ .

If YtfE generates NO during repair, it is possible that YtfE is responsible for the residual NO generation that is still apparent in a *narG nap* double mutant (Figure 3.12). It would be possible to test this hypothesis by making a triple mutant that is defective in *napAB*, *narG* and *ytfE*. The new strain could be transformed with the *phcp::lacZ* plasmid, and the β -galactosidase activity measured. If the activity was as low as the control, it would be clear that YtfE was the remaining protein that generates NO. However, if there was still activity in this triple mutant, it would be possible to test an alternative hypothesis. Perhaps it is a property of several molybdoproteins to be able to convert nitrite to NO and that NarG is the major contributor from the group of molybdoproteins. It would be possible either to assay a *moa* mutant, or to supplement the growth medium with 2 mM tungstic acid (sodium salt) that inhibits molybdenoproteins. If either manner of inhibiting molybdoproteins decreased the rate of NO generation to the levels observed for the unsupplemented control, it would be clear that a molybdoprotein is responsible for the residual NO generation.

Final conclusions

The roles of proteins involved in anaerobic growth in the presence of nitrate and nitrite are shown schematically in Figure 7.6. The nitrite reductases NirBDC and NrfA have a role in removing nitrite in *Escherichia coli* and therefore preventing the build up of this toxic intermediate. The role of NirBDC and NrfA in NO generation is significantly outweighed by the protective effect of the removal of nitrite (Vine *et al.*, 2011). NarG does play a key role in both nitrate reduction in the cytoplasm and also in generating NO from nitrite when the concentration of nitrate is low.

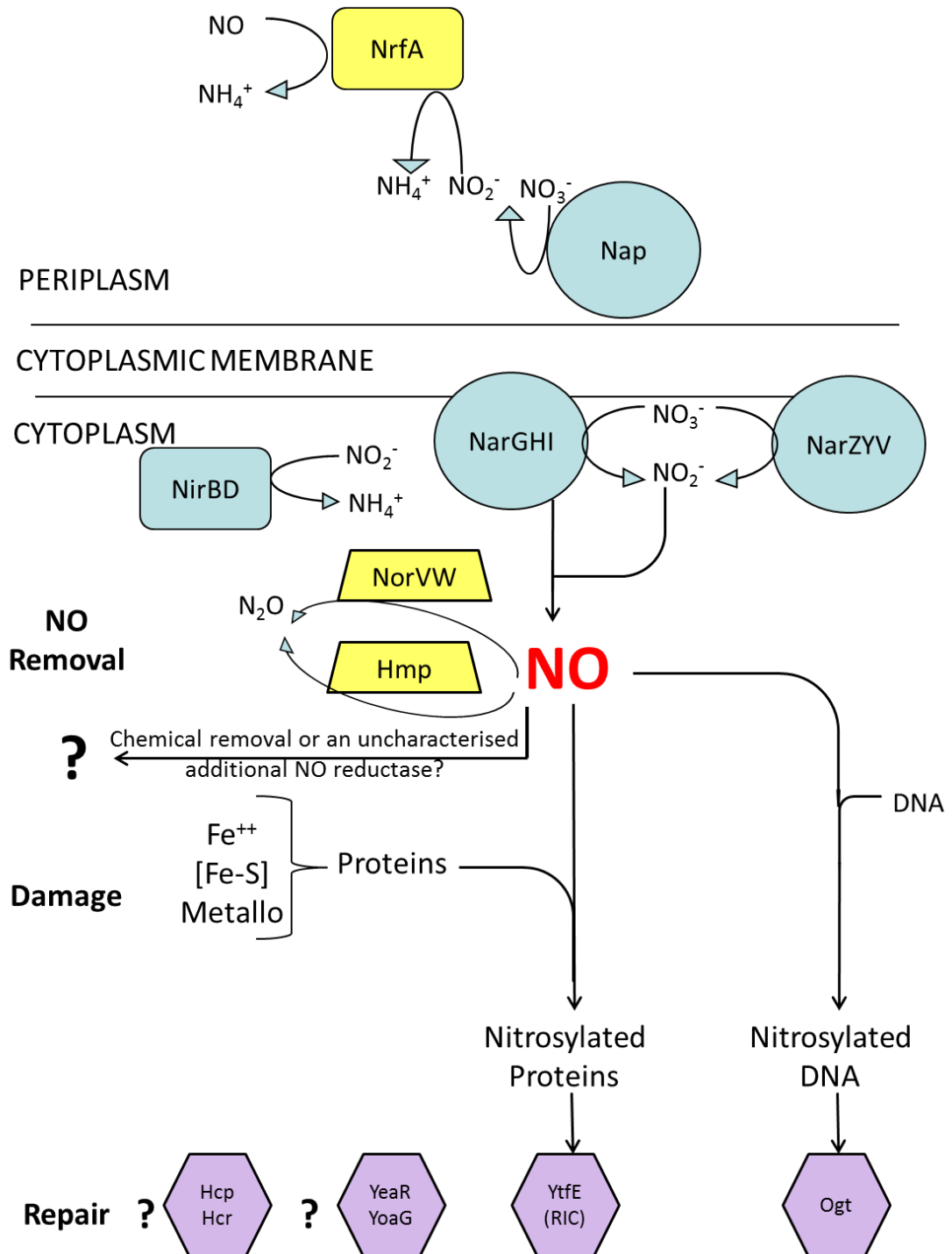
NrfA, NorV and Hmp have been shown by previous *in vitro* studies to reduce NO. However, when all three of these proteins, and NirB, have been deleted, bacteria

are still able to reduce NO at more than 50% of the parental rate, whether grown in the presence of nitrate or nitrite (Vine and Cole, 2011). Synthesis of the protein that is responsible for this residual NO reduction might be activated by NsrR. It is also possible that the apparent NO reduction might be due to nitrosative damage of proteins followed by reductive repair by a protein such as YtfE. This second proposal might explain why the rate of NO reduction of by *ytfE* mutant, and also by a *ytfE* derivative of the quadruple mutant strain, is significantly lower than that of the corresponding parent. YtfE has been characterised to repair iron centres, but the previously unexplained growth defect of the *ytfE* strain LMS 4209 has now been attributed to a secondary mutation and not the deletion of *ytfE* itself (Vine *et al.*, 2010). However, the role of the YtfE protein, and the corresponding roles of the staphylococcal and gonococcal orthologues, ScdA and DnrN, in repair of iron centres is not challenged.

The hybrid cluster protein has an important role during anaerobic metabolism. This role becomes particularly critical in the presence of nitrate or nitrite in the environment. It is still not clear what the precise role of Hcp might be, but further experiments must characterise the purified protein biochemically. The ability of *E. coli* to survive during anaerobic respiration, particularly using nitrate and nitrite reduction to conserve free energy, is critical to the survival of the bacterium both in the host and in the environment when nutrients are scarce. The ability of the bacterium to protect itself against the side products of metabolism, such as NO generated by NarG, are critical for survival.

This work has established the role of NarG, not NrfA or NirB, in NO generation during nitrate respiration. The unexplained anaerobic growth phenotype of the *ytfE* strain, LMS 4209, has been attributed to a secondary mutation. This study prompts further investigation into the precise role of Hcp in anaerobic metabolism, and into NO reduction activity that currently remains uncharacterised.

Figure 7.6.



Proteins in *E. coli* that are implicated in nitrate and nitrite metabolism, and protection against the consequences of the use of these terminal electron acceptors.

The location of proteins implicated in the nitrosative stress response in *E. coli* are depicted schematically. Those involved in nitrate and nitrite reduction, with the exception of NrfA, are coloured blue, and those implicated in NO reduction are coloured yellow. Proteins involved in damage repair are depicted in purple.

References

- Almeida, C.C., Romão, C. V., Lindley, P.F., Teixeira, M. and Saraiva, L.M. (2006) The role of the hybrid cluster protein in oxidative stress defence. *J. Biol. Chem.* **281**: 32445-32450
- Appleman, J.A., Chen, L-L. and Stewart, V. (2003) Probing conservation of HAMP linker structure and signal transduction mechanism through analysis of hybrid sensor kinases. *J. Bacteriol.* **185**: 4872-4882
- Aragão, D., Mitchell, E.P., Frazão, C.F., Carrondo, M.A. and Lindley, P.F. (2008) Structural and functional relationships in the hybrid cluster protein family: structure of the anaerobically purified hybrid cluster protein from *Desulfovibrio vulgaris* at 1.35 Å resolution. *Acta. Cryst.* **D64**: 665-674
- Arends, A.F. Hadden, J., Card, G. *et al.*, (1998) The “prismane” protein resolved: X-ray structure at 1.7 Å and multiple spectroscopy of two novel 4Fe clusters. *J. Biol. Inorg. Chem.* **3**: 81-95
- Barrios, H., Valderrama, B. and Morett, E. (1999) Complication and analysis of σ^{54} – dependent promoter sequences. *Nucleic Acids Res.* **27**: 4305-4313
- van den Berg, W.A.M., Hagen, W.R. and van Dongen, W.M.A.M. (2000) The hybrid-cluster protein (‘prismane protein’) from *Escherichia coli*. Characterisation of the hybrid-cluster protein, redox properties of the [2Fe-2S] and [4Fe-2S-2O] clusters and identification of an associated NADH oxidoreductase containing FAD and [2Fe-2S]. *Eur. J. Biochem.* **267**: 666-676
- Beaumont, H.J.E., Lens, S.I., Reijnders, W.N.M., Westerhoff, H.V. and van Spanning, R.J.M. (2004) Expression of nitrite reductase in *Nitrosomonas europaea* involves NsrR, a novel nitrite-sensitive transcription repressor. *Mol. Microbiol.* **54**: 148-158
- Berks, B.C. (1996) A common export pathway for proteins binding complex redox cofactors? *Mol. Microbiol.* **22**: 393-404
- Berks, B.C., Sargent, F. and Palmer, T. (2000) The Tat export pathway. *Mol. Microbiol.* **35**: 260-274
- Blasco, F., Iobbi, C., Ratouchniak, J., Bonnefoy, V. and Chippeaux, M. (1990) Nitrate reductases of *Escherichia coli*: sequence of the second nitrate reductase and comparison with that encoded by the *narGHJI* operon. *Mol. Gen. Genet.* **222**: 104-111
- Bodenmiller, D.M. and Spiro, S. (2006) The *yjeB* (*nsrR*) Gene of *Escherichia coli* encodes a nitric oxide-sensitive transcriptional regulator. *J. Bacteriol.* **188**: 874-881

- Brondijk, T.H., Nilavongse, A., Filenko, N., Richardson, D.J. and Cole, J.A. (2004) NarGH components of the periplasmic nitrate reductase of *Escherichia coli* K-12: location, topology and physiological roles in quinol oxidation and redox balancing. *Biochem. J.* **379**: 47-55
- Browning, D.F., Grainger, D.C., Beatty, C.M., Wolfe, A.J., Cole, J.A. and Busby, S.J. (2005) Integration of three signals at the *Escherichia coli nrf* promoter: a role for Fis protein in catabolite repression. *Mol. Microbiol.* **57**: 496-510
- Browning, D.F., Lee, D.J., Spiro, S. and Busby, S.J.W. (2010) Down-regulation of the *Escherichia coli* K-12 *nrf* promoter by binding of the NsrR nitric oxide-sensing transcription repressor to an upstream site. **192**: 3824-3828
- Bryk, R., Griffin, P. and Nathan, C. (2000) Peroxynitrite reductase activity of bacterial peroxiredoxins. *Nature* **407**: 211-215
- Cabello, P., Pino, C., Olmo-Miro, M.F., Castillo, F., Roldan, M.D. and Moreno-Vivian, C.M. (2004) Hydroxylamine assimilation by *Rhodobacter capsulatus* E1F1. Requirement of the *hcp* gene (hybrid cluster protein) located in the nitrate assimilation gene region for hydroxylamine reduction. *J. Biol. Chem.* **279**: 45485-45494
- Calmels, S., Ohshima, H. and Bartsch, H. (1988) Nitrosamine formation by denitrifying and non-denitrifying bacteria: implication of nitrite reductase and nitrate reductase in nitrosation catalysis. *J. Gen. Microbiol.* **134**: 221-226
- Cardinale, J.A. and Clark, V.L. (2005) Determinants of nitric oxide steady-state levels during anaerobic respiration by *Neisseria gonorrhoeae*. *Mol. Microbiol.* **58**: 177-188.
- Chaudhry, G.R. and MacGregor, C.H. (1983) Cytochrome *b* from *Escherichia coli* nitrate reductase: its properties and association with enzyme complex. *J. Biol. Chem.* **258**: 5819-5827
- Chiang, R.C., Cavicchioli, R. and Gunsalus, R.P. (1992) Identification and characterisation of *narQ*, a second nitrate sensor for nitrate-dependent gene regulation in *Escherichia coli*. *Mol. Microbiol.* **6**: 1913-1923
- Chismon, D.L., Browning, D.F., Farrant, G.K. and Busby, S.J. (2010) Unusual organisation, complexity and redundancy at the *Escherichia coli hcp-hcr* operon promoter. *Biochem. J.* **430**: 61-68
- Clarke, T.A., Cole, J.A., Richardson, D.J. and Hemmings, A.M. (2007) The crystal structure of the pentahaem *c*-type cytochrome NrfB and characterisation of its solution-state interaction with the pentahaem nitrite reductase NrfA. *Biochem. J.* **406**: 19-30
- Clegg, S.J., Jia, W. and Cole, J.A. (2006) Role of the *Escherichia coli* nitrate transport protein, NarU, in survival during severe nutrient starvation and slow growth. *Microbiol.* **152**: 2091-2100

Clegg, S., Yu, F., Griffiths, L. and Cole, J.A. (2002) The roles of the polytopic membrane proteins NarK, NarU and NirC in *Escherichia coli* K-12: two nitrate and three nitrite transporters. *Mol. Microbiol.* **44**: 145-155

Cole, J. (1996) Nitrate reduction to ammonia by enteric bacteria: redundancy, or a strategy for survival during oxygen starvation? *FEMS Microbiol. Lett.* **136**: 1-11

Constantinidou, C., Hobman, J.L., Griffiths, L., Patel, M.D., Penn, C.W., Cole, J.A. and Overton, T.W. (2006). A reassessment of the FNR regulon and transcriptomic analysis of the effects of nitrate, nitrite, NarXL, and NarQP as *Escherichia coli* K12 adapts from aerobic to anaerobic growth. *J. Biol. Chem.* **281**: 4802-4815

Cooper, S.J., Garner, C.D., Hagen, W.R., Lindley, P.F. and Bailey, S. (2000) Hybrid-cluster protein (HCP) from *Desulfovibrio vulgaris* (Hildenborough) at 1.6 Å resolution. *Biochemistry.* **39**: 15044-15054

Corker, H. and Poole, R.K. (2003) Nitric oxide formation by *Escherichia coli*. *J. Biol. Chem.* **278**: 31584-31592

Costa, C., Macedo, A., Moura, I., Moura, J.J.G., Le Gall, J., Berlier, Y., Liu, M.-Y. and Payne, W.J. (1990) Regulation of the hexaheme nitrite/nitric oxide reductase of *Desulfovibrio desulphuricans*, *Wolinella succinogenes* and *Escherichia coli*. *FEBS Lett.* **276**: 67-70

Cotter, P.A., Chepuri, V., Gennis, R.B. and Gunsalus, R.P. (1990) Cytochrome *o* (*cyoABCDE*) and *d* (*cydAB*) oxidase gene expression in *Escherichia coli* is regulated by oxygen, pH, and the *fnr* gene product. *J. Bacteriol.* **172**: 6333-6338

Cotter, P.A. and Gunsalus, R.P. (1989) Oxygen, nitrate, and molybdenum regulation of *dmsABC* gene regulation in *Escherichia coli*. *J. Bacteriol.* **171**: 3817-3823

Cotter, P.A., Melville, S.B., Albrecht, J.A. and Gunsalus, R.P. (1997) Aerobic regulation of cytochrome *d* oxidase (*cydAB*) operon expression in *Escherichia coli*: roles of Fnr and ArcA in repression and activation. *Mol. Microbiol.* **25**: 605-615

Crack, J.C., Gaskell, A.A., Cheesman, M.R., Le Brun, N.E. and Thomson, A.J. (2008a) Influence of the environment on the [4Fe-4S]²⁺ to [2Fe-2S]²⁺ cluster switch in the transcriptional regulator FNR. *J. Am. Chem. Soc.* **130**: 1749-1758

Crack, J.C., Le Brun, N.E., Thomson, A.J., Green, J. and Jervis, A.J. (2008b) Reactions of nitric oxide and oxygen with the regulator of fumarate and nitrate reduction, a global transcriptional regulator, during anaerobic growth of *Escherichia coli*. *Methods Enzymol.* **437**: 191-209

Cruz-Ramos, H., Crack, J., Wu, G., Hughes, M.N., Scott, C., Thomson, A.J., Green, J. and Poole, R.K. (2002) NO sensing by FNR: regulation of the *Escherichia coli* NO-detoxifying flavohaemoglobin, Hmp. *EMBO J.* **21**: 3235-3244

- Darwin, A.J., Hussain, H., Griffiths, L., Grove, J., Sambongi, T., Busby, S. and Cole, J. (1993a) Regulation and sequence of the structural gene for cytochrome *c*₅₅₂ from *Escherichia coli*: not a hexaheme but a 50 kDa tetrahaem nitrite reductase. *Mol. Micro.* **9**: 1255-1265
- Darwin, A.J., Tormay, P., Page, L., Griffiths, L. and Cole, J. (1993b) Identification of the formate dehydrogenases and genetic determinants of formate-dependent nitrite reduction by *Escherichia coli* K-12. *J. Gen. Microbiol.* **139**: 1829-1840
- Darwin, A.J. and Stewart, V. (1995) Expression of the *narX*, *narL*, *narP* and *narQ* genes of *Escherichia coli* K-12: regulation of the regulators. *J. Bacteriol.* **177**: 3865-3869
- Darwin, A.J., Tyson, K.L., Busby, S.J.W. and Stewart, V. (1997) Differential regulation by the homologous response regulators NarL and NarP of *Escherichia coli* K-12 depends on DNA binding site arrangement. *Mol. Micro.* **25**: 583-595
- Datsenko, K.A. and Wanner, B.L. (2000) One step inactivation of chromosomal genes in *Escherichia coli* K-12 using PCR products. *Proc. Natl. Acad. Sci. USA* **97**: 6640-6645
- D'Autréaux, B., Touati, D., Bersch, B., Latour, J.M. and Michaud-Soret, I. (2002) Direct inhibition by nitric oxide of the transcriptional ferric uptake regulation protein via nitrosylation of the iron. *Proc. Natl. Acad. Sci. USA* **99**: 16619-16624
- D'Autréaux, B., Tucker, N.P., Dixon, R. and Spiro, S. (2005) A non-haem iron centre in the transcription factor NorR senses nitric oxide. *Nature*. **437**: 769-772
- Ding, H. and Dimple, B. (2000) Direct nitric oxide signal transduction via nitrosylation of iron-sulphur centres in the SoxR transcription activator. *Proc. Natl. Acad. Sci. USA* **97**: 5146-5150
- Drew, D., Sjostrand, D., Nilsson, J., Urbig, T., Chin, C.N., de Gier, J.W. and von Heijne, G. (2002) Rapid topology mapping of *Escherichia coli* inner-membrane proteins by prediction and PhoA/GFP fusion analysis. *Proc. Natl. Acad. Sci. USA* **99**: 2690-2695
- Egan, S.M. and Stewart, V. (1990) Nitrate regulation of anaerobic respiratory gene expression in *narX* deletion mutants of *Escherichia coli* K-12. *J. Bacteriol.* **172**: 5020-5029
- Enoch, H.G. and Lester, R.L. (1975) The purification and properties of formate dehydrogenase and nitrate reductase from *Escherichia coli*. *J. Biol. Chem.* **250**: 6693-6705
- Fang, F. C. (2004) Antimicrobial reactive oxygen and nitrogen species: concepts and controversies. *Nat. Rev. Microbiol.* **2**: 820-832

Fileenko, N.A., Browning, D.F. and Cole, J.A. (2005) Transcriptional regulation of a hybrid cluster (prismane) protein. *Biochem. Soc. Trans.* **33**: 195-197

Fileenko, N., Spiro, S., Browning, D.F., Squire, D., Overton, T.W., Cole, J. and Constantinidou, C. (2007) The NsrR regulon of *Escherichia coli* K-12 includes genes encoding the hybrid cluster protein and the periplasmic, respiratory nitrite reductase. *J. Bacteriol.* **189**: 4410-4417

Flatley, J., Barrett, J., Pullan, S.T., Hughes, M.N., Green, J. and Poole, R.K. (2005) Transcriptional responses of *Escherichia coli* to S-Nitrosoglutathione under defined chemostat conditions reveal major changes in methionine biosynthesis. *J. Biol. Chem.* **280**: 10065-10072

Fleischhacker, A.S. and Kiley, P.J. (2011) Iron-containing transcription factors and their roles as sensors. *Curr. Opin. Chem. Biol.* **15**: 335-341

Forget, P. (1974) The bacterial nitrate reductases. Solubilization, purification and properties of the enzyme A of *Escherichia coli* K12. *Eur. J. Biochem.* **42**: 325-332

Forsythe, S.J. and Cole, J.A. (1987) Nitrite accumulation during anaerobic nitrate reduction by binary suspensions of bacteria isolated from the achlorhydric stomach. *J. Gen. Microbiol.* **133**: 1845-1849

Forsythe, S.J., Dolby, J.M., Webster, A.D.B and Cole, J.A. (1988) Nitrate- and nitrite-reducing bacteria in the achlorhydric stomach. *J. Med. Microbiol.* **25**: 253-259

Gardner, A.M. and Gardner, P.R. (2002) Flavohemoglobin detoxifies nitric oxide in aerobic, but not anaerobic, *Escherichia coli*. *J. Biol. Chem.* **277**: 8166-8171

Genest, O., Seduk, F., Ilbert, M., Mejean, V. and Iobbi-Nivol, C. (2006) Signal peptide protection by specific chaperone. *Biochem. Biophys. Res. Commun.* **339**: 991-995

Giel, J.L., Rodiovov, D., Liu, M., Blattner, F.R. and Kiley, P.J. (2006) IscR-dependent gene expression links iron-sulphur cluster assembly to the control of O₂-regulated genes in *Escherichia coli*. *Mol. Microbiol.* **60**: 1058-1075

Gilberthorpe, N.J. and Poole, R.K. (2008) Nitric oxide homeostasis in *Salmonella typhimurium*: roles of respiratory nitrate reductase and flavohemoglobin. *J. Biol. Chem.* **283**: 11146-11154

Gohlke, U., Pullan, L., McDevitt, C.A., Porcelli, I., de Leeuw, E., Palmer, T., Saibil, H.R. and Berks, B.C. (2005) The TatA component of the twin-arginine protein transport system forms channel complexes of variable diameter. *Proc. Natl. Acad. Sci. USA* **102**: 10482-10486

Gomes, C.M., Giuffrè, A., Forte, E., Vicente, J.B., Saraiva, L.M., Brunori, M. and Teixeira, M. (2002) A novel type of nitric-oxide reductase. *J. Biol. Chem.* **277**: 25273-25276

Gon, S., Patte, J.C., Mejean, V. and Iobbi-Nivol, C. (2000) The *torYZ* (*yecK bisZ*) operon encodes a third respiratory trimethylamine *N*-oxide reductase in *Escherichia coli*. *J. Bacteriol.* **182**: 5779-5786

Grove, J., Tanopongpipat, S., Thomas, G., Griffiths, L., Crooke, H. and Cole, J. (1996) *Escherichia coli* K-12 genes essential for the synthesis of *c*-type cytochromes and a third nitrate reductase located in the periplasm. *Mol. Microbiol.* **19**: 467-481

Harrington, J.C., Wong, S.M.S., Rosadini, C.V., Garifulin, O., Boyartchuk, V. and Akerley, B.J. (2009) Resistance of *Haemophilus influenzae* to reactive nitrogen donors and gamma interferon-stimulated macrophages requires the formate-dependent nitrite reductase regulator-activated *ytfE* gene. *Infect. Immun.* **77**: 1945-1958

Hausladen, A., Gow, A. J. and Stamler, J.S. (1998) Nitrosative stress: metabolic pathway involving the flavohemoglobin. *Proc. Natl. Acad. Sci. USA.* **95**: 14100-14105

Hausladen, A., Privalle, C.T., Keng, T., DeAngelo, J. and Stamler, J.S. (1996) Nitrosative stress: activation of the transcription factor OxyR. *Cell.* **86**: 719-729

Hill, B.G., Dranka, B.P., Bailey, S.M., Lancaster, J.R. and Darley-Usmar, V.M. (2010) What part of NO don't you understand? Some questions to the cardinal questions in nitric oxide biology. *J. Biol. Chem.* **285**: 19699-19704

Hobman, J.L., Patel, M.D., Hidalgo-Arroyo, G.A., Cariss, S.J.L., Avison, M.B., Penn, C.W. and Constantinidou, C. (2007). Comparative genomic hybridisation detects secondary chromosomal deletions in *Escherichia coli* K-12 MG 1655 mutants and highlights instability in the *flhDC* region. *J. Bact.* **189**: 8786-8792

Hughes, M.N. (1999) Relationships between nitric oxide, nitroxyl ion, nitrosonium cation and peroxynitrite. *Biochim. Biophys. Acta.* **1411**: 263-272

Hussain, H., Grove, J., Griffiths, L., Busby, S. and Cole, J. (1994) A seven gene operon essential for formate-dependent nitrite reduction to ammonia by enteric bacteria. *Mol. Microbiol.* **12**: 153-163

Hutchings, M.I., Mandhana, N. and Spiro, S. (2002) The NorR protein of *Escherichia coli* activates expression of the flavorubredoxin gene *norV* in response to reactive nitrogen species. *J. Bacteriol.* **184**: 4640-4643

Hutchings, M.I., Shearer, N., Wastell, S., van Spanning, R.J. and Spiro, S. (2000) Heterologous NNR-mediated nitric oxide signaling in *Escherichia coli*. *J. Bacteriol.* **182**: 6434-6439

Ilbert, M., Mejean, V., and Iobbi-Nivol, C. (2004) Functional and structural analysis of members of the TorD family, a large chaperone family dedicated to molybdoproteins. *Microbiol.* **150**: 935-943

- Iobbi, C., Santini, C.L., Bonnefoy, V. and Giordano, G. (1987) Biochemical and immunological evidence for a second nitrate reductase in *Escherichia coli* K12. Eur. J. Biochem. **168**: 451-459
- Iobbi-Nivol, C., Santini, C.L., Blasco, F. And Giordano, G. (1990) Purification and further characterization of the second nitrate reductase of *Escherichia coli* K12. Eur. J. Biochem. **188**: 679-687
- Jackson, R.H., Cole, J.A. and Cornish-Bowden, A. (1981a) The steady-state kinetics of the NADH-dependent nitrite reductase from *Escherichia coli* K 12. Nitrite and hydroxylamine reduction. Biochem. J. **199**: 171-178
- Jackson, R.H., Cornish-Bowden, A. And Cole, J.A. (1981b) Prosthetic groups of the NADH-dependent nitrite reductase from *Escherichia coli* K 12. Biochem. J. **199**: 861-867
- Jayaraman, P.S., Cole, J. and Busby, S. (1989) Mutational analysis of the nucleotide sequence at the FNR-dependent *nirB* promoter in *Escherichia coli*. Nucleic. Acids. Res. **17**: 135-145
- Jayaraman, P.S., Gaston, K.L., Cole, J.A. and Busby, S.J.W. (1988) The *nirB* promoter of *Escherichia coli*: location of nucleotide sequences essential for regulation by oxygen, the FNR protein and nitrite. Mol. Microbiol. **2**: 527-530
- Ji, X.B. and Hollocher, T.C. (1988) Reduction of nitrite to nitric oxide by enteric bacteria. Biochem. Biophys. Res. Commun. **157**: 106-108
- Jia, W., Tovell, N., Clegg, S., Trimmer, M. and Cole, J. (2009) A single channel for nitrate uptake, nitrite export and nitrite uptake by *Escherichia coli* NarU and a role for NirC in nitrite export and uptake. Biochem. J. **417**: 297-304.
- Justino, M.C., Vicente J.B., Texiera, M. and Saraiva, L.M. (2005) New genes implicated in the protection of anaerobically grown *Escherichia coli* against nitric oxide. J Biol. Chem. **280**: 2636-2643
- Justino, M.C., Almeida, C.C., Goncalves, V.L., Teixeira, M. and Saraiva, L.M. (2006) *Escherichia coli* YtfE is a di-iron protein with an important function in assembly of iron-sulphur clusters. FEMS Microbiol. Lett. **257**: 278-84
- Justino, M.C., Almeida, C.C., Teixeira, M. and Saraiva, L.M. (2007) *Escherichia coli* di-Iron YtfE protein is necessary for the repair of stress-damaged iron-sulphur clusters. J. Biol. Chem. **282**: 10352-10359
- Justino, M.C., Baptista, J.M. and Saraiva, L.M. (2009) Di-iron proteins of the Ric family are involved in iron-sulphur cluster repair. Biometals. **22**: 99-108

- Kern, M., Volz, J. and Simon, J. (2011) The oxidative and nitrosative stress defence network of *Wolinella succinogenes*: cytochrome *c* nitrite reductase mediates the stress response to nitrite, nitric oxide, hydroxylamine and hydrogen peroxide. *Environ. Microbiol.* In press.
- Khoroshilova, N., Popescu, C., Munck, E., Beinert, H. and Kiley, P.J. (1997) Iron-sulfur cluster disassembly in the FNR protein of *Escherichia coli* by O₂: [4Fe-4S] to [2Fe-2S] conversion with the loss of biological activity. *Proc. Natl. Acad. Sci. USA.* **94**: 6087-6092
- Kim, C.C., Monack, D. and Falkow, S. (2003) Modulation of virulence by two acidified-nitrite-responsive loci of *Salmonella enterica* serovar Typhimurium. *Infect. Immun.* **71**: 3196-3205
- Kim, S.O., Orii, Y., Lloyd, D., Hughes, M.N. and Poole, R.K. (1999) Anoxic function for the *Escherichia coli* flavohaemoglobin (Hmp): reversible binding of nitric oxide and reduction to nitrous oxide. *FEBS. Lett.* **445**: 389-394
- Kisker, C., Schindelin, H. and Rees, D.C. (1997) Molybdenum-cofactor-containing enzymes: structure and mechanism. *Annu. Rev. Biochem.* **66**: 233-267
- Kitagawa, M., Ara, T., Arifuzzaman, M., Ioka-Nakamichi, T., Inamoto, E., Toyonaga, H. and Mori, H. (2005) Complete set of ORF clones of *Escherichia coli* ASKA library (A Complete Set of E. coli K-12 ORF Archive): Unique Resources for Biological Research. *DNA Res* **12**: 291-299
- Kojima, H., Urano, Y., Kikuchi, K., Higuchi, T., Hirata, Y. and Nagano, T. (1999) Fluorescent indicators for imaging nitric oxide production. *Angew. Chem. Int. Ed. Engl.* **38**: 3902-3212
- Lazazzera, B.A., Beinert, H., Khoroshilova, N., Kennedy, M.C. and Kiley, P.J. (1996) DNA binding and dimerisation of the Fe-S containing FNR protein from *Escherichia coli* are regulated by oxygen. *J. Biol. Chem.* **271**: 2762-2768
- Lee, P.A., Orriss, G.L., Buchanan, G., Greene, N.P., Bond, P.J., Punginelli, C., Jack, R.L., Samsom, M.S., Berks, B.C. and Palmer, T. (2006) Cysteine-scanning mutagenesis and disulfide mapping studies of the conserved domain of the twin-arginine translocase TatB component. *J. Biol. Chem.* **281**: 34072-34085
- Lin, H-Y, Bledsoe, P.J. and Stewart, V. (2007) Activation of *yeaR-yoaG* operon transcription by the nitrate-responsive regulator NarL is independent of oxygen-responsive regulator Fnr in *Escherichia coli* K-12. *J. Bacteriol.* **189**: 7539-7548
- Lodge, J., Fear, J., Busby, S., Gunasekaran, P. and Kamini, N.R. (1992) Broad host range plasmids carrying the *Escherichia coli* lactose and galactose operons. *FEMS Microbiol. Lett.* **74**: 271-276

- Love, C.A., Lilley, P.E. and Dixon, N.E. (1996) Stable high-copy-number bacteriophage λ promoter vectors for overproduction of proteins in *Escherichia coli*. *Gene*. **176**: 49-53
- Lundberg, J.O., Weitzberg, E., Cole, J.A. and Benjamin, N. (2004) Nitrate, bacteria and human health. *Nat. Rev. Microbiol.* **2**: 593-602
- Macdonald, H. and Cole, J. (1985) Molecular cloning and functional analysis of the *cysG* and *nirB* genes of *Escherichia coli* K12, two closely-linked genes required for NADH-dependent nitrite reductase activity. *Mol. Gen. Genet.* **200**: 328-334
- Macedo, S., Aragão, D., Mitchell, E.P. and Lindley, P. Structure of the hybrid cluster protein (HCP) from *Desulfovibrio desulphuricans* ATCC 27774 containing molecules in the oxidised and reduced states. *Acta. Cryst.* **D59**: 2065-2071
- Mason, M.G., Shepherd, M., Nicholls, P., Dobbin, P.S., Dodsworth, K.S., Poole, R.K. and Cooper, C.E. (2009) Cytochrome *bd* confers nitric oxide resistance to *Escherichia coli*. *Nat. Chem. Biol.* **5**: 94-96
- McCrindle, S., Kappler, U. and McEwan, A.G. (2005) Microbial dimethylsulfoxide and trimethylamine-N-oxide respiration. *Adv. Microb. Physiol.* **50**: 147-198
- McLoed, S.M. and Johnson, R.C. (2001) Control of transcription by nucleoid proteins. *Curr. Opin. Microbiol.* **4**: 152-159
- McNicholas, P.M., Chiang, and Gunsalus, R.P. (1998) Anaerobic regulation of the *Escherichia coli dmsABC* operon requires the molybdate-responsive regulator ModE. *Mol. Microbiol.* **27**: 197-208
- McNicholas, P.M. and Gunsalus, R.P. (2002) The molybdate-responsive *Escherichia coli* ModE transcriptional regulator coordinates periplasmic nitrate reductase (*napFDAGHBC*) operon expression with nitrate and molybdate availability. *J. Bacteriol.* **12**: 3253-9
- Méjean, V., Iobbi-Nivol, C., Lepelletier, M., Giordano, G., Chippaux, M. and Pascal, M.-C. (1994) TMAO anaerobic respiration in *Escherichia coli*: involvement for the *tor* operon. *Mol. Microbiol.* **11**: 1169-1179
- Metheringham, R. and Cole, J.A. (1997) A reassessment of the genetic determinants, the effect of growth conditions and the availability of an electron donor on the nitrosating activity of *Escherichia coli* K-12. *Microbiology.* **143**: 2647-2656
- Mills, P.C., Rowley, G., Spiro, S., Hinton, J.C.D. and Richardson, D.J. (2008) A combination of cytochrome *c* nitrite reductase (NrfA) and flavorubredoxin (NorV) protects *Salmonella enterica* serovar Typhimurium against killing by NO in anoxic environments. *Microbiol.* **154**: 1218-1228

- Mills, C.E., Sedelnikova, S., Soballe, B., Hughes, M.N. and Poole, R.K. (2001) *Escherichia coli* flavohaemoglobin (Hmp) with equistoichiometric FAD and haem contents has a low affinity for dioxygen in the absence or presence of nitric oxide. **353**: 207-213
- Moreland, J.L., Gramada, A., Buzko, O.V., Zhang, Q. and Bourne, P.E. (2005) The molecular biology toolkit (MBT): a modular platform for developing molecular visualization applications. *BMC Bioinformatics*, **6**: 21
- Mukhopadhyay, P., Zheng, M., Bedzyk, L.M., LaRossa, R.A. and Storz, G. (2004) Prominent roles of the NorR and Fur regulators in the *Escherichia coli* transcriptional response to reactive nitrogen species. *Proc. Natl. Acad. Sci. USA* **101**: 745-50
- Noriega, C.E., Lin, H.Y., Chen, L.L., Williams, S.B. and Stewart, V. (2010) Asymmetric cross-regulation between the nitrate-responsive NarX-NarL and NarQ-NarP two-component regulatory systems from *Escherichia coli* K-12. *Mol. Microbiol.* **75**: 394-412
- Overton, T.W., Justino, M.C., Li, Y., Baptista, J.M., Melo, A.M.P., Cole, J.A. and Saraiva, L.M. (2008) Widespread distribution in pathogenic bacteria of di-iron proteins that repair oxidative and nitrosative damage to iron-sulphur centers. *J. Bacteriol.* **190**: 2004-2013
- Overton, T. W., Whitehead, R., Li, Y., Snyder, L.A., Saunders, N.J., Smith, H. and Cole, J.A. (2006) Coordinated regulation of the *Neisseria gonorrhoeae*-truncated denitrification pathway by the nitric oxide-sensitive repressor, NsrR, and nitrite-insensitive NarQ-NarP. *J. Biol. Chem.* **281**: 33115-33126.
- Page, L., Griffiths, L. and Cole, J.A. (1990) Different physiological roles of two independent pathways for nitrite reduction to ammonia by enteric bacteria. *Arch. Microbiol.* **154**: 349-354
- Palmer, T. and Berks, B.C. (2003) Moving folded proteins across the bacterial cell membrane. *Microbiology.* **149**: 547-556
- Palmer, R.M.J., Ferrige, A.G. and Moncada, S. (1987) Nitric oxide release accounts for the biological activity of endothelium-derived relaxing factor. *Nature* **327**: 524-526
- Palmer, T., Santini, C-L., Iobbi-Nivol, C., Eaves, D.J., Boxer, D.H. and Giordano, G. (1996) Involvement of the *narJ* and *mob* gene products in distinct steps in the biosynthesis of the molybdoenzyme nitrate reductase in *Escherichia coli*. *Mol. Microbiol.* **20**: 875-884
- Pereira, A.S., Tavares, P., Krebs, C., Huynh, B.H., Rusnak, F., Moura, I. And Moura, J.J.G. (1999) Biochemical and spectroscopic characterisation of overexpressed fuscodoxin from *Escherichia coli*. *Biochem. Biophys. Res. Commun.* **260**: 209-215

- Poock, S.R., Leach, E.R., Moir, J.W.B., Cole, J.A. and Richardson, D.J. (2002) Respiratory denitrification of nitric oxide by the cytochrome *c* nitrite reductase of *Escherichia coli*. *J. Biol. Chem.* **277**: 23664-23669.
- Poole, R.K. (2005) Nitric oxide and nitrosative stress tolerance in bacteria. *Biochem. Soc. Trans.* **33**: 176-180
- Poole, R.K. and Hughes, M.N. (2000) New functions for the ancient globin family: bacterial responses to nitric oxide and nitrosative stress. *Mol. Microbiol.* **36**: 775-783
- Pope, N. R. & Cole, J. A. (1984). Pyruvate and ethanol as electron donors for nitrite reduction by *Escherichia coli* K12. *J. Gen. Microbiol.* **130**: 1279–1284
- Potter, L.C., Millington, P., Griffiths, L., Thomas, G.H. and Cole, J.A. (1999) Competition between *Escherichia coli* strains expressing either a periplasmic or a membrane-bound nitrate reductase: does Nap confer a selective advantage during nitrate-limited growth? *Biochem. J.* **344**: 77-84
- Pullan, S.T., Gidley, M.D., Jones, R.A., Barrett, J., Stevanin, T.M., Read, R.C., Green, J., and Poole, R.K. (2007) Nitric Oxide in chemostat-cultured *Escherichia coli* is sensed by Fnr and other global regulators: unaltered methionine biosynthesis indicates lack of S-Nitrosation. *J. Bacteriol.* **63**: 1845-55
- Rabin, R.S. and Stewart, V. (1992) Either of two functionally redundant sensor proteins, NarX and NarQ, is sufficient for nitrate regulation in *Escherichia coli* K-12. *Proc. Natl. Acad. Sci. USA.* **89**: 8419-8423
- Rabin, R.S. and Stewart, V. (1993) Dual response regulators (Nar L and Nar P) interact with dual sensors (Nar X and Nar Q) to control nitrate- and nitrite-regulated gene expression in *Escherichia coli* K-12. *J. Bacteriol.* **175**: 3259-3268
- Raines K.W., Kang, T.J., Hibbs, Cao G.-L., Weaver, J., Tsai, P., Baillie, L., Cross, A.S., and Rosen, G.M. (2006) Importance of nitric oxide synthase in the control of infection by *Bacillus anthracis*. *Infect. Immun.* **74**: 2268-2276
- Ralt, D., Wishnok, J.S., Fitts, R. and Tannenbaum, S.R. (1988) Bacterial catalysis of nitrosation: involvement of the *nar* operon of *Escherichia coli*. *J. Bacteriol.* **170**: 359-364
- Rankin, L.D., Bodenmiller, D.M., Partridge, J.D., Nishino, S.F., Spain, J.C. and Spiro, S. (2008) *Escherichia coli* NsrR regulates a pathway for the oxidation of 3-nitrotyramine to 4-hydroxy-3-nitrophenylacetate. *J. Bacteriol.* **190**: 6170-6177
- Ray, N., Oates, J., Turner, R.J. and Robinson, C. (2003) DmsD is required for the biogenesis of DMSO reductase in *Escherichia coli* but not for the interaction of the DmsA signal peptide with the Tat apparatus. *FEBS Lett.* **534**: 156-160

- Richardson, D. and Sawers, G. (2002) PMF through the redox loop. *Science*. **295**: 1842-1843
- Robinson, C., Matos, C.F.R.O., Beck, D., Ren, C., Lawrence, J., Vasisht, N. and Mendel, S. (2011) Transport and proofreading of proteins by the twin-arginine translocation (Tat) system in bacteria. *Biochim. Biophys. Acta*. **1808**: 876-884
- Rodionov, D.A., Dubchak, I.L., Arkin, A.P., Alm, E.J. and Gelfand, M.S. (2005) Dissimilatory metabolism of nitrogen oxides in bacteria: comparative reconstruction of transcriptional networks. *PLoS Computational Biol.* **1**: 415-431
- Sambrook, J., Fritsch, E. F. & Maniatis, T. (1989). *Molecular Cloning: a Laboratory Manual*, 2nd edn. Cold Spring Harbor, NY: Cold Spring Harbor Laboratory.
- Sargent, F. (2007) Constructing the wonders of the bacterial world: biosynthesis of complex enzymes. *Microbiology*. **153**: 633-651
- Sargent, F., Bogsch, E.G., Stanley, N.R., Wexler, M., Robinson, C., Berks, B.C. and Palmer, T. (1998) Overlapping functions of a bacterial Sec-independent protein export pathway. *EMBO J.* **17**: 3640-3650
- Sedgwick, B. and Taverna, P. (1996) Generation of an endogenous DNA-methylating agent by nitrosation in *Escherichia coli*. *J. Bacteriol.* **178**: 5105-5111
- Shingler, V. (2011) Signal sensory systems that impact σ^{54} -dependent transcription. *FEMS Microbiol. Rev.* **35**: 425-440
- Simon, G., Mejean, V., Jourlin, C., Chippaux, M. and Pascal, M.-C. (1994) The *torR* gene of *Escherichia coli* encodes a response regulator protein involved in the expression of trimethylamine *N*-oxide reductase genes. *J. Bacteriol.* **176**: 5601-5606
- Smith, M.S. (1983) Nitrous oxide production by *Escherichia coli* is correlated with nitrate reductase activity. *Appl Env Microbiol* **45**: 679-689
- Spector, M.P., Garcia del Portillo, G., Bearson, S.M.D., Mahmud, A., Magut, M., Finlay, B.B., Dougan, G., Foster, J.W. and Pallen, M.J. (1999) The *rpoS*-dependent starvation-stress response locus *stiA* encodes a nitrate reductase (*narZYWV*) required for carbon-starvation-inducible thermotolerance and acid tolerance in *Salmonella typhimurium*. *Microbiology*. **145**: 3035-3045
- Spek, E.J., Wright, T.L., Stitt, M.S., Taghizadeh, N.R., Tannenbaum, S.R., Marinus, M.G. and Engelward, B.P. (2001) Recombinatorial repair is critical for survival of *Escherichia coli* exposed to nitric oxide. *J. Bacteriol.* **183**: 131-138
- Spiro, S. (2007) Regulators of bacterial responses to nitric oxide. *FEMS Microbiol. Rev.* **31**: 193-211

- Squire, D.J., Xu, M., Cole, J.A., Busby, S.J. and Browning, D.F. (2009) Competition between NarL-dependent activation and Fis-dependent repression controls expression from the *Escherichia coli* *yeaR* and *ogt* promoters. *Biochem. J.* **420**: 249-257
- Stanley, N.R., Sargent, F., Buchanan, G., Shi, J.R., Stewart, V., Palmer, T. and Berks, B.C. (2002) Behaviour of topological marker proteins targeted to the Tat protein transport pathway. *Mol. Microbiol.* **43**: 1005-1021
- Stevanin, T.M., Ioannidis, N., Mills, C.E., Kim, S.O., Hughes, M.N. and Poole, R.K. (2000) Flavohemoglobin Hmp affords inducible protection for *Escherichia coli* respiration, catalysed by cytochromes *bo* or *bd* from nitric oxide. *J. Biol. Chem.* **275**: 35868-35875
- Stewart, V. (1993) Nitrate regulation of anaerobic respiratory gene expression in *Escherichia coli*. *Mol. Microbiol.* **9**: 425-434
- Stewart, V. (2003) Nitrate- and nitrite-responsive sensors NarX and NarQ of proteobacteria. *Biochem. Soc. Trans.* **31**: 1-10
- Stewart, V. and Bledsoe, P.J. (2003) Synthetic *lac* operator substitutions for studying the nitrate- and nitrite-responsive NarX-NarL and NarQ-NarP two-component regulatory systems of *Escherichia coli* K-12. *J. Bacteriol.* **185**: 2104-2111
- Stewart, V., Chen, L.L. and Wu, H. (2003) Response to culture aeration mediated by the nitrate and nitrite sensor NarQ of *Escherichia coli* K-12. *Mol. Microbiol.* **50**: 1391-1399
- Stewart, V. and McGregor, C.H. (1982) Nitrate reductase in *Escherichia coli* K-12: Involvement of *chlC*, *chlE*, and *chlG* loci. *J. Bacteriol.* **151**: 788-799
- Sutton, V.R., Mettert, E.L., Beinert, H. and Kiley, P.J. (2004a) Kinetic analysis of the oxidative conversion of the [4Fe-4S]²⁺ Cluster of FNR to a [2Fe-2S]²⁺ cluster. *J. Bacteriol.* **186**: 8018-8025
- Sutton, V.R., Stubna, A., Patschkowski, T., Münck, E., Beinert, H. And Kiley, P.J. (2004b) Superoxide destroys the [2Fe-2S]²⁺ cluster of FNR from *Escherichia coli*. *Biochemistry.* **43**: 791-798
- Tarry, M.J., Schaefer, E., Chena, S., Buchanan, G., Greene, N.P., Lead, S.M., Palmer, T., Saibil, H.R. and Berks, B.C. (2009) Structural analysis of substrate binding by the TatBC component of the twin-arginine protein transport system. *Proc. Natl. Acad. Sci. USA* **106**: 13284-13289
- Taverna, P. and Sedgwick, B. (1996) Generation of an endogenous DNA-methylating agent by nitrosation in *Escherichia coli*. *J. Bacteriol.* **178**: 5105-5111

- Todorovic, S., Justino, M.C., Wellenreuther, G., Hildebrandt, P., Murgida, D.H., Meyer-Klaucke, W. and Saraiva, L.M. (2008) Iron-Sulphur repair YtfE protein from *Escherichia coli*: structural characterisation of the di-iron center. *J. Biol. Inorg. Chem.* **13**: 765-770
- Tucker, N.P., Autreaux, B.D., Spiro, S. and Dixon, R. (2005) Mechanism of transcriptional regulation by the *Escherichia coli* nitric oxide sensor NorR. *Biochem. Soc. Trans.* **34**: 191-194
- Tucker, N.P., Hicks, M.G., Clarke, T.A., Crack, J.C., Chandra, G., Le Brun, N.E., Dixon, R. and Hutchings, M.I. (2008) The transcriptional repressor protein NsrR senses nitric oxide directly via a [2Fe-2S] cluster. *PLoS ONE.* **3**: e3623
- Tucker, N.P., Le Brun, N.E., Dixon, R. and Hutchings, M.I. (2010) There's NO stopping NsrR, a global regulator of the bacterial NO stress response. *Trends. Microbiol.* **18**: 149-156
- Tyson, K., Bell, A., Cole, J. and Busby, S. (1993) Definition of nitrite and nitrate response elements at the anaerobically inducible *Escherichia coli nirB* promoter: interactions between FNR and NarL. *Mol. Microbiol.* **7**: 151-157
- Tyson, K.L., Cole, J.A. and Busby, S.J.W. (1994) Nitrite and nitrate regulation at the promoters of two *Escherichia coli* operons encoding nitrite reductase: identification of common target heptamers for both NarP- and NarL-dependent regulation. *Mol. Microbiol.* **13**: 1045-1055
- Tyson, K., Busby, S. and Cole, J. (1997a) Catabolite repression of two *Escherichia coli* operons encoding nitrite reductases: role of the Cra protein. *Arch. Microbiol.* **168**: 240-244
- Tyson, K., Metheringham, R., Griffiths, L., and Cole, J. (1997b) Characterisation of *Escherichia coli* K-12 mutants defective in formate-dependent nitrite reduction: essential roles for *hemN* and the *menFDBCE* operon. *Arch. Microbiol.* **168**: 403-411.
- Uden, G., Becker, S., Bongaerts, J., Holighaus, G., Schirawski, J. and Six, S. (1995) O₂ sensing and O₂ dependent gene regulation in facultatively anaerobic bacteria. *Arch. Microbiol.* **164**: 81-90
- Uden, G. and Bongaerts, J. (1997) Alternative respiratory pathways in *Escherichia coli*: energetic and transcriptional regulation in response to electron acceptors. *Biochim. Biophys. Acta.* **1320**: 217-234
- van Wonderen, J.H., Burlat, B., Richardson, D.J., Cheesman, M.R. and Butt, J.N. (2008) The nitric oxide reductase activity of cytochrome *c* nitrite reductase from *Escherichia coli*. *J. Biol. Chem.* **283**: 9587-9594

Vasudevan, S.G., Armarego, W.L., Shaw, D.C., Lilley, P.E., Dixon, N.E. and Poole, R.K. (1991) Isolation and nucleotide sequence of the *hmp* gene that encodes a haemoglobin-like protein in *Escherichia coli* K-12. *Mol. Gen. Genet.* **226**: 49-58

Vine, C.E. and Cole, J.A. (2011) Nitrosative stress in *Escherichia coli*: reduction of nitric oxide. *Biochem. Soc. Trans.* **39**: 213-215

Vine, C.E., Justino, M.C., Saraiva, L.M. and Cole, J.A. (2010) Detection by whole genome microarrays of a spontaneous 126-gene deletion during construction of a *ytfE* mutant: Confirmation that a *ytfE* mutation results in loss of repair of iron-sulphur centres in proteins damaged by oxidative or nitrosative stress. *J. Microbiol. Meth.* **81**: 77-79

Vine, C.E., Purewal, S.K. and Cole, J.A. (2011) NsrR-dependent method for detecting nitric oxide accumulation in the *Escherichia coli* cytoplasm and enzymes involved in NO production. *FEMS Microbiol. Lett.* In press

de Vries, S. and Schröder, I. (2002) Comparison between the nitric oxide reductase family and its aerobic relatives, the cytochrome oxidases. *Biochem. Soc. Trans.* **30**: 662-667

Wang, H. and Gunsalus, R.P. (2000) The *nrfA* and *nirB* nitrite reductase operons in *Escherichia coli* are expressed differently in response to nitrate than to nitrite. *J. Bacteriol.* **182**: 5813-5822

Wang, H., Tseng, C.P. and Gunsalus, R.P. (1999) The *napF* and *narG* nitrate reductase operons in *Escherichia coli* are differentially expressed in response to submicromolar concentrations of nitrate but not nitrite. *J. Bacteriol.* **181**: 5303-5308

Watmough, N.J., Butland, G., Cheesman, M.R., Moir, J.W.B., Richardson, D.J. and Spiro, S. (1999) Nitric oxide in bacteria: synthesis and consumption. *Biochim. Biophys. Acta.* **1411**: 456-474

Weiner, J.H., Bilous, P.T., Shaw, G.M., Lubitz, S.P., Frost, L., Thomas, G.H., Cole, J.A. and Turner, R.J. (1998) A novel and ubiquitous system for membrane targeting and secretion of cofactor-containing proteins. *Cell.* **93**: 93-101

Weiss, B. (2006) Evidence for mutagenesis by nitric oxide during nitrate metabolism in *Escherichia coli*. *J. Bacteriol.* **188**: 829-833

Wolfe, M.T., Heo, J., Garavelli, J.S. and Ludden, P.W. (2002) Hydroxylamine reductase activity of the hybrid cluster protein from *Escherichia coli*. *J. Bacteriol.* **184**: 5898-5902

Wu, H., Tyson, K.L., Cole, J.A. and Busby, S.J.W. (1998) Regulation of transcription initiation at the *Escherichia coli nir* operon promoter: a new mechanism to account for co-dependence on two transcription factors. *Mol. Microbiol.* **27**: 493-505

Xie, X., Wong, W. and Tang, Y. (2007) Improving simvastatin bioconversion in *Escherichia coli* by deletion of *bioH*. *Metab. Eng.* **9**: 379-386

Yeo, W.S., Lee, J.H., Lee, K.C. and Roe, J.H. (2006) IscR acts as an activator in response to oxidative stress for the *suf* operon encoding Fe-S assembly proteins. *Mol. Microbiol.* **61**: 206-218

Zhao, G., Ceci, P., Ilari, A., Giangiacomo, L., Laue, T.M., Chiancone, E. and Chasteen, N.D. (2002) Iron and hydrogen peroxide detoxification properties of DNA-binding protein from starved cells. *J. Biol. Chem.* **277**: 27689-27696

Zumft, W.G. (1997) Cell biology and molecular basis of denitrification. *Microbiol. Mol. Biol. Rev.* **61**: 533-616